

---

**GLYCOSIDASES AND NANOVESICLES:  
NOVEL BIOLOGICAL TOOLS FOR  
BIOTECHNOLOGICAL APPLICATIONS.**

---

**Federica De Lise**

Dottorato in Biotecnologie – XXX ciclo

Università di Napoli Federico II





Dottorato in Biotecnologie – XXX ciclo

Università di Napoli Federico II



---

**GLYCOSIDASES AND NANOVESICLES:  
NOVELS BIOLOGICAL TOOLS FOR  
BIOTECHNOLOGICAL APPLICATIONS**

---

**Federica De Lise**

Dottorando: Federica De Lise

Co-Relatore: Prof. Ramaroson  
Andriantsitohaina

Co-Relatore: Prof. Alberto Di Donato

Coordinatore: Prof. Giovanni Sannia



*Why do we fall, Bruce?  
So we can learn to pick ourselves up.  
(Batman Begins)*



# INDEX

---

<b>RIASSUNTO</b>	<b>pag. 5</b>
<b>ABSTRACT</b>	<b>pag. 11</b>
<b>ABBREVIATIONS</b>	<b>pag. 13</b>
<b>CHAPTER I – INTRODUCTION</b>	<b>pag. 15</b>
<b>1.1 Biocatalysis and glycosidases</b>	<b>pag. 17</b>
<b>1.2 <math>\alpha</math>-L-rhamnosidases</b>	<b>pag. 18</b>
<b>1.3 Enzyme immobilization</b>	<b>pag. 20</b>
<i>1.3.1 Outer Membrane Vesicles</i>	<b>pag. 23</b>
<i>1.3.2 Extracellular Vesicles</i>	<b>pag. 25</b>
<b>1.4 Novosphingobium sp. PP1Y: a novel microbial source of OMVs and glycosidases</b>	<b>pag. 26</b>
<b>AIMS OF THE THESIS</b>	<b>pag. 31</b>
<b>CAPTER II – MATERIALS AND METHODS</b>	<b>pag. 33</b>
<b>2.1 Generals</b>	<b>pag. 35</b>
<b>2.2 Cloning of orf PP1YRS05470 and construction of the pET22b(+)/rha-p expression vector</b>	<b>pag. 35</b>
<b>2.3 Construction of the pET22b(+)/rha-his expression vector</b>	<b>pag. 35</b>
<b>2.4 Mutagenesis of the pET22b(+)/rha-his expression vector and construction of rRHA-Phis single mutants</b>	<b>pag. 36</b>
<b>2.5 rRHA-P recombinant expression</b>	<b>pag. 36</b>
<b>2.6 rRHA-P purification</b>	<b>pag. 37</b>
<b>2.7 rRHA-Phis and mutants recombinant expression</b>	<b>pag. 37</b>
<b>2.8 rRHA-Phis and RHA-Phis mutants purification</b>	<b>pag. 38</b>
<b>2.9 Enzyme activity assays</b>	<b>pag. 39</b>
<b>2.10 TLC Analysis for substrate specificity</b>	<b>pag. 40</b>
<b>2.11 Growth of Novosphingobium sp. PP1Y</b>	<b>pag. 40</b>
<b>2.12 OMVs isolation and purification</b>	<b>pag. 40</b>
<b>2.13 AFM analysis</b>	<b>pag. 41</b>
<b>2.14 DLS and Zeta-potential measurements</b>	<b>pag. 41</b>
<b>2.15 Scanning electron microscopy (SEM)</b>	<b>pag. 41</b>
<b>2.16 Proteome Analysis</b>	<b>pag. 41</b>
<b>2.17 Fatty acids analysis</b>	<b>pag. 42</b>

<b>2.18 Carbohydrates analysis</b>	<b>pag. 42</b>
<b>2.19 Cell viability MTT assay</b>	<b>pag. 42</b>
<b>2.20 Cell culture</b>	<b>pag. 43</b>
<b>2.21 Production and isolation of EVs</b>	<b>pag. 43</b>
<b>2.22 Western Blot analysis</b>	<b>pag. 43</b>
<b>2.23 Nanoparticle tracking analysis</b>	<b>pag. 44</b>
<b>2.24 Cytofluorimetric Annexin V binding analysis</b>	<b>pag. 44</b>
<b>CHAPTER III – RESULTS SECTION I. A NOVEL A-L-RHAMNOSIDASE ACTIVITY FROM NOVOSPHINGOBIUM SP. PP1Y</b>	<b>pag. 47</b>
<b>3.1.1 Cloning, recombinant expression and purification of recombinant RHA-P</b>	<b>pag. 49</b>
<b>3.1.2 Biochemical characterization of rRHA-P</b>	<b>pag. 51</b>
<b>3.1.3 Optimization of rRHA-P purification: his-tag cloning</b>	<b>pag. 54</b>
<b>3.1.4 Functional and structural characterization of rRHA-P: Alanine scanning mutagenesis</b>	<b>pag. 57</b>
<b>CHAPTER III– RESULTS SECTION II. EXTRACELLULAR VESICLES IN BIOTECHNOLOGICAL PROCESSES</b>	<b>pag. 63</b>
<b>3.2.1 Outer Membrane Vesicles (OMVs) from Novosphingobium sp. PP1Y</b>	<b>pag. 65</b>
3.2.1.1 Identification of OMVs from PP1Y	pag. 65
3.2.1.2 OMVs purification	pag. 67
3.2.1.3 OMVs characterization	pag. 68
3.2.1.4 Biocompatibility	pag. 72
<b>3.2.2 Extracellular Vesicles (EVs) from macrophages</b>	<b>pag. 73</b>
3.2.2.1 Isolation of extracellular vesicles (EVs) from murine macrophages RAW 264.7 cell lines	pag. 73
3.2.2.2 Characterization of EVs	pag. 74
3.2.2.3 The role of isolated EVs in inflammatory processes	pag. 77
<b>CAPTER IV – DISCUSSION</b>	<b>pag. 83</b>
<b>RERERENCES</b>	<b>pag. 95</b>
<b>APPENDICES</b>	<b>pag. 105</b>
<b>APPENDIX I – List of publications</b>	<b>pag. 107</b>
<b>APPENDIX II – Communications</b>	<b>pag. 108</b>
<b>APPENDIX III –Experiences in foreign laboratories</b>	<b>pag. 109</b>
<b>APPENDIX IV – Other papers</b>	<b>pag. 110</b>





# RIASSUNTO

---

## Base scientifica del progetto

### Biocatalisi e glicosidasi

Le biocatalisi rappresentano uno strumento ampiamente utilizzato nel campo delle biotecnologie. Un valore aggiunto in tale ambito viene fornito dall'utilizzo di enzimi come catalizzatori, i quali possono aumentare la selettività delle reazioni, la resa dei prodotti desiderati ed il cui utilizzo comporta una diminuzione dell'utilizzo di sostanze chimiche inquinanti. Tra gli enzimi utilizzati, le glicosidasi risultano particolarmente interessanti, soprattutto nella produzione di detersivi (cellulasi ed amilasi), di bioetanolo a partire dalla biomassa vegetale, di *soft-drinks* ad alto contenuto zuccherino ecc. Tra le glicosidasi, negli ultimi anni grande attenzione è stata dedicata alle  $\alpha$ -L-ramnosidasi ( $\alpha$ -RHA), enzimi che catalizzano l'idrolisi di un residuo di ramnosio in un'ampia varietà di composti presenti in natura, come i flavonoidi, e che sono prodotte da tessuti di origine animale, da piante, funghi e batteri. Nell'ultimo decennio le  $\alpha$ -RHA hanno attirato un grande interesse per il loro utilizzo come biocatalizzatori nell'industria alimentare, farmaceutica e nei processi di chimica industriale. In particolare, questi enzimi vengono utilizzati nell'industria alimentare per esaltare gli aromi dei vini attraverso l'idrolisi enzimatica dei glicosidi terpenici contenenti L-ramnosio, e per dolcificare e chiarificare i succhi di frutta ottenuti da agrumi. Nonostante le applicazioni finora descritte, ad oggi solo poche  $\alpha$ -L ramnosidasi di origine batterica sono state caratterizzate e attualmente un numero estremamente esiguo di strutture tridimensionali è depositato in banca dati. Tutto questo rende le  $\alpha$ -L ramnosidasi una classe di enzimi ancora poco caratterizzata e con un interessante potenziale biotecnologico ancora da esplorare.

### L'immobilizzazione degli enzimi

L'utilizzo di enzimi in applicazioni industriali è spesso limitato dalla loro instabilità, dal loro elevato costo di purificazione e dall'impossibilità di disporne in grande quantità. Tutte queste problematiche trovano una loro soluzione nell'immobilizzazione degli enzimi su diversi supporti, approccio che può aumentare sia la stabilità di un enzima che la sua attività enzimatica, avvantaggiando l'avanzamento delle reazioni e aumentando la resa dei prodotti desiderati. Diverse tipologie di supporti per l'immobilizzazione sono state fino ad ora utilizzate e studiate ma, negli ultimi anni, di particolare interesse si è rivelato l'utilizzo di nanobiomateriali. In particolare, la ricerca si è recentemente focalizzata sull'isolamento di nanoparticelle di origine biologica quali le Outer Membrane Vesicles (OMVs) originate da batteri gram-negativi e le Extracellular Vesicles (EVs), secrete invece da cellule eucariotiche.

#### -Outer Membrane Vesicles (OMVs) e Extracellular Vesicles (EVs)

Le OMVs sono proteo-liposomi con un diametro di circa 20-200 nm, prodotte dai batteri gram-negativi durante il loro ciclo vitale. Sembra che la loro funzione possa essere quella di veicolare tossine, molecole segnale, nutrienti e attività enzimatiche di vario genere, e che siano quindi implicate in svariati processi. Queste nanostrutture possono essere interessanti in campo biotecnologico sia per l'immobilizzazione di enzimi, sia per creare nuovi supporti per il "drug-delivery". Ad oggi le OMVs maggiormente

studiare derivano da batteri gram-negativi patogeni; al contrario, le OMVs secrete da batteri non patogeni, che dovrebbero essere più indicate in campo farmaceutico, risultano invece essere ancora poco studiate e caratterizzate. Per quanto riguarda le EVs, si tratta di particelle di grandezza variabile tra i 30 e i 2000 nm secrete da gran parte delle cellule eucariotiche, classificate, in base alla loro differente origine, in due principali categorie: esosomi e microparticelle (MP). Tali nanostrutture sono implicate in diversi processi fisiologici quali ad esempio la coagulazione, e sembrano avere un ruolo nell'insorgenza delle patologie cardiovascolari e del cancro [4,6,7 star]; in campo biotecnologico potrebbero avere un grande potenziale nell'ambito della progettazione di nuovi farmaci. Ciò che rende le EVs più idonee delle OMVs batteriche nel campo del drug-delivery deriva dal fatto che tali nanovesicole, essendo di origine eucariotica, dovrebbero essere meno immunogeniche. Le EVs possiedono inoltre uno specifico meccanismo di "cell-targeting", che permetterebbe una veicolazione del farmaco mirata ad uno specifico tessuto.

### **Novosphingobium sp. PP1Y**

Nel laboratorio in cui ho svolto il seguente progetto di dottorato, è stato recentemente isolato, dalle acque superficiali di una piccola baia all'interno del porto di Pozzuoli, un  $\alpha$ -proteobatterio gram-negativo: *Novosphingobium* sp. PP1Y (*N.sp.* PP1Y). *N.sp.* PP1Y appartiene all'ordine degli sfingomonadali ed è in grado di utilizzare un numero sorprendentemente ampio di idrocarburi aromatici mono- e policiclici come unica fonte di carbonio e di energia, con un efficace adattamento alla crescita su miscele complesse di molecole aromatiche disciolte in fasi non polari (come il gasolio e la benzina). Considerate le sue peculiari caratteristiche, *N.sp.* PP1Y risulta essere molto interessante per l'isolamento sia di nuove attività enzimatiche sia di OMVs. L'interesse per l'isolamento di nuove glicosidasi di interesse biotecnologico da tale batterio nasce dalla considerazione che l'analisi del suo genoma, completamente annotato, ha evidenziato un'abbondanza unica di geni codificanti per glicosil-idrolasi (53 ORFs) e glicosil-trasferasi (57 ORFs); tra questi sono stati identificati 8 geni codificanti per proteine con attività ramosidasi.

Altro aspetto interessante è il fatto che PP1Y mostra un complesso dimorfismo planctonico/sessile ed è in grado di colonizzare superfici idrofobiche o interfacce acqua/gasolio. Dati preliminari hanno inoltre mostrato la capacità di PP1Y di formare, in soluzione, flocculi amorfi o un biofilm strutturato. Queste caratteristiche morfologiche e metaboliche, oltre ad evidenziare la potenzialità dello stesso biofilm per applicazioni industriali nelle biotecnologie dei materiali e del biorisanamento, suggerirebbero la produzione di OMVs per l'acquisizione di nutrienti e la comunicazione cellulare.

### **Obiettivi del progetto di ricerca**

Sulla base delle considerazioni descritte nella sezione precedente, le  $\alpha$ -L-rhamnosidasi, le OMVs e le EVs sono considerate interessanti elementi per il miglioramento dei processi biocatalitici nelle industrie biotecnologiche.

Lo scopo di questa tesi è stato quello di: i) caratterizzare una nuova  $\alpha$ -L-rhamnosidasi da *Novosphingobium* sp. PP1Y, un microorganismo gram-negativo recentemente isolato nel porto di Pozzuoli; ii) Isolare e caratterizzare OMVs da *Novosphingobium* sp. PP1Y ed EVs da macrofagi murini.

## Risultati

### **Isolamento e caratterizzazione di una nuova $\alpha$ -L-rhamnosidasi da *Novosphingobium* sp. PP1Y**

Nel laboratorio in cui ho svolto il mio progetto di dottorato, è stata recentemente identificata un'attività  $\alpha$ -L-rhamnosidasi nell'estratto crudo grezzo del batterio *Novosphingobium* sp. PP1Y, cresciuto in presenza di 0.3 mM naringina. Il gene codificante per tale enzima è stato clonato in un vettore di espressione pET22b(+), e la proteina è stata espressa in maniera ricombinante in cellule di *E. coli* BL21(DE3). I primi tentativi di espressione hanno evidenziato la presenza della proteina nella sola porzione insolubile; di conseguenza, la temperatura di induzione è stata diminuita da 37 a 23 °C e la crescita batterica è stata effettuata in terreno LB ad alte concentrazioni di NaCl e in presenza di Betaina e Sorbitolo, due molecole che possono agire da "chaperon molecolari", consentendo un miglioramento del *folding* della proteina stessa. La proteina è stata quindi espressa nelle condizioni ottimizzate e la purificazione è stata effettuata seguendo tre passaggi cromatografici, al termine dei quali la resa ed il fattore di purificazione risultavano però non soddisfacenti. La sequenza amminoacidica di rRHA-P, un monomero di  $101,500 \pm 5,000$  Da, è stata verificata per spettrometria di massa. La successiva caratterizzazione dal punto di vista biochimico di rRHA-P, ha evidenziato una  $K_M$  inferiore rispetto alle altre  $\alpha$ -RHA riportate in letteratura, suggerendo una maggiore affinità di rRHA-P per il substrato sintetico utilizzato. Per valutare l'effettivo potenziale biotecnologico di rRHA-P, sono state inoltre determinate le condizioni ottimali di attività enzimatica in diverse condizioni sperimentali. In particolare, rRHA-P presenta proprietà leggermente basofile con un'attività ottimale a pH 6.9 e a 40.9 °C, conservando una certa stabilità fino a 50°C. L'enzima possiede inoltre una moderata tolleranza ai solventi organici, quali etanolo e DMSO; i risultati ottenuti indicano che rRHA-P mostra diverse caratteristiche di interesse biotecnologico. È stata a tal proposito valutata la capacità di rRHA-P di idrolizzare alcuni flavonoidi naturali, la cui solubilità è più elevata in condizioni di pH basico, alte temperature e in presenza di solventi organici. I risultati ottenuti hanno mostrato che rRHA-P è in grado di convertire, dopo 3h di incubazione, di completamente la naringina nei corrispondenti prunina e ramosio, e parzialmente rutina e neoesperidina. Tali dati supportano ulteriormente l'utilizzo dell'enzima in processi di bioconversione. Le analisi di spettrometria di massa ed il sequenziamento N-terminale effettuati sulla proteina rRHA-P purificata hanno evidenziato l'assenza dei primi 23 aminoacidi codificati dal gene, il che ha suggerito la presenza di un peptide segnale, successivamente allontanato in seguito a modifiche post-traduzionali della stessa. Tale peptide possiede delle caratteristiche peculiari e, da dati presenti in letteratura, sembra essere coinvolto nel "sorting" della proteina nello spazio periplasmatico. Tale ipotesi è stata confermata da esperimenti di espressione analitica, in cui la frazione periplasmatica evidenzia un'attività ramosidasi 400 volte maggiore rispetto alla frazione citoplasmatica. Considerando la bassa resa di purificazione di rRHA-P, si è deciso di clonare e di esprimere in maniera ricombinante la proteina fusa con un *his-tag*, e di utilizzare, come primo step di purificazione, l'estrazione della frazione periplasmatica. Seguendo il protocollo appena descritto, è stato necessario un solo step di purificazione attraverso una cromatografia di affinità che ha permesso di ottenere, con una resa del 25%, una proteina molto pulita caratterizzata da una minima percentuale di contaminanti. Saggi di attività sulla proteina purificata non hanno mostrato una significativa influenza del *tag* di istidine né sulla attività specifica, né sull'efficienza catalitica dell'enzima. Per implementare l'utilizzo biotecnologico di

rRHA-P, sono stati effettuati esperimenti di mutagenesi per ottenere una preliminare identificazione degli ipotetici residui amminoacidici responsabili dell'attività catalitica dell'enzima. È stato quindi effettuato, in primo luogo, un allineamento della sequenza della proteina rRHA-P con sequenze di ramnosidasi della stessa famiglia GH106, già presenti in banca dati. Successivamente, individuati i 5 residui maggiormente conservati (D504, E506, D552, E644 e D763), si è proceduto con un approccio di mutagenesi sito specifica in cui i residui di interesse sono stati sostituiti con alanina ed è stata valutata la loro influenza sull'attività specifica di rRHA-P. Le mutazioni in posizione 504, 506 e 644 sembrano portare ad una totale inattivazione dell'attività catalitica, mentre le mutazioni in posizione 552 e 763 hanno mostrato una ritenzione dell'attività enzimatica di rRHA-P compresa tra il 6 e il 12%. Tali dati suggeriscono un effetto differenziale dei residui amminoacidici individuati dall'allineamento e pongono le basi per futuri interventi di mutagenesi finalizzati al *fine-tuning* dell'attività enzimatica su substrati di interesse biotecnologico.

### **Isolamento di vescicole batteriche e eucariotiche**

Per ottimizzare l'utilizzo degli enzimi come biocatalizzatori, oltre all'ingegnerizzazione, molto utile può essere la loro immobilizzazione su diversi tipi di supporti. In particolare, al fine di sviluppare supporti biocompatibili, sono stati recentemente studiati sistemi di immobilizzazione composti da membrane di origine biologica. Durante la seconda parte del mio periodo di dottorato, mi sono quindi occupata della caratterizzazione di due possibili sistemi di immobilizzazione, uno di origine batterica (Outer Membrane Vesicles OMVs) ed uno di derivazione eucariotica (Extracellular Vesicles EVs).

#### *Isolamento e caratterizzazione di OMVs da *Novosphingobium* sp. PP1Y*

Le OMVs sono state isolate da *N. sp. PP1Y*, un batterio gram-negativo non patogeno. Analisi di microscopia elettronica (SEM) e a forza atomica (AFM) hanno evidenziato, durante la crescita in terreno minimo, una significativa attività di vescicolazione in tarda fase esponenziale, evidenza che spiegherebbe la vescicolazione di *N. sp. PP1Y* come possibile strategia per l'acquisizione di nutrienti. Le OMVs identificate sono state quindi purificate attraverso una serie di ultracentrifugazioni e la loro analisi strutturale ha evidenziato una forma sferica e un diametro di  $\approx 130-150$  nm, in linea con le OMVs descritte in letteratura. Le OMVs da *N. sp. PP1Y*, risultano inoltre avere una peculiare composizione biochimica sia per quanto riguarda le proteine che per quanto concerne gli acidi grassi. L'analisi proteomica ha infatti evidenziato la presenza di una preponderanza di enzimi idrolitici rispetto alle cellule del ceppo PP1Y. Ancor più interessante risulta il fatto che la maggior parte delle proteine maggiormente presenti sulle OMVs, non lo è invece nelle cellule di PP1Y; in particolare le OMVs risultano avere, al contrario delle cellule, una elevata percentuale di proteine di membrana ed enzimi idrolitici ed una quasi totale assenza di enzimi deputati al metabolismo cellulare. Anche la composizione in acidi grassi sembra essere fortemente regolata nelle OMVs, che infatti presentano una grande percentuale di acidi grassi saturi, rispetto alla membrana delle cellule; questo aspetto suggerisce una specifica selezione degli acidi grassi durante la vescicolazione, che avverrebbe in zone della membrana batterica più "rigide" rispetto al resto della cellula.

I dati ottenuti incrementano fortemente l'interesse delle OMVs nel campo delle biotecnologie anche se un limite nel loro utilizzo è rappresentato dalla loro immunogenicità verso le cellule eucariotiche, dovuta alla presenza di LPS sulla membrana esterna. In questo contesto, *N. sp. PP1Y* sembra essere un buon candidato in quanto la sua membrana esterna non presenta LPS. Infatti, il trattamento di cellule

di cheratinociti umani con concentrazioni crescenti di OMVs, non ha mostrato una significativa diminuzione della vitalità cellulare rispetto al controllo; tale dato suggerisce una potenziale biocompatibilità delle OMVs per le cellule eucariotiche, che necessita chiaramente di ulteriori indagini effettuate su altre linee cellulari.

#### Isolamento e caratterizzazione di EVs da macrofagi

Una valida alternativa alle OMVs batteriche per il drug-delivery è rappresentata dalle vescicole isolate da cellule eucariotiche: EVs. Tali nanostrutture sono classificate, in base alla loro origine e dimensione, in Microparticelle (MPs), che hanno una grandezza di  $\approx 400-2000$  nm ed esosomi, di  $\approx 50-200$  nm. Tali vescicole originano da diversi tipi di cellule eucariotiche, il che le rende meno immunogeniche per le stesse e quindi più attraenti per il drug-delivery; inoltre, grazie alla presenza di specifici recettori di membrana, le EVs possono avere uno specifico *cell-targeting* che può aumentare l'efficienza di veicolazione di un farmaco. Nell'ultima parte del mio progetto di dottorato mi sono quindi occupata della caratterizzazione e della valutazione dell'effetto immunogenico di EVs isolate da macrofagi murini. Per l'isolamento delle EVs sono stati valutati differenti stimoli, tra cui l'utilizzo di LPS, acido oleico e acido palmitico, i quali incrementano la vescicolazione rispetto alle cellule non stimolate. Tali vescicole, dopo opportuna purificazione tramite ultracentrifugazione, sono risultate essere omogenee in taglia e conformi rispetto a quelle descritte in letteratura. La valutazione dell'effettivo utilizzo delle EVs in campo biotecnologico passa necessariamente attraverso la determinazione dell'effetto di tali nanostrutture sulle cellule eucariotiche. In particolare, negli ultimi anni è stata riscontrata una correlazione tra le EVs isolate da macrofagi e l'instaurazione di uno stato di infiammazione. Per tale motivo, nelle EVs isolate da cellule sottoposte a stimoli di vescicolazione, è stata valutata l'espressione di Nlrp3, un complesso proteico definito "infiamosoma" responsabile dell'attivazione della gran parte dei processi infiammatori. In particolare, la stimolazione dei macrofagi con LPS e acido palmitico aumenta significativamente l'espressione di Nlrp3, suggerendo un'effettiva differenza anche nell'effetto delle diverse EVs su altre cellule. In particolare, essendo le cellule vascolari le prime coinvolte nell'infiammazione, l'effetto pro-infiammatorio delle EVs, sia MPs che esosomi, è stato valutato su cellule muscolari lisce vascolari (VSMC). In questo modello sperimentale è stato evidenziato un significativo aumento dell'espressione della caspasi-1 attivata in seguito a trattamento delle VSMC con MPs ed esosomi isolate da macrofagi stimolati con LPS e acido palmitico, mentre si è osservato un aumento dell'espressione della caspasi-8 soltanto dopo trattamento con esosomi isolati da macrofagi stimolati con LPS e acido palmitico.

In conclusione, in questo lavoro di dottorato è stato messo a punto un sistema di espressione ricombinante e di purificazione di una nuova  $\alpha$ -RHA, il cui potenziale biotecnologico è stato analizzato e discusso. Inoltre, questo progetto di dottorato ha permesso di caratterizzare due possibili sistemi di immobilizzazione e di veicolamento di attività enzimatiche e/o di piccole molecole organiche, di origine batterica (OMVs) ed eucariotica (EVs). Tutti i sistemi analizzati in questo progetto di dottorato risultano essere molto interessanti dal punto di vista biotecnologico e applicabili in diversi campi.



# ABSTRACT

---

Biocatalysis represents a versatile and valuable tool for industrial biotechnologies. The use of enzymes as biocatalysts has reached its present industrial level, due to their optimal reaction selectivity, high reaction rates, high product purity, and a significant decrease in the generation of chemical waste. The use of enzymes in industrial applications has been limited by several factors, mainly the high cost of enzymes, their instability, and their availability in small amounts. To overcome these problems, the quest for new catalytic activities and the development of new technical approaches, such as enzyme immobilization, to improve their stability and practical applications, remain a central focus of the current biotechnological research. In this PhD thesis, the biotechnological potential of a novel bacterial glycosidase ( $\alpha$ -RHA), and the characterization of two possible immobilization systems, bacterial OMVs and eukaryotic EVs is reported.

More in detail, an optimized expression and purification procedure allowed to characterize a novel  $\alpha$ -RHA from the microorganism *Novosphingobium* sp. PP1Y, which resulted to be appealing from a biotechnological point of view for its interesting catalytic behaviour. Moreover, mutagenesis experiments, allowed a preliminary identification of the aminoacidic residues responsible for the catalytic activity of rRHA-P, which could be further mutagenized to fine-tune rRHA-P catalytic efficiency on selected substrates.

In addition, two different potential scaffolds from bacteria (OMVs) and from an eukaryotic cell line (EVs) were isolated and characterized. Both systems resulted to be appealing either for enzyme immobilization or for drug-delivery strategies. In particular, OMVs isolated from *N. sp. PP1Y* were characterized by a peculiar biochemical composition, which showed some differences with the originating whole cells. EVs isolated from human macrophages resulted to have differential effects on inflammation activation, and their potential as a valid alternative to bacterial OMVs for the development of novel delivery Biosystems is discussed.



# ABBREVIATIONS

---

$\alpha$ -RHA =  $\alpha$ -L-rhamnosidase  
ABS = absorbance  
AFM = atomic force microscopy  
BSA = bovin serum albumin  
DLS = dynamic light scattering  
DMEM = Dulbecco modified Eagle's medium  
DMSO = dimethyl sulfoxide  
EtOH = ethanol  
EVs = extracellular vesicles  
GC-MS = gas chromatography – mass spectrometry  
GFP = green fluorescent protein  
GHs = glycosyl hydrolases  
GTs = glycosyl transferases  
IPTG = isopropyl  $\beta$ -D-1-thiogalactopyranoside  
LB = Luria Bertani  
LC-MS = liquid chromatography – mass spectrometry  
LPS = lipopolysaccharide  
MOPS = morpholinopropanesulphonic acid  
MPs = microparticles  
MUFA = monounsaturated fatty acid  
NTA = nano tracking particles analysis  
OA = oleic acid  
OD = optical density  
OM = outer membrane  
OMPs = outer membrane proteins  
OMVs = outer membrane vesicles  
ORF = open reading frame  
PA = palmitic acid  
PAHs = polycyclic aromatic hydrocarbons  
PBS = phosphate sulphate buffer  
PLs = phospholipids  
pNPR = para-nitrophenyl rhamnopyranoside  
ppb = parts per billion  
PPMM = potassium phosphate minimal medium  
PUFA = polyunsaturated fatty acid  
RT = room temperature  
SDS = sodium dodecyl sulphate  
SEM = scanning electron microscopy  
SFA = saturated fatty acid  
TLC = thin layer chromatography  
TLR4 = Toll-like receptor 4  
UFA = unsaturated fatty acid  
VSMC = vascular smooth muscle cells



---

# **CHAPTER I**

## **INTRODUCTION**

---



# CHAPTER I

## INTRODUCTION

### 1.1 Biocatalysis and glycosidases

Biocatalysis represents nowadays a versatile and valuable tool for industrial biotechnologies. The use of enzymes as biocatalysts gives invaluable advantages over conventional chemical technologies, for achieving high reaction selectivity, higher reaction rate, improved product purity, and a significant decrease in chemical waste generation. More in detail, in the fine chemical and pharmaceutical industries several advantages can be obtained from the use of biocatalytic processes, such as:

- reduction of processing steps (improved productivity and lower costs);
- transfer of processes from organic solvents to water (lower emissions, saving on raw materials and waste treatment);
- use of eco-friendly mild reaction conditions (avoiding very high or very low temperatures, and therefore heating/refrigeration costs).

Biocatalysts can be performed either with whole cells or purified enzymes, in solution or immobilized.

Glycosidases are a class of enzymes particularly suited for biotechnological applications. These enzymes catalyse the hydrolysis of the glycosidic linkage, leading to the formation of a sugar hemiacetal or hemiketal and the corresponding free aglycon [1] (Fig. 1).

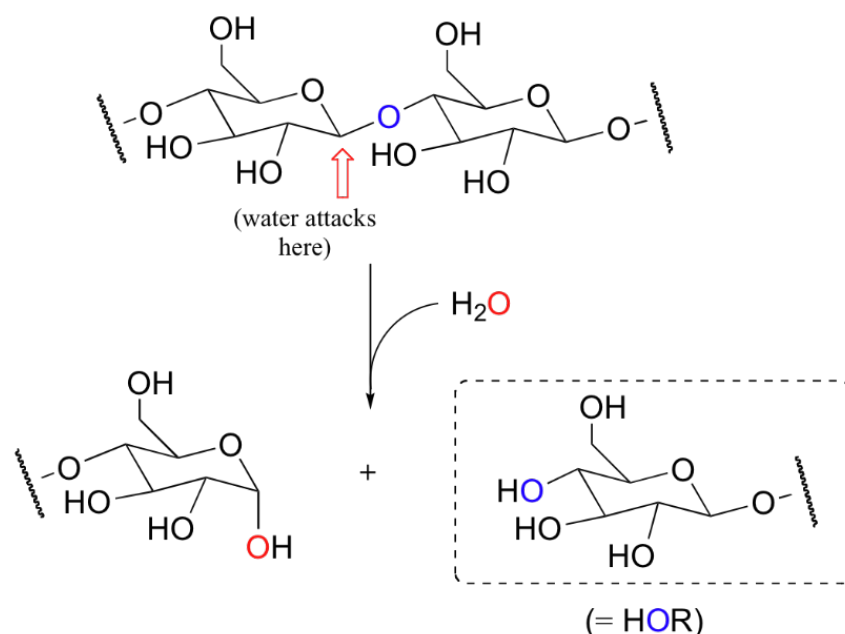


**Figure 1.** Glycosidases reaction mechanism.

Glycosidases (GH) are present in almost all living organisms [2] where they play different roles. Based on the amino acid sequence and folding and the diversity of the reactions catalysed, glycosidases have been classified in many different ways.

Recently, a new type of classification was proposed based on the amino acid similarity within the proteins; this classification is available in the Carbohydrate-Active Enzymes database (CAZy - <http://www.cazy.org/>) [2] and provides a direct relationship between sequence and folding similarities, which can be found in 130 amino acid sequence-based families. In general, GHs belonging to the subfamilies of the same family share a common ancestor, a similar 3D structure and are characterized by an identical catalytic mechanism [2].

Despite all their natural functions, glycosidases are nowadays considered an attractive target for food, paper and pulp industries, as well as in organic chemistry, where glycosidases have proven to be efficient catalysts, able to hydrolyze very stable glycosidic bonds in glycoconjugates, oligo- and poly-saccharides [3]. For this reason, glycosidases have wide and documented applications in several fields of biotechnology. Classical examples of industrial application of these enzymes include detergent formulations (cellulases and amylases) for the removal of glycan spots and fading of the denim color [4] pulp and paper bleaching (xylanases) [5], conversion of lignocellulosic plant biomass into bioethanol (cellulases, glucosidases, xylanases, etc. [6], production of High Fructose Corn Syrup for soft drinks (amylases and glucoamylases) [7], fruit juice processing (pectinases) [8], and many others. Glycosidases have recently attracted the attention of many pharmaceutical industries since they are involved in many biological processes such as cell-cell or cell-virus recognition, immune responses, cell growth, and viral and parasitic infections [9].

In addition to the hydrolytic ability, GHs can also be used under appropriate conditions for the reverse reaction, thus promoting the formation of glycosidic linkages. These reactions are called transglycosylations [10] and generally require high substrate concentration. In this case, the glycosyl donor can be a monosaccharide, an oligosaccharide or an activated glycoside. This specific action of glycosidases, which work either as hydrolases or in the glycosynthetic mode [11], are of great interest for the production of functional foods and drugs, whose biological activities might be improved by either the removal or the addition of specific glycan moieties [12]. In conclusion, glycosidases are biotechnologically attractive for the preparation of structurally well-defined oligosaccharides compared to chemical processes that require instead, complex protection and deprotection steps.

Continuous progress in the study of these enzymes and the application of molecular evolution and site-directed mutagenesis for better performance, is currently improving their potential use in oligosaccharide synthesis [13].

## 1.2 $\alpha$ -L-rhamnosidases

$\alpha$ -L-Rhamnosidases ( $\alpha$ -RHAs) are a subset of GHs that have gained much attention in recent years. These enzymes catalyse the hydrolysis of a terminal L-rhamnose from a large number of natural products [14].

L- Rhamnose is widely distributed in plants as component of flavonoid glycosides, terpenyl glycosides, pigments, signalling molecules, and in cell walls as a component of complex heteropolysaccharides, such as rhamnogalacturonan and arabinogalactan-proteins [15-18]. In bacteria, L-rhamnose appears to be included in membrane rhamnolipids [19-20] and polysaccharides [21]. According to the GHs classification,  $\alpha$ -RHAs are grouped in the CAZy (carbohydrate-active enzymes) database ([www.cazy.org](http://www.cazy.org)) into four different families: GH28, GH78, GH106, and NC (non-classified).

$\alpha$ -RHAs are produced by a large number of animal tissues, plants, fungi, bacteria and bacteriophages [16], but their physiological role is still not well understood. The

hypothesis can be advanced that the role of  $\alpha$ -RHAs is linked to the broad distribution of L-rhamnose as a component in bacterial and plant cell walls, glycosides, biofilms and glycolipids [16,22].

In the last decade,  $\alpha$ -RHAs have attracted a great deal of attention due to their potential application as biocatalysts in a variety of industrial processes and in particular in the food industry [1]. Among  $\alpha$ -RHAs substrates, particularly interesting results natural flavonoids (Fig. 2), polyphenolic compounds generally characterized by a three-ring structure, which consists of two phenyl rings (A and B) and a heterocyclic ring (C). These molecules are naturally produced in plants in glycosylated forms, showing the presence of either a rutinose (6- $\alpha$ -l-rhamnosyl- $\beta$ -d-glucose) or a neohesperidoside (2- $\alpha$ -l-rhamnosyl- $\beta$ -d-glucose) disaccharidic unit bound in different positions. These molecules are intriguing due to their potential antioxidant, antitumor and anti-inflammatory properties [23-24]. In particular, naringin, hesperidin and rutin, flavanone glycosides found in grapefruit juices, lemons, sweet oranges and vegetables, have gained increasing recognition for their potential antioxidant, antitumor and anti-inflammatory properties [25-28]. In humans, endogenous  $\beta$ -glucosidases are responsible for removing in the small intestine glucose (or possibly arabinose or xylose) moiety from flavonoids thus allowing their effective absorption; these enzymes, however, are not able to cleave terminal rhamnose units, thereby limiting the bioavailability of rhamnosylated flavonoids that are further converted by the colon local microflora [29-30]. Therefore, enzymatic rhamnose removal from potentially bioactive flavonoids might be the key point to improve their intestinal absorption and their beneficial properties on human health [31-32]. In addition, the ability to hydrolyze glycosylated flavonoids has been used, in the industrial field, to mitigate the bitterness of citrus juices, which is primarily caused by naringin [33-34]. Moreover, the corresponding de-rhamnosylated compound, prunin, is endowed with antimicrobial properties [28], and shows an improved intestinal assimilation when compared to naringin. Other applications of  $\alpha$ -RHAs are gaining popularity in the oenological industry, where these enzymes are used to hydrolyze terpenyl glycosides and enhance aroma in wine, grape juices and derived beverages [35-37].

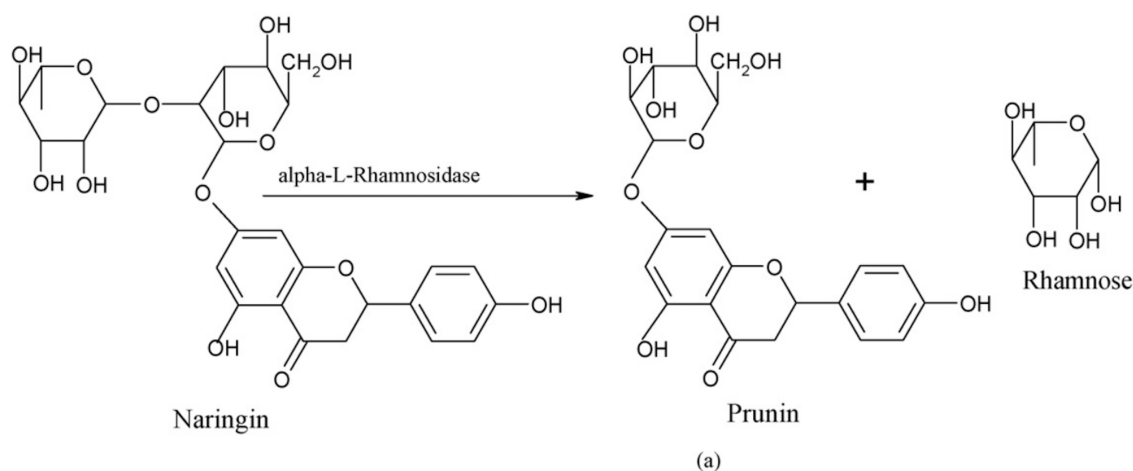


**Figure 2.** Hydrolysis of naringin to prunin by  $\alpha$ -L-rhamnosidase in the corresponding product: prunin (a) and rhamnose.

Moreover, in their glycosynthetic mode of action  $\alpha$ -L-rhamnosides can “decorate” flavonoids in fruit juices and wine, antibiotic and antitumoral drugs [38].

It is worth to note that the use of an  $\alpha$ -RHA for the synthesis of rhamnose-containing chemicals by reverse hydrolysis was recently reported, suggesting a yet unexplored potential of these class of enzymes in the chemical and pharmaceutical industry [39]. Despite their potential as industrial biocatalysts, only a limited number of bacterial rhamnosidases have been extensively studied and characterized [40-44]. In fact, commercial preparations of  $\alpha$ -RHAs, naringinases and hesperidinases available and currently used in oenology, are all isolated from fungal sources (*Aspergillus niger* and *Penicillium decumbens*) [45-47].

Different features of these two families of enzymes, especially pH optimum, suggest different applications for fungal and bacterial enzymes. As an example, fungal enzymes show more acidic pH optima compared to bacterial counterparts, for which neutral and alkaline optimal pH values have generally been reported [48-49]. This feature suggested that bacterial  $\alpha$ -RHAs might be considered, for example, an alternative source of biocatalysts to use in basic conditions for the biotransformation of flavonoids such as naringin or hesperidin, whose solubility strongly increases at higher pH value [48-49]. Most importantly, few attempts have been described so far to engineer bacterial  $\alpha$ -RHAs to unravel the molecular details concerning their catalytic mechanism, to modify their substrate specificity or to improve their catalytic efficiency towards different substrates [50]. A major stumbling is represented by the limited number of  $\alpha$ -RHAs crystal structures currently available, with a consequent lack of structural data of these enzymes. To date, only two bacterial  $\alpha$ -RHAs belonging to the GH106 family were described, one from *Sphingomonas paucimobilis* FP2001 [51] and the  $\alpha$ -RHA BT0986 from *Bacteroides thetaiotaomicron* [52]. Moreover, only five crystal structures of bacterial  $\alpha$ -RHA have been solved so far, which include the putative  $\alpha$ -RHA BT1001 from *Bacteroides thetaiotaomicron* VPI-5482 [53], the  $\alpha$ -RHA B (BsRhaB) from *Bacillus* sp. GL1[54],  $\alpha$ -RHA (SaRha78A) from *Streptomyces avermitilis* [55], and  $\alpha$ -RHA (KoRha) from *Klebsiella oxytoca* [56]. All these enzymes belong to the GH78 group. Only one example of a GH106  $\alpha$ -RHAs crystal structure was recently reported and in the  $\alpha$ -RHA BT096 expressed by *Bacteroides thetaiotaomicron* [52].

Therefore, it is evident that bacterial  $\alpha$ -RHAs represent a yet unexplored reservoir of potential biocatalysts for which more functional and structural data are required.

### 1.3 Enzyme immobilization

The use of enzymes in industrial applications has been limited by several factors, mainly the high cost of the enzymes, their instability, and availability in small amounts. In addition, enzymes are soluble in aqueous media and it is difficult and expensive to recover them from reactor effluents at the end of the catalytic process. These limits the use of soluble enzymes to batch operations, followed by disposal of the spent enzyme-containing solvent [57]. Over the last few decades, intense research in the area of enzyme technology has provided many approaches that facilitate their practical applications. Among these, technological developments in the field of immobilized biocatalysts resulted to be a very powerful tool to improve almost all enzyme properties, such as stability, activity, specificity selectivity, and enzyme inhibition [58]. Enzyme immobilization offers the possibility of a wider and more economical exploitation of biocatalysts in industry, waste treatment, drug delivery, and bioprocess monitoring devices, like biosensors [57]. Besides the application in industrial processes, immobilization techniques could be the basis for the developing a large

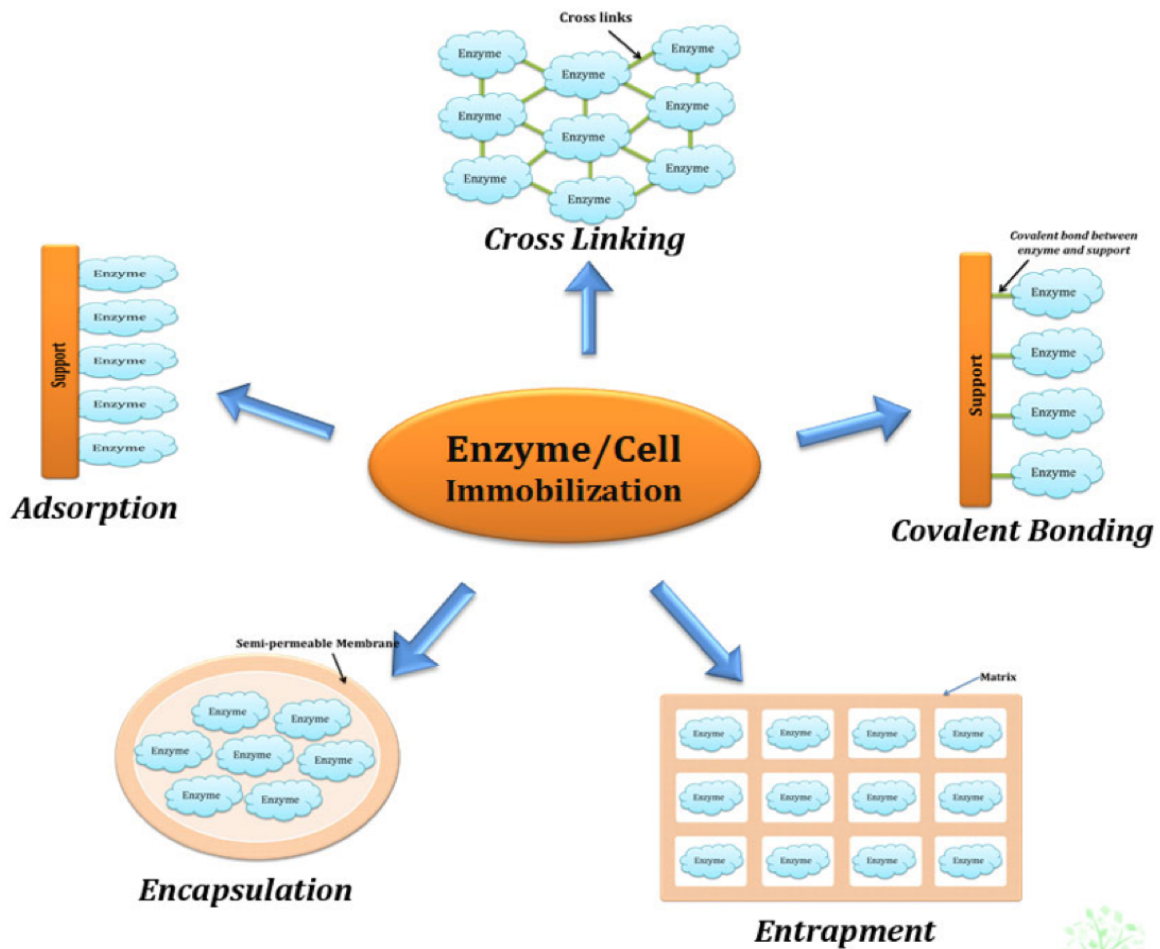
number of biotechnological devices with applications in diagnostics and biosensors [59].

Immobilization means associating the biocatalysts with an insoluble matrix, so that it can be retained in a proper reactor geometry for its economic reuse under stabilized conditions (Fig.3) [60]. Immobilization helps in the development of continuous processes allowing more economic organization of the operations, automation, and investment/capacity ratio. Immobilized biocatalysts offer several other advantages such as, for example, the availability of the product in greater purity. Purity of the product is crucial, for example, in food processing and pharmaceutical industry since contamination could cause serious toxicological, sensory, or immunological problems [60].

Another major advantage includes greater control over enzymatic reaction, as well as high volumetric productivity, with lower residence time, which are of great significance in the food industry [57]. Moreover, compared to their free forms, immobilized enzymes are generally more stable and easier to handle [57]. In addition, reaction products are not contaminated with the enzyme (especially useful in the food and pharmaceutical industries), and in the case of proteases, the rate of the autolysis process can be dramatically reduced upon immobilization [61].

To date, more than one hundred techniques to immobilize enzymes have been developed, such as entrapment, adsorption, ionic binding, and disulphide bonds formation. Enzymes can be attached to the support by interactions, ranging from reversible physical adsorption and ionic linkages to stable covalent bonds (Fig.3) [62]. Ideal support properties include physical resistance to compression, hydrophilicity, inertness toward enzymes ease of derivatization, biocompatibility, resistance to microbial attack, and availability at low cost [62-64]. Supports can be classified as inorganic and organic according to their chemical composition, and organic supports can be subdivided into natural and synthetic polymers [65]. The most common are synthetic polymers, biopolymers (cellulose, starch, agarose, carragenans, and chitosan), inorganic supports (alumina, silica, zeolites), hydrogels and so on.

In this framework, nanobiotechnology is gaining much attention from the scientific community, and "Nanobiocatalysis" is one direct application of this growing field [66]. In early approaches to nanobiocatalysis, enzymes were immobilized on various nanostructured materials using conventional approaches, such as simple adsorption and covalent attachment. This approach was used by immobilizing enzymes onto nanostructured materials, such as nanoporous materials and magnetic nanoparticles [67]. Nanosized particles of noble metals, for example, were used due to their attractive electronic, optical, and thermal properties as well as catalytic properties and potential applications in the fields of physics, chemistry, biology, medicine, and material science [68]. Recently, new immobilization studies were performed by using, as immobilization systems, artificial or natural lipid bilayers of biological membranes. Lipid vesicles (liposomes) have been recently used for this purpose, despite the fact that the long-term stability of liposomes may be problematic [69]. Lipid vesicles, generally, are not thermodynamically stable and do not assemble 'spontaneously' (without input of external energy); they are only kinetically stable, and their physical properties may depend on how and under which conditions lipid vesicles have been prepared. To overcome all these limitations, a recent interest for the immobilization of enzymes and biocatalysts in general focuses on the isolation of bilayer membranes from both prokaryotic and eukaryotic sources.



<http://www.easybiologyclass.com>

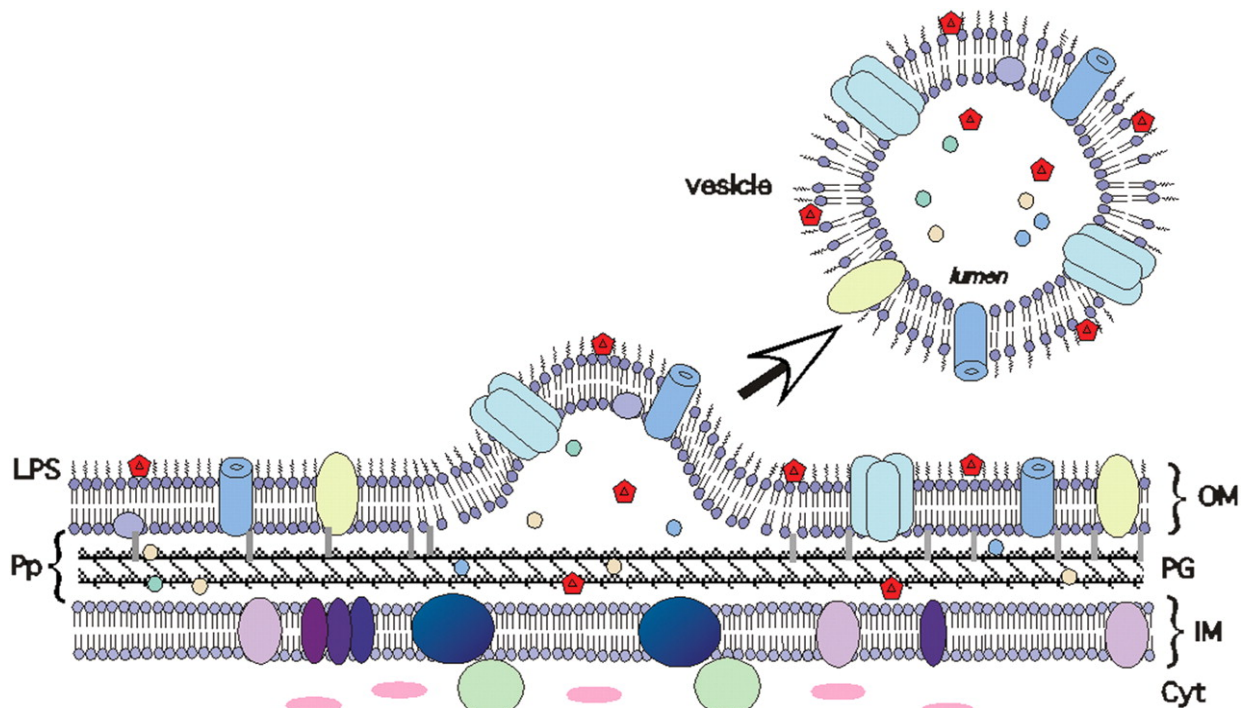
**Figure 3.** Enzyme immobilization examples.

In this context, extracellular nanostructures, such as bacterial Outer Membrane Vesicles (OMVs) and eukaryotic Extracellular Vesicles (EVs), proteoliposomes of 20-2000 nm diameter, have been recently investigated as biotechnological scaffolds alternative to liposomes [70-71].

### 1.3.1 Outer Membrane Vesicles

Outer membrane vesicles (OMVs) are nanoscale proteoliposomes of 20-200 nm diameter, naturally derived from the surface of some Gram-negative and Gram-positive bacteria as part of their natural growth cycle. In Gram-negative bacteria, OMVs are initially formed as a bulge arising from the outer membrane (Fig 4) [70]. Thus, they are generally surrounded by a single phospholipidic bilayer derived from the outer membrane and are primarily composed of lipopolysaccharides, membrane phospholipids (PLs) and outer membrane proteins (OMPs) [70-73]. In addition, a portion of periplasmic space is often enclosed in these vesicles, which includes proteins, toxins or effectors that are delivered to the environment to accomplish several biological functions (Fig 4).

The production of OMVs has been reported from a large number of Gram-negative bacteria, [73-75] in a variety of environments, including planktonic cultures, fresh and salt water, biofilms, inside eukaryotic cells and within mammalian hosts [76-78]. Among OMV-producing Gram-negative bacteria, pathogenic microorganisms such as *Escherichia coli*, *Helicobacter pylori*, *Pseudomonas aeruginosa*, have been so far major targets for OMV studies [79-81]. The main interest towards pathogenic-OMVs was driven from their cargo proteins, identified as major virulence factors or agents of inflammatory responses. Some examples include *E. coli* cytolysin A (ClyA), *E. coli* heat labile enterotoxin (LT) [82]. However, OMVs functions are far from being limited to pathogenicity, and the role of these carrier structures has proven to be far more complex than what initially supposed.



<http://genesdev.cshlp.org/content/19/22/2645/F1.large.jpg>

**Figure 4.** OMVs example. LPS: lipopolysaccharide; OM: outer membrane; Pp: periplasm; Cyt: cytosol; IM: inner membrane.

Indeed, it is currently well known that OMVs are also involved in interspecies communication and competition, biofilm formation, DNA lateral gene transfer, antibiotic resistance and nutrient acquisition [79,83-87]. This system allows signalling proteins

or effectors to be delivered, even over great distances, at high concentration in close proximity of an acceptor site. Ultimately, the binding specificity between surface-exposed bacterial adhesins and environmental ligands or receptors guarantees a high target specificity. Several hypotheses on OMVs biogenesis have been proposed, although they are not fully comprehensive and often restricted to a few species of bacteria [74-75, 86, 88]. However, OMV production occurs at a constitutive level for a wide variety of bacteria, suggesting that this is a highly conserved process [74-75, 86]. Furthermore, vesiculation levels can be altered by factors such as temperature, nutrient availability, oxidation, quorum sensing and envelope-targeting antibiotics [86-87, 89]. So far, only few examples of OMVs isolated from non-pathogen gram-negative bacteria have been reported. Some examples of non-pathogenic, environmental bacteria from which OMVs have been isolated include the halophilic marine bacterium *Novosphingobium pentaromativorans* US6-1, and the soil bacterium *Pseudomonas putida* K2440 [90-91]. These environmental OMV-producing bacteria are endowed with the ability to use various aromatic compounds, including polycyclic aromatic hydrocarbons (PAHs) and several other pollutants, as major carbon and energy sources. Little is still known about the vesicles produced by these organisms, however two main roles of these OMVs have been suggested. The first one involves the use of OMVs as carriers of hydrolytic enzymes, such as proteases and glycosidases, which play a role in the acquisition of nutrients from the surrounding environment [18]. This system would improve nutrient acquisition and thus bacterial survival, particularly in starving growth conditions [71, 90- 93]. The second hypothesis suggests that these structures might be involved in *i*) the formation of the biofilm matrix [20], *ii*) the onset and maintaining of biofilm communities [71, 83, 88, 93] and *iii*) the antibiotic resistance expressed by the biofilm bacterial community. Beyond a role in biofilm onset, OMVs might mediate interactions within and external to the biofilm through OMV-associated quorum-signalling molecules [88, 93-94].

In recent years, a great deal of attention was also devoted to the study of OMVs for their potential use in biotechnological industry. Drug delivery, enzyme immobilization and construction of innovative biosensors are some of the major research fields of interest. Bacterial OMVs can be foreseen as platforms for the immobilization of proteins and enzymatic complexes and be employed as carriers for drugs and molecules, allowing these latter to be conveyed to a highly specific target site and in a protected environment [95-98]. By taking advantage of the unique feature to embed outer membrane proteins into OMVs, a wide range of functional proteins such as green fluorescence protein (GFP) and  $\beta$ -lactamase, have been genetically tethered to the surface of a hyper-vesiculating *Escherichia coli* strain- therefore to the corresponding OMVs- using the virulence factor cytotoxin ClyA as the surface anchor [95]. Unlike complex enzyme assembly onto liposomes or polymerosomes, these results indicate the feasibility of designing OMVs as synthetic nanoreactors, using only standard molecular biology techniques. This approach has been recently used for example, to immobilize three glycosidase activities on engineered *E. coli* OMVs [98]. A trivalent protein scaffold was genetically tethered onto the OMVs to enable the positional specific recruitment of three different cellulases. This work reported that the assembled enzyme complex, not only retained full activity, but also hydrolyzed cellulose 23-fold faster than non-complexed enzyme [98]. The biotechnological use of OMVs isolated from gram-negative bacteria, for example as drug delivery systems, is currently limited, among others, by the presence in their outer membrane of the immunogenic LPS. Several studies have in fact demonstrated how LPS is sensed by the Toll-like receptor 4 (TLR4) complex, triggering a pro-inflammatory response and playing an important

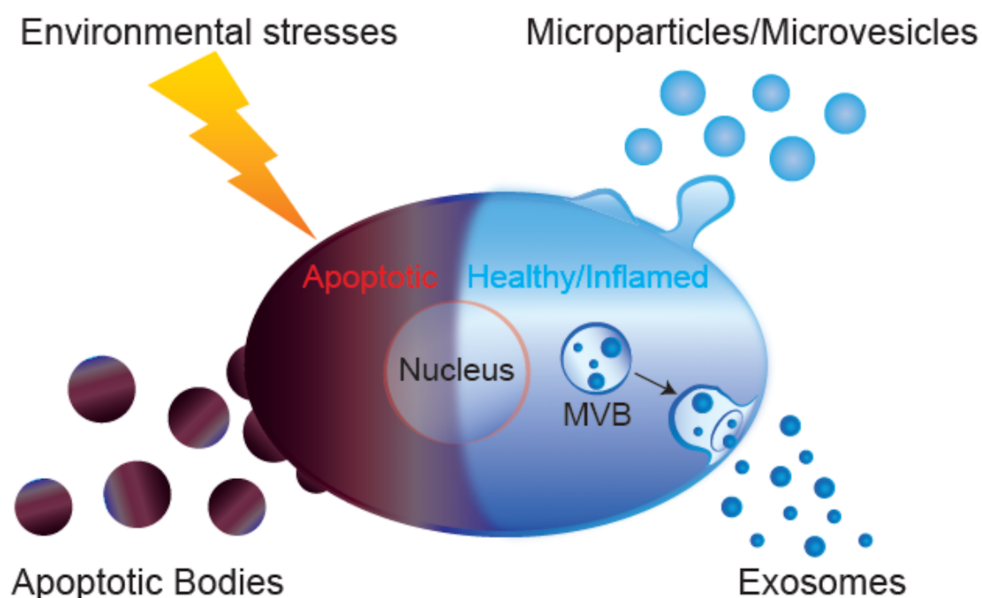
role in septic shock [99]. As a consequence, much interest is currently devoted to vesiculating non-pathogen strains that do not produce LPS.

### 1.3.2 Extracellular Vesicles

Extracellular vesicles (EVs) are membrane-derived particles with a diameter size ranging from 30 nm to 2,000 nm, surrounded by a (phospho)lipid bilayer and released by cells in the human body [100]. EVs are classified, based on their cellular origin, biological function or biogenesis, in three main groups: exosomes, microvesicles and apoptotic bodies [101]. Distinct processes responsible for vesicle release from cells have been identified; in particular, exosomes are derived from the multivesicular endosomal cell compartment [71, 101-103] whereas EVs originate by direct budding from the cell plasma membrane [102-106]. Both extracellular vesicle types contain cytoplasmic proteins, certain lipid raft-interacting proteins and RNAs but, owing to their highly regulated biogenesis, exosomes typically accommodate some additional defined components [71]. Apoptotic bodies represent another type of membrane-limited vesicle. These are larger than exosomes and EVs [108] and are formed exclusively during the late stage of apoptosis (Fig. 5).

Within the past decade, extracellular vesicles have gained attention as important mediators of intercellular communication [108].

Shedding of EVs is considered to be a physiological phenomenon that leads cell activation and growth. Many stimuli have been shown to increase vesicle secretion, including hypoxia, oxidative stress and inflammation [109-111]. These evidences suggested that EVs are implicated in physiological responses such as immune surveillance [112], blood coagulation [113], tissue repair [114] or in pathological disorders, for example cancer [115] and cardiovascular diseases [116].



Yamamoto S, Azuma E, Muramatsu M, Hamashima T, Ishii Y, Sasahara M. (2016) Significance of extracellular vesicles: pathological roles in disease. *Cell Struct Funct*

**Figure 5.** EVs classification and origin.

EVs could also carry and deliver multiple information through lipids, proteins or nucleic acids transfer. Proteins sorting into shedding vesicles is selective; specific proteins may be included or excluded from membrane EVs, leading to the expression of proteins arrays that differ from those present on the surface of the cells from which they originated [117-118]. It is also possible that EVs may interact with specific target cells after their release. For example, EVs shed from platelets interact with macrophages and endothelial cells but not with neutrophils, [119] whereas EVs from neutrophils interact with platelets, macrophages, and dendritic cells [120-121]. Due to their specific targeting, the current biotechnological interest in EVs derives from their great potential as a new way, for innovative therapies, to deliver drugs to specific target cells [115]. Thus, EVs can be engineered to over-express different therapeutic proteins, mRNA or miRNA - by driving their synthesis from the relevant EV producing cells [122]. Indeed, EVs possess a lot of peculiarities that give them ideal drug-delivery features. More specifically, EVs are stable within the body. EVs do not induce (ii) tumour generation [123], or (iii) immune rejection after allogenic administration [124]. In addition, EVs carrying proteins and/or nucleic acids can be easily modulated to confer them specific pharmacological functions [125].

EVs have been also studied, in particular from macrophages, for the identification of new potential therapeutic targets associated to inflammatory response and for the development of a new drug delivery strategy. All these features suggest that EVs, as well as bacterial OMVs, could be used for biotechnological purposes. The interest in using eukaryotic EVs rather than OMVs, lies in their specific drug delivery application. Indeed, the fact that EVs derives from eukaryotic cells, could make these latter less immunogenic than OMVs. Moreover, their composition can be physiologically determined or driven by exogenous modulations either on their origin cells or directly on purified EVs populations [126]. Another advantage in using EVs as novel natural bio-carriers, lies in their specific cell-targeting, which has already been described in literature [127-129]. For this reason, EVs appear to be a suitable alternative to traditional delivery systems currently in development, limiting inflammation processes and improving target-specific delivery.

#### **1.4 *Novosphingobium* sp. PP1Y: a novel microbial source of OMVs and glycosidases**

In the laboratory in which my PhD project has been developed, a novel gram-negative strain has been isolated and characterized, named *Novosphingobium* sp. PP1Y [99,120]. The microorganism was isolated from surface waters of a small dock bay in the harbour of Pozzuoli which is used for the storage of small boats and is characterized by a severe pollution of the water by mono-, poly- and heterocyclic aromatic hydrocarbons (Fig. 6)

The microbiological analysis of the bacterium indicated that the microorganism belongs to the order of *Sphingomonadales*, a class of bacteria whose outer membrane is characterized by the presence of glycosphingolipids, instead of the more common lipopolysaccharides.

This peculiarity makes the surface of their cells more hydrophobic than those of the other Gram-negative strains and has probably contributed to the ability of these microorganisms to degrade mono- and polycyclic aromatic hydrocarbons (PAHs). *N. sp.* PP1Y, however, shows different characteristics if compared to other members of the order, as it appears not only to be able to grow using, as the sole source of carbon and energy, a wide range of mono-and polycyclic aromatic substrates such as pyrene,

naphthalene and phenanthrene, but also to have evolved an effective adaptation to the growth on complex mixtures of aromatic molecules dissolved in non-polar phases such as diesel and gasoline.

Due to its peculiar natural environment and metabolism, this strain might be considered a valuable reservoir of novel biotechnological tools.

In particular, *Sphingomonadales* show the presence of a great abundance of both glycosyl hydrolases (GHs) and glycosyltransferases (GTs), activities that are probably involved in the biosynthesis of complex extracellular polysaccharides and microbial biofilms [130].

The interest for *Novosphingobium* sp. PP1Y carbohydrate-active enzymes has grown as the sequencing and annotation of the whole genome, recently completed, has revealed peculiar biochemical and biotechnological properties, namely some metabolic pathways specifically involved in the degradation of several aromatic hydrocarbons, and the resistance to toxic compounds. A great number of genes encoding for both GHs (53 orfs) and GTs (57 orfs) were identified in this microorganism [99]. In particular, the number of GHs is remarkable when compared, respectively, to the 16 GHs and the 32 GHs of the closely related strains of *Sphingomonas wittichii* and *Sphingobium chlorophenolicum*. The 53 GHs of strain PP1Y are distributed among 27 different families. The most represented families are GH3, GH13 and GH23 with 9, 5 and 9 members respectively. Among these, there are 8 genes encoding for  $\alpha$ -RHAs. A novel  $\alpha$ -RHA activity in *N. sp.* PP1Y crude extract was recently described, which was used, among others, for bioconversion experiments on substrates such as naringin, rutin and hesperidin [131].

Strain PP1Y shows a very high propensity to adopt the sessile phenotype and efficiently colonise several types of hydrophobic surfaces including water/oil interfaces (Fig. 7) [99]. In addition to these features, strain PP1Y has a surprisingly high tolerance to diesel oil, which allows its growth in biphasic diesel oil/water cultures containing more oil than water. To the best of our knowledge, such behaviour has never been reported for a *Sphingomonas*. *Sphingomonas* sp. Ant 17, the sole Sphingomonads known to use fuels as a sole carbon and energy source, has been reported to grow in 1:1000 (v/v) fuel/water biphasic systems [131]. Several details suggested also the production of OMVs in strain PP1Y, which might play a potential role in biodegradation and nutrient supply in natural habitats, as well as being involved in cell-cell communication and genetic transfer. *N. sp.* PP1Y can grow as either planktonic free cells or sessile-aggregated macroscopic “flocks” of 1-10 mm long, with a composition in fatty acids similar to the cell membrane (Izzo V., unpublished results); noteworthy, this behaviour has already been described for other *Sphingomonads*, which show the so-called “planktonic/sessile dimorphism” [132-133]. Most importantly, cell free supernatants from cultures of *N. sp.* PP1Y were able to effectively stabilize paraffin drops, obtained by shaking a paraffin/water biphasic system, which remained stable for more than 1 week. These last data in particular suggested that strain PP1Y produced an extracellular emulsifier, and it was shown that secretion was dependent upon the presence of neither aromatic hydrocarbon nor an oil phase in the growth medium [133]. Interestingly, culture supernatants showed a low total carbohydrate level and no detectable polysaccharides [134].

Thus, *N. sp.* PP1Y might be particularly appealing for OMVs isolation and characterization in order to shed light on vesiculation mechanisms related to environment adaptation. Noteworthy, the lack of LPS on the membrane surface of strain PP1Y, and the availability for this microorganism of a completely sequenced and

annotated genome [134], are extremely appealing to develop a novel molecular tool for drug delivery systems and enzyme immobilization. During my PhD work, specific aspects of the biotechnological potential of *N. sp. PP1Y* were investigated, focusing the attention on the use of this microorganism to isolate and characterize novel examples of *i*)  $\alpha$ -RHA activities and *ii*) OMVs for industrial applications and biotechnological purposes.



**Figure 6.** An overview of the harbour of Pozzuoli, where *Novosphingobium sp. PP1Y* was isolated.

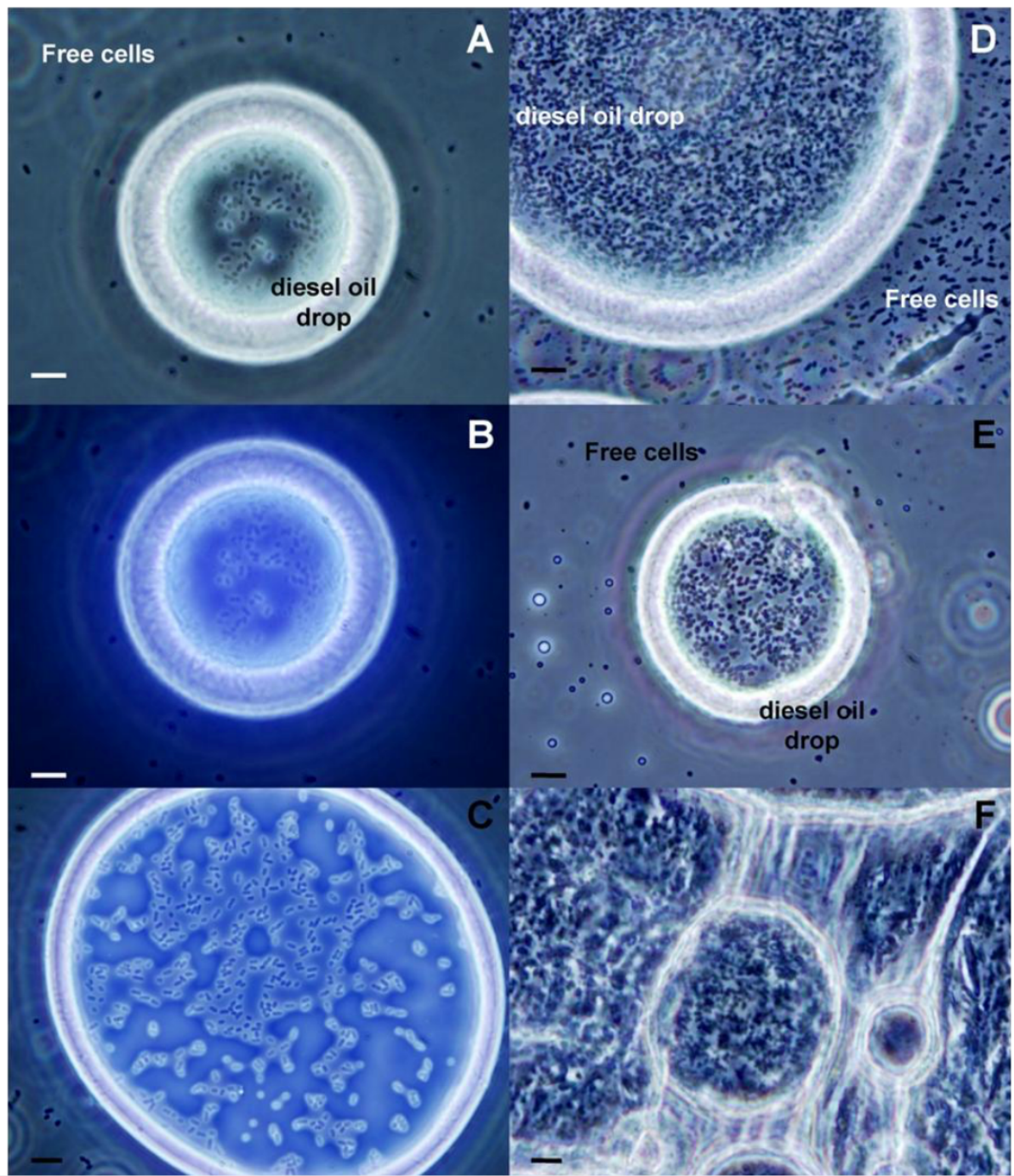


**Figure 7.** Phase contrast microscopy analysis of coated diesel oil drops isolated from a culture of *Novosphingobium* sp. PP1Y grown using diesel oil as sole carbon and energy source. A) and B) Coated diesel oil drop after 2 days of incubation observed using visible light only or UV/visible light, respectively. C) Coated diesel oil drop after 2 days of incubation observed using UV/visible light. D) and E) Coated diesel oil drops after 10 days of incubation. F) Super-aggregates of coated drops. Bar = 10  $\mu$ m.



# AIMS OF THE THESIS

---

Both  $\alpha$ -L-rhamnosidases and extracellular vesicles are elements of great interest for the development and implementation of novel biocatalysis processes of biotechnological importance. A great deal of attention is being devoted by the biotech community to the use of these two systems for applications in the food and pharmaceutical industries. Main aim of this PhD project has been to characterize the biotechnological potential of a bacterial  $\alpha$ -L-rhamnosidase isolated from *Novosphingobium* sp. PP1Y, and of novel examples of vesicles, Outer Membrane Vesicles (OMVs) isolated from the same microorganism and Extracellular Vesicles (EVs) from macrophages.

This general aim has been pursued through the following activities:

1. Purification and characterization of a novel  $\alpha$ -L-rhamnosidases from *N. sp.* PP1Y;
- 2a. Isolation, purification and characterization of OMVs from *N. sp.* PP1Y;
- 2b. Isolation, purification and characterization of Extracellular Vesicles (EVs) from human macrophages.

Tasks 1 and 2a were performed in the laboratory of Professor Alberto Di Donato, university of Naples, Federico II. The 2b task was developed, starting September 2016 through March 2017, at INSERM (University of Angers, France) in the laboratories of the “Stress oxidant et pathologies métaboliques U1063” of Prof. Ramarason Andriantsitohaina.



---

# **CHAPTER II**

## **MATERIALS AND METHODS**

---



## CHAPTER II

### MATERIALS AND METHODS

---

#### 2.1 Generals

*N. sp.* PP1Y was isolated from polluted seawater in the harbor of Pozzuoli (Naples, Italy) as already described [1]. Bacterial growth was followed by measuring the optical density at 600 nm (OD/mL, from now on referred to as OD<sub>600</sub>). Nanosize analysis for the determination of OMVs size was performed by IZON technical service using qNANO GOLD (<http://www.izon.com>). Protein quantification was performed using BCA kit assay purchased from Thermo Scientific.

Protein concentration was measured using the Bio-Rad Protein System [52] using bovine serum albumin (BSA) as standard. Polyacrylamide gel electrophoresis was carried out using standard techniques [53]. SDS-PAGE 15% Tris-glycine gels were run under denaturing conditions and proteins were stained with Coomassie brilliant blue G-250. "Wide range" (200–6.5 kDa) molecular weight standard was from Sigma (ColorBurst™ Electrophoresis Marker).

#### 2.2 Cloning of orf PP1YRS05470 and construction of the pET22b(+)/rha-p expression vector.

Genomic DNA was extracted from a 50mL saturated culture of *N. sp.* PP1Y as described elsewhere [130]. OrfPP1Y RS05470 coding for the  $\alpha$ -RHA activity was amplified in two contiguous fragments, owing to the considerable length of the orf (3441 bp). The first fragment, named rha-up (1816 bp), was amplified using an internal downstream primer, RHA-Intdw (5'-AGGCGGCCATGGGAATGT-3'), which included an internal NcoI site already present in orfPP1Y RS05470, and an upstream primer, RHA-up (5'-GGGAATTCCATATGCCGCGCCTTTCGCT-3'), designed to add a NdeI restriction site at 5' of orf PP1Y RS05470. The second half to the gene, named rha-dw (1625 bp), was amplified using the upstream primer RHA-Intup (5'-ACATTCCCATGGCCGCCT-3'), complementary to RHA-Intdw, and the downstream primer RHA-dw (5'-AAAACCGAGCTCTCAATGCCCGCCCGTG-3') that was intended to incorporate a SacI restriction site downstream of the amplified orf. The amplified fragments, rha-up and rha-dw, were purified from agarose gel, digested, respectively, with NdeI/NcoI and NcoI/SacI, and individually cloned in pET22b(+) vector previously cut with the same enzymes. Ligated vectors were used to transform *E. coli*, strain Top10 competent cells. The resulting recombinant plasmids, named pET22b(+)/rha-up and pET22b(+)/rha-dw, were verified by DNA sequencing. Next, the construction of complete rha-p gene in pET22b(+) was performed. First, both pET22b(+)/rha-dw and pET22b(+)/rha-up were digested with NcoI/SacI restriction endonucleases to obtain, respectively, fragment rha-dw and linearized pET22b(+)/rha-up. Digestion products were purified from agarose gel electrophoresis, eluted and ligated. Ligation products were used to transform *E. coli* Top10 competent cells and the resulting recombinant plasmid, named pET22b(+)/rha-p was verified by DNA sequencing.

#### 2.3 Construction of the pET22b(+)/rha-his expression vector.

To obtain the pET22b(+)/rha-his expression vector, which expresses a recombinant RHA-P fused to a C-terminus His-tag, a single point mutagenesis (TGA to CGA) on the STOP codon of the coding sequence of RHA-P, previously cloned, was performed. In this way, an arginine residue was inserted and the coding sequence was extended on the pET22b(+) plasmid, thus including a linker sequence and the coding region for

a 6-His-tag domain at 3' of the gene. The plasmid pET22b(+)/rha-dw, bearing only the C-terminus 1,625 bp-long fragment of the gene and already present in our laboratory, was chosen to perform the mutagenesis, in order to use a smaller plasmid for the amplification procedure. The mutagenesis experiment was done using specific designed complementary primers named RHAmutUP (5'ACCACGGGCGGGCATCGAGCCGTCGACAAGC3') and RHAmutDW (5'GCTTGTGCGACGGCTCGATGCCCGCCCGTGGT3') containing the desired mutated codon. Quickchange II site directed mutagenesis kit (Agilent technologies) was used for this experiment, following the manufacturer protocol. Mutagenesis was then verified by DNA sequencing. A fragment containing the mutated codon was identified between the single restriction sites AatII - NotI. The cassette was excised from the pET22b(+)/rha-dw plasmid, purified from agarose gel and subcloned in a pET22b(+)/rha-p total vector, by digesting both mutagenized fragment and pET22b(+)/rha-p with AatII / NotI restriction endonucleases. Digestion products were separated by agarose gel electrophoresis, purified and ligated. Ligation products were used to transform *E. coli* Top10 competent cells and the resulting recombinant plasmid, named pET22b(+)/rha-his was verified by DNA sequencing.

#### **2.4 Mutagenesis of the pET22b(+)/rha-his expression vector and construction of rRHA-Phis single mutants.**

A mutagenesis cassette containing all the residues to modify was identified in pET22b(+)/rha-his sequence, between the single restriction sites AatII and KpnI. The mutagenesis cassette was excised from pET22b(+)/rha-his vector, purified from agarose gel and ligated into a pGEM-3Z vector digested using the same enzymes. Ligation products were used to transform *E. coli* Top10 competent cells and the resulting recombinant plasmid, named pGEM-3Z/rha, was verified by DNA sequencing. The plasmid pGEM-3Z/rha was then used in five different mutagenesis experiments where for the identified conserved aminoacids D503, E506, D552, E644, and D763 were mutated into alanine codons. For D503, D552 and D763 the codon GAT was converted in GTC, for E506 the codon GAG was converted in GCG and for E644 the codon GAA was converted in GCA. Therefore, five couple of specific mutagenic primers were designed and the QuikChange II Site-Directed Mutagenesis Kit (Agilent Technologies) was used on pGEM-3Z/rha in five separate reactions, following the manufacturer protocol. Mutagenized fragments in pGEM-3Z/rha vector were then individually subcloned into pET22b(+)/rha-his vector using AatII/KpnI restriction endonucleases. Mutagenized clones were verified by DNA sequencing and named: pET22b(+)/D503A, pET22b(+)/E506A, pET22b(+)/D552A, pET22b(+)/E644A, and pET22b(+)/D763A (pET22b(+)/D-EXXXXA).

**2.5 rRHA-P recombinant expression.** Protein expression was carried out in *E. coli* BL21(DE3) strain transformed with pET22b(+)/rha-p plasmid. All the media described in this paragraph contained 100 g/mL of ampicillin.

##### -Analytical expression:

*E. coli* BL21(DE3) competent cells transformed with plasmid pET22b (+)/rha-p were inoculated in a sterile 50mL Falcon tube containing 12.5 mL of either LB or LB containing a final concentration of 0.5 M NaCl (LB-N). Cells were grown under constant shaking at 37 ° C up to 0.6–0.7 OD<sub>600</sub>. This preinoculum was diluted 1:100 in 12.5 mL of either one of the four following media: LB, LB-N, LB supplemented with 1 mM of both betaine and sorbitol (LB-BS), or LB containing a final concentration of 0.5 M NaCl and 1 mM of both betaine and sorbitol (LB-NBS). Cells were grown under constant

shaking at 37°C up to 0.7–0.8 OD<sub>600</sub>. rRHA-P recombinant expression was induced with 0.1 mM IPTG at either 23 °C or 37 °C; growth was continued in constant shaking for 3h. Cells were collected by centrifugation (5,524×g for 15min at 4°C) and suspended in 25 mM MOPS pH 6.9 at a final concentration of 14 OD<sub>600</sub>. Cells were disrupted by sonication (12 times for a 1-min cycle, on ice) and an aliquot of each lysate was centrifuged at 22,100 × g for 10 min at 4 °C. Both soluble and insoluble fractions were analyzed by SDS- PAGE. The soluble fraction was assayed for the presence of α-RHA enzymatic activity.

-Large scale expression:

Fresh transformed cells were inoculated into 10 mL of LB-N and incubated in constant shaking at 37 °C O/N. The preinoculum was diluted 1:100 in four 2 L Erlenmeyer flasks containing each 500 mL of LB-NBS and incubated in constant shaking at 37 °C up to 0.7–0.8 OD<sub>600</sub>. Expression of the recombinant protein, named rRHA-P, was induced with 0.1mM IPTG and growth was continued for 3h at 23 °C. Cells were collected by centrifugation (5,524×g for 15min at 4 °C) and stored at –80 °C until needed.

## **2.6 rRHA-P purification.**

rRHA-P was purified following three chromatographic steps. Cell paste was suspended in 25 mM MOPS pH 6.9, 5% glycerol (buffer A), at a final concentration of 100 OD<sub>600</sub> and cells were disrupted by sonication (10 times for a 1- min cycle, on ice). Cell debris were removed by centrifugation at 22,100 × g for 60 min at 4 °C and the supernatant was collected and filtered through a 0.45 m PVDF Millipore membrane. Afterwards, cell extract was loaded onto a Q Sepharose FF col- umn (30 mL) equilibrated in buffer A. The column was washed with 50 mL of buffer A, after which bound proteins were eluted by using a 300-mL linear gradient of buffer A from 0 to 0.4 M NaCl at a flow rate of 15 mL/h. The chromatogram was obtained by analyzing fractions absorbance at λ= 280 nm and the presence of the recombinant α-RHA activity was detected using the pNPR assay. Relevant fractions were analyzed by SDS-PAGE, pooled and concentrated at a final vol- ume of ~ 0.5 mL using a 30 kDa Amicon ultra membrane, Millipore. The sample was then loaded onto a Sephacryl HR S200 equilibrated with buffer A containing 0.2 M NaCl (buffer B). Proteins were eluted from the gel filtration column with 250 mL of buffer B at a flow rate of 12 mL/h. Fractions were collected, analyzed and screened for the presence of α-RHA activity as previously described. At this stage, NaCl was removed from pooled fractions by repeated cycles of ultrafiltration and dilution with buffer A. The sample was then loaded on a Q Sepharose FF column (30 mL) equilibrated in buffer A. The column was washed with 50 mL of buffer A, after which bound proteins were eluted with 300 mL of a linear gradient of buffer A from 0 to 0.25 M NaCl at a flow rate of 13 mL/h. Fractions were collected, analyzed by SDS- PAGE and screened for the presence of α-RHA activity. Relevant fractions were pooled, concentrated, purged with nitrogen, and stored at –80 °C until use.

## **2.7 rRHA-Phis and mutants recombinant expression.**

Protein expression was carried out in *E. coli* BL21(DE3) strain transformed with either pET22b(+)/rha-his or pET22b(+)/D-EXXXA plasmids. All the media described in this paragraph contained 100 µg/mL of ampicillin.

-Analytical expression:

*E. coli* BL21(DE3) competent cells were transformed with plasmid pET22b(+)/rha-his and inoculated in a sterile 50 mL Falcon tube containing 12.5 mL of either LB or LB containing a final concentration of 0.5 M NaCl (LB-N). Cells were grown under constant shaking at 37°C up to 0.6–0.7 OD<sub>600</sub>. These preinoculum were diluted 1:100 in 2 sterile

50 mL Falcon tubes containing 12.5 mL of LB, and 2 sterile 50 mL Falcon tubes containing 12.5 mL of LB-N. Cells were grown under constant shaking at 37°C up to 0.7–0.8 OD<sub>600</sub>. Then, rRHA-Phis recombinant expression was induced with 0.1 mM IPTG and growth was continued in constant shaking for 3hrs, at either 23°C or 37°C for both LB or LB-N. Cells were collected by centrifugation (5,524 x g for 15 min at 4°C) and suspended in 25 mM MOPS pH 6.9 at a final concentration of 14 OD<sub>600</sub>/mL. Cells were disrupted by sonication (12 times for a 1-min cycle, on ice) and an aliquot of each lysate was centrifuged at 22,100 x g for 10 min at 4°C. Both soluble and insoluble fractions were analyzed by SDS-PAGE. The soluble fraction was assayed for the presence of α-RHA enzymatic activity.

A second analytical expression experiment was performed by transforming *E. coli* BL21(DE3) competent cells with plasmid pET22b(+)/rha-his. Five colonies were inoculated from the transformation plate in a sterile 50 mL Falcon tube containing 12.5 mL of LB, and were grown under constant shaking at 37°C up to 0.6–0.7 OD<sub>600</sub>. This preinoculum was diluted 1:100 in either one of the following media: LB, LB supplemented with 1 mM of both betaine and sorbitol (LB-BS), LB supplemented with 5 mM of both betaine and sorbitol (LB-BS), LB supplemented with 10 mM of both betaine and sorbitol (LB-BS) and cells were grown under constant shaking at 37°C up to 0.7–0.8 OD<sub>600</sub>. Then, rRHA-Phis recombinant expression was induced by testing 0.1 mM IPTG or 1 mM IPTG, for all condition mentioned above and, in all cases, growth was continued in constant shaking for 3hrs, at 23°C. Cells were collected by centrifugation (5,524 x g for 15 min at 4°C) and suspended in 25 mM MOPS pH 6.9, 5% glycerol at a final concentration of 14 OD<sub>600</sub>/mL. Cells were disrupted by sonication (12 times for a 1-min cycle, on ice) and an aliquot of each lysate was centrifuged at 22,100 x g for 10 min at 4°C. Both soluble and insoluble fractions were analyzed by SDS-PAGE. The soluble fraction was assayed for the presence of α-RHA enzymatic activity.

*-Large scale expression:*

*E. coli* BL21(DE3) cells fresh transformed with pET22b(+)/rha-his, pET22b(+)/D503A, pET22b(+)/E506A, pET22b(+)/D552A, pET22b(+)/E644A, or pET22b(+)/D763A, were inoculated from the transformation plate into 5 mL of LB and incubated in constant shaking at 37°C up to ~ 0.5 OD<sub>600</sub>. The first preinoculum was diluted 1:10 in 4 sterile 50 mL Falcon tubes containing 12.5 mL of LB and incubated in constant shaking at 37°C up to ~ 0.6 – 0.7 OD<sub>600</sub>. The second preinoculum was diluted 1:40 in four 2 L Erlenmeyer flasks containing each 500 mL of LB-BS and incubated in constant shaking at 37°C up to 0.7– 0.8 OD<sub>600</sub>. Expression of rRHA-Phis or rRHA-Phis mutants, was induced with 1 mM IPTG and growth was continued for 3 hrs in constant shaking at 23°C. Cells were collected by centrifugation (5,524 x g for 15 min at 4°C) and periplasm extraction of the culture was performed.

## **2.8 rRHA-Phis and rRHA-Phis mutants purification.**

*E. coli* BL21(DE3) cells were collected by centrifugation (5,524 x g for 15 min at 4°C), after 3 hrs of induction of rRHA-Phis or rRHA-Phis mutants expression. To periplasmic extraction, cell paste was suspended in 100 mM Tris/HCl pH 7.4, 20% sucrose, 1 mM EDTA (Lysis buffer) at a final concentration of 84 OD<sub>600</sub>/mL. 48 µg of native Lysozyme from chicken egg white (L6876 Sigma-Aldrich) for each OD<sub>600</sub> of cells were added to the suspension buffer, and cultures were incubated at RT for 15 min. Then, distilled water was added to the cultures in equal volume respect to the Lysis buffer, and cultures were incubated at RT for 15 min. Cells were centrifuged at 5,524 x g for 15 min at 4°C. The supernatant was collected as the periplasmic fraction of the induced

cultures. Debris were removed by centrifugation at  $22,100 \times g$  for 60 min at  $4^{\circ}\text{C}$  and the supernatant was collected and filtered through a  $0.45 \mu\text{m}$  PVDF Millipore membrane. Afterwards, the periplasmic fraction was loaded overnight in batch under constant shaking at  $4^{\circ}\text{C}$ , onto a Ni-Sepharose FF resin (using  $\sim 3.5 \text{ mg}$  of total proteins for each mL of resin) equilibrated with 15 column volumes of 50 mM Tris/HCl pH 7, 5% glycerol (buffer A). Then, the unbound portion was removed by centrifugation at  $3200 \times g$  for 10 min at  $4^{\circ}\text{C}$ . The resin was washed with 15 column volumes of buffer A, and protein elution was directly carried out in column using a 2 steps gradient at a flow rate of  $\sim 1 \text{ mL/min}$ . In the first step 5 column volumes of buffer A containing 30 mM Imidazole were used, in the second step protein was eluted using 5 column volumes of buffer A containing 250 mM Imidazole. 1 mL fractions were collected and the chromatogram was obtained by analyzing absorbance at  $\lambda = 280 \text{ nm}$  and the presence of rRHA-Phis, or rRHA-Phis mutants activity was detected using the pNPR assay. Relevant fractions were analyzed by SDS-PAGE and pooled. At this stage, imidazole was removed from the pooled fractions by repeated cycles of ultrafiltration and dilution with buffer A, the protein sample was purged with nitrogen, and stored at  $-80^{\circ}\text{C}$  until use.

## 2.9 Enzyme activity assays.

rRHA-P activity was determined using pNPR as substrate (pNPR assay). Otherwise stated, all activity assays were performed at RT. The reaction mixture contained, in a final volume of 0.5 mL of 50 mM MOPS pH 6.9, pNPR at a final concentration of 600  $\mu\text{M}$  and variable amounts of the sample tested. The reaction was blocked after 10 and 20 min by adding 0.5 M  $\text{Na}_2\text{CO}_3$ ; the product, p-nitrophenolate (pNP), was detected spectrophotometrically at  $\lambda = 405 \text{ nm}$ . The extinction coefficient used was  $\lambda_{405} = 18.2 \text{ mM}^{-1} \text{ cm}^{-1}$ . One unit of enzyme activity was defined as the amount of the enzyme that releases one micromole of pNP per min.

### -Kinetic parameters determination:

Kinetic parameters were obtained at pH 6.9 using a pNPR concentration in the range 0.025–1 mM. All kinetic parameters were determined by a non-linear regression curve using GraphPad Prism (GraphPad Software; [www.graphpad.com](http://www.graphpad.com)).

### -pH optimum:

pH optimum for rRHA-P activity was determined in the range 4.7–8.8. Enzyme assays were performed as described above, using the following buffers: 50 mM potassium acetate (pH 4.7–5.7), 50 mM MOPS/NaOH (pH 5.7–7.7) and 50 mM Tris/HCl (pH 7.7–8.8).

### -Temperature optimum and stability:

Optimum temperature was evaluated by performing the standard pNPR assay and incubating the reaction mixture at different temperatures, in the range  $25\text{--}55^{\circ}\text{C}$ . The thermal stability of the enzyme was determined by incubating the enzyme for one and 3 h at 30, 40, 50,  $60^{\circ}\text{C}$  and measuring, after each incubation, the residual specific activity.

### -Organic solvents tolerance:

The tolerance of the enzymatic activity to the presence of organic solvents in the reaction mixture, such as DMSO, acetone or ethanol, was evaluated by performing the standard pNPR assay in 50 mM MOPS pH 6.9 to which either 10% or 50% of solvent was added.

### - Whole cells pNPR assay:

Samples were assayed in a total volume of 0.5 mL. The reaction mixtures contained, 50 mM MOPS pH 6.9, pNPR at a final concentration of 600  $\mu\text{M}$ , and variable amounts of rRHA-Phis or rRHA-Phis mutants expressing cells preincubated in M9 minimal

medium containing 0.4% glucose, and at a cell density ranging from 0.05 to 0.2 OD/mL. Reactions were incubated at RT and after 6 and 12 min aliquots of 0.2 mL were collected and centrifuged at  $5,524 \times g$  for 3 min in order to remove bacterial cells. Supernatants were collected and added to 0.5 M  $\text{Na}_2\text{CO}_3$  in cuvette. The product, p-nitrophenolate (pNP), was detected spectrophotometrically at  $\lambda = 405 \text{ nm}$ . The extinction coefficient used was  $\epsilon_{405\text{nm}} = 18.2 \text{ mM}^{-1} \text{ cm}^{-1}$ . One unit of enzyme activity was defined as the amount of the enzyme that releases one micromole of pNP per min. The Specific Activity was reported as  $\text{mU}/\text{OD}_{600}$ .

### **2.10 TLC Analysis for substrate specificity.**

Reactions were carried out in 0.6 mL of 50 mM Na-phosphate buffer pH 7.0 under magnetic stirring at  $40^\circ\text{C}$  in the presence of 20 mM of either aryl glycoside and 0.25 U of rRHA-P. Reactions were monitored over time (0–24 h) by TLC analysis. Compounds on TLC plates were visualized under UV light or charring with naphthol reagent. Hydrolysis reactions of maltose, pullulan, starch, amylopectin, sucrose, raffinose, lactose, xylan from birchwood, xylan from oat spelt, hyaluronic acid, cellulose, cellobiose, chitosan, Glucan from barley, laminarin, curdlan, fucoidan from *Fucus vesiculosus*, rhamnogalacturonan, rutinose were performed using 2.5 mg of each substrate, which was suspended in 0.5 mL of 50 mM Na-phosphate buffer pH 7.0. Reactions were checked over time by TLC analysis ( $t = 0, 15, 30, 60, 90, 120, 150, 180 \text{ min}, 24 \text{ h}$ ) with the following solvent system: EtOAc:MeOH:H<sub>2</sub>O 70:20:10. An additional hydrolysis reaction of naringin was performed in conditions similar to those reported above in the presence of 10% DMSO, and the reaction was monitored over time. In all experiments, TLC standard solutions of pure reagents and products were used for comparison.

### **2.11 Growth of *Novosphingobium* sp. PP1Y**

*N. sp.* PP1Y cells were grown either in Potassium Phosphate Minimal Medium (PPMM) supplemented with 0.4% glutamic acid as sole carbon and energy source or in Luria Bertani (LB) medium at  $30^\circ\text{C}$  under orbital shaking at 220 rpm. A pre-inoculum in LB was prepared by transferring 50  $\mu\text{L}$  from a glycerol stock stored at  $-80^\circ\text{C}$  to a 50 mL Falcon tube containing 12.5 mL of sterile LB medium. The pre-inoculum was allowed to grow at  $30^\circ\text{C}$  for 10 hrs under orbital shaking and then used to inoculate 1 L of either PPMM or LB at an initial cell concentration of 0.02 OD<sub>600</sub>.

### **2.12 OMVs isolation and purification**

OMVs naturally secreted into the medium were collected from the supernatant in exponential phase by centrifuging cells at  $7,500 \text{ g}$  for 20 min at  $4^\circ\text{C}$ .

Supernatants (2L) were then filtered through a  $0.45 \mu\text{m}$  PVDF (Millipore) membrane, concentrated up to a final volume of 25 mL by using ultrafiltration with an Amicon device equipped with a Millipore YM30 membrane (cut-off 30 kDa). The concentrated sample was first centrifuged at  $25,930 \text{ g}$  for 30 min at  $4^\circ\text{C}$ ; supernatant was subjected to high-speed centrifugation at  $180,000 \text{ g}$  for 2.30 h at  $4^\circ\text{C}$  and pellets were stored at  $-80^\circ\text{C}$  until use.

OMV-containing pellets were suspended in 100  $\mu\text{L}$  of sterile PBS (pH 7.0) and ultracentrifuged using a sucrose gradient density at  $164,000 \text{ g}$  for 6 h at  $4^\circ\text{C}$ . Sucrose gradient was obtained by slowly stratifying, starting from the bottom of an ultracentrifugation vial, 70%, 60% and 20% sucrose solutions prepared in sterile PBS (pH 7.0). Sucrose fractions were separately collected and sucrose was removed using several cycles (at least 10) of concentration/dilution with sterile PBS (pH 7.0).

Concentration cycles were performed by ultrafiltration using an Amicon Ultra 30 K (Millipore) centrifuge tube, at 1,880 g and 4°C. Purified samples were stored at -80°C until needed. OMVs were quantified by evaluating the total amount of protein.

### **2.13 AFM analysis**

OMV samples for AFM analysis were prepared by placing a 20µl droplet of a purified sample on plasma-cleaned microscope slides and letting it dry out O/N at RT. Measurements were performed by using the WiTec alpha300 system, endowed with a closed-loop scan stage with a resolution less than 1 nm. AFM tips (Nano World, Arrow-FMR) were specified by the manufacturer with a resonance frequency at ca. 75 kHz and an elastic spring constant of 2.8 N/m. All AFM images were captured in AC mode, in which the tip is in intermittent contact with the surface, therefore assuring a delicate tip-sample interaction. Typically, images were acquired with a scan step of 15 nm and a scan rate of 200 points/s. The driving frequency was set in correspondence to 90% of the peak amplitude of the cantilever oscillation.

### **2.14 DLS and Zeta-potential measurements**

OMVs size distribution was evaluated using Dynamic Light Scattering (DLS) technique. A commercial apparatus Zetasizer Mod. ZSP – Malvern was used, which measured size distribution and Zeta-potential values.

DLS measurement was carried out by placing samples in an appropriate cuvette. A laser beam emitting a maximum power of 4 mW at 633 nm was focused in the middle part of the cuvette. The scattered light was collected at an angle of 135° and, through an optical fiber, detected with an avalanche photodiode. The fluctuation intensities, originated by the Brownian motion of the OMVs, were analysed by a digital autocorrelator. The correlation curve was fitted to obtain size distribution of the particles. The operating range of our apparatus discriminates particles size varying from 0.3 nm to 20 µm. The Z-potential measurement was performed using a Doppler anemometry function using the Zetasizer Nano ZS.

### **2.15 Scanning electron microscopy (SEM)**

PP1Y cells were grown in either PPMM or LB medium as described above (par. 2.2). Cell pellets were fixed in 2.5 % glutaraldehyde in phosphate buffer (65 mM, pH 7.2–7.4) for 2 hrs at room temperature and washed three times in PBS for 10 min. Samples were then post-fixed with 1% osmium tetroxide in the same phosphate buffer for 1.5 hrs at room temperature, and dehydrated with through consecutive steps of a graded series of ethanol (30%, 50%, 70%, 95% and 100%); in each step the sample was incubated for 15 min at RT. Samples were then mounted on aluminium stubs, coated with a thin gold film using an Edward E306 Evaporator, and observed with a FEI (Hillsboro, OR, USA) Quanta 200 ESEM in high vacuum mode at 30 kV voltage.

### **2.16 Proteome Analysis**

1 mg of total proteins-containing OMVs was used for proteome analysis. Protein extracts from PP1Y cells and OMVs underwent LC-MS/MS-based proteomic analyses. Briefly, 30 µg of proteins were resolved on a 12 % 1D SDS-PAGE. Each resulting gel line was divided in 10 bands that were reduced to smaller pieces, washed with water and dehydrated in acetonitrile, reduced with dithiothreitol and alkylated with iodoacetamide. All bands underwent over-night in-gel digestion using trypsin. Resulting peptide were analyzed by LC/MS/MS using an Orbitrap XL instrument (Thermo Fisher, Waltham, MA, USA) equipped with a nano-ESI source coupled with a

nano-ACQUITY capillary UPLC (Waters): peptide separation was performed on a capillary BEH C18 column (0.075 mm × 100 mm, 1.7 μm, Waters) using aqueous 0.1% formic acid (A) and CH<sub>3</sub>CN containing 0.1% formic acid (B) as mobile phases. Peptides were eluted by means of a linear gradient from 5% to 50% of B in 90 minutes and a 300 nL min<sup>-1</sup> flow rate. Mass spectra were acquired over an m/z range from 400 to 1800. To achieve protein identification, MS and MS/MS data underwent MxQuant software (version 1.4.1.2) analysis: Andromeda search engine was used on NCBI protein database. Parameters sets were: trypsin cleavage; carbamidomethylation of cysteine as a fixed modification and methionine oxidation as a variable modification; a maximum of two missed cleavages; false discovery rate (FDR), calculated by searching the decoy database, 0.05. Only proteins from *Ns. sp. PP1Y* were considered as acceptable. Proteomic analyses were performed in triplicate on two different OMVs preparations and on two PP1Y cells samples.

### **2.17 Fatty acids analysis**

1 mg of total proteins-containing OMVs was used for fatty acid analysis. To obtain fatty acid composition of isolated OMVs, each sample was dried for 90 min over P<sub>2</sub>O<sub>5</sub> and then treated for 30 min at 60 °C with a solution of boron trifluoride/methanol 10% (1.3 M, 1.5 mL) and 50 μL of dimethoxypropane. Afterwards, each solution was extracted twice with hexane and the organic phase was filtered on a Millex filter 0,45μm and dried. The fatty acid methyl esters were re-dissolved in hexane (100 μL) and injected into a gas chromatograph. Gas chromatography analyses were obtained on a Shimadzu model GC2010 instrument equipped with a SP52–60 capillary column (Sigma-Aldrich, St Louis, MO, USA; 100 m x 0.25 inside diameter x 0.20 film thickness); flow rate 1.0 mL/min; injector temperature: 275 °C; splitting ratio: 1:20; detector temperature: 275 °C; carrier gas: helium for chromatography at a pressure of 1.8 psi; auxiliary gas: hydrogen for chromatography, under a pressure of 18 psi; air chromatography at a pressure of 22 psi; sensitivity of instrument: 4 to 16 times the minimum attenuation; amount of sample injected: 1.0 μL. Analyses were performed with the following temperature program: 170 °C for 7 min, 170–225 °C at 2.0 °C min<sup>-1</sup>, and 225 °C for 20 min. Fatty acid methyl esters were identified by comparing their retention times with those of 22 commercial fatty acid standards purchased from Supelco (Sigma-Aldrich Group, St. Louis, MO, USA), with the limit of quantitation of 14 ppb.

### **2.18 Carbohydrates analysis**

1 mg of total proteins-containing OMVs was used for carbohydrates analysis. The determination of the sugar residues by GC–MS analysis was carried out as described in De Castro C et al. [43-44]. Briefly, monosaccharides were identified as acetylated O-methyl glycoside derivatives. After methanolysis (1.25 M HCl/MeOH, 85°C, 24 h) and acetylation with acetic anhydride in pyridine (85°C, 30 min), the sample was analyzed by GC–MS.

### **2.19 Cell viability MTT assay**

HaCaT cells were seeded on 96-well plates at a density of 4×10<sup>3</sup> cells/well in 0.1 mL of complete DMEM 24 h prior to the treatment.

Cells were incubated in the presence of OMVs sample at a final concentration of 10 and 25 μg/mL, for 1,5 and 4 hours. As control, cells were incubated with PBS 1X buffer diluted in medium. Cell viability was evaluated by MTT assay, adding tetrazolium MTT (3-(4,5-dimethylthiazol-2-yl)-2,5-diphenyltetrazolium bromide) diluted at 0.5 mg/mL in

DMEM without red phenol (0.1 mL/well). After 4 h of incubation at 37°C, the resulting insoluble formazan salts were solubilized in 0.04 M HCl in anhydrous isopropanol, and quantified by measuring the absorbance at  $\lambda = 570\text{nm}$ , using an automatic plate reader spectrophotometer (Synergy HTX Multi-Mode Reader-BIOTEK). Cell survival was expressed as means of the percentage values compared to control. Standard deviations were always  $< 5\%$  for each repeat (values in quadruplicate of at least three independent experiments).

## 2.20 Cell culture

HaCaT keratinocytes cell line were cultured in high-glucose Dulbecco's modified Eagle's medium (DMEM) with 10% FBS, 1% Pen/strep at 37°C and 5% carbon dioxide (CO<sub>2</sub>).

Murine macrophage Raw 264,7 cells were cultured in high-glucose Dulbecco's modified Eagle's medium (DMEM) with 10% FBS, 1% Pen/strep at 37°C and 5% carbon dioxide (CO<sub>2</sub>). EVs were isolated from 24 h serum-free conditioned media of 600,000 cells for a T75 flask.

Treatment for EVs isolation was performed for 24 h (with the following agents: Palmitic Acid (PA) 400  $\mu\text{M}$ , Oleic Acid (OA) 400  $\mu\text{M}$ , LPS 5  $\mu\text{g/mL}$  and non-stimulated. Murine vascular smooth muscle cells (VSMC) were isolated from murine adult Aorta and cultured in Dulbecco's modified Eagle medium (DMEM) supplemented with 10% fetal bovine serum (FBS), 4mM L-glutamine, 1% v/v penicillin/streptomycin solution (100 U/ml) and 1mM sodium pyruvate (Euroclone, Milano, Italy) at 37°C in 5% CO<sub>2</sub> incubator.

## 2.21 Production and isolation of EVs

Serum-free conditioned media were collected to isolate total EVs. The conditioned medium was first centrifuged at 1,500  $\times g$  for 15 min in order to eliminate cells and cellular debris. Supernatants containing total EVs were pelleted two times at 15,000  $g$  for 50 min in order to isolate Microparticles (MPs). Pellets (MPs) were finally suspended in 200  $\mu\text{L}$  of 0.9% NaCl and stored at 4 °C. Supernatants, containing exosomes, were ultracentrifuged at 200,000  $\times g$  for 2hrs at 4°C (rotor MLA-50, Beckman Coulter Optima MAX-XP Ultracentrifuge). After two washing steps in NaCl 0.9%, exosomes pellets were suspended into 200  $\mu\text{L}$  of PBS 1X and stored at 4 °C.

The protein amount in the EV preparations was estimated by a DC protein assay (BioRad, Marnes la Coquette, France) using BSA as a standard.

## 2.22 Western Blot analysis

VSMC were resuspended in lysis buffer [50 mM Tris pH 7.4, 0.27 M sucrose, 1 mM Na-orthovanadate pH 10, 1 mM ethylenediaminetetraacetic acid (EDTA), 1 mM ethylene glycol-bis( $\beta$ -aminoethyl ether)-N,N,N',N'-tetraacetic acid (EGTA), 10 mM Na  $\beta$ -glycerophosphate, 50 mM NaF, 5 mM Na pyrophosphate, 1% (w/v) Triton X-100, 0.1% (v/v) 2-mercaptoethanol and cOmplete™ Protease Inhibitor Cocktail, (Roche Diagnostics, Meylan, France)] and left on ice for 30 min. Whole cell lysates were centrifuged at 15,000  $\times g$  for 10 min at 4°C and stored at -80°C.

Cell lysates (8  $\mu\text{g}$ ), MPs and exosomes preparations (15  $\mu\text{g}$ ) were diluted with Laemmli Buffer 6X (in reducing conditions), subjected to SDS-PAGE on 4–12% bis-acrylamide resolving gels (Novex® NuPAGE® precast gels; Life Technologies, Saint Aubin, France) and transferred on to nitrocellulose membranes (GE Healthcare, Pittsburgh, PA, USA). The membrane was blocked for 90 min at room temperature in 5% (w/v)

BSA/ Tris-buffered saline (TBS) (50 mM Tris-HCl pH 7.6, 150 mM NaCl) supplemented with 0.1% (v/v) Tween-20.

Antibodies for Western blot were: Alix (#611620; BD Biosciences, Le Pont de Claix, France),  $\beta$ -actin (#4970, clone 13E5; Cell Signaling), CD9 (#553758; BD Biosciences), CD63 (#D263-3, MBL International, Woburn, Massachusetts, USA), CD81 (#sc- 18877; Santa Cruz Biotechnology), and Nlrp3 (NLRP3 (D4D8T) Rabbit mAb #15101 Cell Signaling). Nitrocellulose membranes were washed three times in TBS 0.1% Tween-20 (v/v) for 5 min and visualization was performed with horseradish peroxidase (HRP)-coupled secondary antibodies (Jackson Immuno-Research, West Grove, Pennsylvania, USA). Protein signals were visualized using enhanced chemiluminescence (Immunocruz, Santa Cruz Biotechnology) with a Chemi-smart 5000 imager system (Vilber-Lourmat, Marne La Vallée, France).

### **2.23 Nanoparticle tracking analysis**

EV samples were diluted in sterile NaCl 0.9% before nanoparticle tracking analysis (NTA). NTA was undertaken using the NanoSight NS300 (Malvern Instruments, Malvern, UK) equipped with a 405-nm laser. Ninetysecond videos were recorded in five replicates per sample with optimised set parameters (the detection threshold was set to 7 and 5, respectively, for IEVs and sEVs). Temperature was automatically monitored and ranged from 20°C to 21° C. Videos were analysed when a sufficient number of valid trajectories was measured. Data capture and further analysis were performed using the NTA software version 3.1. At least three independent biological samples of each EV subtype were analysed, and the presented results correspond to the mean of the five videos taken for a given biological sample.

### **2.24 Cytofluorimetric Annexin V binding analysis**

Annexin V binding properties was measured by flow cytometry using the kit Annexin V-FITC (Miltenyi Biotec). Five microlitres of MPs (corresponding to 0.5  $\mu$ g of MPs content) were washed with annexin V 1X binding buffer, centrifuged at 13,000  $\times$  g for 15 min, then incubated with 5  $\mu$ L of annexin V-FITC in annexin V 1X buffer in the dark for 45 min. Following staining, MPs were washed twice in 1X buffer, pelleted and resuspended in 200  $\mu$ L 1X buffer for flow cytometry analysis. Annexin V positivity was determined on a MACSQuant flow cytometer. Data were further analysed using MACSQuant analysis software.





---

## **CHAPTER III**

### **RESULTS SECTION I**

#### **A NOVEL $\alpha$ -L-RHAMNOSIDASE ACTIVITY FROM *NOVOSPHINGOBIUM* sp. PP1Y**

---



## CHAPTER III- RESULTS SECTION I

### 3.1.1 Cloning, recombinant expression and purification of recombinant RHA-P

$\alpha$ -RHA activity was previously detected and isolated, in the laboratory in which this PhD project was developed, in the crude extract of *N. sp.* PP1Y grown in minimal medium and in the presence of 0.3 mM naringin [132]. In order to express, purify and characterize this novel enzymatic activity, PP1Y genomic DNA was cloned in a pET22b(+) recombinant plasmid as described in Materials and Methods [135]. Recombinant plasmid pET22b(+)/rha-p was used to transform *E. coli* BL21(DE3) strain, and first attempts to express the recombinant protein (rRHA-P) at 37°C showed the presence of a protein band with the expected molecular weight of 120 kDa almost exclusively in the insoluble fraction of the induced culture. At this stage, the induction temperature was lowered to 23°C and a SDS-PAGE analysis highlighted the presence of an analogous protein band also in the soluble portion of the induced culture (Fig. 8), thus suggesting a possible further improvement of the yield of soluble rRHA-P by modifying the experimental conditions of the recombinant expression. Neither the use of different IPTG concentrations nor the variation of the induction time seemed to further influence the presence of rRHA-P in the soluble fractions. However, it has been shown that the addition of osmolytes such as betaine and sorbitol, which behave as “chemical chaperones”, to the culture medium of induced recombinant cells of *E.coli* helps in assisting protein folding and might increase protein solubility. This effect can be improved by the presence in the growth medium of a high salt concentration that is responsible for increasing the uptake rate of betaine and sorbitol from the extracellular environment. It has been shown, in fact, that in the presence of an osmotic shock, caused for example by the presence of a high salt concentration, some bacteria equilibrate the osmotic pressure by accumulating both intracellular metabolites such as aspartate, glutamate, and proline and osmolytes present in the medium such as betaine and sorbitol [136].

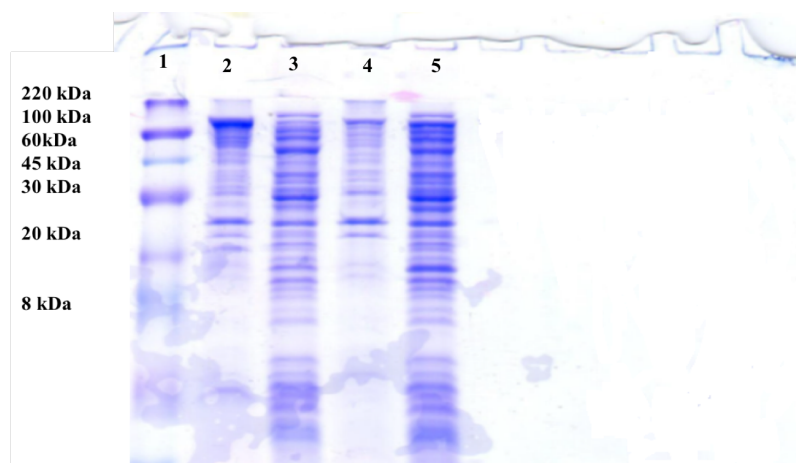


**Figure 8:** SDS-PAGE of analytical expression of rRHA-P in *E.coli*, strain BL21(DE3). Lane 1: MW standard. Lane 2: insoluble fraction of induced cultures after 3 hrs of induction at 37°C. Lane 3: soluble fraction of induced cultures after 3 hrs of induction at 37°C. Lane 4: insoluble fraction of induced cultures after 3 hrs of induction at 23°C. Lane 5: soluble fraction of induced cultures after 3 hrs of induction at 23°C.

Therefore, analytical expression experiments were performed to optimize the yield of active rRHA-P in the soluble fraction of the induced culture. To this purpose, cell growth was performed in media of different composition that included a) LB, b) LB

supplemented with 0.5 M NaCl (LB-N), c) LB supplemented with 1 mM of both betaine and sorbitol (LB-BS), and d) LB containing 0.5 M NaCl, and 1 mM of both betaine and sorbitol (LB-NBS). rRHA-P expression was induced with 0.1 mM IPTG at either 23 °C or 37 °C. Data obtained showed that the best condition involved an induction at 23 °C using LB-NBS as growth medium, with a 46-fold-increase of the specific activity in the soluble fraction after cell lysis when compared to cultures grown in LB and induced at 37 °C.

Large-scale recombinant expression was performed by using the optimized experimental conditions suggested by the analytical experiments described above.

rRHA-P purification was carried out following three different chromatographic steps. Cell extract obtained after lysis, was loaded onto a Q Sepharose FF column and protein separation was carried out using a linear gradient from 0 to 0.4 M NaCl at a flow rate of 15mL/h. The chromatogram was obtained by analysing fractions absorbance at  $\lambda = 280$  nm and the presence of the recombinant  $\alpha$ -RHA activity was detected by using the pNPR assay. Relevant fractions were analysed by SDS-PAGE, pooled and concentrated and then loaded onto a Sephacryl HR S200 gel filtration column; proteins were eluted at a flow rate of 12 mL/h. Fractions were collected, analysed and screened for the presence of  $\alpha$ -RHA activity as previously described. The last chromatographic step involved a second ion exchange chromatography; sample was loaded on a Q Sepharose FF column and eluted with a linear gradient from 0 to 0.25 M NaCl at a flow rate of 13mL/h. Relevant fractions were pooled, concentrated, purged with nitrogen, and stored at -80 °C until use.

The purification table (Table1) showed a final purification factor (PF) of 6.9.

	<i>Tot U.#</i>	<i>Specific Activity (U/mg)</i>	<i>P.F.</i>	<i>Yield (%)</i>
<b>Cell lysate</b>	13,728.8	49.8		
<b>I Q-Sepharose</b>	5,939.6	54.7	1.1	43.3
<b>Gel filtration</b>	1,370.6	66.1	1.3	9.9
<b>II Q-Sepharose</b>	920.9	346.9	6.9	6.7

**Table 1:** Purification table of rRHA-P. #Total Units

SDS-PAGE analysis of peak fractions representative of all purification steps showed in the final purified sample of rRHA-P the presence of a major contaminant with an approximate molecular weight of ~35 kDa. This protein band was excised, digested *in situ* and analysed by LC-MS/MS. The protein was identified by searching in the *E. coli* sequence database and resulted to be the subunit of Glyceraldehyde 3-phosphate dehydrogenase which is composed of four identical subunits, as identified by 17 peptides matches for a global sequence coverage of 71%.

Purified rRHA-P amino acidic sequence was verified up to a 94% coverage, by MS Mapping analysis carried out by MALDI-TOF and LC-MS/MS after both an *in-situ* and an *in-solution* digestion with either trypsin or chymotrypsin. However, it is worth noting that the protein N-terminus, detected by MS analysis, lacks the first 23 amino acids from the expected cloned sequence (data not shown). To confirm the lack of the putative N-terminal peptide, purified rRHA-P was subjected, after an N-terminus labelling, to both MALDI-TOF and LC-MS/MS analysis. Mass spectrometry analysis

allowed the identification of peptides 23 ESRDDAAEVAPSTRPEPSLEQAF45 (MH+ 2502.17 ppm) and 23 ESRDDAAEVAPSTR36 (MH+ 1503.70) when rRHA-P was digested with chymotrypsin or trypsin, respectively. This evidence was also confirmed by Edman degradation N-terminus sequencing, which showed that the first 5 amino acids of the recombinant protein are ESRDD. It should be noted that the same N-terminal peptide was also found in native RHA-P.

### 3.1.2 Biochemical characterization of rRHA-P

The oligomeric state of rRHA-P was verified by analytical gel filtration using a Superdex 200 analytical column, in collaboration with prof. Antonio Molinaro of the Department of Chemical Sciences (University Federico II of Naples). The protein was eluted as a single peak with an apparent molecular weight of  $101,500 \pm 5,000$  Da, which indicates that rRHA-P is a monomer.

To gain a deeper insight into the biotechnological potential of rRHA-P, the reaction mechanism, the kinetic parameters, the optimal reaction conditions in terms of pH and temperature and the solvent tolerance were investigated.

In order to understand the mechanism of action of rRHA-P,  $^1\text{H}$  NMR spectroscopy was used to monitor the stereochemical course of pNPR cleavage in collaboration with Prof. Antonio Molinaro, of the Department of Chemical Sciences, University of Naples Federico II. The data obtained suggest that rRHA-P acts as an inverting enzyme. Moreover, to investigate rRHA-P substrate specificity in hydrolysis and self-condensation processes, several pNP and pNP derivatives were used as substrates in enzymatic assays performed as described in Materials and Methods. Reactions were followed over time by TLC analysis and purified enzyme showed activity only on pNPR, confirming that rRHA-P is indeed an  $\alpha$ -L-rhamnosidase (data not shown). Moreover, no activity on pNP- $\beta$ -d-Glucose was detected. Furthermore, oligo- and polysaccharides such as rutinose, maltose, sucrose, lactose, pullulan, starch, amylopectin, raffinose, xylan from birchwood, xylan from oat spelt, hyaluronic acid, cellulose, cellobiose, chitosan, Glucan from barley, laminarin, curdlan, fucoidan from *Fucus vesiculosus*, were also tested as substrates for rRHA-P. TLC analysis of all these reactions showed the lack of activity of this enzyme on any of these compounds. Kinetic parameters were estimated at pH 6.9 using a pNPR concentration ranging between 0.025-1 mM. All kinetic parameters were determined with a non-linear regression curve using GraphPad Prism (GraphPad Software; [www.graphpad.com](http://www.graphpad.com)). The reaction rate ( $\mu\text{M}/\text{min}$ ) plotted as a function of the substrate concentration ( $\mu\text{M}$ ) showed a typical Michaelis-Menten trend (Fig. 9 and Table 2).  $K_M$  constant of  $160.2 (\pm 17.3) \mu\text{M}$ ,  $V_{\text{max}}$  of  $21.1 (\pm 8.0) \mu\text{M min}^{-1}$ , a  $k_{\text{cat}}$  of  $734.4 (\pm 212.9) \text{sec}^{-1}$  and a  $K_S$  of  $4.6 (\pm 1.7) \text{sec}^{-1} \mu\text{M}^{-1}$  were obtained.

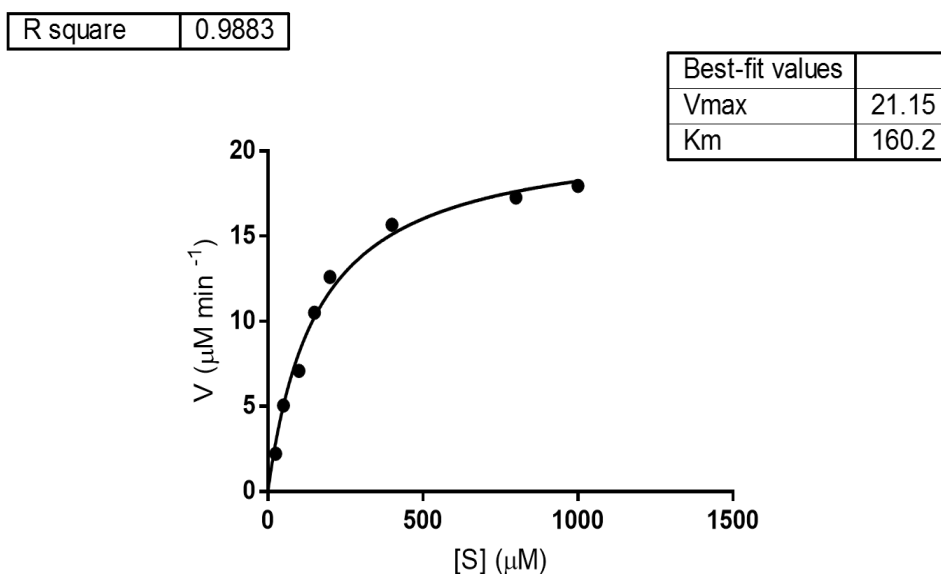


**Figure 9.** rRHA-P kinetic behavior using pNPR as substrate. Reaction rate expressed in  $\mu\text{M}/\text{min}$  is plotted as a function of pNPR  $\mu\text{M}$  concentration.

	$K_M$ ( $\mu\text{M}$ )	$V_{\text{max}}$ ( $\mu\text{M min}^{-1}$ )	$K_{\text{cat}}$ ( $\text{sec}^{-1}$ )	$K_S$ ( $\text{sec}^{-1} \mu\text{M}$ )
rRHA-P	160.2 ( $\pm$ 17.3)	21.1( $\pm$ 8.0)	734.4 ( $\pm$ 212.9)	4.6 ( $\pm$ 1.7)

**Table 2.** Kinetic parameters determined for rRHA-P on pNPR substrate.

To further characterize rRHA-P, pH optimum was determined by performing pNPR assay in buffers with different pH (range 4.7-8.8). The recombinant protein revealed an optimal activity in the range 6.0-7.5 with an optimum at pH 6.9, retaining 47% and 36% of activity at pH 7.9 and 8.8, respectively (Fig. 10A). In addition, rRHA-P optimum temperature activity was evaluated by performing the standard pNPR assay in the temperature range 25°C-55°C. Data, reported in Figure 10B, showed an optimal activity temperature at 40.9 °C. Moreover, to verify the thermal stability of rRHA-P in the same range used to determine the optimal temperature, an incubation of the purified protein for 1h and 3h was performed at each different temperature. The results indicate that the enzymatic activity is stable between 25 and 40 °C, and retains 44% of its value up to 50°C. At 40° C, the temperature optimum, the activity is stable up to 24h.

In addition, rRHA-P tolerance to the presence of organic solvents was assessed by performing the standard pNPR assay in 50mM MOPS pH 6.9 to which 10% and 50% of either DMSO, acetone or ethanol (EtOH) were added. Results, reported in Figure 11, pointed up a drastic decrease of the activity in the presence of either concentration of acetone and in 50% DMSO and EtOH, while  $\approx$  66% of residual activity was detected in the presence of 10% of DMSO and EtOH.

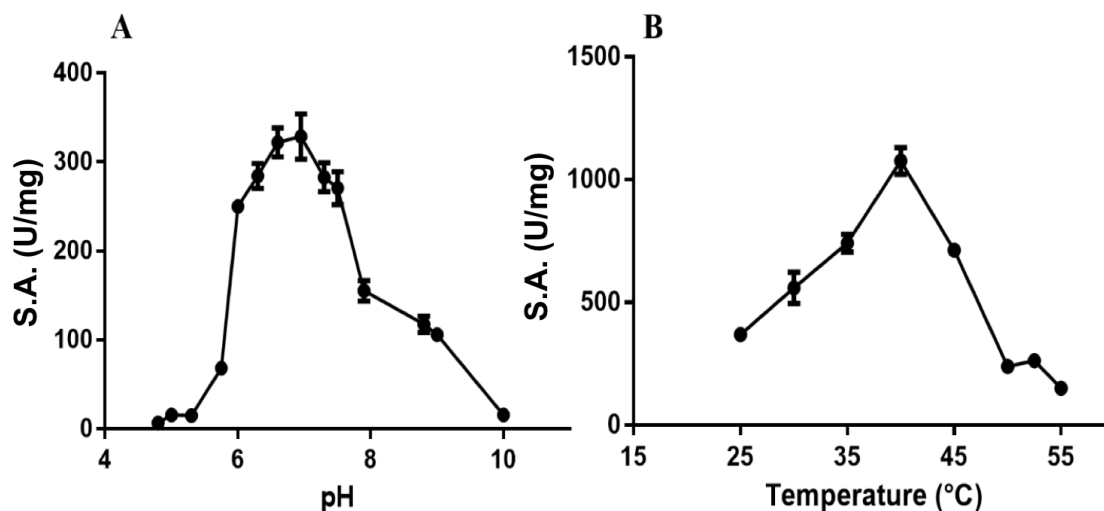


**Figure 10.** rRHA-P pH (A) and temperature (B) optimum curves.

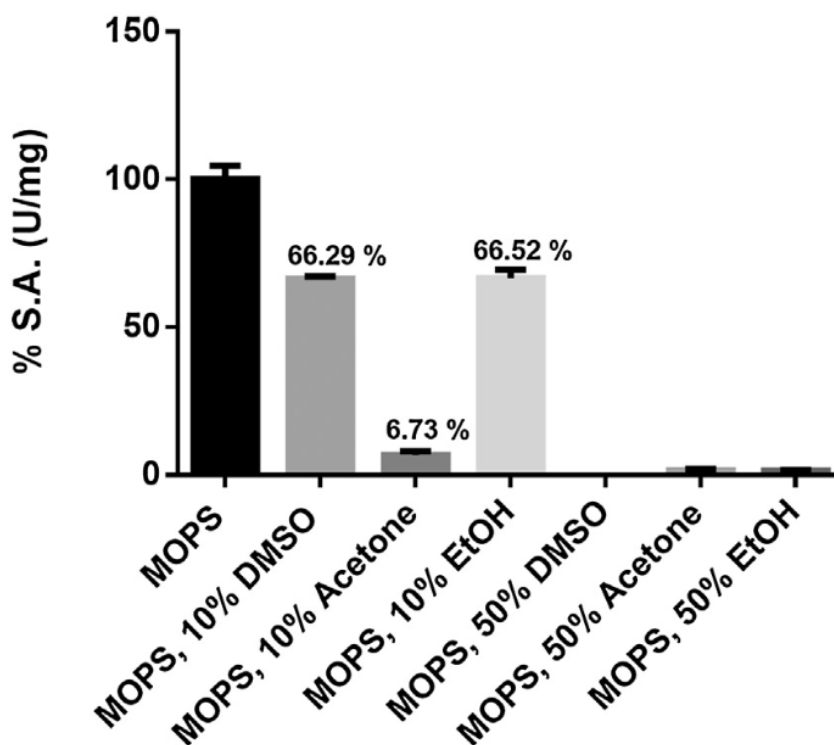


**Figure 11.** Organic solvents resistance of rRHA-P. Specific activity is reported in terms of %, compared to control. Data are resulting of three independent experiments. Errors were always within 20%.

In light of these encouraging outcomes, the ability of rRHA-P to hydrolyze natural flavonoids was investigated. Enzymatic assays using naringin, rutin and neohesperidin dihydrochalcone were performed and followed by TLC analysis, as described in Materials and Methods. To this purpose, a 6 mM solution of each compound was incubated with purified rRHA-P in 50 mM Na-phosphate buffer pH 7.0 at 40 °C, and

the reaction was monitored by TLC analyses over time. After 3 h of incubation, TLC analysis of the reaction mixtures showed a 40–60% hydrolysis of neohesperidin dihydrochalcone and rutin in the corresponding derhamnosylated neohesperidin dihydrochalcone and isoquercitrin. Besides, a total conversion of naringin was observed as the corresponding products, rhamnose and prunin, were the only compounds observed on the TLC plate. Reaction on naringin was also carried out in the presence of 10% DMSO. In this case, in our experimental conditions, the complete conversion of naringin in prunin and rhamnose occurred after 1h.

### 3.1.3 Optimization of rRHA-P purification: his-tag cloning

Considering the low purification yield of rRHA-P previously obtained for the untagged recombinant protein and the burden of the previous purification protocol, the recombinant expression of rRHA-P fused to a His-tag was implemented. To this purpose, the recombinant plasmid pET22b(+)/rha-his was obtained through a site directed mutagenesis on the STOP codon of the coding sequence (TGA to CGA). Gene coding sequence was thus extended on the pET22b(+) plasmid, to include a 6-His-tag coding region at 3' of the gene, as described in Materials and Methods. In this way, a rRHA-P fused to a C-terminal His-tag was obtained (Fig. 12).

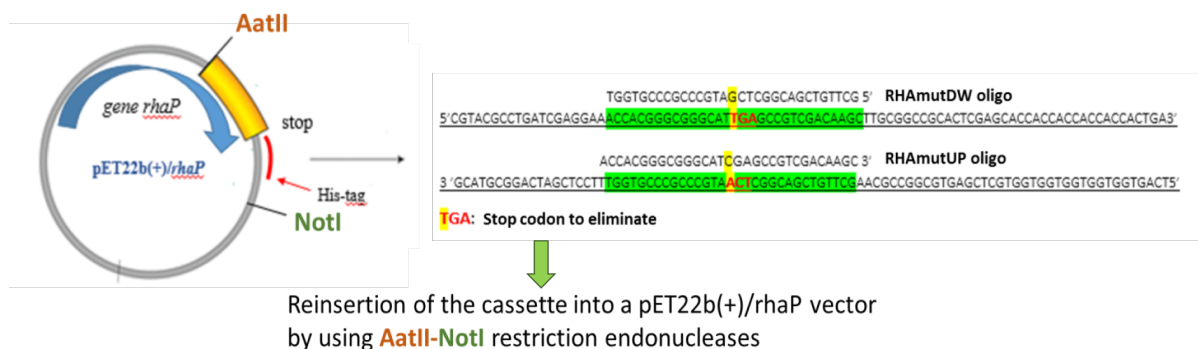


**Figure 12.** rha-his Cloning strategy.

In order to evaluate rRHA-P-his expression, the plasmid pET22b(+)/rha-his was used to transform *E. coli* BL21(DE3) cells and analytical expression experiments were performed. As previously underlined, recombinant expression of rRHA-P (untagged) significantly increased when BL21(DE3) cells were induced at a temperature of 23°C, and were grown in a high-salt concentration (0.5 M NaCl) LB medium, containing betaine and sorbitol [135]. Therefore, a first analytical expression experiment was set-up to evaluate the recombinant expression of rRHA-Phis as described in Materials and Methods.

The SDS-PAGE analysis of the soluble and insoluble fractions of the induced cultures showed the foremost presence of a protein band at the expected molecular weight for rRHA-Phis in the soluble fraction, only in cultures induced at 23°C (data not shown). The soluble fractions were assayed for the presence of  $\alpha$ -RHA enzymatic activity and, differently from what observed for rRHA-P, the presence of 0.5 M NaCl in the culture medium had no effect in raising the levels of active rRHA-Phis in the soluble fraction (data not shown). Data showed that the best expression conditions involved an induction with 1 mM IPTG, at 23°C, using LB supplemented with 5 mM of both betaine

and sorbitol [51]. Once defined the recombinant expression conditions for rRHA-Phis, another optimization of the previous rRHA-P purification protocol was set-up. As described above, the protein N-terminus expected from genomic sequence had been detected neither in the native nor in the recombinant rRHA-P, suggesting the presence of a signal peptide that is presumably cleaved through post-translational proteolytic processing. In order to verify the presence of rRHA-Phis in the periplasmic fraction, an analytical expression experiment was performed (Material and Methods). Starting from the same cell growth, an 8 OD<sub>600</sub> aliquot was collected and sonicated, while another 8 OD<sub>600</sub> aliquot was used to perform periplasmic extraction as described in Materials and Methods section. Fractions containing the total cell extract, periplasm and cytoplasm were analyzed by SDS-PAGE and the  $\alpha$ -RHA activity was evaluated. As evident from SDS PAGE (Fig. 13), the amount of rRHA-P his is comparable in both periplasmic fraction (lane3) and total cell extract (lane 2), whereas only a slight amount of protein was observed in cytoplasm. Moreover, enzymatic assays showed that the specific activity expressed in the periplasmic space (9,38U/mg) was more than 400 times higher than that detected in the cytoplasmic fraction (0,02 U/mg). Therefore, large-scale recombinant expression of rRHA-Phis was performed using the optimized condition described above and, in order to implement the yield of the purified rRHA-Phis, a large-scale extraction of the periplasm fraction was set-up as described in Materials and Methods. rRHA-Phis purification was then carried out in a single step affinity chromatography using a Ni-sepharose 6 fast flow column. SDS-PAGE analysis of purified rRHA-Phis showed a quite pure protein (Fig.14) and the purification table (Table 3) showed a final purification factor (PF) of 5.6 and a total yield of 24.8%, corresponding to a 1.6 total mg of rRHA-Phis recovered for liter of culture

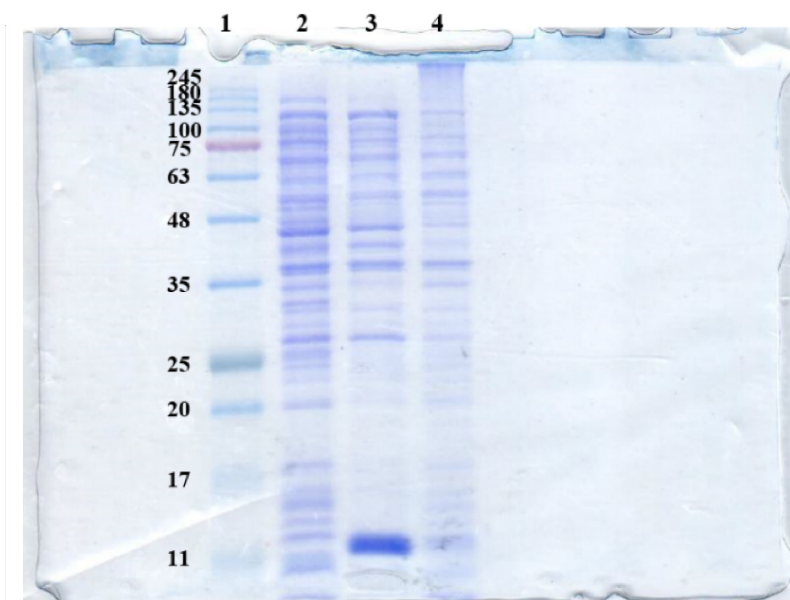


**Figure 13.** SDS PAGE gel analysis of analytical expression of rRHAP-his. Lane 1: standard molecular weight, lane 2: total cell extract, lane 3. Periplasmic fraction, lane 4: cytoplasmic fraction.

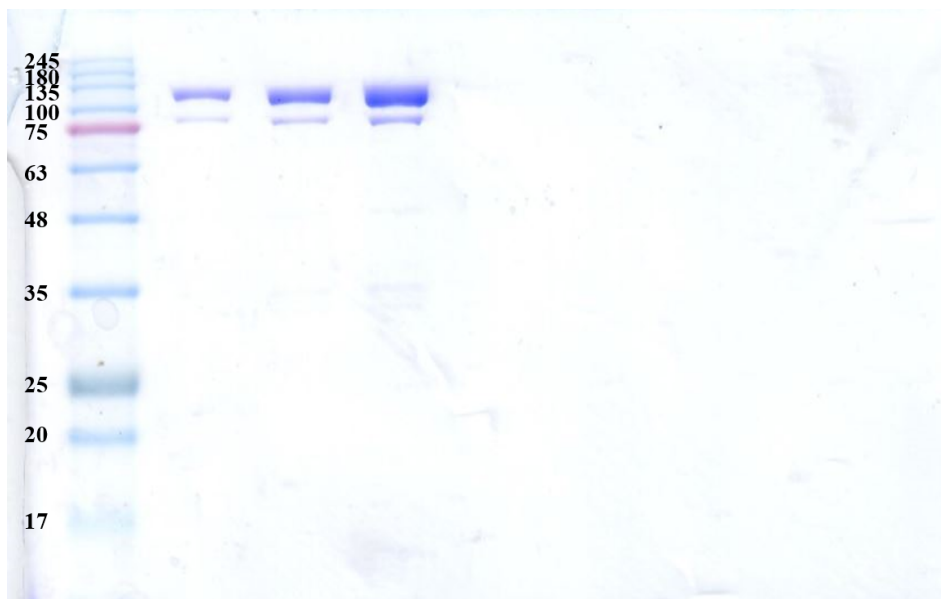


**Figure 14.** SDS PAGE analysis of purified rRHA-Phis. Lane 1: standard molecular weight, lane 2-4: 1,2,4 µg of purified rRHA-Phis

<b>Sample</b>	<b>Total Units</b>	<b>Specific Activity (U/mg)</b>	<b>P.F.</b>	<b>Yield (%)</b>
<b>Periplasm</b>	3212.5	41.2		
<b>RHA-Phis</b>	798.40	230.4	5.6	24.8

**Table 3.** Purification table of rRHA-Phis. S.A: specific activity. U tot: total units

To evaluate the potential effect of the his-tag on protein functionality, specific activity of the purified rRHA-Phis was compared to the specific activity of the native rRHA-P. Data showed a small decrease of the specific activity on pNPR, with rRHA-Phis displaying 87% of the native rhamnosidase activity (Fig. 15). Kinetic constants on pNPR for rRHAP-his were also evaluated. Results (Fig. 15) showed that  $K_M$  and  $K_S$  values evaluated for RHA-Phis are comparable to those of the the untagged protein ( $160.2 \mu\text{M}^{-1}$  and  $4.6 \text{sec}^{-1} \mu\text{M}^{-1}$  respectively).

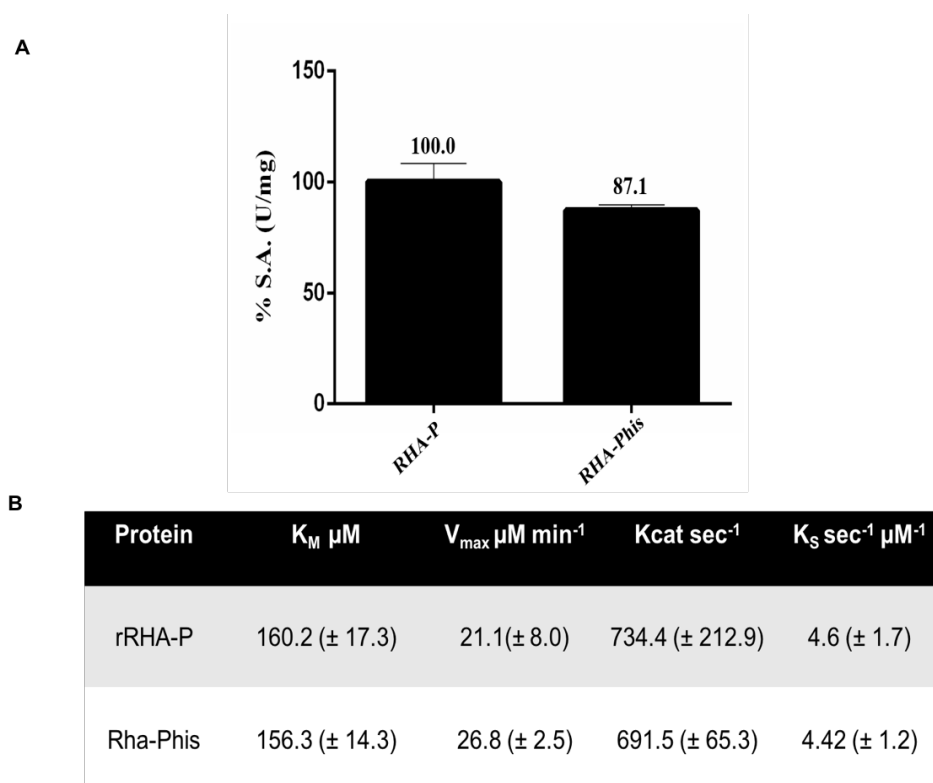


**Figure 15.** Specific activity (A) and Kinetics parameters (B) of rRHA-P his compared with native rRHA-P. Data are resulting of three independent experiments. Errors were always within 20%.

### 3.1.4 Functional and structural characterization of rRHA-P: Alanine scanning mutagenesis

In order to further characterize rRHA-P catalytic activity and specificity, an alanine scanning mutagenesis of putative catalytic residues was performed. Therefore, an alignment of the rRHA-P amino acid sequence with other 130 GH106 protein sequences available from the online database, was performed using the BLAST alignment tool (<http://blast.ncbi.nlm.nih.gov/Blast.cgi>) in collaboration with Prof. Marco Moracci and Dr. Andrea Strazzulli, Department of Biology, Federico II of Naples. Five conserved residues with a consensus of > 90% were found: D503, E506, D552, E644, and D763. An “alanine scanning” strategy was set-up for all 5 residues. This approach would lead to a loss of function of mutants, in which the catalytic residue is replaced with an alanine, through site-directed mutagenesis (Fig. 16). pET22b(+)/D-EXXXXA mutated plasmids were obtained by the construction of a mutagenesis cassette, after digesting pET22b(+)/rhaPhis with AatII/KpnI endonucleases. This cassette contained all residues to mutagenize, as described in Materials and Methods. Mutagenesis

experiments were performed using QuikChange II Site-Directed Mutagenesis Kit (Agilent Technologies) and mutagenized fragments, cloned into pGEM-3Z vector, were then individually cloned back into pET22b(+)/rha his vector using AatII/KpnI restriction endonucleases. Mutagenized clones were named: pET22b(+)/D504A, pET22b(+)/E506A, pET22b(+)/D552A, pET22b(+)/E644A, and pET22b(+)/D763A and were used, separately, to transform *E. coli* BL21(DE3) competent cells (Fig. 16).

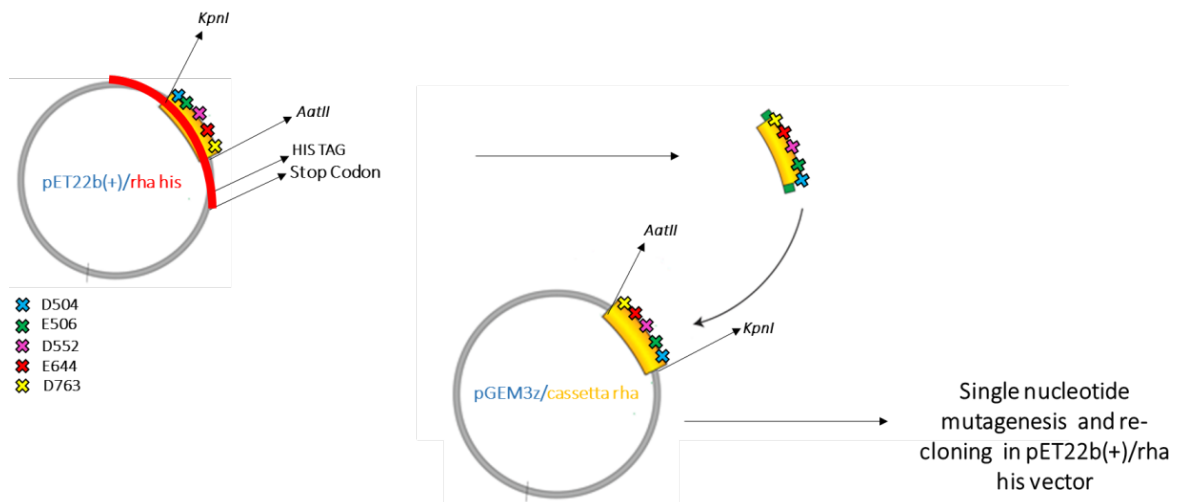


**Figure 16:** Mutagenesis strategy of rRHA-P gene.

Preliminary analytical expressions confirmed the same experimental conditions used for *wt* rRHA-Phis. Therefore, large-scale expressions were performed in order to evaluate, for each clone, specific activity on pNPR of either recombinant whole cells or cell extracts. To this purpose, an initial screening for the  $\alpha$ -RHA activity expressed by the recombinant cells was performed using *E. coli* BL21(DE3) whole cells, according to the procedures described in Materials and Methods. No activity was detected for mutants rRHA-Phis/D503A and rRHA-Phis/E644A, and a significant reduction in  $\alpha$ -RHA activity for mutants rRHA-Phis/E506A (0.57%), rRHA-Phis/D552A (11.3%) and rRHA-Phis/D763A (12.2%) was observed (Fig. 17A). Enzymatic activity was also assayed on the corresponding cell lysates. Results, shown in Figure 17B, confirmed the data obtained by using recombinant whole cells.

rRHA-P-his mutants were purified from crude extracts following the same protocol used for rRHA-P-his, and the specific activity of the purified mutants was evaluated. As underlined in figure 18, mutation in residues D503, E506 and E644, led to an almost total inactivation of the enzyme; on the contrary, mutations in positions D552 and D763 allowed maintaining a residual activity of 47.87% and 15.75% respectively (Fig. 18).

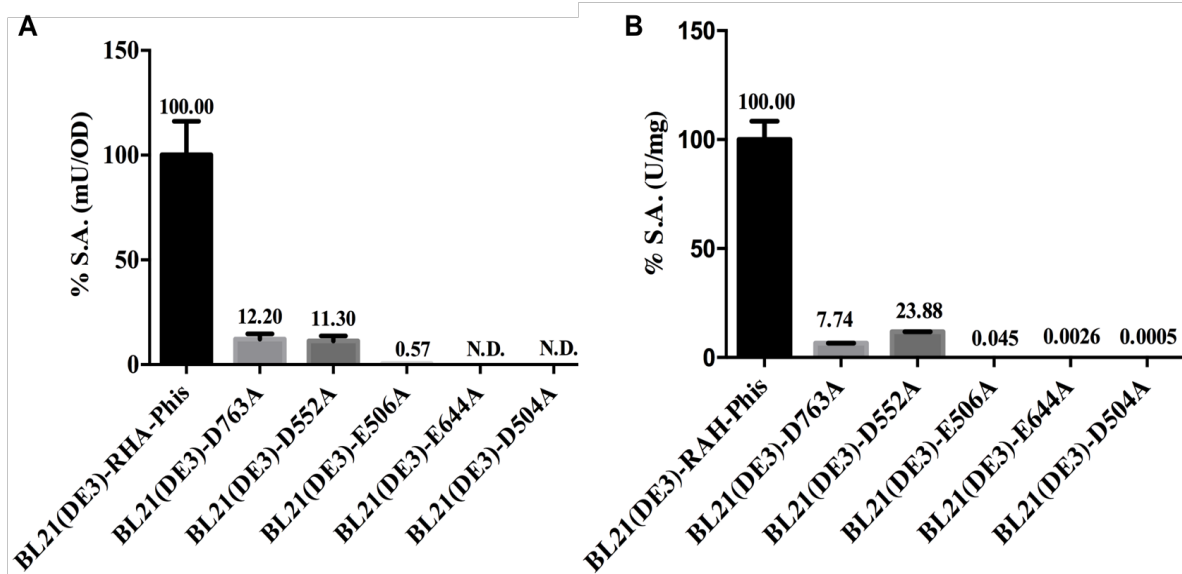


**Figure 17.** Residual specific activity of RHA-Phis mutants. A) pNPR assays on whole cells of *E. coli* BL21(DE3) transformed with pET22b(+)/D-EXXXA, compared to the control recombinant cells transformed with pET22b(+)/rha-his. Rhamnosidase specific activity is reported as the percentage of residual activity, expressed as mU/OD<sup>600</sup>, compared to the control. B) pNPR assays of lysates of *E. coli* BL21(DE3) transformed with pET22b(+)/D-EXXXA, compared to the control recombinant cells transformed with pET22b(+)/rha-his. Rhamnosidase specific activity is reported as percentage of residual activity, expressed as U/mg, compared to the wt protein. Data are resulting of three independent experiments. Errors were always within 20%.

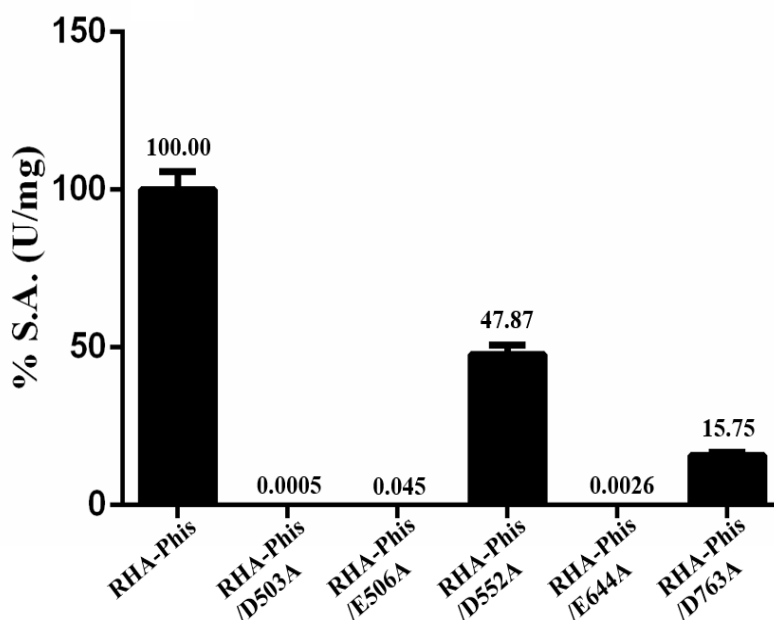


**Figure 18.** pNPR assays of purified RHA-Phis mutants, compared to wt RHA-Phis. Rhamnosidase specific activity is reported as percentage of residual activity, expressed as U/mg, compared to the wt protein. Data are resulting of three independent experiments. Errors were always within 20%.

In addition, Kinetics experiments were performed as described in Materials and Methods section. The reaction rate ( $\mu\text{M}/\text{min}$ ) was plotted as a function of the substrate concentration ( $\mu\text{M}$ ), showing the typical Michaelis-Menten trend. Table 4 summarizes the kinetic constants measured for rRHA-Phis and for the active mutants. Firstly, results showed that  $K_M$  and  $K_S$  value found for rRHA-Phis are quite close to the ones measured for the untagged protein ( $160.2 \mu\text{M}^{-1}$  and  $4.6 \text{sec}^{-1} \mu\text{M}^{-1}$  respectively). Moreover,  $K_S$  values obtained for rRHA-Phis/D552A and rRHA-Phis/D763A mutants were equivalent to the  $\sim 65\%$  and  $\sim 21\%$  of rRHA-Phis  $K_S$ , respectively.

<b><i>Protein</i></b>	<b><i>K<sub>M</sub> (<math>\mu\text{M}</math>)</i></b>	<b><i>V<sub>max</sub> (<math>\mu\text{M min}^{-1}</math>)</i></b>	<b><i>K<sub>cat</sub> (<math>\text{sec}^{-1}</math>)</i></b>	<b><i>K<sub>S</sub> (<math>\text{sec}^{-1} \mu\text{M}^{-1}</math>)</i></b>
<b>RHA-Phis</b>	156.30	26.76	691.47	4.42
<b>RHA-Phis D552A</b>	158.80	26.83	457.69	2.88
<b>RHA-Phis D763A</b>	138.20	25.57	126.08	0.94

**Table 4.** RHA-Phis, RHA-Phis/D552A and RHA-Phis/D763A kinetic constants using pNPR as substrate. Errors were always within 20%.





---

# **CHAPTER III**

## **RESULTS SECTION II**

### **EXTRACELLULAR VESICLES IN BIOTECHNOLOGICAL PROCESSES**

---



## CHAPTER III- RESULTS SECTION II

### EXTRACELLULAR VESICLES IN BIOTECHNOLOGICAL PROCESSES

#### 3.2.1 Outer Membrane Vesicles (OMVs) from *Novosphingobium sp. PP1Y*

Outer membrane vesicles (OMVs) are bacterial extracellular vesicles, with a diameter range of 20-200 nm. Current research is focusing on the use of OMVs for their biotechnological potential as immobilization scaffolds and drug delivery systems. The second activity planned in my PhD project was to isolate, purify and characterize OMVs from the microorganism *Novosphingobium sp. PP1Y*.

##### 3.2.1.1 Identification of OMVs from PP1Y

To verify *N. sp. PP1Y* vesiculation and identify the best growth conditions for OMVs production, cells were grown either in PPMM supplemented with 0.4% glutamic acid as the sole carbon and energy source (minimal medium) or in LB (rich medium) as described in Materials and Methods section. Cells were harvested during both exponential (16 hrs) and stationary phase (20 hrs) at 7,500 g for 20 min at 4°C. Cell pellets were processed for SEM visualization and each sample was spotted on aluminium stubs and analyzed. The images obtained (Figure 19), showed the presence of rod-shaped PP1Y cells embedded in an extracellular matrix rich of small globular nanostructures that appeared quite heterogenous in size. This occurred only when PP1Y was grown in PPMM (Fig 19 A) and mainly during the exponential growth phase; noteworthy, PP1Y grown in LB did not show the presence of extracellular vesicles (Fig 19 B).

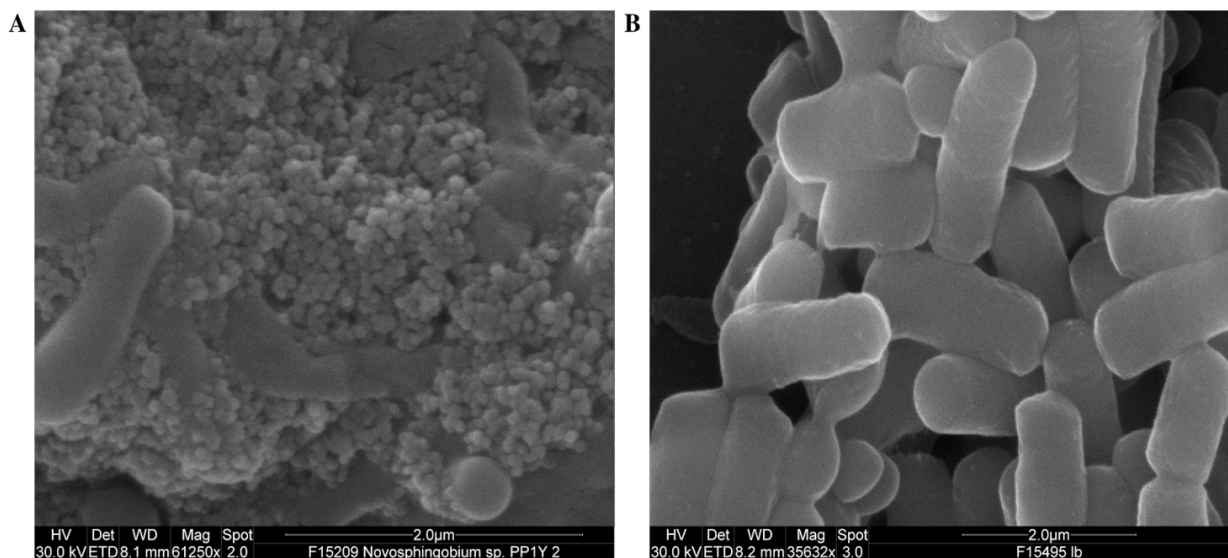


**Figure 19.** SEM images of PP1Y cells. SEM images of PP1Y cells grown either in PPMM (A) or LB (B). Scale bars: 2 μm.

Further attempts to analyse by SEM cell-free exhausted growth media to obtain images of free-floating vesicles failed to give positive results.

To overcome this problem, cell free supernatants of PP1Y cells grown under different conditions were collected and analysed using Atomic Force Microscopy (AFM) in collaboration with Dr. Giulia Rusciano and Prof. Antonio Sasso at the Department of Physics, University Federico II of Naples. *N. sp.* PP1Y was grown in the same experimental conditions described for SEM using either PPMM or LB. Two litres of exhausted growth medium were collected in both exponential and stationary phase, concentrated at a final volume of ~15 mL using a 30 kDa Amicon ultra (Millipore) membrane and filtered through a 0.45  $\mu\text{m}$  PVDF Millipore membrane. Samples were ultracentrifuged at 180,000  $\times$  g for 2.5 h at 4°C and were analyzed for the presence of OMVs as described in Materials and Methods. AFM data were processed in order to obtain 3D images, which confirmed the presence of globular nanostructures in the exhausted media collected during the exponential phase growth of *N. sp.* PP1Y in PPMM (Fig. 20). In addition, AFM analysis indicated an average size for these structures of ~ 100-200 nm, in agreement with data reported in literature [78, 80, 90, 93, 140]. It is worth noting that AFM highlighted, at this stage, the presence of a heterogeneous sample (Fig. 20), which confirmed what previously observed with SEM and prompted the need for a further purification of the sample.

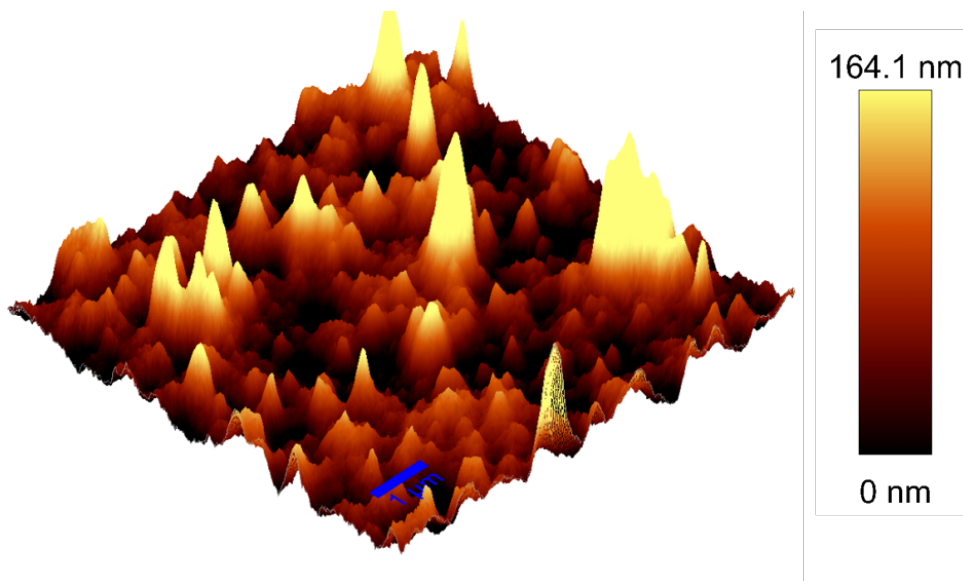


**Figure 20.** AFM analysis of *N. sp.* PP1Y OMVs. AFM images of OMVs isolated in late exponential phase from *N. sp.* PP1Y grown in PPMM. Scale bar 1  $\mu\text{m}$ .

### 3.2.1.2 OMVs purification

PP1Y cells were grown in PPMM supplemented with 0.4% glutamic acid, in the same experimental conditions described above, and 2 L of exhausted growth media were processed as described above. Vesicles were purified through ultracentrifugation by stratifying the sample on a sucrose gradient density (Materials and Methods). The fractions obtained from this procedure, one for each sucrose concentration, were separately recovered and analysed using AFM analysis. The sample before the density gradient separation (Fig. 21A) resulted to be heterogeneous in terms of particles shape and morphology. Figure 21B and 21D show the 20% and the 70% sucrose fractions, respectively, where size and morphology heterogeneity is still evident. The 60% fraction (Fig. 21C), instead, showed the presence of a homogenous population of small circular particles with the expected size of 100-200 nm [78, 80, 90, 93, 140]. Therefore, we focused our attention exclusively on the vesicles isolated in the 60% sucrose fraction, from now on referred to as OMVs. The total protein concentration of purified OMVs was performed, and indicated that these latter had a total protein concentration of ca.  $\sim 340 \mu\text{g/mL}$ .

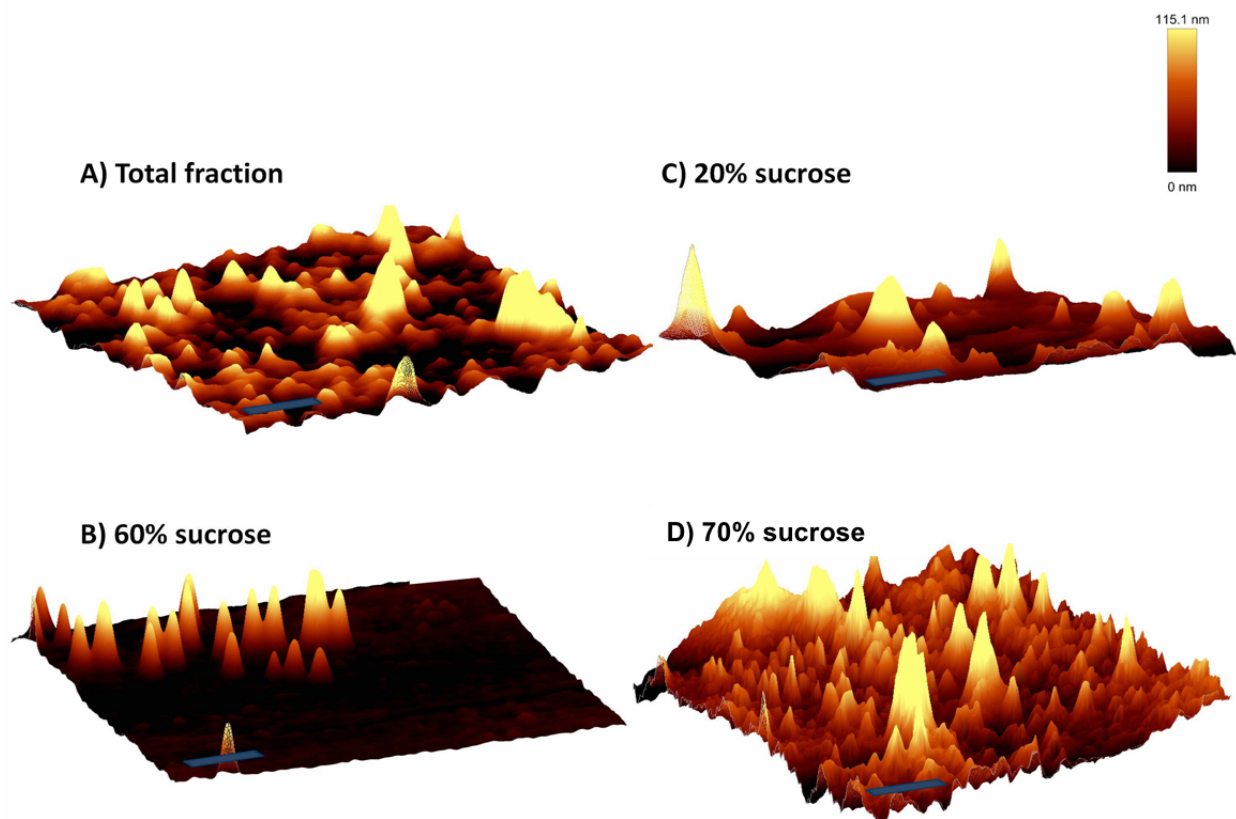


**Figure 21.** AFM images of OMVs total fraction (**A**), 20% sucrose fraction (**B**), 60% sucrose fraction (**C**) and 70% sucrose fraction (**D**). Scale bars 1  $\mu\text{m}$ . Data are resulting of three independent experiments.

### 3.2.1.3 OMVs characterization

#### - Size determination

To better define their size and morphology, purified OMVs were analysed using dynamic light scattering (DLS) technique, which indicated the presence of a homogenous population owning a size of 130-150 nm (Fig. 22). The same sample was also analyzed through Nanotracking particles Analysis (NTA). This methodology allows knowing, as a function of particles movement in a fluid medium, the size of nanoparticles and their concentration (particles/mL). NTA analysis confirmed for these OMVs an average size of ~ 130 nm (Figure 23) and a concentration of about  $1.02 \times 10^9$  particles/mL. Z-potential and electrophoretic mobility of these novel OMVs were measured using the Doppler anemometry function of the Zetasizer Nano ZS. Results showed a Z-potential of -11.0 mV ( $\pm 0.757$ ) with an electrophoretic mobility of -0.864 ( $\mu\text{m} \times \text{cm}$ )/Vs ( $\pm 0.0616$ ). The net negative charge of these nanostructures was consistent with a cell wall charge as other OMVs reported in literature [140].

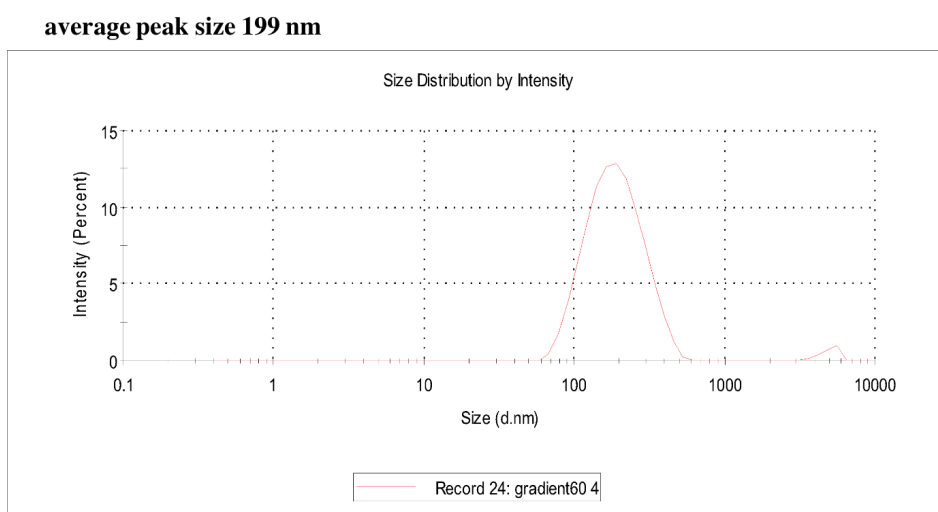


**Figure 22:** DLS size distribution of purified OMVs. Figure is representative of 3 independent experiments. The average peak size resulted to be 199 nm. All measurements resulting of three independent experiments.

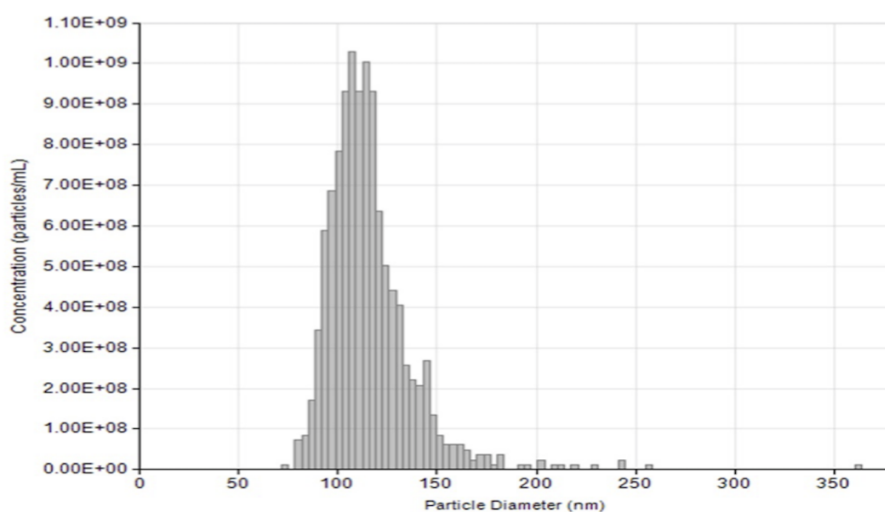


**Figure 23.** NTA analysis of purified OMVs. All measurements derive from three independent experiments.

*- Proteomic analysis*

To obtain protein composition of purified OMVs, an LC-MS/MS- based approach was used in collaboration with Dr. Fabrizio Dal Piaz (Department of Medicine, Surgery and Dentistry at the University of Salerno). Results were compared with those obtained on whole *N. sp.* PP1Y cells. At least six analyses for each sample type were performed: only those proteins that were detected in all measurements were taken into account. Using such a restrictive approach it was possible able to positively identify 17 proteins (Table 5). An high score was achieved for Protease IV; in addition, other hydrolytic enzymes were identified such as Amidase, 3-oxoacyl-(Acyl-carrier-protein) reductase, alpha-L-fucosidase, aldehyde dehydrogenase (Table 5 and figure 24D). A comparison between proteins identified in OMVs and in whole PP1Y cells showed that many proteins that resulted highly abundant in the bacterium were completely absent in OMVs proteome. In particular, as underlined in figure 24, PP1Y OMVs contained a higher percentage of hydrolytic enzymes and other enzymatic activity and a total absence of enzymes implicated in metabolic processes (Fig. 24D), compared to PP1Y whole cells (Fig. 24C). Moreover, PP1Y OMVs contained more membrane proteins (37%) (Fig. 24B) compared to whole cells (12%) (Fig. 24A), and only a little presence of intracellular proteins (19%) was detected (Fig 24B).

Score	significant matches	significant sequences	Description	Gene
11820	499	18	Protease IV	PP1Y_AT18626
577	6	5	Molecular chaperone GroEL	PP1Y_AT4091
232	5	3	Peptidase M48, Ste24p	PP1Y_AT37085
209	5	3	Methylmalonyl-CoA epimerase	PP1Y_AT13590
189	4	3	TonB-dependent siderophore receptor	PP1Y_Mpl5927
176	4	3	Amidase	PP1Y_Mpl2820
161	3	3	Outer membrane protein	PP1Y_Mpl9648
159	4	3	Two-component system, NtrC family, response regulator	PP1Y_AT21969
143	4	3	3-oxoacyl-(Acyl-carrier-protein) reductase	PP1Y_AT18239
138	3	3	Carboxypeptidase-related protein	PP1Y_AT34079
124	3	2	Alpha-L-fucosidase	PP1Y_Mpl858
114	3	2	Acetyl-CoA hydrolase/transferase	PP1Y_AT33599
105	3	3	Methylitaconate delta2-delta3-isomerase	PP1Y_Mpl10392
97	2	2	Aldehyde dehydrogenase	PP1Y_AT13240
93	2	2	Dimethylmenaquinone methyltransferase	PP1Y_AT31205
89	2	2	Adenosylmethionine-8-amino-7-oxononanoate aminotransferase	PP1Y_AT5612
75	2	2	Major facilitator transporter	PP1Y_AT12732

**Table 5.** Proteins profile identified by LC-MS/MS-based proteomic analysis of OMVs.

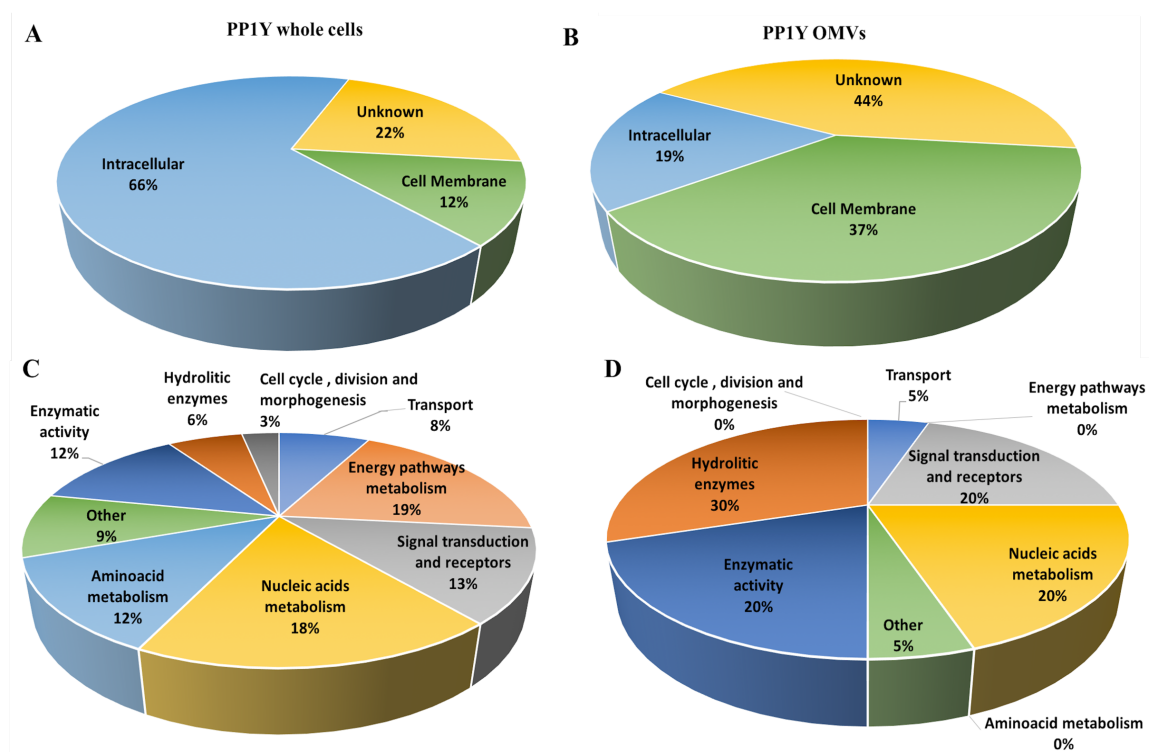


**Figure 24.** Proteomic profile analysis. Subcellular localization (A-B) and biological function (C-D) of PP1Y whole cell (A, C) and OMVs (B, D) proteins.

#### - Fatty acids and carbohydrate analysis

OMVs fatty acid profile was also evaluated [141-143]. A gas chromatography analysis was performed in collaboration with Dr. Armando Zarrelli (Department of Chemical Sciences, University of Naples Federico II) on purified OMVs and fatty acid methyl esters were identified by comparing their retention times with those of 22 commercial fatty acid standards, with the limit of quantitation of 14 *parts per billion* (ppb). Results (Table 7 and Fig. 25) underlined differences between PP1Y whole cells and OMVs. More in detail, OMVs membrane showed a greater abundance of Saturated Fatty Acids (SFAs) compared to PP1Y cell membranes. A more significative evidence could be obtained by grouping fatty acids into four different groups (Figure 25): Unsaturated Fatty Acids (UFAs), Poly-Unsaturated Fatty Acids (PUFAs), Mono-Unsaturated Fatty Acids (MUFAs) and Saturated Fatty Acids (SFAs) [143].

Comparison between OMVs and PP1Y cells composition, reported in Figure 6, revealed that OMVs membrane had a great abundance of SFAs, corresponding to 71% of total fatty acids, and about 9% of MUFAs, whereas PP1Y cell membrane contained only 4% of SFAs, almost the same percentage of MUFAs (8.8%) and 87.2% of PUFAs.

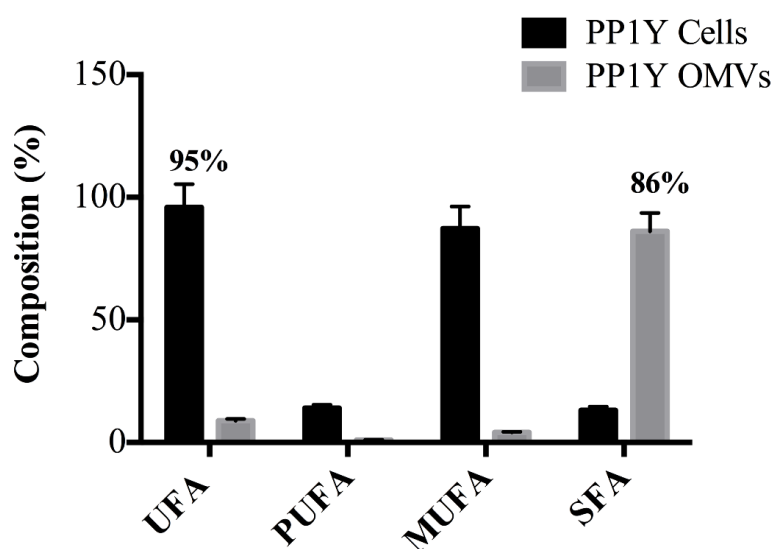


**Figure 25.** Fatty acid composition of PP1Y membranes (raw black) and OMVs (raw grey) are reported in terms of percentage of total amount. Data are resulting of three independent experiments. Errors were always within 20%.

Fatty acid	PP1Y cells	OMVs
Myristic (14:0)	0.1	27.4
Palmitic (16:0)	0.6	29.4
Trans Palmitoleic (16:1 n7)	1.7	0.5
Palmitoleic (16:1 n7)	3.0	0.0
Stearic (18:0)	1.7	29.3
Trans oleic (18:1 n9)	0.0	0.2
Oleic (18:1 n9)	3.0	0.0
Trans linolenic (18:2 n6)	0.8	4.2
Linolenic (18:2 n6)	0.0	1.6
Alpha-linolenic (18:3 n3)	23.3	1.6
Gamma-linolenic (18:3 n6)	0.0	0.2
Eicosenoic (20:1 n9)	1.1	0.0
Arachidonic (20:4 n6)	51.5	2.9
Eicosadienoic (20:2 n6)	0.7	0.0
Dihomo-gamma-linolenic (20:3 n6)	8.8	0.0
Nervonic (24:1 n9)	0.0	0.2
Lignoceric (24:0)	1.6	0.0
Eicosapentaenoic (20:5 n3)	0.0	0.0
Docosatetraenoic (22:4 n6)	0.1	0.0
Docosapentaenoic-3 (22:5 n3)	1.1	0.0
Docosapentaenoic-6 (22:5 n6)	0.2	0.0
Docosahexaenoic (22:6 n3)	0.7	2.5

**Table 7.** Fatty acids composition of *N. sp* PP1Y OMVs and whole cells.

As for carbohydrate analysis, OMVs showed as main component glucose, likely deriving from the sucrose contamination used for the gradient. Beside this monosaccharide, vesicles contained (in low amounts) galacturonic acid and galactose (data not shown). The heavy contamination of sucrose unfortunately hampered a quantitative evaluation of these and other sugars present in the vesicles.

### 3.2.1.4 Biocompatibility

In order to use these isolated OMVs as drug delivery systems, their biocompatibility was preliminary evaluated using, as a model, human normal keratinocytes (HaCaT) cells. Biocompatibility of purified OMVs was assessed by performing an MTT assay. Cells were seeded on 96-well plates and treated with 10 and 25  $\mu\text{g}/\text{mL}$  of purified OMVs. After 1,5 and 4 hours of incubation, a MTT stock solution in 1X PBS was added to the cells to a final concentration of 0.5  $\text{mg}/\text{mL}$  and, after a 4h incubation, MTT formazan salts were dissolved in 100  $\mu\text{L}$  of 0.1 N HCl in anhydrous isopropanol. Cell survival was expressed as the ABS of blue formazan measured at 570 nm with an automatic plate reader. Three independent experiments were performed and, for each experiment, standard deviations were always  $<5\%$ . Results shown in Figure 26, underlined that cell viability was not affected at any of the concentration and incubation time tested, indicating that OMVs does not affect human keratinocytes viability.

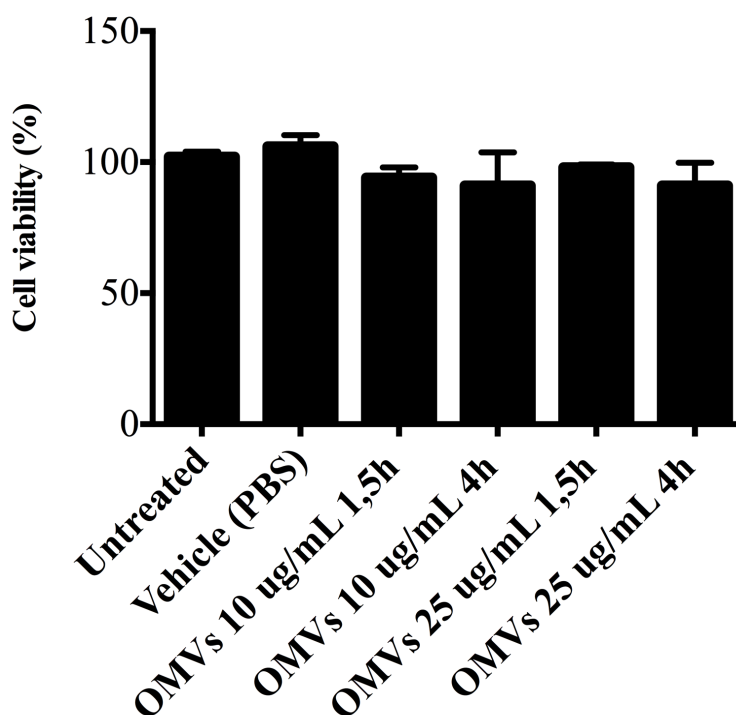


**Figure 26.** MTT assay on HaCaT cell line. Cell survival is expressed as percentage compared to control. Data are resulting of three independent experiments. Standard deviations were always  $<5\%$  for each experiment.

### **3.2.2 Extracellular Vesicles (EVs) from macrophages**

Extracellular vesicles (EVs) are membrane-derived particles of 30-2,000 nm diameter, released by cells in the human body [108]. EVs are classified, based on their cellular origin, biological function or biogenesis, in exosomes and microparticles (MPs) [71]. Within the past decade, EVs have gained much attention as biotechnological tools for enzyme immobilization and drug delivery systems. However, to evaluate their effective use, their inflammatory properties need to be better investigated. Among others, we decided to focus our attention on monocyte-derived EVs, a system well described in literature, that are characterized by pro-inflammatory effects, mostly through interaction with endothelial cells, but also with other cells, including monocytes themselves, fibroblasts, and smooth muscle cells [124]. Main aim of this part of my PhD project, which was performed at the laboratory of Professor Ramarosan Andriantsitohaina of the University of Angers (INSERM), France, has been to better characterize monocytes/macrophages-derived EVs.

#### **3.2.2.1 Isolation of extracellular vesicles (EVs) from murine macrophages RAW 264.7 cell lines**

In order to isolate and characterize EVs (Both MPs and Exosomes) from macrophages, a murine cell line (RAW 264.7) was selected and different types of stimulations were chosen, such LPS, Oleic Acid (OA) and Palmitic Acid (PA) [146]. Different concentrations were tested for each type of stimulation, and optimal vesiculation conditions were set-up. Two million RAW 264.7 cells were plated in T75 flasks and cultured in DMEM high glucose at 37°C, 5%CO<sub>2</sub>, as described in Materials and Methods. To get rid of serum-contaminating EVs, cells were pre-incubated in a medium deprived of FBS for 24 hrs and stimulated for additional 24 hrs either by using LPS (5 µg/mL), or oleic acid (400 µM), or palmitic acid (400 µM).

It is important to underline that EVs are classified in two principal groups: exosomes and microparticles (MPs) [71] and their purification is carried out following a combination of centrifugation steps at different *g* values [147]. Supernatants recovered from the three different stimulation conditions were first centrifuged at 1,500 *g* for 15 min to eliminate cellular debris. Cell supernatants were then centrifuged twice at 15,000 *g* for 50 min to isolate Microparticles (MPs) first. Pellets containing MPs were suspended in 200 µL of 0.9% NaCl in sterile water and stored at 4 °C. Supernatants were ultracentrifuged twice at 200,000 *g* for 2 h and pellets, which contain exosomes, were suspended in 200 µL of PBS 1X and stored at 4 °C.

A first protein quantification, performed using Biorad quantification kit, indicated that LPS stimulation increased both the MPs and exosomes amount; oleic acid stimulation increased mostly MPs secretion, whereas palmitic acid treatment increased exosomes vesiculation (Fig. 27)

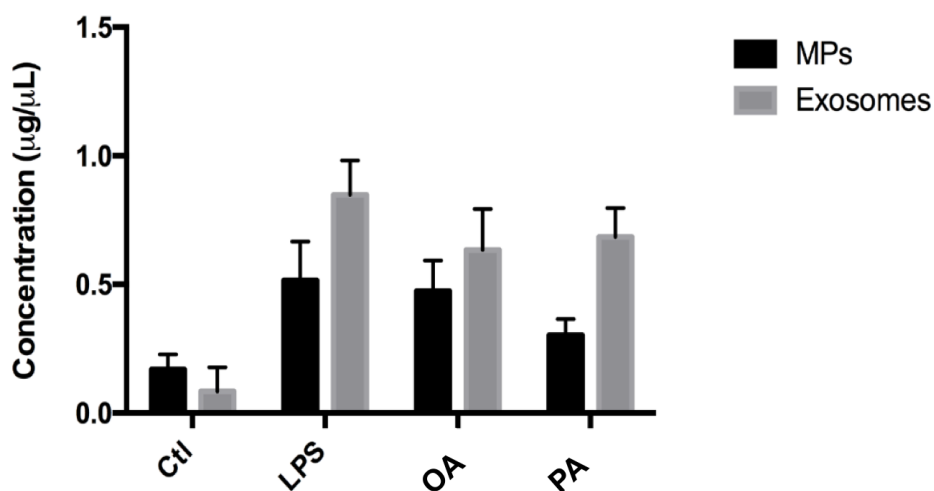


**Figure 27.** Vesicular protein quantification. Data are resulting of three independent experiments. Errors were always within 20%.

### 3.2.2.2 Characterization of EVs

#### - Size determination

Exosomes were analysed by Nanoparticle Tracking Analysis (NTA) technique, using Malvern NanoSight instrument. Exosomes samples were diluted at a final concentration of 0.02 µg/mL and loaded on Malvern NanoSight instrument. Three independent experiments were performed and results are shown in Figure 28 A-B. It is evident that all exosomes are characterized by an average diameter of  $\approx 100$  nm (Fig 28A) and no significant variation between vesicles derived from different growth conditions were evidenced. Conversely, particles concentration (Fig. 28B) underlined important differences among all conditions tested. In particular, stimulation with LPS and Palmitic Acid increased the amount of exosomes isolated compared to both control (non-stimulated cells) and macrophages stimulated with Oleic Acid (Fig 28B).

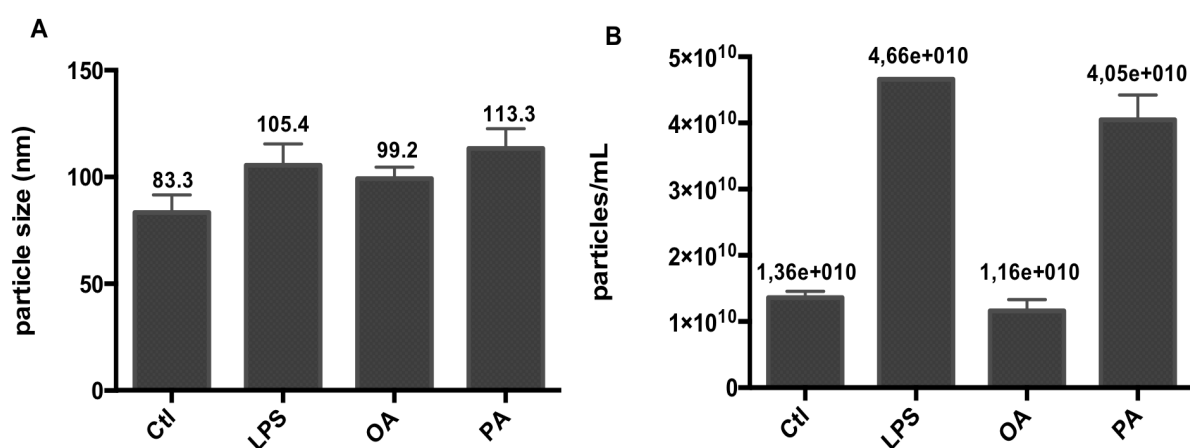


**Figure 28.** NTA exosomes analysis. Comparison of size distribution (A) and exosomes concentration (B). Data are resulting of three independent experiments. Standard errors were always within 20%.

MPs were instead analysed using flow cytometry (FC) analysis [148-149] and using annexin V as a marker for MPs [147,150]. 5  $\mu$ L of each MPs sample were incubated with Annexin V for 30' at RT, and charged on FC500 Beckman coulter, France cytometer. Results, obtained from three independent experiments (Fig 29), revealed that all MPs were Annexin V-positive with a diameter of  $\approx$  400 nm. Interestingly, MPs amount mainly increased when RAW 264,7 cells were treated with LPS and Oleic Acid (Fig. 29).

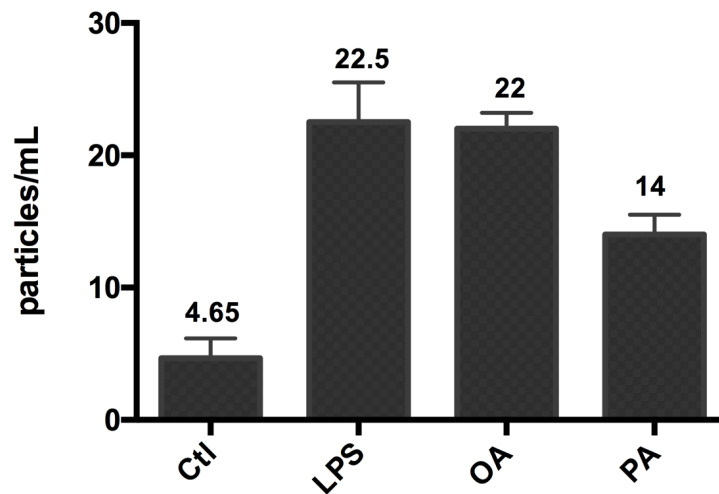


**Figure 29.** Microparticles cytometric analysis. Data shown, derived from 3 independent experiments and p value is always under 0,005.

#### - Protein content analysis

To investigate the presence of some exosomes and MPs target proteins, such as CD63, CD81, CD9, Alix and  $\beta$ -Actin [107,152], in the isolated nanostructures, a western blot analysis was performed. To this purpose, 20  $\mu$ g of total proteins was loaded on SDS-PAGE precast gel and western-blot analysis was performed as described in Materials and Methods. From the results obtained,  $\beta$ -Actin was exclusively recovered in the MPs fraction and was instead undetectable in the Exosome fraction (Fig. 30), in agreement with data reported in literature [153]. In contrast, exosomes were significantly enriched with Alix (Fig. 31 C), the endosomal sorting complex required for transport I (ESCRT-I) component and the tetraspanins CD9 and CD81 (Fig. 31 A-B). No significative difference was observed between EVs isolated under the different conditions tested.

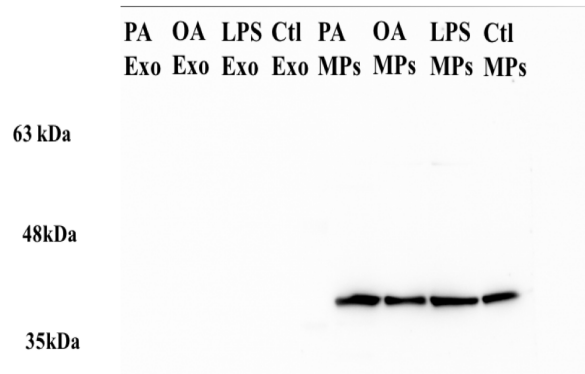


**Figure 30:**  $\beta$ -actin expression in exosomes and MPs. Lane 1: exosomes isolated from macrophages stimulated with palmitic acid; lane 2: exosomes isolated from macrophages stimulated with oleic acid; lane 3: exosomes isolated from macrophages stimulated with LPS; lane 4: exosomes isolated from unstimulated macrophages; lane 5: MPs isolated from macrophages stimulated with palmitic acid; lane 6: MPs isolated from macrophages stimulated with oleic acid; lane 7: MPs isolated from macrophages stimulated with LPS; lane 8: MPs isolated from unstimulated macrophages. The figure shows a representative example of three independent Western blot analysis.

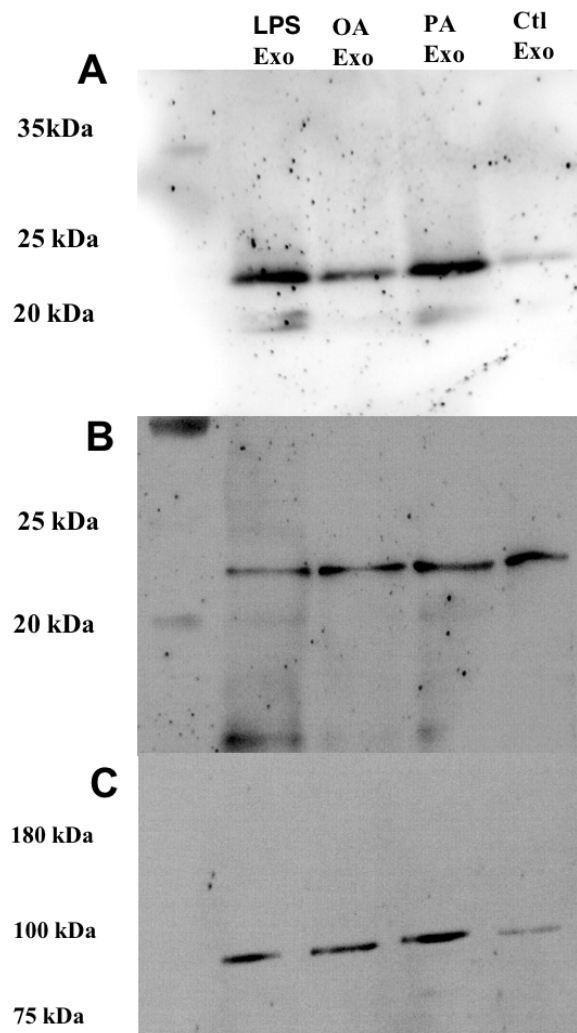


**Figure 31:** CD9 (A) CD81 (B) and Alix (C) expression in exosomes. Lane 1: molecular weight standard; lane 2 exosomes isolated from macrophages stimulated with LPS; lane 3: exosome isolated from macrophages stimulated with oleic acid; lane 4: exosome isolated from macrophages stimulated with palmitic acid; lane 5: exosomes isolated from unstimulated macrophages. The figure shows a representative example of three independent Western blot analysis.

### 3.2.2.3 The role of isolated EVs in inflammatory processes

#### - *Nlrp3* presence on isolated EVs

EVs appear to be a suitable alternative to traditional delivery systems currently in development, limiting inflammation processes and enhancing specific delivery. For this reason, studying the effect of macrophages-derived EVs in the inflammatory process could be particularly beneficial for the development of a future drug delivery strategy. In recent years a strict correlation between EVs derived from macrophages and the presence of inflammatory states was demonstrated [154]. In particular, these pathologies are caused by the action of a specific complex, named “inflammasome”, and Nlrp3 (Nucleotide-binding domain and leucine rich repeat containing family pyrin domain containing) remains the best-studied model of inflammasome [154].

In this context, the presence of Nlrp3 was evaluated on both exosomes and MPs isolated from murine macrophages.

All EVs isolated from macrophages cultured in all conditions previously described (*i.e.* LPS, OA, PA) were quantified as described in paragraph 4.1; 20  $\mu$ g of total proteins were loaded on a SDS-PAGE, transferred on a nitrocellulose membrane and WB analysis were performed as described in Materials and Methods. Results, showed in Figure 32, underlined a marked increase of Nlrp3 expression on both exosomes and MPs isolated from macrophages stimulated with PA and LPS, in accordance with what is described in literature [155-156]. Conversely, oleic acid does not seem to modify Nlrp3 expression in EVs (both MPs and exosomes), as already described in literature [157]

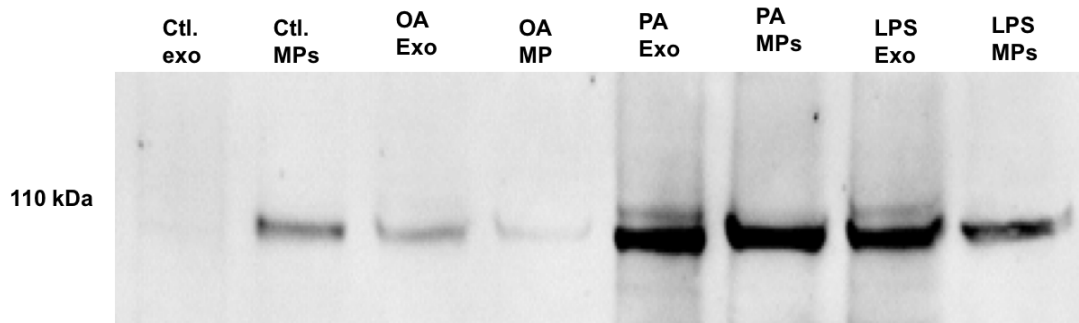


**Figure 32.** Western blot analysis of Nlrp3 in MPs and exosomes isolated from macrophages. Lane 1: exosomes isolated from unstimulated macrophages; lane 2: MPs isolated from unstimulated macrophages; lane 3: exosome isolated from macrophages stimulated with oleic acid; lane 4: MPs isolated from macrophages stimulated with oleic acid; lane 5: exosome isolated from macrophages stimulated with palmitic acid; lane 6: MPs isolated from macrophages stimulated with palmitic acid; lane 7: exosomes isolated from macrophages stimulated with LPS; lane 8: MPs isolated from macrophages stimulated with LPS. The figure shows a representative example of three independent Western blot analysis.

-Effects of EVs on vascular smooth muscle cells.

To evaluate possible different effects of EVs on inflammatory processes, cardiovascular cells, and in particular murine vascular smooth muscle cells (VSMC), were used as a model [158]. The induction of inflammation *via* inflammasome activation occur once the protein complexes have formed and the inflammasome activate caspase-1, which proteolytically activates the pro-inflammatory cytokines interleukin-1 $\beta$  (IL-1 $\beta$ ) and IL-18 [160] causing a rapid, pro-inflammatory form of cell death called pyroptosis [161]. In addition, inflammasome activation could stimulate cell apoptosis mechanism through the activation of caspase 8 [162] (Fig.33).

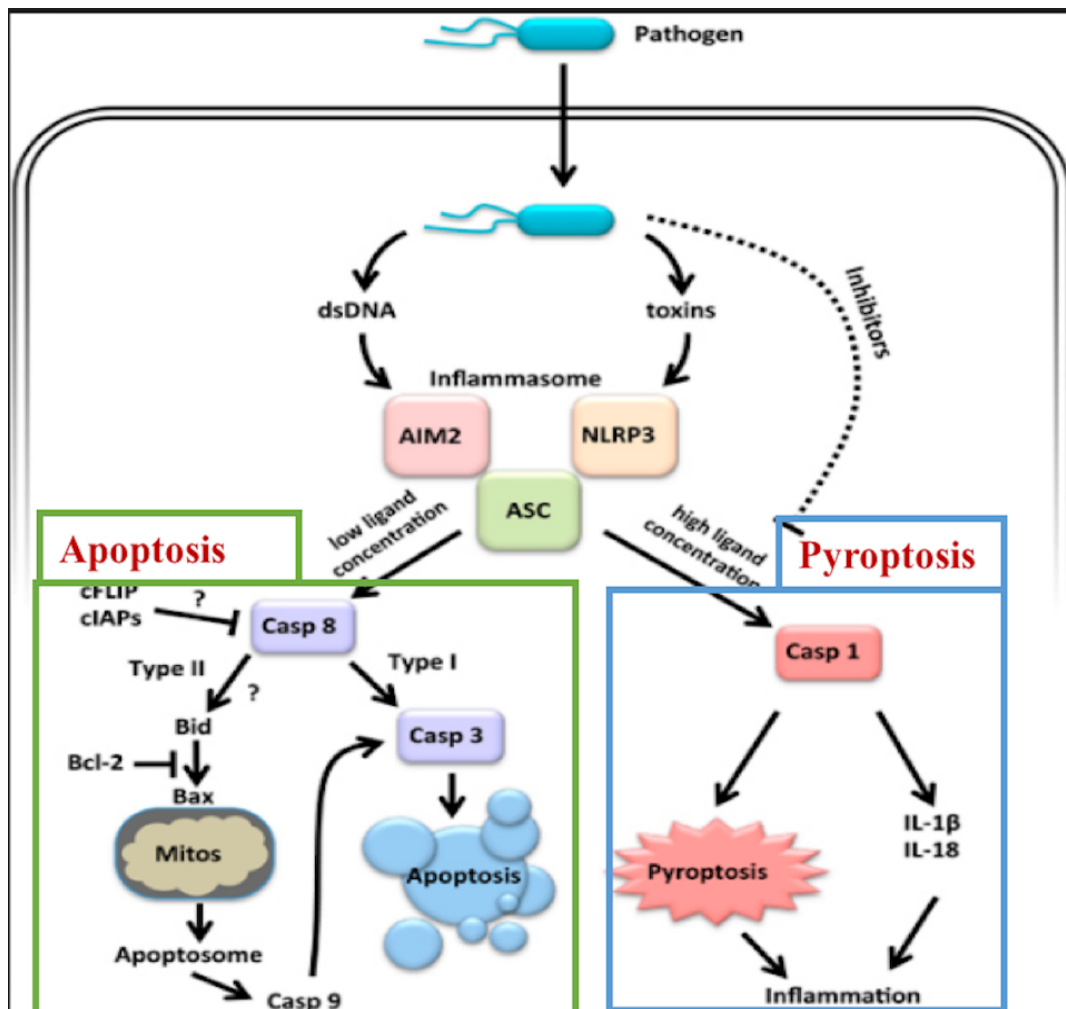


**Figure 33.** Framework of Nlrp3 inflammasome activation. Pyroptosis activation is indicated in the blue square, while in the green one induction of apoptosis is depicted.

In order to understand EVs inflammation mechanism induction, VSMC were isolated from a murine Aorta as described in Materials and Methods, and cultured in DMEM supplemented with 10% FBS, 4mM L-glutamine, 1% v/v penicillin/streptomycin solution (100 U/ml) and 1mM sodium pyruvate (Euroclone, Milano, Italy) at 37°C in 5% CO<sub>2</sub> incubator. VSMC cells were treated with 40  $\mu$ g/mL of all EVs samples and, after 4 hrs of incubation, cells were detached, collected and lysed. In all experiments 10

µg/mL LPS was used as positive control; moreover, to confirm Nlrp3 involvement in this mechanism, all conditions were also tested by pre-treating VSMC cells with a Nlrp3 inhibitor (MCC95 at a final concentration of 0,5 µM) [163]. Cell lysates were used to perform western-blot analysis, where 20 µg of total proteins were loaded on SDS-PAGE precast gel and western-blot experiments were performed as already described (Materials and Methods).

Figure 34 showed EVs (both MPs and exosomes) effect on caspase-1 activation. It is evident that MPs and exosomes isolated from macrophages stimulated with LPS increased the concentration of activated caspase-1 in VSMC cells; in this case, control performed with cells pre-treated Nlrp3 inhibitor (MCC95) does not show the same effect (Fig 34A). The same outcome occurs for both exosomes and MPs isolated from macrophages stimulated with palmitic acid (Fig 34B). For what concerns oleic acid stimulation, only exosomes showed a caspase-1 activation Nlrp3-dependent (Fig 34B). Figure 35 shows EVs (both MPs and exosomes) effect on caspase-8 activation. It is evident that caspase-8 levels increased only when VSMC cells were treated with exosomes isolated from macrophages stimulated with LPS (fig 35A). When considering palmitic acid stimulation, only exosomes isolated showed a caspase-8 activation, whereas control with Nlrp3 inhibitor does not influence caspase-8 activation (Fig. 35B). Exosomes isolated from macrophages stimulated with oleic acid increased caspase-8 amount, also in presence of MCC95 (Fig. 35B). EVs isolated from unstimulated macrophages did not increase either caspase-1, nor caspase-8 activation.

\* : pvalue ≤ 0,05

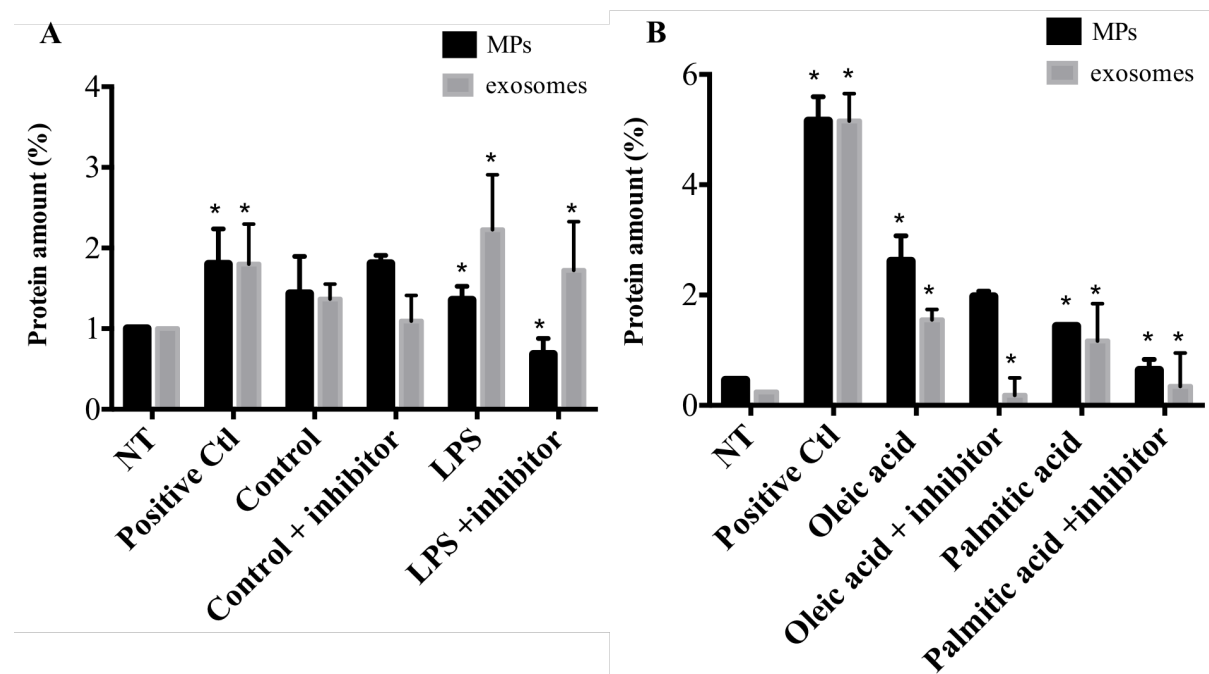


**Figure 34.** Western blot analysis of Caspase-1 expression in VSMC cells treated with EVs isolated. NT: Non-treated VSMC; positive control: VSMC treated with LPS 5 µg/mL; control: VSMC treated with EVs isolated from unstimulated macrophages; LPS: VSMC treated with macrophages stimulated with LPS; Oleic acid: VSMC treated with macrophages stimulated with oleic acid; Palmitic acid: VSMC treated with macrophages stimulated with palmitic acid. Data reported are representative of Three independent experiments.

\* : pvalue  $\leq$  0,05

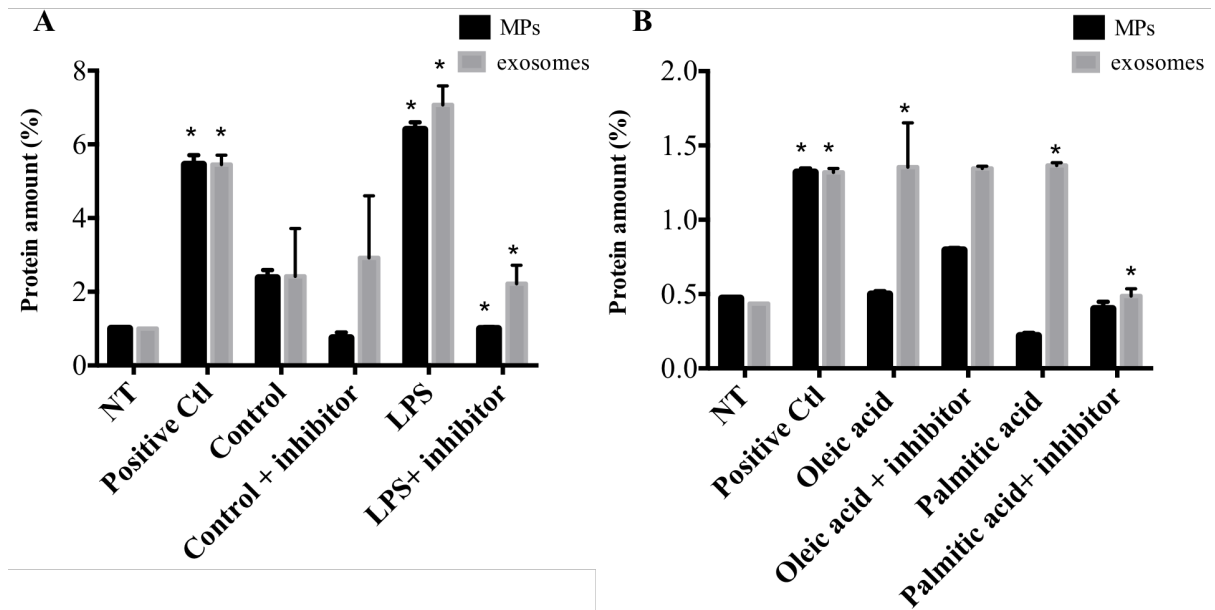


**Figure 35.** Western blot analysis of Caspase-8 expression in VSMC cells treated with EVs isolated. NT: Non-treated VSMC; positive control: VSMC treated with LPS 5  $\mu$ g/mL; control: VSMC treated with EVs isolated from unstimulated macrophages; LPS: VSMC treated with macrophages stimulated with LPS; Oleic acid: VSMC treated with macrophages stimulated with oleic acid; Palmitic acid: VSMC treated with macrophages stimulated with palmitic acid. Data reported are representative of Three independent experiments.





---

# **CHAPTER IV**

## **DISCUSSION**

---



## CHAPTER 4

---

### DISCUSSION

Nowadays, biocatalysis represents a versatile and valuable tool for the development of industrial biotechnologies and can be performed with either whole cells or purified enzymes. Whereas whole cells generally offer a simple and effective option for cofactor regeneration and enhanced enzyme stability, protein engineering and the use of single enzymes continues to be considered more economic and practical. Nevertheless, the use of enzymes in industrial applications is still limited by several factors, mainly the high cost of enzymes, their instability, and their availability in small amounts. To overcome these problems, the quest for new catalytic activities from one side, and the development of new technical approaches to improve their stability and practical applications from the other, remain a central focus of current biotechnological research. Among these, technological developments in the field of immobilized biocatalysts resulted to be a very powerful tool to improve almost all enzyme properties, such as stability, activity, specificity selectivity, and enzyme inhibition [58, 59]. In this framework, nanobiotechnology is gaining much attention from the scientific community, and “nanobiocatalysis” is one direct application of this growing field [66] in which artificial or natural lipid bilayers of biological membranes from bacteria (Outer Membrane Vesicles) and eukaryotic cells (Extracellular Vesicles) might be used as versatile immobilization systems.

In this PhD thesis, the quest for new enzymatic activities and the need to explore new biological systems for the immobilization of biotechnologically relevant enzymes were investigated by *i*) expressing and characterizing a recently identified bacterial rhamnosidase, and *ii*) isolating and characterizing both bacterial OMVs and eukaryotic vesicles (EVs) to be used as innovative scaffolds for the immobilization of enzymes or as delivery systems.

For what it concerns the first aim, a novel  $\alpha$ -RHA (rRHA-P) was successfully isolated and characterized from *Novosphingobium* sp. PP1Y, a gram-negative bacterium isolated from surface waters of a small dock bay in the harbor of Pozzuoli.  $\alpha$ -RHAs are a group of glycosyl hydrolases (GHs) that have attracted a great deal of attention due to their potential application as biocatalysts in a variety of industrial processes. These enzymes are of particular interest for the biotransformation of several natural compounds that are used in pharmaceutical and food industry, as the removal of the terminal rhamnose residues might improve their bioavailability in the small intestine.

The recombinant expression in *E. coli* was optimized and the purification protocol was implemented to obtain a protein suitable for a further biochemical and structural characterization. More in detail, first attempts of expression of the recombinant protein, rRHA-P, resulted in the foremost presence of the protein in the insoluble portion of the induced cultures. A lower induction temperature, shifted from 37 °C to 23 °C, along with the use of a high-salt LB formulation containing both betaine and sorbitol, which presumably act as “chemical chaperones”, efficiently concurred in improving the yield of soluble, active rRHA-P. It is well known that the induction temperature is considered as one of the main determinants responsible for protein misfolding in recombinant expression and consequent formation of inclusion bodies. In addition, several evidences in literature have shown that the addition of osmolytes such as betaine and sorbitol to the culture medium of induced recombinant cells of *E. coli* helps in assisting protein folding and might increase protein solubility [135-136]. This effect can be improved by the presence in the growth medium of a high salt concentration that might be responsible for both increasing the uptake rate in the cytoplasm of betaine and

sorbitol from the extracellular environment and adjuvating the effect of the osmolytes themselves by inducing the expression of additional heat-shock proteins that help in assisting protein folding [136]. Indeed, by combining a lower temperature with the presence of osmolytes and a 2.9% final concentration of NaCl in the growth medium, we succeeded in obtaining a reasonable amount of active protein, which was purified following a three-step purification protocol, but with a relatively poor yield.

A preliminary structural characterization showed that rRHA-P is a monomeric protein with an approximate molecular weight of  $101,500 \pm 5,000$  Da. Mechanism of action, kinetic parameters and optimum reaction conditions were determined using a synthetic substrate, pNPR. As for the reaction mechanism, GHs are generally grouped in two main classes, inverting and retaining. These different hydrolysis mechanisms lead to a retention or an inversion of the anomeric oxygen configuration of the substrate [137]. NMR experiments showed that rRHA-P acts as an inverting GH, although further investigation is needed to better investigate the details of the catalytic mechanism.

rRHA-P catalytic efficiency, defined by a  $K_S$  value of  $4.6 \text{ s}^{-1} \text{ M}^{-1}$ , underlined an activity comparable or even higher than that of other bacterial  $\alpha$ -RHAs described in literature. When clearly reported, such as in lactic acid bacteria *Lactobacillus plantarum*, and *Pediococcus acidilactici*,  $K_S$  values on pNPR range from  $0.01 \text{ s}^{-1} \text{ M}^{-1}$  to  $0.019 \text{ s}^{-1} \text{ M}^{-1}$  [42-43]. In addition, rRHA-P  $K_S$  resulted to be approximately 3 times higher than the one reported for the  $\alpha$ -RHA isolated from *S. paucimobilis* FP2001 [51] and the comparison among the  $K_M$  values present in literature, ranging from 1.18 mM for *S. paucimobilis* FP 2001 to 16.2 mM for the  $\alpha$ -RHA isolated from *P. acidilactici*, showed a higher apparent affinity of rRHA-P for pNPR ( $K_M$  of 160  $\mu\text{M}$ ). In addition, rRHA-P appeared to be a valuable biocatalyst in the biotransformation of flavonoids, due to its optimal reaction conditions in terms of pH, temperature and presence of organic solvents. More in detail, rRHA-P, in line with other bacterial  $\alpha$ -RHAs, has an optimal activity at pH 6.9, but retains a significative percentage of its enzymatic activity at pH 8.0, which is suitable for the conversion of flavonoids that are scarcely soluble at lower values of pH. rRHA-P shows also an optimal activity at  $40.9^\circ\text{C}$  and a significant overall thermal stability, retaining ~66% of the activity up to  $45^\circ\text{C}$ , a temperature range mainly used in most industrial processes. A great majority of other fungal and bacterial enzymes exhibit also similar values of temperature stability and optimal activity [35,37,42-44], whereas only a limited number of  $\alpha$ -RHAs is more thermophilic and has an optimum of temperature at ca.  $60^\circ\text{C}$  [42,47]. In addition, rRHA-P has a moderate tolerance to organic solvents, which are usually employed for the biotransformation of flavonoids that are poorly soluble in water, retaining the 66% of activity in solutions containing 10% of either DMSO or ethanol. These data suggest a higher tolerance of rRHA-P to the presence of solvents compared to  $\alpha$ -RHAs described in literature for which a residual 20 – 30% activity in 12% ethanol and a 24% activity in 25% DMSO has been reported [35]. It is worth mentioning that rRHA-P residual activity in ethanol-containing buffers might be of additional importance as many biologically relevant rhamnosylated flavonoids are found in wine and possibly citrus derived alcoholic beverages.

In this framework, experiments to verify the hydrolytic properties of rRHA-P on few natural flavonoids containing either  $\alpha$ -1,2 or  $\alpha$ -1,6 glycosidic linkages were performed. TLC analysis showed a total conversion of naringin ( $\alpha$ -1,2 linkage) in the corresponding prunin and rhamnose, while a partial hydrolysis of rutin and

neohesperidin ( $\alpha$ -1,6 linkage) was observed, thus confirming the ability of this enzyme to hydrolyze both  $\alpha$ -1,2 and  $\alpha$ -1,6 linkages. Likewise, the majority of other bacterial and fungal  $\alpha$ -RHAs exhibit similar substrate specificity, even though these enzymes often show a slight preference for the hydrolysis of  $\alpha$ -1,6 linkages [42-43,47,138]. rRHA-P specificity on natural flavonoids resulted to be peculiar when compared to fungal counterparts, thus paving the way to the use of this enzyme for a new array of bioconversion applications.

However, despite all the interesting biotechnological aspects described so far, the poor yield of purification of rRHA-P was a major drawback to its use in large scale processes. We approached this problem with a dual strategy, *i.e.* by better investigating the initial sorting of the recombinant protein in the bacterial cell (periplasm vs. cytoplasm), and by fusing a His-tag to rRHA-P, thus reducing the purification steps to be used.

rRHA-P amino acid sequence, verified by MS mapping, showed the lack of the N-terminal peptide, suggesting the presence of a signal peptide presumably cleaved through a post-translational proteolytic processing. A similar evidence has been described for the  $\alpha$ -RHA isolated from *S. paucimobilis* FP2001, recombinantly expressed in *E. coli* [51]. The analysis of the amino acid sequence of the putative signal peptide revealed several features owned by bacterial signal peptides. These features encompass the presence of a charged region (2 – 5 residues) followed by a hydrophobic stretch of ~ 12 aa and, 1-3 aa upstream the cleavage site, the occurrence of small and hydrophobic residues. The functional role of this cleavage sequence, also in the native bacterium, is possibly due to the sorting of these proteins in the periplasmic space to accomplish their function. The presence of rRHA-P in the periplasmic space was confirmed by comparing specific activities separately measured in the cytoplasmic and the periplasmic fractions of the recombinant cells.

The use of the periplasmic fraction as starting material and the presence of a unique purification step concurred in improving the purification yield from 6.7% (untagged rRHA-P from the crude extract) to 25.3%, (His-tagged rRHAP from periplasm).

The analysis of the kinetic constants evaluated on *p*NPR suggested that the His-tag did not significantly affect the activity of the recombinant protein on this synthetic substrate.

Once improved the purification yield, we focused our attention on gathering more insights into the catalytic mechanism of rRHA-P, by identifying the residues involved in catalysis for a future fine-tuning of its activity, an important aspect in view of the biotechnological application of this enzyme.

Alignment of the RHA-Phis amino acid sequence with other 130 protein sequences belonging to the GH106 family was performed. Five highly conserved residues of glutamic and aspartic acid were identified, *i.e.* D503, E506, D552, E644 and D763, which were subjected to a “alanine scanning” mutagenesis.

RHA-Phis single mutants were successfully expressed and purified. Activity assays performed again on *p*NPR, both using recombinant whole cells and purified proteins, highlighted that mutations at positions D503, E506 and E644 led to an almost total inactivation of the enzyme, thus suggesting that these amino acids might be part of the catalytic residues present in the active site. On the other hand, mutations at positions D552 and D763 allowed maintaining a residual activity of 47.9% and 15.7% respectively, thus suggesting that residues D552 and D763 are not directly implicated in the functionality of the enzyme active site. After the initial screening procedure using whole recombinant cells, the evaluation of residual specific activity was performed on purified proteins. The hypotheses on the role of mutated residues were also supported

by the analysis of the kinetic constants measured on pNPR for these two partially active mutants. In fact, the decrease in the efficiency of catalysis, expressed by the  $K_s$ , is almost exclusively dependent on the  $k_{cat}$  value and not on a difference in the apparent affinity of the enzyme for the substrate, thus suggesting that the mutagenized residues might not be directly involved in the binding or positioning of the substrate in the active site.

The data collected would indicate the presence of better properties in comparison with similar enzymes and suggest a possible use of the enzyme for a large number of biotechnological purposes, in particular in the food industry. The possibility to fine-tune the activity of this enzyme can be foreseen, but undoubtedly more residues need to be mutagenized to gain a larger picture of the molecular determinants responsible for rRHA-P substrate specificity.

In this context, the determination of the 3D structure of the enzyme, either by homology modelling or by solving the crystal structure of the protein, is an important task to fulfil in the near future for better exploring the biotechnological potential of this bacterial rhamnosidase.

As underlined in the first part of the Discussion, the use of enzymes in industry is generally limited by their instability and availability in small amounts. Over the last few decades, intense research in the area of enzyme technology has provided many approaches that facilitate their practical applications. Among these, technological developments in the field of immobilized biocatalysts resulted to be a very powerful tool to improve almost all enzyme properties, such as stability, activity, specificity and selectivity.

Besides their application in industrial processes, immobilization techniques could pave the way to the development of a large number of biotechnological devices with applications in diagnostics and biosensors.

During the second part of my PhD project, two different potential immobilization scaffolds from bacteria (Outer Membrane Vesicles: OMVs) and from eukaryotic cell lines (Extracellular Vesicles: EVs) were isolated and partially characterized.

OMVs are spherical buds of the outer membrane (OM) filled with periplasmic content commonly produced by Gram-negative bacteria which can be foreseen as platforms for the immobilization of proteins and enzymatic complexes and could be employed as carriers for drugs. The possibility to use these structures for different biotechnological purposes has prompted a recent attention towards the isolation and characterization of OMVs from non-pathogenic bacteria [84,90]. During my PhD, OMVs were isolated from a non-pathogen Gram-negative microorganism lacking LPS, *Novosphingobium* sp. PP1Y. SEM analyses on PP1Y cells grown in minimal medium and collected during exponential phase showed the presence of rod-shaped cells in a matrix of globular nanostructures that resembled “canonical” OMVs described in literature.

Further attempts to analyze by SEM cell-free exhausted growth media to obtain images of free-floating vesicles failed to give positive results. To overcome this problem, cell free supernatants of PP1Y cells grown under different conditions were collected and analyzed using Atomic Force Microscopy (AFM). This technique is currently considered a gold standard for biological imaging compared to conventional microscopes such as SEM and TEM, because AFM does not require, among others, conducting materials for imaging, staining, labelling or coating of samples. By far, the greatest advantage of AFM is that cells and biomolecules can be imaged in physiological environments, in solution and under controlled temperatures [139]. Indeed, AFM analysis allowed us to identify OMVs in cell-free supernatants, before

and after an ultracentrifugation purification procedure on a sucrose gradient. AFM images confirmed OMVs production in *N. sp.* PP1Y grown in minimal medium during the late exponential phase, which could be explained as a physiological strategy of this microorganism to overcome a possible nutrients depletion in these conditions [84,88,92]. AFM, DLS and Nanosizer (NTA) data showed that purified OMVs from strain PP1Y are predominantly spherical in shape, with an average size of  $\approx 130$ -150 nm, which is in agreement with the description of other OMVs from different Gram-negative bacteria [85,90,95]. These vesicles were normally distributed, resulted to be homogeneous and owned a negative zeta potential of -11.0 mV ( $\pm 0.757$ ). The net negative charge of these nanostructures was consistent with a cell wall charge and with the values reported in literature for similar nanostructures [140]. Several studies described for OMVs a peculiar protein pattern characterized by a marked presence of OM proteins (e.g. OmpW) and some proteolytic enzymes for nutrient acquisition [80,91-92]. Proteins from these OMVs belong to different functional categories, including OM structural proteins, porins, ion channels, transporters, periplasmic and cytoplasmic enzymes, and proteins related to stress response [89,92]. Proteomic analysis of purified OMVs from PP1Y showed the presence of at least 17 proteins of *N. sp.* PP1Y among which the expression of Protease IV was predominant. This might be the direct consequence of the presence in the minimal medium of glutamic acid as sole carbon and energy source. In addition, other hydrolytic enzymes were identified, such as Amidase, 3-oxoacyl-(Acyl-carrier-protein) reductase, alpha-L-fucosidase, aldehyde dehydrogenase, which are in accordance with a physiological role of PP1Y vesiculation for environmental adaptation and nutrient acquisition. Interestingly, a comparison between proteins identified in OMVs and in whole PP1Y cells showed that many proteins that resulted highly abundant in the bacterium were completely absent in OMVs proteome, thus suggesting that proteins internalization in these vesicles might be finely regulated. Noteworthy, OMVs displayed a marked presence of membrane proteins when compared to PP1Y whole cells, thus confirming their peculiar composition and their origin from the outer membrane of this microorganism. In OMVs secretion, a finely controlled fatty acids distribution in the outer membrane has been already described, which is probably related to a complex relationship between membrane fluidity and vesicles biosynthesis [141-143]. In fact, fatty acids analysis underlined differences between PP1Y whole cells and OMVs. More in detail, OMVs membrane showed a greater abundance of Saturated Fatty Acids (SFA) compared to PP1Y cell membranes. This aspect has been already described for *P. aeruginosa*, where OMVs isolated from this bacterium contained a 71% of SFA vs. a 49% of these fatty acids present in the cell membrane [143]. It is worth to note that phospholipids that contain UFAs are more flexible than those richer in SFA [141-142]. Hence, it can be argued that OMVs show a more rigid membrane compared to "parental" cells. The decrease in membrane fluidity of PP1Y OMVs could confirm that these structures are released from membrane sites where the outer membrane is relatively rigid, as already suggested in literature [144]. Intriguingly, as a rigid membrane does not appear to easily adapt to changes in environment, it was also hypothesized that the release of OMVs could be an additional strategy to increase OM fluidity and thus bacterial survival in harsh environments [141,143-144]. However, the detailed mechanism of OMVs biosynthesis is still under investigation, both in pathogenic and non-pathogenic bacteria. Among the diverse applications, a great deal of attention was also devoted to the potential use of OMVs in drug delivery, enzyme immobilization and construction of innovative biosensors [78,96-97].

In this context, a preliminary evaluation of the biocompatibility of these structures for a possible use with eukaryotic cells was performed, by using human normal keratinocytes (HaCaT). In recent years, skin has been shown to contain a broad spectrum of enzymes capable to metabolize a wide range of topically applied drugs. This metabolic capacity may have consequences for the topical, as well as the transdermal delivery of drugs. For this reasons, there is growing interest in studying biocompatibility of drugs on skin cells lines. The spontaneously immortalized human keratinocyte cell line HaCaT represent a readily available *in vitro* model and has already been used as model for skin toxicity studies [164]. Biocompatibility of purified OMVs was assessed by performing an MTT assay, which suggested that OMVs do not affect human keratinocytes viability. However, the effect of OMVs on other cell lines such epithelial intestinal cells, endothelial cells and vascular smooth muscle cells should be also evaluated in the near future, to better investigate the biotechnological potential of OMVs as novel drug delivery systems.

EVs from eukaryotic cells, as well as bacterial OMVs, are ideal target for biotechnological purposes. The interest in using eukaryotic EVs rather than OMVs lies in their specific drug delivery application. Indeed, their specific cell-targeting might help in improving target-specific delivery [120,126-129]. Moreover, the fact that EVs derive from eukaryotic cells, could make these latter less immunogenic than OMVs, even if the presence of histocompatibility factors on EVs surface need to be further investigated.

Main aim of this part of my PhD project has been to better characterize macrophages-derived EVs, a system already well described in literature, which are characterized by pro-inflammatory effects, mostly through the interaction with endothelial cells, fibroblasts, and smooth muscle cells [14].

EVs are classified in two principal groups: exosomes and microparticles (MPs) [71]. MPs are small bioactive vesicles with a diameter between 0.1 to 1 $\mu$ m, whereas Exosomes have a diameter of 30-100 nm [126]. EVs, both exosomes and MPs, were isolated from murine macrophages and their release resulted to be stimulated by specific types of stress such as LPS, oleic acid and palmitic acid [145]. More in detail, LPS induces macrophage activation and stimulates immune responses by inducing the generation of cytokines such as tumor necrosis factor (TNF)-alpha, interleukin (IL)-1, and IL-6 [145]. Fatty acids such as oleic acid (OA) and palmitic acid (PA) seem to directly influence inflammatory gene expression [146]; in particular, palmitic acid increases pro-inflammatory gene expression like TNF- $\alpha$ , whereas oleic acid increases anti-inflammatory gene expression in macrophages [146].

In order to purify EVs (Exosomes and MPs), a combination of centrifugation steps at different *g* values was performed [147]. A differential production was observed for either exosome, where macrophages were stimulated with LPS and PA, or MPs, whose secretion was incremented by LPS and oleic acid stimulation. This differential effect could be explained by the fact that MPs and exosomes have different secretion mechanisms, which might be triggered by different molecular signals and cellular stress [126,145-146].

Exosomes were analyzed by Nanoparticle Tracking Analysis (NTA) technique, whereas MPs were analyzed by flow cytometry (FC) analysis [148-149] and using annexin V as a marker for MPs [147,150].

NTA is an advantageous technique to study nanoparticles from 10-1000 nm in solution, which are individually but simultaneously analyzed by direct observation and measurement of diffusion events. This particle-by-particle methodology produces high

resolution results for particle size distribution and concentration and allows to measure both particle size and concentration. Conversely, FC is a widely used method for MPs detection and recently, there have been improvements in the standardization of membrane vesicles FC measurements [148-149]. With this technique, it is possible to specifically identify particles of  $\approx$  300-500 nm diameter, using microbeads of the desired diameter, as standards, and evaluate their concentration in terms of particles/mL.

Results obtained for exosomes and MPs, underlined that the different vesiculation conditions did not affect EVs size. On the contrary, different cell stimulations influenced EVs amount. In particular, LPS cell stimulation caused an increase of both exosome and MPs number, whereas Palmitic Acid and Oleic Acid seemed to have different effects. More specifically, palmitic acid is responsible for the increase of exosomes production, whereas oleic acid increases MPs secretion. This differential effect could be explained by the fact that MPs and exosomes have different secretion mechanisms, which might be stimulated by different molecular signals [126].

Both exosomes and MPs have a well-defined protein profile. In particular, exosomes feature phosphatidylserine markers of tetraspanin family proteins including CD63, CD81, CD9, [107,152] and the endosomal protein Alix. Conversely,  $\beta$ -Actin was generally described in literature in the MPs fraction, in agreement with the critical role of cytoskeleton remodeling in the process of microvesicle shedding. Western Blot experiments performed on purified exosomes and MPs, showed a typical protein expression for each [152] and no contamination between MPs and exosomes was found.

In the overall goal to use EVs as novel drug delivery systems, it is important to better detail the effect of macrophages-derived EVs on the inflammatory process. In recent years, in fact, a strict correlation between EVs derived from macrophages and the presence of inflammatory states, such as type 2 diabetes and atherosclerosis, was demonstrated [154]. In particular, these pathologies seem to be caused by the action of a specific complex, named “inflammasome”, a large, multiprotein complex that oligomerizes in the cytoplasm of innate immune cells to cleave and activate pro-IL-1 $\beta$ . Nlrp3 (Nucleotide-binding domain and leucine rich repeat containing family pyrin domain containing) is a component of the inflammatory complex and remains the best-studied model of inflammasome [154]. In the light of this evidence, it was hypothesized that there could be an association between Nlrp3, Extracellular Vesicles and inflammatory diseases. In particular, it would be of interest to understand whether Nlrp3 could be conveyed by EVs from activated macrophages thus contributing to the induction of the inflammation process.

In this context, the presence of Nlrp3 was evaluated on both exosomes and MPs isolated from murine macrophages. Western Blot analysis underlined a marked increase of Nlrp3, in exosomes and MPs isolated after macrophages stimulation with LPS and PA, in accordance with what reported in literature [155-156]. It is already well known, in fact, that LPS chronic stimulation activates the NLRP3 inflammasome in macrophages [155-156]; moreover, fatty acids, in particular PA have recently been proposed as triggers of the NLRP3 inflammasome [157]. Conversely, OA does not seem to modify Nlrp3 expression in EVs (both MPs and exosomes), thus confirming what is already reported in literature [157].

Vascular smooth muscle cells (VSMCs) [158] were used in this part of my PhD project as a model to study the effect of macrophages-derived EVs in the inflammatory process. These cells undergo a unique, coordinated morphological and functional transition between contractile and synthetic states in injury and disease [158]. VSMC

inflammatory activation contributes to vessel pathophysiology, vascular disease progression and ultimately, adverse clinical outcome [159].

The inflammation induction that occurs *via* inflammasome activation begins once the protein complexes have formed and the inflammasome activate caspase-1 proteolitically activates the pro-inflammatory cytokines interleukin-1 $\beta$  (IL-1 $\beta$ ) and IL-18 [160], thus pyroptosis [161]. In addition, inflammasome activation could stimulate cell apoptosis mechanism through the activation of caspase 8 [162] (Fig.31). VSMC were isolated from a murine Aorta and treated with 40  $\mu$ g/mL of all EVs for 4 hrs. In all experiments 10  $\mu$ g/mL LPS was used as positive control; moreover, to confirm Nlrp3 involvement in this mechanism, all conditions were also tested by pre-treating VSMC cells with a Nlrp3 inhibitor [163].

Results obtained suggest a different effect among EVs on inflammation and vascular dysfunction. In fact, MPs and exosomes isolated from macrophages stimulated with LPS and PA increased active caspase-1 levels, in a Nlrp3 dependent manner, causing a canonical pyroptosis pathway. Conversely, only exosomes isolated from macrophages stimulated with both LPS and palmitic acid activated caspase-8, and subsequently apoptosis pathway. These results underlined a complex mechanism for inflammasome activation. Because of the great number and diversity of NLRP3 stimuli known to activate the NLRP3 inflammasome, it seems unlikely that they all bind to the NLRP3 structure to activate the inflammasome. Thus, a major question in the field relates to the exact molecular activation mechanism of the NLRP3 inflammasome.

Noteworthy, EVs naturally derived from macrophages (unstimulated), do not stimulate either inflammation or apoptosis pathways, suggesting these latter to be the real valid alternative to bacterial OMVs. However their large-scale production is still a major problem, therefore it is still useful to focus at the moment our attention on the EVs derived from stimulated macrophages to evaluate in the near future their potential as drug delivery systems. The know-how acquired will be then transferred for the biotechnological use of naturally derived EVs.





# REFERENCES

---

1. Kötztler, M. P., Hancock, S. M., and Withers, S. G. *Glycosidases: Functions, Families and Folds*. eLS 2014.
2. Cantarel B. L., et al. *The Carbohydrate-Active EnZymes database (CAZy): an expert resource for Glycogenomics*. Nucleic Acids Research. 2009. **37(1)**:D233–D238.
3. Bojarova P., and Kren V. *Biotechnol. Glycosidases: a key to tailored carbohydrates*. Trends in Biotechnol. 2009. **27(4)**:199-209.
4. Ito S., Kobayashi T., Ara K., Ozaki K., Kawai S., Hatada Y. *Alkaline detergent enzymes from alkaliphiles: enzymatic properties, genetics, and structures*. Extremophiles. 1998. **2(3)**:185-90
5. Kulkarni N., Shendye A., Rao M. *Molecular and biotechnological aspects of xylanases*. FEMS Microbiol Rev. 1999. **23(4)**:411-56
6. Bayer E.A., Lamed R., Himmel M.E. *The potential of cellulases and cellulosomes for cellulosic waste management*. Curr Opin Biotechnol. 2007. **18(3)**:237-45.
7. James, J.A.; Lee, B.H. *Glucoamylases: Microbial sources, industrial applications and molecular biology*. Journal of Food Biochemistry. 1997 **21(1)**:1-52
8. Kashyap, D.R.; Vohra, P.K.; Chopra, S. et al. *Applications of pectinases in the commercial sector: a review*. Bioresource.Technology. 2001. **77(3)**:215-227
9. Brás N.F., et al. *Glycosidases: A Mechanistic Overview*. Intech. 2012.
10. Bras N. F., Fernandes P. A., Ramos M. J. *Docking and molecular dynamics studies on the stereoselectivity in the enzymatic synthesis of carbohydrates*. Theoretical Chem. Acc. 2009. **122(5-6)**:283.
11. Plou, F. J., Segura, A. G. D., and Ballesteros, A. *Application of glycosidases and transglycosidases in the synthesis of oligosaccharides*. Ind. Enz. 2007. 141-157.
12. Cobucci-Ponzano B., Moracci M. *Glycosynthases as tools for the production of glycan analogs of natural products*. Nat Prod Rep. 2012. **29(6)**:697-709
13. Planas, A., and Faijes, M. *Glycosidases and glycosynthases in enzymatic synthesis of oligosaccharides. An overview*. Afinidad. 2002. **59(500)**:295-313.
14. Manzanares P., Vallés S., Ramón D., Orejas M.  *$\alpha$ -L-Rhamnosidases: Old and New Insights*. Industrial Enzymes. 2007. 117–140.
15. Mutter M., Beldman G., Schols H.A., Voragen A.G.J. *Rhamnogalacturonan  $\alpha$ -L-Rhamnopyranohydrolase' a novel enzyme specific for the terminal nonreducing rhamnosyl unit in rhamnogalacturonan regions of pectin*. Plant Physiol. 1994. **106(1)** 241-250.
16. Hashimoto R.W., Miyake O., Nankai H., Murata K. *Molecular identification of an  $\alpha$ -l-rhamnosidase from Bacillus sp. strain GL1 as an enzyme involved in complete metabolism of gellan*. Arch. Biochem. Biophys. 2003. **415(2)**:235-44.
17. Rahim R., Ochsner U.A., Olvera C., Graninger M., Messner P., Lam J.S, Soberón-Chávez G. *Cloning and functional characterization of the Pseudomonas aeruginosa rhlC gene that encodes rhamnosyltransferase 2, an enzyme responsible for di-rhamnolipid biosynthesis*. Mol. Microbiol. 2001. **40(3)**:708–718.
18. Maxwell E.G., Colquhoun I.J., Chau H.K., Hotchkiss A.T., Waldron K.W, Morris V.J., Belshaw N.J., *Rhamnogalacturonan I containing homogalacturonan inhibits colon cancer cell proliferation by decreasing ICAM1 expression*. Carbohydr. Polym. 2015. **132**:546–553
19. Nguema-Ona E., Vicré-Gibouin M., Gotté M., Plancot B., Lerouge P., Bardor M., Driouch A. *Cell wall O-glycoproteins and N-glycoproteins: aspects of*

- biosynthesis and function*. Front. Plant. Sci. 2014. 5-499.
20. Nereus W., Gunther I.V., Nunñez A., Fett W., Solaiman D.K.Y. *Production of Rhamnolipids by Pseudomonas chlororaphis, a Nonpathogenic Bacterium*. Appl. Env. Microb. 2005. **71(5)**:2288–2293.
  21. Champion E., Andre I., Mulard L.A., Monsan P., Remaud-Simeon M., Morel S., *Synthesis of L-Rhamnose and N-Acetyl-D-Glucosamine Derivatives Entering in the Composition of Bacterial Polysaccharides by Use of Glucansucrases*. J. Carbohydr. Chem. 2009. **28**:142–160.
  22. Seifert, G. J. *Nucleotide sugar interconversions and cell wall biosynthesis: how to bring the inside to the outside*. Curr. Op. in plan. Biol. 2004. **7(3)**:277-284.
  23. Panche A.N., Diwan A.D, Chandra S.R. *Flavonoids: an overview*. J Nutr Sci. 2016 5-47.
  24. Benavente-García O., Castillo J. *Update on uses and properties of citrus flavonoids: new findings in anticancer, cardiovascular, and anti-inflammatory activity*. J Agric Food Chem. 2008. **56(15)**:6185-205.
  25. Middleton E.Jr., Kandaswami C., Theoharides T.C., *The Effects of Plant Flavonoids on Mammalian Cells: Implications for Inflammation, Heart Disease, and Cancer*. Pharmacol. Rev. 2000. **4(52)**:673-751.
  26. Perez-Vizcaino F.L., Duarte J. *Flavonols and cardiovascular disease*, Mol. Aspects Med. 2010. **31(6)**:478-94.
  27. Fresco P., Borges F., Marques M.P.M., Diniz C. *The Anticancer Properties of Dietary Polyphenols and its Relation with Apoptosis*. Curr. Pharm. Des. 2010.**16**:114-134.
  28. Ce'liz G., Audisio M.C., Daz M. *Antimicrobial properties of prunin, a citric flavanone glucoside, and its prunin 6"-O-lauroyl ester*. J. Appl. Microbiol. 2010. **109(4)**:1450–1457.
  29. Németh K., Plumb G.W., Berrin J.G., Juge N., Hassan R.J., Naim H.Y., Williamson G., Swallow D.M., Kroon P.A. *Deglycosylation by small intestinal epithelial cell  $\beta$ -glucosidases is a critical step in the absorption and metabolism of dietary flavonoid glycosides in humans*. Eur. J. Nutr. 2003. **42**:29–42.
  30. Bokkenheuser V. D., Shackleton C. H., Winter J. *Hydrolysis of dietary flavonoid glycosides by strains of intestinal Bacteroides from humans*. Biochem J. 1987. **248(3)**:953–956.
  31. Hollman P.C., Bijlsman M.N., van Gameren Y., Crossen E.P., de Vries J.H., Katan M.B. *The sugar moiety is a major determinant of the absorption of dietary flavonoid glycosides in man*, Free Radic. Res. 1999. **31(6)**:569-73.
  32. Day A.J., Gee J.M., DuPont M.S., Johnson I.T., Williamson G. *Absorption of quercetin-3-glucoside and quercetin-4'-glucoside in the rat small intestine: the role of lactase phlorizin hydrolase and the sodium-dependent glucose transporter*. Biochem. Pharmacol. 2003. **65(7)**:1199-2006.
  33. Puri M., Marwaha S.S., Kothari R.M., Kennedy J.F. *Biochemical basis of bitterness in citrus fruit juices and biotech approaches for debittering*. Crit. Rev. Biotechnol. 1996. **16**:145–155.
  34. González-Barrio R., Trindade L. M., Manzanares P., de Graaff L. H., Tomás-Barberán F. A., Espín J. C., *Production of bioavailable flavonoid glucosides in fruit juices and green tea by use of fungal alpha-L-rhamnosidases*. J. Agric. Food Chem. 2004. **52(20)**:6136-42.
  35. M.V. Gallego, F. Piñaga, D. Ramón, S. Vallés, *Purification and Characterization of an  $\alpha$ -L-Rhamnosidase from Aspergillus terreus of Interest in Winemaking*, J. Food Sci. 66(2) (2001) 204 - 209.

36. Gunata Z., Bitteur S., Brillouet J. M., Bayonove C., Cordonnier R. *Sequential enzymatic hydrolysis of potentially aromatic glycosides from grape*. Carbohydr. Res. 1988. **184**:139–149.
37. Manzanares P., Orejas M., Gil J. Vde Graaff L. H. , Visser J., Ramón D., *Construction of a Genetically Modified Wine Yeast Strain Expressing the Aspergillus aculeatus rhaA Gene, Encoding an  $\alpha$ -L-Rhamnosidase of Enological Interest*. Appl. Environ. Microbiol. 2003. **69(12)**:7558–7562.
38. Gantt R. W., Peltier-Pain P., Thorson J.S. *Enzymatic methods for glyco(diversification/randomization) of drugs and small molecules*. Natural Product Reports. 2011. **28(11)**:1811-1853.
39. Xu L., Liu X., Yin Z., Liu Q., Lu L., Xiao M. *Site-directed mutagenesis of  $\alpha$ -L-rhamnosidase from Alternaria sp. L1 to enhance synthesis yield of reverse hydrolysis based on rational design*. Appl Microbiol Biotechnol. 2016. **100(24)**:10385-10394.
40. Hashimoto W., Nankai H., Sato N., Kawai S., Murata K. *Characterization of  $\alpha$ -L-rhamnosidase of Bacillus sp. GL1 responsible for the complete depolymerization of gellan*, Arch. Biochem. Biophys. 1999. **415(2)**:56–60.
41. Zverev V.V., Hertel C., Bronnenmeier K., Hroch A., Kellermann J., Schwarz W.H. *The thermostable  $\alpha$ -L-rhamnosidase RamA of Clostridium stercorarium: biochemical characterization and primary structure of a bacterial  $\alpha$ -L-rhamnoside hydrolase, a new type of inverting glycoside hydrolase* Mol. Microbiol. 2000. **35**:173–179.
42. Avila M., Jaquet M., Moine D., Requena T., Peláez C., Arigoni F., Jankovic I., *Physiological and biochemical characterization of the two alpha-L-rhamnosidases of Lactobacillus plantarum NCC245*. Microbiol. 2009. **155**:2739–2749.
43. Beekwilder J., Marcozzi D., Vecchi S., de Vos R., Janssen P., Francke C., van Hylckama Vlieg J., Hall R.D. *Characterization of rhamnosidases from Lactobacillus plantarum and Lactobacillus acidophilus*. Appl. Environ. Microbiol. 2009. **75**:3447–3454.
44. Miake F., Satho T., Takesue H., Yanagida F., Kashige N., Watanabe K. *Purification and characterization of intracellular alpha-L-rhamnosidase from Pseudomonas paucimobilis FP2001*. Arch. Microbiol. 2000. **173(1)**:65-70.
45. Li L., Yu Y., Zhang X., Jiang Z., Zhu Y., Xiao A., Ni H., Chen F., *Expression and biochemical characterization of recombinant  $\alpha$ -L-rhamnosidase r-Rha1 from Aspergillus niger JMU-TS528*. Int J Biol Macromol. 2016. **85**:391-9.
46. Young N.M., Johnston R.A.Z., Richards J.C. *Purification of the  $\alpha$ -L-rhamnosidase of Penicillium decumbens and characteristics of two glycopeptide components*. Carbohydr. Res. 1989. **191**:53–62.
47. Koseki T., Mese Y., Nishibori N., Masaki K., Fujii T., Handa T., Yamane Y., Shiono Y., Murayama T., Iefuji H. *Characterization of an alpha-L-rhamnosidase from Aspergillus kawachii and its gene*. Appl. Microbiol. Biotechnol. 2008. **80(6)**:1007-13.
48. Puri M. *Updates on naringinase: structural and biotechnological aspects*. Applied Microbiology and Biotechnology. 2012. **93(1)**:49-60
49. Elíades, L. A., et al.  *$\alpha$ -L-Rhamnosidase and  $\beta$ -D-glucosidase activities in fungal strains isolated from alkaline soils and their potential in naringin hydrolysis*. J. of basic microbiol. 2011. **51(6)**:659-665.
50. Yadav V., Yadav P., Yadav S., Yadav K.D.S.  *$\alpha$ -L-Rhamnosidase: A review*. Process Biochemistry. 2010. **45**:1226-1235.

51. Miyata T., Kashige N., Satho T., Yamaguchi T., Aso Y., Miake F. *Cloning, sequence analysis, and expression of the gene encoding Sphingomonas paucimobilis FP2001 alpha-l-rhamnosidase*. *Curr Microbiol.* 2005. **51**:105–109.
52. Ndeh D., Rogowski A., Cartmell A., Luis A.S., Baslé A., Gray J., Venditto I., Briggs J., Zhang X., Labourel A., Terrapon N., et al. *Complex pectin metabolism by gut bacteria reveals novel catalytic functions*. *Nature.* 2017. **544(7648)**:65-70.
53. Bonanno J.B., et al. *New York-Structural GenomiX Research Consortium (NYSGXRC): a large scale center for the protein structure initiative*. *J. Struct. Funct. Genomics.* 2005. **6(2)**:225-32.
54. Cui Z., Maruyama Y., Mikami B., Hashimoto W., Murata K. *Crystal structure of glycoside hydrolase family 78  $\alpha$ -l-rhamnosidase from Bacillus sp. GL1*. *J. Mol. Biol.* 2007. **374(2)**:384–398.
55. Fujimoto Z., Jackson A., Michikawa M., Maehara T., Momma M., et al. *The structure of a Streptomyces avermitilis  $\alpha$ -L-rhamnosidase reveals a novel carbohydrate-binding module CBM67 within the six-domain arrangement*. *J. Biol. Chem.* 2013. **288(17)**:12376-85.
56. O'Neill E.C., Stevenson C.E., Paterson M.J., Rejzek M., et al. *Crystal structure of a novel two domain GH78 family  $\alpha$ -rhamnosidase from Klebsiella oxytoca with rhamnose bound*. *Proteins.* 2015. **83(9)**:1742-9.
57. D'Souza S. F. *Immobilized enzymes in bioprocess*. *Curr. Sci.* 1999. 69-79.
58. Mateo C., Palomo J.M., Fernandez-Lorente G., Guisan J.M, et al. *Improvement of enzyme activity, stability and selectivity via immobilization techniques*. *Enz. and Microb. Technol.* 2007. **40**:1451–1463
59. Brena B.M., and Batista-Viera F. *Immobilization of Enzymes. A Literature Survey*. *Immobil. Enz. and cells.* 2006. 15-30.
60. Wubbolts M.G., Bucke C., Bielecki S. *How to get the biocatalyst*. *Appl. Biocat.* 2000. 153.
61. Massolini G., Calleri E. *Immobilized trypsin systems coupled on-line to separation methods: recent developments and analytical applications*. *J. Sep. Sci.* 2005. **28**:7–21
62. Trevan M.D. *Immobilized Enzymes: an Introduction and applications in biotechnology*. Wiley. 1980. 1–9.
63. Brodelius, P., Mosbach, K. *Immobilization Techniques for Cells/Or ganelles*. *Methods in Enzymol.* 1987. **135**:173–454.
64. Buchholz K., Klein J. *Characterization of Immobilized Biocatalysts*. *Methods in Enzymol.* 1987. **135**:3–30.
65. Cabral J.M.S., Kennedy, J. F. *Covalent and coordination immobilization of proteins*. *Protein immobilization.* 1991. 73–138.
66. Girelli A.M., Mattei E. *Application of immobilized enzyme reactor in on-line high-performance liquid chromatography: a review*. *J. Chromatogr. B.* 2005. **819**:3–16.
67. Chow D.C., Johannes M-S., Lee W.K. et al. *Nanofabrication with biomolecules*. *Mater. Today* 2005. **8**:30–39.
68. Aniel M.C., Astruc D. *Gold nanoparticles: assembly, supramolecular chemistry, quantum-size-related properties, and applications toward biology, catalysis, and nanotechnology*. *Chem. Rev.* 2004. **104**:293–346.
69. Heeremans, J. L. M., et al. *Long-term stability of liposomes containing both tissue-type plasminogen activator and glu-plasminogen*. *Int. J. of pharm.* 1996. **129(1-2)**:191-202.
70. Mashburn-Warren L., McLean R. J., Whiteley M. *Gram negative outer membrane*

- vesicles: beyond the cell surface*. Geobiol. 2008. **6(3)**:214–219.
71. Yáñez-Mó M., et al. *Biological properties of extracellular vesicles and their physiological functions*. 2015. J Extracell. Vesicles. 2015. **4(1)**:27066.
  72. Roier, S., et al. *A novel mechanism for the biogenesis of outer membrane vesicles in gram negative bacteria*. Nature Commun. 2016. **7**:10515.
  73. Sullivan C., et al. *Envelope control of outer membrane vesicle production in Gram-negative bacteria*. Biochem. 2013. **52**:3031–3040.
  74. Kulp A., and Kuehn M. J. *Biological functions and biogenesis of secreted bacterial outer membrane vesicles*. Annu. Rev. Microbiol. 2010. **64**:163–184.
  75. Zhou, L., et al. *On the origin of membrane vesicles in Gram-negative bacteria*. FEMS Microbiol. Lett. 1998. **163**:223–228.
  76. Biller, S. J. et al. *Bacterial vesicles in marine ecosystems*. Science **343**, 183–186 (2014).
  77. Hellman, J. et al. *Release of gram-negative outer-membrane proteins into human serum and septic rat blood and their interactions with immunoglobulin in antiserum to Escherichia coli J5*. J. Infect. Dis. 2000. **181**:1034–1043.
  78. Kim G. H., et al. *Isolation and proteomic characterization of bacterial extracellular membrane vesicles*. Curr. Protein Pept. Sci. 2014. **15**:719–731.
  79. Lee, E. Y. et al. *Global proteomic profiling of native outer membrane vesicles derived from Escherichia coli*. Proteomics. 2007. **7(17)**:3143–3153.
  80. Yonezawa, H., et al. *Outer membrane vesicles of Helicobacter pylori TK1402 are involved in biofilm formation*. BMC Microbiol. 2009. **9**:197.
  81. Bauman, S. J., and Kuehn, M. J. *Purification of outer membrane vesicles from Pseudomonas aeruginosa and their activation of an IL-8 response*. Microbes Infect. 2006. **8**:2400–2408.
  82. Wai, S. N. et al. *Vesicle-mediated export and assembly of pore-forming oligomers of the enterobacterial ClyA cytotoxin*. Cell. 2003. **115**:25–35.
  83. Schooling, S. R., Hubley, A. and Beveridge, T. J. *Interactions of DNA with biofilm-derived membrane vesicles*. J. Bacteriol. 2009. **13**:4097–4102.
  84. Schwechheimer, C., and Kuehn, M. J. *Outer-membrane vesicles from Gram-negative bacteria: biogenesis and functions*. Nat. Rev. Microbiol. 2015. **13(10)**:605–619.
  85. Manning, S. J., and Kuehn, M. J. *Contribution of bacterial outer membrane vesicles to innate bacterial defense*. BMC Microbiol. 2011. **11**:258.
  86. Li, Z., Clarke, A. J., and Beveridge, T. J. *Gram-negative bacteria produce membrane vesicles which are capable of killing other bacteria*. J. Bacteriol. 1998.**20**:5478–5483.
  87. Mashburn-Warren, L. M. and Whiteley M. *Special delivery: vesicle trafficking in prokaryotes*. Mol. Microbiol. 2006. **61(4)**:839–846.
  88. Heramb, M. K. and Medicharla, V. J. *Biogenesis and multifaceted roles of outer membrane vesicles from Gram-negative bacteria*. Microbiol. 2014. **160(10)**:2109–2121.
  89. McBroom, A. J. and Kuehn, M. J. *Release of outer membrane vesicles by Gram-negative bacteria is a novel envelope stress response*. Mol. Microbiol. 2007. **63**:545–558.
  90. Yun, S. H. et al. *Proteomic characterization of the outer membrane vesicle of the halophilic marine bacterium Novosphingobium pentaromativorans*. J. Microbiol. 2014. **55(1)**:56–62.
  91. Choi, C. W. et al. *Proteomic characterization of the outer membrane vesicle of Pseudomonas putida KT2440*. J. Proteome Res. 2014. **13**:4298–4309.

92. Frias, A., et al. *Membrane vesicles: a common feature in the extracellular matter of cold-adapted antarctic bacteria*. *Microb. Ecol.* 2010. **59**:476–486.
93. Mashburn-Warren, L. et al. *Interaction of quorum signals with outer membrane lipids: insights into prokaryotic membrane vesicle formation*. *Mol. Microbiol.* 2008. **69**:491–502.
94. Kesty, N. C. and Kuehn M. J. *Incorporation of heterologous outer membrane and periplasmic proteins into Escherichia coli outer membrane vesicles*. *J. Biol. Chem.* 2004. **279**:2069–2076.
95. Kim, J. Y. et al. *Engineered bacterial outer membrane vesicles with enhanced functionality*. *J. Mol. Biol.* 2008. **380**(1):51–66.
96. Gujrati, V. et al. *Bioengineered bacterial outer membrane vesicles as cell-specific drug-delivery vehicles for cancer therapy*. *ACS Nano.* 2014. **8**(2):1525–1537.
97. Ellis, T. N. and Khuen, M. J. *Virulence and Immunomodulatory Roles of Bacterial Outer Membrane Vesicles*. *Microbiol. Mol. Biol. Rev.* 2010. **1**:81–94.
98. Park M., et al. *Positional assembly of enzymes on bacterial outer membrane vesicles for cascade reactions*. *PLoS One.* 2014. **9**(5):e97103
99. Notomista, E. et al. *The Marine Isolate Novosphingobium sp. PP1Y Shows Specific Adaptation to Use the Aromatic Fraction of Fuels as the Sole Carbon and Energy Source*. *Microb. Ecol.* 2011. **61**(3):582–594.
100. van der Meel R., et al. *Extracellular vesicles as drug delivery systems: Lessons from the liposome field*. *J Control Release.* 2014. **195**:72-85.
101. Baglio S.R., Pegtel D.M., and Baldini N. *Mesenchymal stem cell secreted vesicles provide novel opportunities in (stem) cell-free therapy*. *Front Physiol.* 2012. **3**:359.
102. Heijnen H.F., Schiel A.E., Fijnheer R., Geuze H.J., Sixma J.J. *Activated platelets release two types of membrane vesicles: microvesicles by surface shedding and exosomes derived from exocytosis of multivesicular bodies and alpha-granules*. *Blood* 1999. **94**:3791–3799.
103. Lai R.C., et al. *Exosomes for drug delivery - a novel application for the mesenchymal stem cell*. *Biotechnol. Adv.* 2013. **31**:543–551.
104. Rozmyslowicz T., et al. *Platelet- and megakaryocyte-derived microparticles transfer CXCR4 receptor to CXCR4-null cells and make them susceptible to infection by X4-HIV*. *AIDS.* 2003. **17**:33–42.
105. Boulanger C.M. *Microparticles, vascular function and hypertension*. *Curr. Opin. Nephrol. Hypertens.* 2010. **19**:177–180.
106. Cocucci E., Racchetti G., and Meldolesi J. *Shedding microvesicles: artefacts no more*. *Trends. Cell. Biol.* 2009. **19**:43–51.
107. Dignat-George F., and Boulanger C.M. *The many faces of endothelial microparticles*. *Arterioscler. Thromb. Vasc. Biol.* 2011. **31**:27–33.
108. György B., et al. *Membrane vesicles, current state-of-the-art: emerging role of extracellular vesicles*. *Cell. Mol. Life Sci.* 2011. **68**:2667–2688.
109. EL Andaloussi S., et al. *Extracellular vesicles: biology and emerging therapeutic opportunities*. *Nat. Rev. Drug. Discov.* 2013. **12**(5):347-57.
110. Barry O.P., and FitzGerald G.A. *Mechanisms of cellular activation by platelet microparticles*. *Thromb. Haemost.* 1999. **82**:794–800.
111. Horstman L.L., et al. *New horizons in the analysis of circulating cell-derived microparticles*. *Keio J. Med.* 2004. **53**:210–230.
112. VanWijk M.J., et al. *Microparticles in cardiovascular diseases*. *Cardiovasc. Res.* 2003. **59**:277–287.
113. Raposo G. and Stoorvogel W. *Extracellular vesicles: Exosomes, microvesicles,*

- and friends*. J. Cell. Biol. 2013. **200(4)**:373-83.
114. Del Conde I., *et al.* *Tissue-factor-bearing microvesicles arise from lipid rafts and fuse with activated platelets to initiate coagulation*. Blood. 2005. **106(5)**:1604-11.
  115. Martinez M.C. and Andriantsitohaina R. *Microparticles in angiogenesis: therapeutic potential*. Circ. Res. 2011. **109(1)**:110-9.
  116. De Toro J., *et al.* *Emerging roles of exosomes in normal and pathological conditions: new insights for diagnosis and therapeutic applications*. Front. Immunol. 2015. **6**:203.
  117. Iraci, N., *et al.* *Focus on Extracellular Vesicles: Physiological Role and Signalling Properties of Extracellular Membrane Vesicles*. International J. of Mol. Sci. 2016. **17(2)**:171.
  118. Cocucci E., *et al.* *Enlargeosome traffic: exocytosis triggered by various signals is followed by endocytosis, membrane shedding or both*. Traffic. 2007. **8**:742–757.
  119. Moskovich O., and Fishelson Z. *Live cell imaging of outward and inward vesiculation induced by the complement c5b-9 complex*. J. Biol. Chem. 2007. **282**:29977–29986.
  120. Lösche W., *et al.* *Platelet-derived microvesicles transfer tissue factor to monocytes but not to neutrophils*. Platelets. 2004. **15**:109–115.
  121. Eken C., *et al.* *Polymorphonuclear neutrophil-derived ectosomes interfere with the maturation of monocyte-derived dendritic cells*. J. Immunol. 2008. **180**:817–824.
  122. Pluskota E., *et al.* *Expression, activation, and function of integrin alphaMbeta2 (Mac-1) on neutrophil-derived microparticles*. Blood. 2008. **112**:2327–2335.
  123. Fais S., *et al.* *Evidence-Based Clinical Use of Nanoscale Extracellular Vesicles in Nanomedicine*. ACS Nano. 2016. **10(4)**:3886–3899.
  124. Schneider D. J., *et al.* *Signed, Sealed, Delivered: Microenvironmental Modulation of Extracellular Vesicle-Dependent Immunoregulation in the Lung*. Front. Cell Dev. Biol. 2016. **4**.
  125. Bruno S., *et al.* *Mesenchymal stem cell-derived microvesicles protect against acute tubular injury*. J. Am. Soc. Nephrol. 2009. **20(5)**:1053-67.
  126. Milbank E., *et al.* *Extracellular vesicles: pharmacological modulators of the peripheral and central signals governing obesity*. Pharmacol Ther. 2016. **157**:65-83.
  127. Andriantsitohaina R., *et al.* *Microparticles as regulators of cardiovascular inflammation*. Trends in cardiovasc. med. 2012. **22(4)**:88-92.
  128. Gaceb A., *et al.* *Extracellular vesicles: new players in cardiovascular diseases*. The int. J. Biochem. & cell biol. 2014. **50**:24-28.
  129. Martinez, M. C., *et al.* *Microparticles: targets and tools in cardiovascular disease*. Trends pharm. Sci. 2011. **32(11)**:659-665.
  130. D'Argenio V., *et al.* *De Novo Sequencing and Assembly of the Whole Genome of *Novosphingobium* sp. Strain PP1Y*. J. Bacteriol. 2011. **193(16)**:4296.
  131. Hashimoto K. *et al.* *alpha-L-rhamnosidase of *Sphingomonas* sp. R1 producing an unusual exopolysaccharide of sphingan*. Biosci. Biotechnol. Biochem. 1998. **62(6)**:1068-74.
  132. Izzo V., *et al.* *Rhamnosidase activity in the marine isolate *Novosphingobium* sp. PP1Y and its use in the bioconversion of flavonoids*, J. Mol. Catal. B: Enzym. 2014. **105**:95–103.
  133. Baraniecki C.A., Aislabie J., and Foght J.M. *Characterization of *Sphingomonas* sp. Ant 17, an aromatic hydrocarbon-degrading bacterium isolated from Antarctic soil*. Microb. Ecol. 2002. **43**:44–54.
  134. Leahy, J.G. and Colwell R.R., *Microbial degradation of hydrocarbons in the*

- environment*. Microbiol. Rev. 1990. **54(3)**:305-15.
135. De Lise F., et al. *RHA-P: isolation, expression and characterization of a novel -L-rhamnosidase from Novosphingobium sp. PP1Y*. J. Mol. Cat.: Enzymatic. 2016. **134**:136-147.
  136. Oganesyanyan N., et al. *Effect of Osmotic Stress and Heat Shock in Recombinant Protein Overexpression and Crystallization*. Prot. Express. and purif. 2007. **52(2)**:280-285.
  137. Vuong T.V., and Wilson D.B. *Glycoside Hydrolases: Catalytic Base/Nucleophile Diversity*. Biotechnol. Bioeng. 2010. **107**:195–205.
  138. Manzanares P., et al. *Purification and characterization of two different alpha-L-rhamnosidases, RhaA and RhaB, from Aspergillus aculeatus*. Appl. Environ. Microbiol. 2001. **67(5)**:2230-4.
  139. Allison, D. P., et al. *Atomic force microscopy of biological samples*. Wiley Interdiscip. Rev. Nanomed. Nanobiotechnol. 2010. **2(6)**:618–634.
  140. Eddy, J. L., et al. *Production of Outer Membrane Vesicles by the plague pathogen Yersinia pestis*. PLOS One. 2014. **9(9)**: e107002.
  141. Mansilla, M. C., et al. *Control of membrane lipid fluidity by molecular thermosensors*. J. Bacteriol. 2004. **186**:6681–6688.
  142. Crescenzo, R., et al. *Fat quality influences the obesogenic effect of high fat diets*. Nutrients. 2015. **7(11)**:9475-9491.
  143. Bacia, K., Schwille, P., and Kurzchalia, T. *Sterol structure determines the separation of phases and the curvature of the liquid-ordered phase in model membranes*. PNAS 2005. **102(9)**:3272-3277.
  144. Denich, T. J., et al. *Effect of selected environmental and physicochemical factors on bacterial cytoplasmic membranes*. J. Microbiol. Meth. 2003. **52**:149–182.
  145. Meng F., and Lowell C.A. *Lipopolysaccharide (LPS)-induced macrophage activation and signal transduction in the absence of Src-family kinases Hck, Fgr, and Lyn*. J. Exp. Med. 1997. **185(9)**:1661-1670.
  146. Reyes A.D, et al. *The Effects of Palmitic Acid and Oleic Acid on Macrophage Gene Expression*. 2013. FASEB J. **27(1 Supplement)**:1192-6.
  147. Durcin M., et al. *Characterisation of adipocyte-derived extracellular vesicle subtypes identifies distinct protein and lipid signatures for large and small extracellular vesicles*. J. of Extracell. Vesicles. 2017 **6(1)**:1305677.
  148. Opal, S. M. *The host response to endotoxin, antilipopolysaccharide strategies, and the management of severe sepsis*. Int. J. Med. Microbiol. 2007. **297(5)**:365–377.
  149. Robert S., et al. *Standardization of platelet-derived microparticle counting using calibrated beads and a Cytomics FC500 routine flow cytometer: a first step towards multicenter studies?* J. Thromb. Haemost. 2009. **7(1)**:190–197.
  150. Lacroix R., et al. *Standardization of platelet-derived microparticle enumeration by flow cytometry with calibrated beads: Results of the International Society on Thrombosis and Haemostasis SSC Collaborative workshop*. J. Thromb. and Haemost. 2010. **8(11)**:2571-2574.
  151. Dachary-Prigent J., et al. *Annexin V as a probe of aminophospholipid exposure and platelet membrane vesiculation: a flow cytometry study showing a role for free sulfhydryl groups*. Nurden. Blood. 1993. **81**:2554-2565.
  152. Chaput N., They C. *Exosomes: immune properties and potential clinical implementations*. Semin. Immunopathol. 2010. **33(5)**:419.440.
  153. Fox J.E., Austin C.D., and Boyles J.K. *Role of the membrane skeleton in preventing the shedding of procoagulant-rich microvesicles from the platelet*

- plasma membrane*. J Cell Biol. 1990. **111(2)**:483–493.
154. Vanaja S.K., et al. *Mechanisms of inflammasome activation: recent advances and novel insights*. Trends Cell Biol. 2015. **25(5)**:308-15.
  155. Gurung P., et al. *Chronic TLR Stimulation Controls NLRP3 Inflammasome Activation through IL-10 Mediated Regulation of NLRP3 Expression and Caspase-8 Activation*. Scientific Reports. 2015. **5**:14488.
  156. Martinon F., Burns K., and Tschopp J. *The Inflammasome: A Molecular Platform Triggering Activation of Inflammatory Caspases and Processing of proIL-1 $\beta$* . Mol. Cell. 2001. **10**:417–426.
  157. Legrand-Poels S., et al. *Free fatty acids as modulators of the NLRP3 inflammasome in obesity/type 2 diabetes*. Biochem. Pharmacol. 2014. **92(1)**:131-41.
  158. Owens G.K., Kumar M.S., and Wamhoff B.R. *Molecular regulation of vascular smooth muscle cell differentiation in development and disease*. Physiol. Rev. 2004. **84**:767–801.
  159. Sprague A.H., and Khalil R.A. *Inflammatory cytokines in vascular dysfunction and vascular disease*. Biochem Pharmacol. 2009. **78**:539–552.
  160. Latz E.T., Xiao S., and Stutz A. *Activation and regulation of the inflammasomes*. Nat. Rev. Immunol. 2013. **13(6)**.
  161. Miao E.A., Rajan J.V., and Aderem A. *Caspase-1-induced pyroptotic cell death*. Immunol. Rev. 2011. **243**:206–214
  162. Sagulenko V., et al. *AIM2 and NLRP3 inflammasomes activate both apoptotic and pyroptotic death pathways via ASC*. Cell Death Differ. 2013. **20(9)**:1149-60.
  163. Coll R.C. et al. *A small-molecule inhibitor of the NLRP3 inflammasome for the treatment of inflammatory diseases*. Nat. Med. 2015. **21(3)**:248-55.
  164. Altenburger, R. and Kissel, T. *The human Keratinocytes cell Line HaCaT: An In Vitro Cell Culture Model for Keratinocyte Testosterone Metabolism*. Pharm. Res. 1999. **16**:766.
  165. Van der Meel R., et al. *Extracellular vesicles as drug delivery systems: Lessons from the liposome field*. Journal of Contr. Real. 2014. **195**:72-85.



---

# APPENDICES

---



## APPENDIX I

### SCIENTIFIC PUBLICATIONS.

---

- P1)** Donadio G, Sarcinelli C, Pizzo E, Notomista E, Pezzella A, Di Cristo C, **De Lise F**, Di Donato A, Izzo V. *The Toluene o-Xylene Monooxygenase Enzymatic Activity for the Biosynthesis of Aromatic Antioxidants*. PLoS One. (2015) 10(4), e0124427. doi: 10.1371/journal.pone.0124427.
- P2)** Conti V., Izzo V., Corbi G., Russomanno G., Manzo V., **De Lise F.**, Di Donato A., Filippelli A. *Antioxidant supplementation in the treatment of aging-associated diseases*. Front Pharmacol. 2016 Feb 12;7:24. doi: 10.3389/fphar.2016.00024. eCollection 2016. Review.v.
- P3)** **De Lise F.**, Mensitieri F., Tarallo V., Ventimiglia N., Vinciguerra R., Tramice A., MarchettiR., Pizzo E., Notomista E., Cafaro V., Molinaro A., Birolo L., Di Donato A. and Izzo V. *RHA-P: isolation, expression and characterization of a novel  $\alpha$ -L-rhamnosidase from *Novosphingobium* sp. PP1Y*. Journal of Molecular Catalysis B: Enzymatic 134 (2016) 136–147.
- P4)** Pingeon M., Charlier B., **De Lise F.**, Mensitieri F. , Dal Piaz F., Izzo V. *Novel Drug Targets for the Treatment of Cardiac Diseases*. Current Pharmacogenomics and Personalized Medicine, 2017, 15, 1-13.
- P5)** **De Lise F.**, Mensitieri F.,Rusciano G., Dal Piaz F., Di Lorenzo F., Molinaro A., Zarrelli A., Romanucci V., Valeria Cafaro<sup>1</sup>, Sasso A., Filippelli A., Di Donato A., Izzo V. *Isolation and Purification of Extracellular Nanostructures from *Novosphingobium* sp. PP1Y: a Novel Example of Outer Membrane Vesicles*. Scient. Rep. 2017. Under Review

## APPENDIX II

### COMMUNICATIONS.

---

- A1)** Manzo V., Donadio G., Notomista E., Russomanno G., Sarcinelli C., **De Lise F.**, Mensitieri F., Ventimiglia N., Di Cristo C., Pizzo E., Pezzella A., Di Donato A., Izzo V. *Microbial Oxygenase Activities for the Biosynthesis of Novel Aromatic Antioxidant Compounds*. Giornate della Facoltà di Farmacia e Medicina a Salerno. 22-23 maggio 2014, Università degli Studi di Salerno. Translational Medicine @ UniSa (2014) - ISSN 2239-9747 2014, Special Issue (1): 9
- A2)** Di Donato A., **De Lise F.**, Mensitieri F., Donadio G., Tramice A., Trincone A., Cafaro V., Notomista E., Izzo V. *From Bioremediation to Biocatalysis: biotechnologically relevant enzymes from microorganisms adapted to polluted environments*. Japan-Italy Symposium on New Trends in Science and Engineering of Enzyme and Microbiology for Sustainable Society, Lecture T3, Nara, Japan (2014). **(This abstract was selected for an oral presentation)**.
- A3)** **De Lise F.**, Mensitieri F., Rusciano G., Molinaro A., dal Piaz F., Di Cosmo A., Sasso A., Di Donato A., Izzo V. *Isolation and purification of extracellular nanostructures from N. sp. PP1Y: a novel example of Outer Membrane Vesicles?* "ISEV 2016". Rotterdam, The Netherlands. May 2016.
- A4)** Mensitieri F., **De Lise F.**, Strazzulli A., Del sorbo M., Tramice A., Molinaro A., Birolo L., Moracci M., Di Donato A., Izzo V. *RHA-P: insight into a Novel Bacterial  $\alpha$ -L-Rhamnosidase from Novosphingobium sp. PP1Y*. CBM12, Wien. April 2017.
- A5)** Mensitieri F., **De Lise F.**, Cafaro V., Lumacone M., Strazzulli A., Notomista E., Moracci M., Di Donato A., Izzo V. *RHA-P: a novel bacterial  $\alpha$ -L-rhamnosidase of biotechnological relevance from Novosphingobium sp. PP1Y*. SIB 2017. Caserta. September 2017.
- A6)** **De Lise F.**, Mensitieri F., Castaldi S., Rusciano G., Dal Piaz F., Sasso A., Zarrelli A., Di Donato A., Izzo V. *Purification and characterization of extracellular nanostructures from N.sp. PP1Y: a novel example of Outer Membrane Vesicles*. SIB 2017. Caserta. September 2017. **(This abstract was selected for an oral presentation)**.
- A6)** Mensitieri F., **De Lise F.**, Siepi M., Cafaro V., Notomista E., Izzo V., Di Donato A., Oliva R., Del Vecchio P., Petraccone R., Isticato R., Ricca E., Donadio G. *BIOBLUE BIOSENSOR – a new biosensor for the detection of environmental pollutants*. SIB 2017. Sao Paulo School of Advanced Science on Biophysical Methods to study Biomolecular Interactions. 10/2017.

## APPENDIX III

### EXPERIENCES IN FOREIGN LABORATORIES.

From September 21<sup>st</sup> 2016 to March 21<sup>st</sup> 2017, the research activity of Dr. Siepi has been carried out at the INSERM institute (University of Angers, France) in the laboratories of the "Stress oxydant et pathologies métaboliques U1063". The work was supervised by Prof. Ramaroson Andriantsitohaina.



STRESS OXYDANT ET PATHOLOGIES MÉTABOLIQUES  
UMR INSERM U1063

Le 04 Avril 2017

To Whom it may concern,

This is to certify that Ms. Federica De Lise, PhD student in biotechnology from University Federico II, Naples (Italy), has been in our research group at university of Angers, "Institute de Biologie en Santé, Unité INSERM 1063 SOPAM" from 21<sup>st</sup> September 2016 to 21<sup>st</sup> march 2017, under direct supervision of Prof. Ramaroson Andriantsitohaina.



## APPENDIX IV

### PUBLISHED PAPERS.

---

#### **Isolation and purification of extracellular nanostructures from *Novosphingobium sp.* PP1Y: a novel example of Outer Membrane Vesicles?**

Federica De Lise<sup>1</sup>, Francesca Mensitieri<sup>1</sup>, Giulia Rusciano<sup>2</sup>, Fabrizio Dal Piaz<sup>3</sup>, Flaviana Di Lorenzo<sup>4</sup>, Antonio Molinaro<sup>4</sup>, Armando Zarrelli<sup>4</sup>, Giovanni Di Fabio<sup>4</sup>, Valeria Cafaro<sup>1</sup>, Antonio Sasso<sup>2</sup>, Alberto Di Donato<sup>1</sup>, Viviana Izzo<sup>3</sup>.

<sup>1</sup> Department of Biology, University of Federico II Naples, Italy.

<sup>2</sup> Department of Physics, University of Federico II Naples, Italy.

<sup>3</sup> Department of Medicine, Surgery and Dentistry, University of Salerno, Italy.

<sup>4</sup> Department of Chemical Sciences, University of Federico II Naples, Italy.

Corresponding author:

**Dr. Viviana Izzo, PhD**

**Tel/Fax. +39(0)89965225/5116 email: [vizzo@unisa.it](mailto:vizzo@unisa.it)**

Under Revision 2017.

RESEARCH ARTICLE

# The Toluene *o*-Xylene Monooxygenase Enzymatic Activity for the Biosynthesis of Aromatic Antioxidants

Giuliana Donadio<sup>1</sup>\*, Carmen Sarcinelli<sup>1</sup>\*, Elio Pizzo<sup>1</sup>, Eugenio Notomista<sup>1</sup>, Alessandro Pezzella<sup>2</sup>, Carlo Di Cristo<sup>3</sup>, Federica De Lise<sup>1</sup>, Alberto Di Donato<sup>1</sup>, Viviana Izzo<sup>1,4</sup>\*

**1** Department of Biology, University of Naples Federico II, Via Cinthia I, 80126, Napoli, Italy, **2** Department of Chemical Sciences, University of Naples Federico II, via Cinthia I, 80126, Napoli, Italy, **3** Department of Sciences and Technologies, University of Sannio, Via Port'Arsa, 11, Benevento, Italy, **4** Department of Medicine and Surgery, University of Salerno, via S. Allende, 84081, Baronissi (SA), Italy

\* These authors contributed equally to this work.

\* [vizzo@unisa.it](mailto:vizzo@unisa.it)



 OPEN ACCESS

**Citation:** Donadio G, Sarcinelli C, Pizzo E, Notomista E, Pezzella A, Di Cristo C, et al. (2015) The Toluene *o*-Xylene Monooxygenase Enzymatic Activity for the Biosynthesis of Aromatic Antioxidants. PLoS ONE 10 (4): e0124427. doi:10.1371/journal.pone.0124427

**Academic Editor:** Jamshidkhan Chamani, Islamic Azad University-Mashhad Branch, Mashhad, Iran, IRAN, ISLAMIC REPUBLIC OF

**Received:** December 18, 2014

**Accepted:** March 13, 2015

**Published:** April 27, 2015

**Copyright:** © 2015 Donadio et al. This is an open access article distributed under the terms of the [Creative Commons Attribution License](https://creativecommons.org/licenses/by/4.0/), which permits unrestricted use, distribution, and reproduction in any medium, provided the original author and source are credited.

**Data Availability Statement:** All relevant data are within the paper and its Supporting Information files.

**Funding:** This research was supported by FARB 2013 ORSA 132082. Dr. C. Sarcinelli was supported by grant POR CAMPANIA FSE 2007/2013, Progetto CARINA CUP B25B0900080007. The funders had no role in study design, data collection and analysis, decision to publish, or preparation of the manuscript.

**Competing Interests:** The authors have declared that no competing interests exist.

## Abstract

Monocyclic phenols and catechols are important antioxidant compounds for the food and pharmaceutical industries; their production through biotransformation of low-added value starting compounds is of major biotechnological interest. The toluene *o*-xylene monooxygenase (ToMO) from *Pseudomonas* sp. OX1 is a bacterial multicomponent monooxygenase (BMM) that is able to hydroxylate a wide array of aromatic compounds and has already proven to be a versatile biochemical tool to produce mono- and dihydroxylated derivatives of aromatic compounds. The molecular determinants of its regioselectivity and substrate specificity have been thoroughly investigated, and a computational strategy has been developed which allows designing mutants able to hydroxylate non-natural substrates of this enzyme to obtain high-added value compounds of commercial interest. In this work, we have investigated the use of recombinant ToMO, expressed in cells of *Escherichia coli* strain JM109, for the biotransformation of non-natural substrates of this enzyme such as 2-phenoxyethanol, phthalan and 2-indanol to produce six hydroxylated derivatives. The hydroxylated products obtained were identified, isolated and their antioxidant potential was assessed both *in vitro*, using the DPPH assay, and on the rat cardiomyoblast cell line H9c2. Incubation of H9c2 cells with the hydroxylated compounds obtained from ToMO-catalyzed biotransformation induced a differential protective effect towards a mild oxidative stress induced by the presence of sodium arsenite. The results obtained confirm once again the versatility of the ToMO system for oxyfunctionalization reactions of biotechnological importance. Moreover, the hydroxylated derivatives obtained possess an interesting antioxidant potential that encourages the use of the enzyme for further functionalization reactions and their possible use as scaffolds to design novel bioactive molecules.

## Introduction

In living organisms, aerobic metabolic processes such as respiration and photosynthesis cause the generation of reactive species of either oxygen (ROS) or nitrogen (RNS) in specific organelles such as mitochondria, chloroplasts, and peroxisomes. Both ROS and RNS share a well-documented role in stimulating physiological events such as signaling and cell differentiation. However, these molecules are also highly unstable and tend to acquire electrons from nucleic acids, lipids, proteins, carbohydrates causing a sequence of chain reactions that are responsible for cellular damage [1,2]. The correct balance inside the cell between the prooxidant action of both ROS and RNS and the antioxidant activity of either enzymatic (such as superoxide dismutase, catalase, glutathione peroxidase and glutathione reductase) or non-enzymatic (such as vitamin C, vitamin E, selenium, zinc, taurine, hypotaurine, glutathione,  $\beta$ -carotene) systems is indeed a very delicate equilibrium which is maintained through the activity of a complex array of molecular mechanisms [1,3].

Evidence has been accumulating which shows that oxidative stress, the condition deriving from an imbalance between prooxidants and antioxidants in the cell, might represent a common element for the onset of several pathologies such as cancer, neurodegenerative and cardiovascular diseases, and the occurrence of complications in diabetes [4,5].

The quest for novel natural and synthetic antioxidants has undoubtedly drawn the attention of the scientific community in recent years. In this context, several antioxidant pharmacophores have been identified, among which phenols and catechols have been given much attention as they are very susceptible to oxidation by acting as electron donors [6, 7].

Phenols are endowed with the property of suppressing or delaying spontaneous autoxidation of organic molecules and might be useful to prevent *in vivo* the consequences of the autoxidation of biomolecules [6,8]. Thus, it is not surprising that fruits and vegetables, which are characterized by a high content of phenolic compounds such as phenolic acids and flavonoids, have been so far the main suppliers of molecules analyzed as potential antioxidant drugs, and their consumption in a healthy and varied diet has been demonstrated to significantly reduce the risk of cancer [9,10–13]. In addition, synthetic phenolic antioxidants such as butylated hydroxyanisole (BHA), butylated hydroxytoluene (BHT), tert-butylhydroquinone (TBHQ) and propyl gallate (PG) have been also studied and used, although the use of BHA and BHT has been restricted by legislative rules due to uncertainties concerning their toxic and carcinogenic effects [6].

Despite all the interest towards phenolic antioxidants, there are still many issues to unravel concerning their biological activity. The analysis of kinetic and thermodynamic data available so far in the literature indicates that the efficiency of phenols as inhibitors of the autoxidation of organic matter depends on a variety of factors, and this becomes undoubtedly challenging in complex systems such as living organisms [6].

Other antioxidant pharmacophores have been identified, among which catechols, 1,2-dihydroxybenzenes, have been given much attention [7]. It should be noted that the Comprehensive Medicinal Chemistry (CMC) database shows the presence of many drugs containing the catechol moiety for which several pharmacological effects have been described [14,7]. For these molecules, it is commonly accepted that their antioxidant effect depends on the fact that the semiquinone radical derived from H-atom donation of catechol can be stabilized by both an intramolecular hydrogen bond and by the electron-donating properties of the *ortho*-OH [15–16]. Thus, the chemical versatility of both phenols and catechols and the numerous pharmacological effects described for some of their derivatives, encourage their use as scaffolds to design novel bioactive molecules where the different nature of the substituents bound to the aromatic

ring may influence the reactivity of these molecules towards oxidizing agents, their pharmacokinetics, and their tissue and cellular distribution [14,7].

However, the synthesis of substituted phenols and catechols by chemical methods is often complex and may involve severe reaction conditions, resulting in low yields and the formation of racemic mixtures [17,18]. These complications have boosted the research for the development of biotransformations, also known as bioconversions, which make use of the metabolic versatility of either purified enzymes or whole microorganisms, for the selective hydroxylation of commercially available, low-added-value, aromatic precursors [19].

The toluene *o*-xylene monooxygenase (ToMO) from *Pseudomonas* sp. OX1 is a bacterial multicomponent monooxygenase (BMM) [19–23] that has been extensively characterized in the last decade from both a biochemical and a biotechnological point of view [24–26]. The molecular determinants of its regioselectivity and substrate specificity have been thoroughly investigated, and a computational strategy has been developed which analyzes the interactions between the active-site residues of its hydroxylase component ToMOA and the substrates [26–31]. Recently, mutants of the ToMO multicomponent system were used to produce tyrosol (4-hydroxyphenylethanol, bearing a phenol moiety) and hydroxytyrosol (3,4-dihydroxyphenylethanol, bearing a catechol moiety), strong antioxidants commonly found in extra virgin olive oil [32–36,13], using a cheap and commercially available aromatic precursor such as 2-phenylethanol (S1 Fig) [18]. The results obtained showed the great versatility of ToMO and suggested the potential use of this enzyme for the hydroxylation of other non-natural aromatic substrates to produce antioxidant phenols and catechols of interest for both the food and pharmaceutical industries.

In the present study we have used the recombinant ToMO system, expressed in strain JM109 of *E.coli*, to hydroxylate three commercially available aromatic monocyclic molecules that are non-natural substrates of the enzyme, to obtain mono- and dihydroxylated derivatives analogous to natural antioxidants tyrosol and hydroxytyrosol, but with some structural differences that might influence their antioxidant potential.

The three aromatic molecules used in this study as starting compounds are benzene derivatives bearing one or two substituents in *ortho* (Fig 1B):

- 2-phenoxyethanol, is a benzene derivative with a  $\text{-O-(CH}_2\text{)}_2\text{-OH}$  substituent bound to the aromatic ring. This compound differs from 2-phenylethanol (Fig 1A), the starting substrate used for the biosynthesis of tyrosol and hydroxytyrosol [18] (S1 Fig), for the presence of an additional oxygen atom directly linked to the aromatic ring;

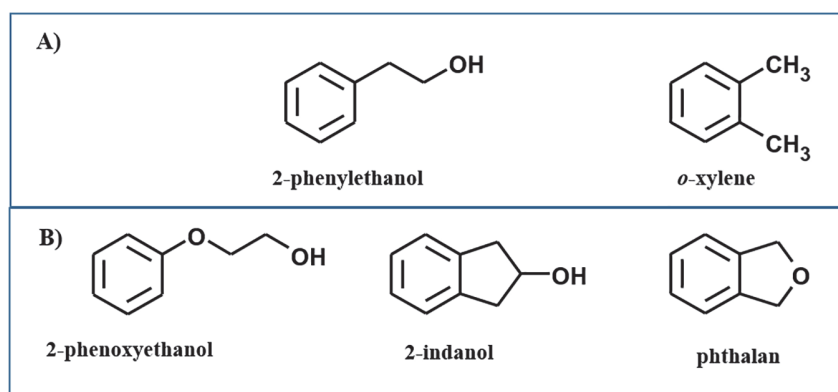


**Fig 1. Starting substrates.** (A) Structures of 2-phenylethanol and *o*-xylene. (B) Substrates used for the ToMO-catalyzed biotransformations presented in this study.

doi:10.1371/journal.pone.0124427.g001

- 2-indanol, is similar to 2-phenylethanol but with an additional methylene group, linking the ethanol moiety to the ring, which makes the structure more rigid;
- phthalan, which differs from *o*-xylene, a natural substrate of ToMO (Fig 1A), for the presence of an oxygen atom bridging the two methyl substituents.

Phenols and catechols obtained from the hydroxylation of these compounds were isolated, purified and identified by NMR and mass spectrometry analysis. Their antioxidant potential was first assessed *in vitro* using the DPPH chemical assay [37–38], and then on the rat cardiomyoblast cell line H9c2 [39–40] to evaluate their effect during a mild oxidative stress induced by sodium arsenite (SA). Exposure to SA inhibits protein synthesis in eukaryotic cells and activates multiple stress signaling pathways such as the generation of what is usually referred to as “stress granules” [4,41–43]. Confocal microscopy analysis suggested that in stressed H9c2 cells, pretreatment with optimal concentrations of the hydroxylated compounds resulted in a lower percentage of cells containing stress granules, thus highlighting a potential antioxidant activity of these molecules in the cellular *milieu*, and paving the way to their future functionalization to increase and diversify their biological activities.

## Materials and Methods

### Generals

Bacterial cultures, plasmid purifications, and transformations were performed according to Sambrook et al [44]. *E. coli* strain JM109 was from Novagen. Plasmid pGEM3Z/Tou *wt* and mutant E103G/F176A were prepared as already described [18]. 2-phenoxyethanol, phthalan, and 2-indanol were purchased from Sigma-Aldrich. Water and methanol used for HPLC experiments were from Romil. Formic acid was from Carlo Erba.

### Docking of substrates in ToMOA active site

Reaction intermediates were docked into the active site of ToMO by using the Monte Carlo energy minimization strategy as previously described [18], except that the 2010 version of the ZMM software was used, and the dielectric constant was calculated using the default option of this version. The PDB files for the initial manually generated complexes and the ZMM instruction files containing the lists of mobile residues, constraints, and parameters used during calculations are available upon request.

### ToMO-catalyzed bioconversion of 2-phenoxyethanol, phthalan and 2-indanol: isolation and purification of the reaction products

Cells of *E. coli* strain JM109 transformed with either plasmid pBZ1260 or variant E103G/F176A, were routinely grown in LB to which ampicillin was added to a final concentration of 100 µg/mL (LB/amp). Several well-isolated colonies were picked from LB/amp agar plates, inoculated into 12.5 mL of LB/amp in a sterile 50 mL Falcon Tube and incubated in constant shaking at 37°C up to 0.6 OD<sub>600</sub>. The preinoculum was diluted 50-fold in two 500 mL Erlenmeyer flasks containing each 250 mL of LB/amp, and incubated under constant shaking at 37°C up to 0.7–0.8 OD<sub>600</sub>. Expression of the recombinant ToMO proteins was induced with 0.2 mM IPTG at 37°C and in the presence of 0.2 mM Fe(NH<sub>4</sub>)<sub>2</sub>(SO<sub>4</sub>)<sub>2</sub>; this latter was necessary for the assembly of the iron-containing catalytic center of the recombinant ToMO. After 1 hour of induction, cells were collected by centrifugation (1,880 x g for 15' at 4°C), resuspended in M9 medium containing 0.4% glucose (M9-G) at a final concentration of 6 OD<sub>600</sub> and incubated with 2 mM of either 2-phenoxyethanol, phthalan, or 2-indanol dissolved in methanol (final methanol concentration was 2%). After

a 16h incubation at 28°C under constant shaking at 230 rpm, cells were collected by centrifugation at 1,880 x g for 15' at 4°C; an aliquot of the cell-free supernatants was loaded on HPLC to check for the presence of hydroxylated products before their purification (S2 Fig). To this purpose, an HPLC system equipped with a Waters 1525 binary pump coupled to a Waters photodiode array detector was used. Substrates and hydroxylated derivatives were separated using a Ultrasphere C<sub>18</sub> reverse-phase column (4.6 x 250 mm; particle size 10 μm, pore size 100 Å). Separation was carried out at a flow rate of 1 mL/min by using a two-solvent system consisting of a 0.1% formic acid solution in water (solvent A) and a 0.1% formic acid solution in methanol (solvent B). Compounds were separated using a 3-min isocratic elution with 10% solvent B, followed by a 20-min linear gradient from 10 to 75% solvent B and an isocratic 5-min step at 98% solvent B.

For the purification of the hydroxylated products identified by analytical HPLC, cell-free supernatants, prepared as described above, were extracted twice with ethyl acetate added in a 1:2 ratio with respect to the aqueous phase. The organic phase was recovered, dried with a Rotavapor apparatus, and the pellet was dissolved in 100% methanol and stored at -20°C. The sample was then diluted to a final 10% concentration of methanol and loaded on HPLC using an Econosil C18 reverse-phase semi-preparative column (10 x 250 mm, particle size 10 μm, pore size 100 Å). Separation was carried out at a flow rate of 2 mL/min by using a two-solvent system consisting of a 0.1% formic acid solution in water (solvent A) and a 0.1% formic acid solution in methanol (solvent B). Compounds were separated using a 10-min isocratic elution with 10% solvent B, followed by a first 10-min linear gradient from 10 to 40%, a second 10-min linear gradient from 40% to 75%, a third 5-min gradient from 75% to 90%, an isocratic 10-min step at 90% of solvent B and a final 15-min step at 10% of solvent B. Each peak of interest was individually collected, concentrated, and stored at -20°C.

### Identification by NMR and mass spectrometry analysis

For NMR analysis, aliquots of the purified cell-free supernatants, prepared as described in the previous paragraph and fractionated by HPLC, were lyophilized, and directly used for NMR analysis in deuterated methanol. <sup>1</sup>H NMR spectra were recorded at 600, 400, or 300 MHz, and <sup>13</sup>C NMR spectra were recorded at 75 MHz. <sup>1</sup>H and <sup>13</sup>C distortionless enhancement by polarization transfer heteronuclear single-quantum correlation and <sup>1</sup>H and <sup>13</sup>C heteronuclear multiple-quantum correlation (HMBC) experiments were run at 600 and 400 MHz, respectively, on instruments equipped with a 5 mm <sup>1</sup>H/broadband gradient probe with inverse geometry using standard pulse programs. The HMBC experiments used a 100-ms long-range coupling delay. Chemical shifts are reported in δ values (ppm) downfield from tetramethylsilane. Regioisomers were distinguished according to the spin-coupling pattern in the aromatic region of the <sup>1</sup>H NMR spectra (S3 Fig). Compound eluting in peak 1 (S2 Fig), indicated from now on as compound 1, showed only two signals featuring a doublet shape as a consequence of the ortho-type coupling. On this basis, the direct attribution of the symmetric para-substituted structure to compound 4HEP, recognized as the 4-(2-hydroxyethoxy)phenol, was allowed. In the case of compounds eluting in peaks 2 and 3 (compounds 2 and 3) a more complex pattern in the aromatic region of the <sup>1</sup>H NMR spectra was present, suggesting, respectively, a meta and an ortho substitution of the aromatic rings (S3 Fig). The characterization of compounds 2 and 3 as 3-(2-hydroxyethoxy)phenol (3HEP) and 2-(2-hydroxyethoxy)phenol (2HEP), respectively, resulted from the ratios of shielded and unshielded signals. Indeed, the <sup>1</sup>H integration for compound 3HEP is accounted with the two H atoms in ortho (H<sub>o</sub>) and the one H atom in para (H<sub>p</sub>) to the OH group. For compound 2HEP, the ratio H<sub>o</sub>/H<sub>p</sub> is 1 which is coherent with the presence of only two shielded H atoms, the one in ortho and one in para to the OH group.

HR ESI+/MS spectra (S4 Fig) were obtained in 0.5% Formic Acid/methanol 1:1 v/v and were recorded on a Agilent 1100 LC/MSD/ESI apparatus.

## Evaluation of the concentration of the hydroxylated derivatives of 2-phenoxyethanol, phthalan and 2-indanol

To evaluate the concentration of the compounds obtained from the ToMO-catalyzed hydroxylation reaction we selected, for each of them, a similar compound whose UV-vis spectrum and corresponding extinction coefficient was available in the literature (S5 Fig). All the spectroscopic data used for calculations were obtained from the “Organic Electronic Spectral Data” book series (*Analytical chemistry*. 58. 1886. G. Norwitz et al Wiley eds).

### DPPH assay

2,2-diphenyl-1-picrylhydrazyl (DPPH) is a stable free radical with  $\lambda_{\text{max}}$  at 515 nm (purple,  $\epsilon_{515}$  in methanol =  $12 \text{ mM}^{-1} \text{ cm}^{-1}$ ). The neutralization of the DPPH radical is responsible for the disappearance of the absorbance at 515 nm and is commonly used as a readout of radical scavenging of an antioxidant compound [37–38]. The reaction mixture contained, in a final volume of 1 mL of methanol, different concentrations of our hydroxylated compounds and 0.1 mM of a freshly prepared DPPH solution in methanol. It is important to note that, as recommended by Kedare and coauthors [38] the initial DPPH concentration should give an absorbance  $\leq 1.0$ . The reaction was allowed to proceed at RT until completion, and was followed at  $\lambda = 515 \text{ nm}$ .

### Cell cultures and treatments

H9c2 cells (Rat Embryonic Myocardium Cells, CRL-1446) were purchased from American Type Culture Collection (ATCC) and grown in Dulbecco's modified Eagle medium (DMEM) supplemented with 10% fetal bovine serum (FBS), 4 mM L-glutamine, 1% v/v penicillin/streptomycin solution (100 U/mL) and 1 mM sodium pyruvate (Euroclone, Milano, Italy) at 37°C in 5% CO<sub>2</sub> incubator. Oxidative stress was induced by adding sodium arsenite (Sigma Aldrich), freshly prepared in stock aqueous solutions and added to the conditioned medium at a final concentration of 0.25 mM.

### MTT assay

H9c2 cells were seeded on 96-well plates at a density of  $2.5 \times 10^3$  cells/well in 0.1 mL of DMEM 24 h prior to the treatment with the different compounds. As control, cells were incubated with buffer diluted in medium.

After 72 h of incubation, cell viability was evaluated by MTT assay, adding tetrazolium MTT (3-(4,5-dimethylthiazol-2-yl)-2,5-diphenyltetrazolium bromide) diluted at 0.5 mg/mL in DMEM without red phenol (0.1 mL/well). After 4 h of incubation at 37°C, the resulting insoluble formazan salts were solubilized in 0.04 M HCl in anhydrous isopropanol, and quantified by measuring the absorbance at  $\lambda = 570 \text{ nm}$ , using an automatic plate reader spectrophotometer (VICTOR<sup>3</sup> Multilabel Counter; Perkin Elmer, Shelton, CA, USA). Cell survival was expressed as means of the percentage values compared to control. Standard deviations were always  $< 5\%$  for each repeat (values in quadruplicate of at least three experiments).

The hydroxylated derivatives of 2-phenoxyethanol, phthalan and 2-indanol were used at a concentration close to their EC<sub>50</sub> value (5 to 10  $\mu\text{M}$  higher) obtained from the DPPH assay. When the EC<sub>50</sub> was not available, as in the case of tyrosol, 3HEP, DHI, and DHIBF (S4 Fig), two arbitrary concentrations were initially tested, 40 and 80  $\mu\text{M}$ . As results obtained with these two concentrations were comparable, the lower concentration (40  $\mu\text{M}$ ) was used to test the

potential antioxidant activity of these compounds in the following experiments such as the apoptosis assay and the analysis of stress granules.

The non-hydroxylated precursors, when assayed, were used at a concentration equal to the higher concentration used for any of their hydroxylated derivatives. In conclusion, the concentrations used in the experiments with H9c2 cells presented in the “Results and Discussion” section of this manuscript were: 25  $\mu$ M for hydroxytyrosol, 40  $\mu$ M for phenylethanol, tyrosol, **4HEP**, **3HEP**, phthalan, **DHiBF**, 2-indanol, **DHI**, **THI**, and 90  $\mu$ M for 2-phenoxyethanol and **2HEP** (S4 Fig).

### EB and AO staining assay

Apoptosis was evaluated by ethidium bromide (EB) and acridine orange (AO) staining of nuclei [45]. AO is a fluorescent DNA binding dye that permeates all the cells staining the nuclei green, whereas EB is only taken up by the cells when cytoplasmic membrane integrity is compromised, staining apoptotic nuclei red. H9c2 cells were seeded in 6-well plates at a density of  $1.5 \times 10^5$  cells/well in 2 mL of DMEM and grown up to nearly 60% confluence. The cells were then incubated at 37°C for 3 h in the presence of the tested compounds. Afterwards, the SA-induced oxidative stress (0.25 mM for 90 min) was performed. Cells were trypsinized, collected by centrifugation, and washed with ice-cold PBS. Cells were re-suspended in 50  $\mu$ L of PBS containing the EB/AO dye mixture (5  $\mu$ g/mL) and incubated at 37°C for 20 min. Stained cells were placed on a microscope slide and covered with coverslips. Images were taken at a 100 X magnification. Both apoptotic (red) and live (green) cells were counted in five microscopic fields for each sample, to estimate the percentage of apoptotic cells.

### Immunofluorescence analysis and confocal microscopy

H9c2 cells were seeded onto coverslips in 24-well plates at a density of  $2.5 \times 10^4$  cells/well in 0.5 mL of DMEM and grown for 48 h, up to nearly 60% confluence. Cells were incubated at 37°C for 3 h with either the starting aromatic compounds or their hydroxylated derivatives. Afterwards, an incubation with 0.25 mM SA for 90 min was performed. As negative and positive controls of the stress effect, cells were treated with either buffer or 0.25 mM SA, respectively, in the absence of any exogenous compound. Cells were then fixed in 4% paraformaldehyde in PBS 1X at room temperature for 15 min and rinsed three times with PBS 1X. Quenching of free aldehydic sites of the fixative was performed by adding 50 mM  $\text{NH}_4\text{Cl}$  in PBS 1X, at room temperature for 15 min. After washing with PBS 1X, cells were permeabilized using 0.1% Triton X-100 in PBS 1X at room temperature for 30 min, then rinsed in PBS 1X for three times. After incubating the cells in a blocking solution consisting of 5% bovine serum albumin (BSA) in PBS 1X at room temperature for 1 hour under constant shaking, PABP monoclonal antibody (Sigma Aldrich), a specific marker used to evidence the presence of stress granules in the cell, was used at 2  $\mu$ g/mL in blocking buffer at 4°C overnight. After washing in PBS 1X, cells were incubated with secondary antibody Cy3 conjugated goat anti-mouse F(ab')<sub>2</sub> (1:1,000 dilution in blocking buffer) (Jackson Immuno Research Laboratories, UK), at room temperature for 1 hour. For nuclear counterstaining, cells were incubated with DAPI, diluted at 0.1  $\mu$ g/mL in PBS 1X, at room temperature for 10 min. After washing, coverslips were mounted in 50% glycerol in PBS 1X. Images were captured using a Zeiss confocal laser-scanning microscope LSM 510 using suitable lasers. Image analyses on stress granules was performed using “Stress granule counter” and “Analyze particles” ImageJ (<http://rsbweb.nih.gov/ij/index.html>) plugins. Nuclear counterstaining was used to count the total number of cells. Statistical analyses were performed using GraphPad (Prism) software ver. 5.0.

## Results and Discussion

### ToMO-catalyzed hydroxylation of 2-phenoxyethanol, phthalan and 2-indanol

The aromatic substrates used in this study (Fig 1B) were used without any further purification. For each compound the corresponding UV-vis spectrum was recorded after dilution in methanol;  $\lambda_{\max}$  of 2-phenoxyethanol, phthalan and 2-indanol were respectively 269.7, 270.9 and 272.1 nm. ToMO-catalyzed biotransformation of these aromatic substrates, used at a final concentration of 2 mM in the incubation medium M9-G, was performed by using recombinant cells of *E.coli*, strain JM109, transformed with the plasmid coding for the complete ToMO *wt* enzymatic system, as described in detail in Materials and Methods.

After incubation for different time intervals (0, 30 min, 1 h, and 16 h) at 30°C under constant shaking (220 rpm), samples were withdrawn, cells were collected by centrifugation, and an aliquot of the exhausted medium was loaded on HPLC to check for the presence of hydroxylated products (Materials and Methods, and S2 Fig). As evident from the chromatographic profiles obtained, ToMO *wt* was able to hydroxylate 2-phenoxyethanol and phthalan. Three different peaks eluting respectively at 10.4 min (compound 1,  $\lambda_{\max} = 287.5$  nm), at 12.6 min (compound 2,  $\lambda_{\max} = 273.5$  nm) and 15.2 min (compound 3,  $\lambda_{\max} = 275.3$  nm) were evident when using 2-phenoxyethanol as the substrate (Panel A in S2 Fig). Formation rates of compounds 1, 2 and 3 were of  $0.89(\pm 0.04)$ ,  $1.15(\pm 0.20)$  and  $0.510(\pm 0.001)$   $\mu\text{M min}^{-1}$ , respectively. Compounds 1, 2 and 3 accounted respectively for the  $37.8(\pm 3.1)$ , the  $43.8(\pm 1.3)$  and the  $18.3(\pm 1.8)\%$  of the total yield of product which was of  $15.3(\pm 1.3)\%$  (total  $\mu\text{M products}/\mu\text{M substrate}$ ) and was calculated after 2h of incubation, the maximum time at which the products yield was still proportional to the time of incubation (data not shown). When using phthalan as substrate a single peak of product was eluted at 14.3 min (compound 4,  $\lambda_{\max} = 279.2$  nm) (Panel B in S2 Fig) with a formation rate of  $1.79(\pm 0.03)$   $\mu\text{M min}^{-1}$  and a yield of  $10.8(\pm 0.2)\%$  after 2h of incubation. No evident hydroxylation product was instead observed when the substrate used for the ToMO-catalyzed bioconversion was 2-indanol (data not shown).

The exhausted media obtained from the ToMO *wt*-catalyzed bioconversion of 2-phenoxyethanol and phthalan were further purified through organic extraction, as described in detail in Materials and Methods. Samples were then loaded on a semi-preparative HPLC C-18 column. Each peak was manually collected, lyophilized and analyzed by NMR and mass spectrometry analysis (Materials and Methods, and S3 and S4 Figs). Fig 2A and 2B show the starting compounds 2-phenoxyethanol and phthalan and the corresponding products identified through these analyses.

### Selection of an efficient catalyst for the hydroxylation of 2-indanol

The conversion of 2-phenoxyethanol to a mixture of the three mono-hydroxylated products is not surprising as this result is very similar to what previously observed in the case of 2-phenylethanol [18]. As for phthalan, the most similar substrate we have previously tested, *o*-xylene is converted to a mixture of 3,4-dimethylphenol (80%) and 2,3-dimethylphenol (20%) [27]. We have previously suggested that this result is due to the fact that the site for the ortho substituents is more hindered than the site for the para substituents [26]. Likely, in the case of phthalan the steric hindrance caused by the additional oxygen atom (Fig 1B) further disfavors the proximal hydroxylation of this compound, thus providing exclusively the hydroxylation product corresponding to 3,4-dimethylphenol *i.e.* 1,3-dihydro-5-hydroxyisobenzofuran (DHIBF), (Fig 2B and S4 Fig).

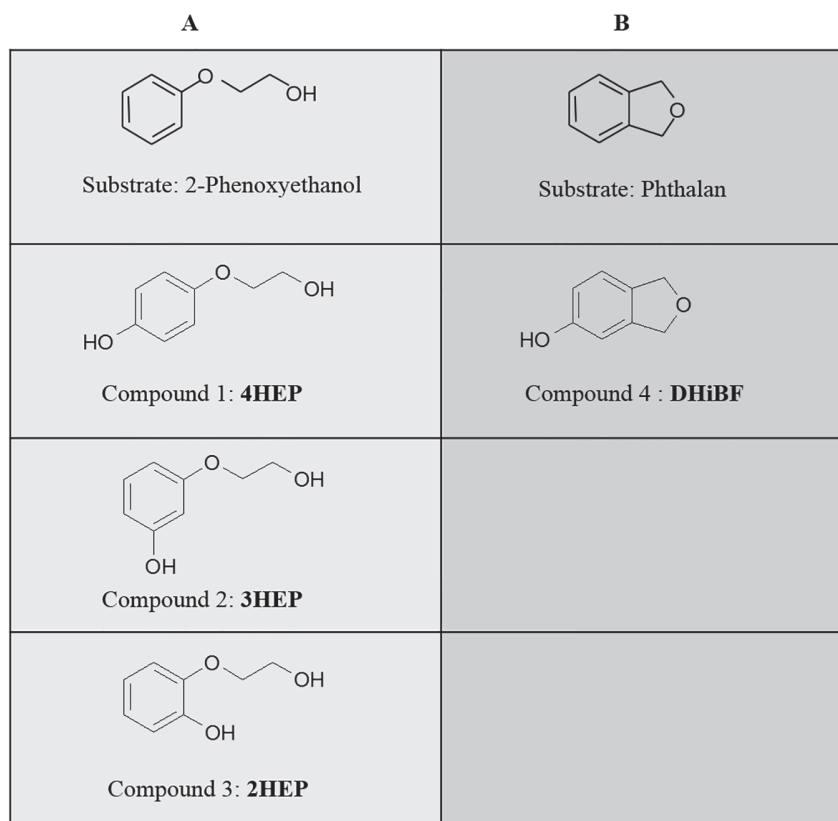


**Fig 2. Hydroxylated products.** Starting substrates and corresponding hydroxylated products obtained through ToMO-catalyzed biotransformation of (A) 2-phenoxyethanol and (B) phthalan.

doi:10.1371/journal.pone.0124427.g002

In order to identify a ToMO variant able to hydroxylate 2-indanol, we have analyzed the interaction of 2-indanol and phthalan (this latter considered as our positive control) with the active site of ToMO using a Monte Carlo modelling strategy previously applied to ToMO natural substrates and to 2-phenylethanol [26, 18]. Briefly, this strategy is based on the docking of a crucial intermediate of the hydroxylation reaction *i.e.* the “arenium intermediate”. By comparing the geometrical parameters for any desired complex ToMO (ToMO-variant)/intermediate to those found for the complex ToMO *wt*/arenium intermediate for para-hydroxylation of the optimal substrate toluene (the “reference complex”), it is possible to predict if an aromatic compound will be a good substrate and which product(s) will be produced. As described previously [26,18], two geometrical parameters defining the orientation of the arenium ring with respect to the diiron cluster were used for the comparison: (i) the distance between the carbon atom of the substrate that accepts the oxygen atom from the diiron cluster during the hydroxylation reaction (herein called  $C_n$ ) and the C4 atom of the reference complex, and (ii)  $\Delta\theta$ , a parameter that measures the angle deviation of the plane of the arenium ring in a ToMO mutant/intermediate complex with respect to the plane of the arenium ring in the reference structure.  $\theta$  is the torsion angle Fe2-O- $C_n$ - $C_m$  where  $C_m$  is the carbon atom of the substrate adjacent to  $C_n$  closer to the substituent bound to the benzene ring (Fig 3). In the reference structure,  $\theta$  angle (Fe2-O-C4-C3) is 103.6°. Previously [26, 18] we have demonstrated that  $C_n$ -C4 distances lower than about 0.2 Å, and  $\Delta\theta$  values in the range  $-10^\circ/+5^\circ$  are predictive of high  $k_{cat}$  values (similar to or even higher than those measured for ToMO *wt* on its natural substrate toluene).

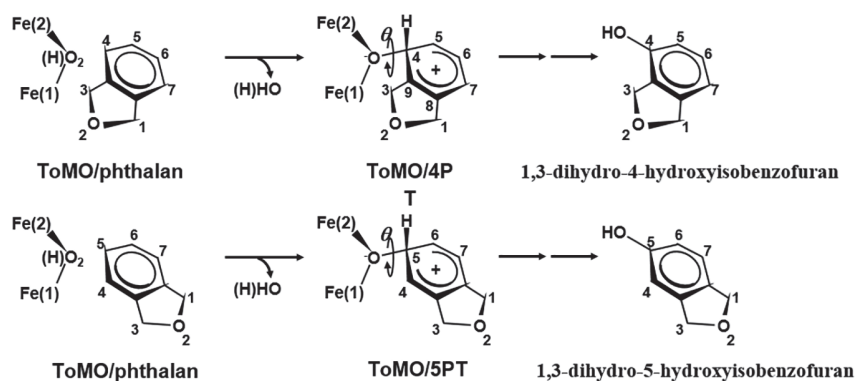


**Fig 3. Docking of intermediates in ToMO active site.** Docking of the two possible arenium intermediates (4PT and 5PT) deriving from phthalan in the active site of ToMOA. In the case of 4PT,  $\theta$  is the torsion angle Fe(2)-O-C4-C9, whereas, in the case of 5PT,  $\theta$  is the torsion angle Fe(2)-O-C4-C5. Similar arenium intermediates can be hypothesized for the hydroxylation of 2-indanol.

doi:10.1371/journal.pone.0124427.g003

Data in Table 1 show that in the case of phthalan only the arenium intermediate leading to 1,3-dihydro-5-hydroxyisobenzofuran (DHIBF) docks in an orientation very similar to that of the reference structure suggesting that this isomer can be efficiently produced by ToMO. On the contrary, the arenium intermediate leading to 1,3-dihydro-4-hydroxyisobenzofuran adopts an orientation very different from that of the reference intermediate described above. According to our model this would indicate poor or none production of the 4-hydroxy isomer in spite of a non-covalent binding energy value (ncBE in Table 1) more negative than that of the 5-hydroxy isomer. Overall, data in Table 1 allow to predict that ToMO can convert phthalan only to 1,3-dihydro-5-hydroxyisobenzofuran in agreement with the experimental finding. In the case of 2-indanol both arenium intermediates 24I and 25I leading to the two possible products,

**Table 1. Geometrical parameters and non covalent binding energies (ncBE) of the complexes between ToMO or E103G/F176A-ToMO and the arenium intermediates for the phthalan/1,3-dihydro-4-hydroxyisobenzofuran (4PT), the phthalan/1,3-dihydro-5-hydroxyisobenzofuran (5PT), the 2-indanol/2,4-dihydroxyindan (24I) and the 2-indanol/2,5-dihydroxyindan (25I) reactions.**

Arenium intermediate	Geometrical parameters	ToMO	
		wild type	E103G/F176A
4PT	C4-C4 (Å)	0.42	- <sup>a</sup>
	$\Delta\theta$ (°)	+36.7	-
	ncBE (kcal mol <sup>-1</sup> )	-42.4	-
5PT	C4-C5 (Å)	0.25	-
	$\Delta\theta$ (°)	-6.7	-
	ncBE (kcal mol <sup>-1</sup> )	-33.5	-
24I	C4-C4 (Å)	0.49	0.45
	$\Delta\theta$ (°)	+28.8	+35.6
	ncBE (kcal mol <sup>-1</sup> )	-40.0	-39.6
25I	C4-C5 (Å)	0.43 <sup>b</sup>	0.25
	$\Delta\theta$ (°)	+36.1 <sup>c</sup>	-7.6
	ncBE (kcal mol <sup>-1</sup> )	-23.6	-35.3

<sup>a</sup> not determined.

<sup>b</sup> in the case of phenylethanol we previously found C4-C4 distances of 0.3 and 0.23 Å for the para- and meta-hydroxylation, respectively.

<sup>c</sup> in the case of phenylethanol we previously found  $\Delta\theta$  values of +41° and +22° for the para- and meta-hydroxylation, respectively.

doi:10.1371/journal.pone.0124427.t001

2,4-dihydroxyindan and 2,5-dihydroxyindan respectively, dock into the active site with orientations very different from that adopted by the natural substrate toluene. An accurate examination of the complex ToMO/25I showed that the steric hindrance of phenylalanine 176 prevents the correct accommodation of the intermediate in a manner similar to that previously described for the *meta*- and *para*-hydroxylation of phenylethanol [18]. However, in the case of 2-indanol the presence of the additional methylene group and the rigidity caused by the ring structure markedly increase the deviation from the ideal geometry (Table 1) in agreement with the fact that ToMO slowly converts phenylethanol to tyrosol isomers but seems to be almost completely inactive on 2-indanol.

Since we have previously demonstrated that mutations F176A and E103G, removing the hindrance at the “para site”, allow the accommodation of large substituents in para, we have modeled the complexes between the double mutant and the arenium intermediates 24I and 25I. Data in Table 1 and the models in S6 Fig show that the two mutations selectively improve the geometrical parameters calculated for the intermediate 25I. The two mutations also increase the non-covalent binding energy of 25I indicating that this intermediate not only could dock with a better geometry but could bind more tightly to the active site.

According to the analysis described above, the ToMO variant E103G/F176A was used for the bioconversion of 2-indanol under the same experimental conditions used for the recombinant ToMO *wt* system (Materials and Methods). The HPLC chromatogram in Fig 4 shows in this case the presence of two peaks of products eluting respectively at 13 min (compound 5,  $\lambda_{\max} = 280.3$  nm) and 10 min (compound 6,  $\lambda_{\max} = 288$  nm). It is worth noting that the presence of compound 6 was evident only after at least 16h of incubation (Panel C in S2 Fig). Due to a partial loss of viability of *E.coli* cells strain JM109 after this time, neither the formation rate nor the yield of this compound were calculated. Rate of formation of compound 5 was of  $5.77 (\pm 1.35) \mu\text{M min}^{-1}$ ; the yield after 2h of incubation was of  $28.9(\pm 0.4)\%$ . By NMR and mass spectrometry analysis (Materials and Methods, and S3 and S4 Figs) compound 5 was identified as 2,5-dihydroxyindan (DHI) in agreement with the docking analysis. Moreover, compound 6 was identified as 2,5,6-trihydroxyindan (THI, Fig 4 and S4 Fig), thus indicating that in the ToMO variant E103G/F176A the active site is wide enough not only to accommodate 2-indanol in a catalytically productive orientation, but also to permit a second hydroxylation at the position adjacent to the first hydroxyl group, as usually observed when ToMO *wt* acts on its natural substrates toluene and *o*-xylene which are respectively converted to 3-/4-methylcatechol and 4,5-dimethylcatechol [27].

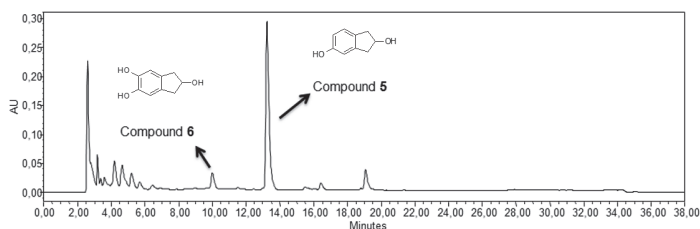


**Fig 4. E103G/F176A ToMO-catalyzed biotransformation of 2-indanol.** HPLC chromatogram at  $\lambda = 280$  nm of an aliquot of the exhausted medium deriving from the 16 hrs, E103G/F176A ToMO-catalyzed biotransformation of 2-indanol.

doi:10.1371/journal.pone.0124427.g004

### *In vitro* antioxidant potential of the hydroxylated derivatives of 2-phenoxyethanol, phthalan and 2-indanol

The capacity of the isolated hydroxylated compounds to scavenge the stable radical 2,2-diphenyl-1-picrylhydrazyl (DPPH) was determined spectrophotometrically by measuring the loss of absorbance of DPPH at  $\lambda = 515$  nm (see [Materials and Methods](#) for details). 0.1 mM DPPH and different concentrations of each hydroxylated compound were added, in a final volume of 1 mL of methanol, in the range 1–200  $\mu$ M, and the loss of absorbance at 515 nm (from now on indicated as  $ABS_{515}$ ) was monitored for 30 min. At this time, the percentage of DPPH effectively reduced ( $\%DPPH_{red}$ ) was calculated evaluating the initial DPPH concentration at  $t = 0$ , indicated as  $[DPPH]_{t=0}$ , and the final DPPH concentration at  $t = 30$ , referred to as  $[DPPH]_{t=30}$ , and using the following formula:

$$\%DPPH_{red} = [1 - ([DPPH]_{t=30} / [DPPH]_{t=0})] \times 100$$

The concentration of hydroxylated compound used in each experiment was plotted against  $\%DPPH_{red}$  ([S7 Fig](#)). The concentration that caused a decrease in the initial DPPH concentration of 50% was defined as EC50 and was obtained by a non-linear regression of the experimental curves using the Graphpad Prism software (<http://www.graphpad.com/>). Each EC50 is the result of at least three independent experiments.

Once obtained the EC50 value for a specific compound we estimated also-at that specific concentration- the time (expressed in minutes) needed to reach a stable value of the  $ABS_{515}$ , a parameter indicated in literature as TEC50 [[37,46](#)]. At this point we calculated what has been defined [[46](#)] as the “antiradical efficiency” (AE) a parameter that is expressed by the following formula:  $AE = 1 / (EC50 \times TEC50)$ . The AE value, taking into account not only the EC50 but also the reaction time, is more informative than the EC50 value alone on the antioxidant behavior of a compound tested with this specific assay [[46](#)].

In all the experiments, described in this and in the following paragraphs, natural aromatic antioxidants such as tyrosol and hydroxytyrosol have also been tested [[32–36](#)] as reference molecules, in parallel with the hydroxylated compounds obtained by ToMO-catalyzed bio-transformation of 2-phenoxyethanol, phthalan and 2-indanol.

Results are shown in [Table 2](#), where it is evident that some among the phenols and catechols produced by the ToMO-catalyzed reaction on non-natural aromatic substrates show an AE value comparable to the strong natural phenolic antioxidant hydroxytyrosol. Interestingly, compounds such as tyrosol, which has been reported to have antioxidant activity *in vivo* [[47](#)], **3HEP**, **DHiBF**, and **DHI** ([S4 Fig](#)) were almost non responsive to the DPPH assay causing negligible losses of  $ABS_{515}$  even when used at concentrations up to 2mM (data not shown).

DPPH reduction curves obtained for each compound tested ([S7 Fig](#)) and the AE values calculated ([Table 2](#)) clearly demonstrate the relevant reducing potential of **2HEP**, **4HEP** and of **THI** compared to hydroxytyrosol activity. Although this could be expected in the case of **THI**,

**Table 2. Evaluation of the antioxidant activity using the DPPH assay.**

Compound	EC50 ( $\mu$ M Antioxidant/ $\mu$ M DPPH)	TEC50 (min)	AE
Hydroxytyrosol	0.21 ( $\pm$ 0.01)	18.0 ( $\pm$ 2.0)	<b>0.27</b> ( $\pm$ 0.01)
4HEP	0.40 ( $\pm$ 0.04)	19.0 ( $\pm$ 1.0)	<b>0.140</b> ( $\pm$ 0.006)
2HEP	1.00 ( $\pm$ 0.02)	25.3 ( $\pm$ 2.1)	<b>0.040</b> ( $\pm$ 0.002)
THI	0.40 ( $\pm$ 0.01)	15.3 ( $\pm$ 2.5)	<b>0.15</b> ( $\pm$ 0.03)

EC50, TEC50 and antioxidant efficiencies (AE) values of hydroxytyrosol, 4 HEP, 2HEP and THI. Standard deviations (SD) are reported in parentheses.

doi:10.1371/journal.pone.0124427.t002

as it shares a catechol moiety with the hydroxytyrosol structure, results obtained from **2HEP** and **4HEP** (phenols like tyrosol, **DHiBF**, and **DHI**) deserve some comments. In both structures the aromatic ring hosts two oxygens either in ortho (**2HEP**) or para (**4HEP**); thus these two molecules share an important structural similarity with catechol and hydroquinone, respectively, two known antioxidants [48]. **3HEP**, instead, shows the additional atom oxygen in a meta position respect to the -OH already present on the aromatic ring, thus resembling resorcinol. Compared to catechol and hydroquinone, where the -OH group in either ortho or para position has an electron donating effect, the reaction of resorcinol with a radical such as DPPH would theoretically be reduced by the electron-withdrawing effect of the -OH group in the meta position [9]. The same rationale seems to apply to the three hydroxylated derivatives we obtained from the biotransformation of 2-phenoxyethanol.

Interestingly, the **THI** plot shows a sigmoidal profile that was not observed for the other compounds tested. Although a more detailed investigation would be necessary to account for such a behaviour, it may be argued that a two-step oxidation path is available for **THI** as a consequence of the -OH substituted five member ring condensed with the catechol system (S8 Fig and explicative notes).

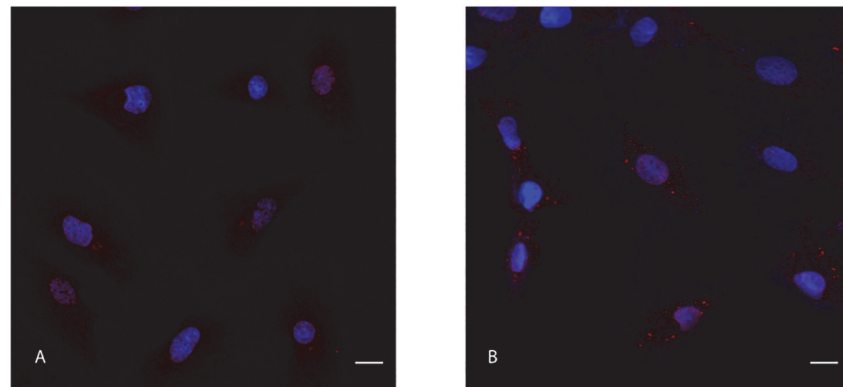
### Antioxidant potential of **4HEP**, **3HEP**, **2HEP**, **DHiBF**, **DHI**, **THI** in cultured H9c2 cells

The potential antioxidant activity of the hydroxylated compounds described in this study was also evaluated testing their effect in a eukaryotic cell system such as the rat cardiomyoblast cell line H9c2. These latter are non-malignant cardiac-like cells, commonly used to study the molecular response to oxidative damage [39–40]. We first examined the effect of the hydroxylated compounds on cell viability, by using the MTT assay (Panel A in S9 Fig), to verify that a cytotoxic effect did not occur. To this purpose, cells were cultured for 72 hours under normal growth conditions in the presence of each purified hydroxylated compound, previously diluted in the growth medium at optimized concentrations (Materials and Methods). The percentage of viable cells, compared to the control, never significantly decreased as shown in Panel A in S9 Fig, thus showing that the compounds tested are not cytotoxic on this specific cell line. Indeed, in the presence of the non-hydroxylated precursors (Panel A in S9 Fig, dark white bars) used as substrates in the ToMO-catalyzed biotransformations, the percentage of viable cells was almost close to the 100%. It is worth to note that hydroxytyrosol and tyrosol induced a significant increase of cell survival (Panel A in S9 Fig, black bars) ( $p$  value < 0.01). A slight positive effect on cell viability was also observed when using the hydroxylated products obtained from 2-phenoxyethanol, with a significant increase of the viable cells number ( $p$  value < 0.01 for **4HEP**,  $p$  value < 0.05 for **3HEP** and **2HEP**). Conversely, **DHiBF**, **DHI** and **THI** did not produce any apparent change in cell viability.

Optimized concentrations obtained in this assay were used in all subsequent experiments (Materials and Methods). In order to validate the data obtained on cell viability, we investigated whether the tested compounds had any effect on cell apoptosis. Apoptotic cells were identified by acridine orange (AO) and ethidium bromide (EB) staining of nuclei [45], as described in Materials and Methods; results are presented in Panel B and C in S9 Fig. When cells were cultured under normal growth conditions, the hydroxylated compounds did not induce an increase in cell apoptosis (Panel C in S9 Fig, white bars). This is consistent with the results obtained from the MTT assay. Moreover, tyrosol, **3HEP**, **DHI** and **THI** induced a significant decrease of the number of apoptotic cells ( $p$  value < 0.05 for **DHI**,  $p$  value  $\leq$  0.01 for the other compounds; Panel C in S9 Fig). Exposure of H9c2 to 0.25 mM of SA for 90 min induced, *per se*, a 37% increase in the percentage of apoptotic nuclei (Panel C in S9 Fig, first black bar).

Since this stress condition was sufficient to elicit a detectable but still sub-lethal cell stress response, it was considered suitable for further experiments aimed at investigating the potential protective effect of our compounds towards the SA-induced effect. Pretreatment for 3h with 4HEP, 2HEP, DHI and THI resulted in a significant reduced percentage of apoptotic nuclei, which decreased from 37% of the control to around 20% (Panel C in S9 Fig, black bars) ( $p$  value  $< 0.05$  for 2HEP and DHI,  $\leq 0.01$  for 4HEP and THI). The other hydroxylated compounds did not significantly alter the sodium arsenite (SA)-induced apoptotic effect.

To better assess a potential antioxidant activity of our hydroxylated compounds, a cell stress response was analyzed, which is activated under mild stress conditions when a transient translational arrest occurs. As underlined in the Introduction section, exposure to SA inhibits protein synthesis and activates multiple stress signaling pathways, including the formation of stress granules (SGs) [4,41–43]. SGs are cytoplasmic foci composed of 40S ribosomal subunits, initiation translation factors and their associated mRNA transcripts, which aggregate when translation initiation is stalled. The SGs formation is reversible and the protein synthesis can be restored, if the stress condition is recovered. To investigate the potential antioxidant effect of our hydroxylated compounds, we examined the occurrence and the number of stress granules (SGs) in H9c2 cells both under normal growth and SA-induced stress conditions. SGs were detected by immunofluorescence and confocal microscopy analysis using the marker PABP (poly-A binding protein) (Materials and Methods and Fig 5). To estimate the antioxidant



C

Substance	Number of SGs/cell	p-value
SA	55.29 ± 3.72	
2HEP	9.12 ± 1.45	**
3HEP	11.05 ± 1.60	*
4HEP	12.77 ± 6.07	*
DHiBF	14.41 ± 5.66	*
DHI	14.68 ± 3.01	*
THI	7.22 ± 4.22	**
Tyr	7.13 ± 3.71	**
Hyd	14.92 ± 1.15	*

**Fig 5. Immunofluorescence assay.** Effect of sodium arsenite on the formation of stress granules: immunofluorescence and statistical analysis. PABP mAb and Cy3-conjugated goat anti-mouse F(ab')<sub>2</sub> were used to detect SGs in H9c2 cells cultured under normal growth (A) and SA-stress conditions (B). Nuclei are stained with DAPI. Scale bars: 10µm. (C) Effect of pretreatment with hydroxylated compounds in SA-treated H9c2 cardiomyoblasts. The table reports SGs number for cell (Mean ± SEM) that was obtained by using “Analyze Particles” plugin of the image software ImageJ (pixel unit: 1,5–2,0; Circularity: 0,99–1,00). Statistical analysis (unpaired t test, two tailed; \*,  $p \leq 0.05$ ; \*\*,  $p \leq 0.01$ ). Tyr: tyrosol; Hyd: hydroxytyrosol.

doi:10.1371/journal.pone.0124427.g005

activity, SGs number per cell was calculated by using a statistical analysis, applied to at least three images acquired analyzing a minimum of 350–400 cells. When H9c2 cells were cultured under normal growth conditions, in the presence of the hydroxylated compounds, no significant change in SGs formation was observed ( $11.7 \pm 4.4$ ) when compared to the control, confirming that the compounds tested do not alter the cellular status (data not shown). In SA-treated cells, SGs were instead easily identified and the statistical analysis revealed the presence of  $55.3 \pm 3.7$  SGs per cell (Fig 5). When pre-treatment with the hydroxylated compounds was performed before the SA-induced oxidative stress, a strong and statistically significant decrease in SGs number was observed (Fig 5). **2HEP** and **THI**, again, showed a higher antioxidant activity compared to the other hydroxylated compounds. A putative antioxidant activity of the aromatic non-hydroxylated substrates used was also evaluated. Their effect on SGs in stressed H9c2 cells was analyzed (data not shown), and no significant decrease in SGs number was observed, when compared to the control.

## Conclusions

Aromatic nuclei are, for their chemical versatility, ideal candidates to create molecules with multiple pharmacological effects. Phenols and catechols, in particular, are promising starting points to merge with other pharmacophores thus obtaining multipotent agents with antioxidant effects and beyond. The different studies presented on the ToMO multicomponent system in more than a decade [18,20–21,23–31] described the unique versatility of the catalytic activity of this enzyme, which allows to obtain hydroxylated derivatives from a wide array of aromatic substrates, highlighting its role as a potential resource for the biosynthesis of phenolic and catecholic compounds.

We have previously shown that a fine-tuning of the regioselectivity and of the catalytic efficiency of ToMO on 2-phenylethanol, a non-natural substrate, to produce known antioxidants such as tyrosol and hydroxytyrosol could be achieved by using an optimized computational model that allows a careful alteration of the shape of the active site [26,18].

In this work we investigated the use of ToMO for the biosynthesis of six aromatic antioxidants, starting from three commercially available aromatic compounds that are non-natural substrates of the enzyme. By using either the *wt* enzyme or ToMO mutant E103G/F176A-catalyzed biotransformations, six hydroxylated compounds were obtained. Although not all of them were able to reduce the DPPH stable radical, a common test system for determining the scavenging properties of putative antioxidants *in vitro*, all hydroxylated compounds shared a common, although differential, antioxidant effect on eukaryotic cells of the H9c2 cell line subjected to a mild oxidative stress induced by sodium arsenite. The discrepancy between the two assays showed from one side a possible limitation in the use of the DPPH assay as the unique methodology to assess the *in vitro* antioxidant potential of hydroxylated aromatic compounds, and on the other hand confirms that the antioxidant effect of phenols and catechols frequently observed in cells might not be due to a simple scavenge of free radicals, but might be dependent on other molecular events that have not been completely elucidated yet.

The availability of the molecules produced under the present study undoubtedly opens new possibilities for obtaining a whole new set of antioxidant molecules by using the ToMO multicomponent system as biocatalyst using a wide array of commercially available monocyclic aromatic compounds as starting substrates.

## Supporting Information

**S1 Fig. Bioconversion of 2-phenylethanol.** Natural antioxidants tyrosol and hydroxytyrosol produced from the hydroxylation of 2-phenylethanol catalyzed by ToMO mutants E103G/

F176T and E103G/F176I (Notomista E., Scognamiglio R., Troncone L., Donadio G., Pezzella A., Di Donato A., and Izzo V. Tuning the specificity of the recombinant multicomponent toluene *o*-xylene monooxygenase from *Pseudomonas* sp. strain OX1 for the biosynthesis of tyrosol from 2-phenylethanol. *Appl. Environ. Microbiol.* 2011;77(15): 5428–37. <http://aem.asm.org/content/77/15/5428.full>).

(TIF)

**S2 Fig. Time course chromatograms.** Time course formation of the hydroxylated products deriving from the ToMO-catalyzed bioconversion of: (**Panel A**) 2-phenoxyethanol, (**Panel B**) phthalan and (**Panel C**) 2-indanol. Chromatograms were extracted at  $\lambda = 280$  nm. The 2-indanol bioconversion was performed by using ToMO mutant E103G/F176A.

(TIF)

**S3 Fig. NMR analysis.** NMR analysis of the isolated products deriving from the ToMO-catalyzed bioconversion of: 2-phenoxyethanol (Compounds **1**, **2** and **3**), phthalan (Compound **4**) and 2-indanol (Compounds **5** and **6**). The structures deduced for each new compound obtained are also presented.

(TIF)

**S4 Fig. Mass spectrometry analysis.** Mass spectrometry analysis and molecular weights obtained for the isolated products deriving from the ToMO-catalyzed bioconversion of: 2-phenoxyethanol (Compounds **1**, **2** and **3**), phthalan (Compound **4**) and 2-indanol (Compounds **5** and **6**).

(TIF)

**S5 Fig. Estimation of extinction coefficients.** For each hydroxylated compound isolated, the  $\epsilon$  at  $\lambda_{\max}$  of a similar model compound is reported which was used for the determination of the concentration throughout this study.

(TIF)

**S6 Fig. Modelling.** Monte Carlo minimized models of the complexes between ToMO or (E103G,F176A)-ToMO and the arenium intermediates for the toluene/*p*-cresol (S4M) and the 2-indanol/2,5-dihydroxyindan (25I) reactions. Carbon atoms are shown in green (ToMO/S4M), magenta (ToMO/25I) and yellow [(E103G,F176A)-ToMO/25I]. Oxygen atoms are shown in red, nitrogen atoms in blue, sulphur atoms in dark yellow. Hydrogen atoms are not shown. Iron ions are shown as orange spheres.

(TIF)

**S7 Fig. DPPH assay.** DPPH reduction (expressed as the percentage of the DPPH effectively reduced, Y axis) as a function of the  $\mu$ M concentration of the compound tested (X axis). 4-(2-Hydroxyethoxy)phenol (**4HEP**); 2-(2-Hydroxyethoxy)phenol (**2HEP**); 2,5,6-trihydroxyindan (**THI**); Hydroxytyrosol.

(TIF)

**S8 Fig. Oxidation pathway.** Two-step oxidation pathway proposed for THI as a consequence of its peculiar structure showing an-OH substituted five member ring condensed with the catechol moiety. First oxidation step results in the formation of expected orthoquinone moiety which can itself undergoes tautomerization affording via transient quinone methides a cyclopentanone condensed catechol, again susceptible to act as reductant (Pezzella A., Lista L., Napolitano A., and d'Ischia M. Tyrosinase-catalyzed oxidation of 17 $\beta$ -estradiol: structure elucidation of the products formed beyond catechol estrogen quinones. *Chem. Res. Toxicol.*

2005.18(9): 1413–9. <http://pubs.acs.org/doi/abs/10.1021/tx050060o>.

(TIF)

**S9 Fig. MTT viability assay and apoptosis assay. (Panel A)** H9c2 cells were cultured under normal growth conditions, incubated in the presence of either the substrates (dark white bars) or the hydroxylated derivatives (black bars) for 72 hours. Cell viability was determined by means of ABS<sub>570</sub> compared to the control (white bar), that is cells without any treatment. Data shown are the means  $\pm$  s.d of at least three repeats, of a representative experiment. A statistical analysis by two-tailed Student's *t* was performed. **(Panel B)** and **(Panel C)** Acridine orange (AO) and ethidium bromide (EB) staining of nuclei to identify apoptotic nuclei. H9c2 cells were cultured under either normal growth conditions (image on the left, panel B, and white bars in panel C), or SA-induced oxidative stress (image on the right, panel B, and black bars in panel C).

(TIF)

## Acknowledgments

Authors are indebted to Dr. Giovanna Benvenuto at the Microscopy Service of Stazione Zoologica "A. Dohrn" (Naples, Italy) for technical assistance.

## Author Contributions

Conceived and designed the experiments: GD CS EN VI. Performed the experiments: GD CS AP FDL. Analyzed the data: GD CS FDL EP CDC AP ADD VI. Contributed reagents/materials/analysis tools: EN EP AP. Wrote the paper: EN AP CDC ADD VI.

## References

1. Agarwal A, Gupta S, Sharma RK. Role of oxidative stress in female reproduction. *Reprod. Biol. Endocrinol.* 2005; 3:28–48. Available: <http://www.ncbi.nlm.nih.gov/pmc/articles/PMC1215514/>. PMID: [16018814](https://pubmed.ncbi.nlm.nih.gov/16018814/)
2. Apel K, Hirt H. Reactive oxygen species: metabolism, oxidative stress, and signal transduction. *Annu Rev Plant Biol.* 2004.; 55:373–399. Available: [http://www.annualreviews.org/doi/abs/10.1146/annurev.arplant.55.031903.141701?url\\_ver=Z39.88-2003&rfr\\_dat=cr\\_pub%3Dpubmed&rfr\\_id=ori%3Arid%3Acrossref.org&journalCode=arplant](http://www.annualreviews.org/doi/abs/10.1146/annurev.arplant.55.031903.141701?url_ver=Z39.88-2003&rfr_dat=cr_pub%3Dpubmed&rfr_id=ori%3Arid%3Acrossref.org&journalCode=arplant). PMID: [15377225](https://pubmed.ncbi.nlm.nih.gov/15377225/)
3. Marco S, Rullo R, Albino A, Masullo M, De Vendittis E, Amato M. The thioredoxin system in the dental caries pathogen *Streptococcus mutans* and the food-industry bacterium *Streptococcus thermophilus*. *Biochimie.* 2013; 95(11):2145–56. Available: <http://www.ncbi.nlm.nih.gov/pubmed/23954859>. doi: [10.1016/j.biochi.2013.08.008](https://doi.org/10.1016/j.biochi.2013.08.008) PMID: [23954859](https://pubmed.ncbi.nlm.nih.gov/23954859/)
4. Anderson P, Kedersha N. Stressful initiations. *J Cell Sci.* 2002; 115:3227–34. Available: <http://jcs.biologists.org/content/115/16/3227.long>. PMID: [12140254](https://pubmed.ncbi.nlm.nih.gov/12140254/)
5. Conti V, Corbi G, Russomanno G, Simeon V, Ferrara N, Filippelli W, et al. Oxidative stress effects on endothelial cells treated with different athletes' sera. *Med Sci Sports Exerc* 2012; 44(1):39–49. Available: <http://journals.lww.com/acsm-msse/pages/articleviewer.aspx?year=2012&issue=01000&article=00006&type=abstract>. doi: [10.1249/MSS.0b013e318227f69c](https://doi.org/10.1249/MSS.0b013e318227f69c) PMID: [21659898](https://pubmed.ncbi.nlm.nih.gov/21659898/)
6. Foti MC. Antioxidant properties of phenols. *J Pharm Pharmacol.* 2007; 59(12):1673–85. Available: <http://onlinelibrary.wiley.com/doi/10.1211/jpp.59.12.0010/abstract>. PMID: [18053330](https://pubmed.ncbi.nlm.nih.gov/18053330/)
7. Yang DP, Ji HF, Tang GY, Ren W, Zhang HY. How many drugs are catecholics. *Molecules.* 2007; 12(4):878–84. Available: <http://www.mdpi.com/1420-3049/12/4/878>. PMID: [17851440](https://pubmed.ncbi.nlm.nih.gov/17851440/)
8. Ingold KU. Inhibition of the autoxidation of organic substances in the liquid phase. *Chem. Rev.* 1961; 61: 563–589.
9. Gülçin I. Antioxidant activity of food constituents: an overview. *Arch. Toxicol.* 2012; 86:345–391. Available: <http://link.springer.com/article/10.1007/s00204-011-0774-2>. doi: [10.1007/s00204-011-0774-2](https://doi.org/10.1007/s00204-011-0774-2) PMID: [22102161](https://pubmed.ncbi.nlm.nih.gov/22102161/)

10. Kelsey NA, Wilkins HM, Linseman DA. Nutraceutical antioxidants as novel neuroprotective agents. *Molecules*. 2010; 15:7792–7814. Available: <http://www.mdpi.com/1420-3049/15/11/7792>. doi: [10.3390/molecules15117792](https://doi.org/10.3390/molecules15117792) PMID: [21060289](https://pubmed.ncbi.nlm.nih.gov/21060289/)
11. Liu RH. Health-promoting components of fruits and vegetables in the diet. *Adv. Nutr.* 2013; 4(3):384S–392S. Available: <http://advances.nutrition.org/content/4/3/384S.long>. doi: [10.3945/an.112.003517](https://doi.org/10.3945/an.112.003517) PMID: [23674808](https://pubmed.ncbi.nlm.nih.gov/23674808/)
12. Raederstorff D. Antioxidant activity of olive polyphenols in humans: a review. *Int J Vitam Nutr Res.* 2009; 79(3):152–65. Available: <http://www.ncbi.nlm.nih.gov/pubmed/20209466> doi: [10.1024/0300-9831.79.3.152](https://doi.org/10.1024/0300-9831.79.3.152) PMID: [20209466](https://pubmed.ncbi.nlm.nih.gov/20209466/)
13. Visioli F, Bernardini E. Extra virgin olive oil's polyphenols: biological activities *Curr Pharm Des.* 2011; 17(8):786–804. Available: <http://www.ncbi.nlm.nih.gov/pubmed/21443485>. PMID: [21443485](https://pubmed.ncbi.nlm.nih.gov/21443485/)
14. Schweigert N, Zehnder AJ, Eggen RI. Chemical properties of catechols and their molecular modes of toxic action in cells, from microorganism to mammals. *Environ Microbiol* 2001; 3(2):81–91. Available: <http://www.ncbi.nlm.nih.gov/pubmed/11321547>. PMID: [11321547](https://pubmed.ncbi.nlm.nih.gov/11321547/)
15. Zhang HY. Theoretical Investigation on Free Radical Scavenging Activity of 6,7-Dihydroxyflavone. *Quant Struct-Act Relat.* 2000; 19:50–53. Available: <http://onlinelibrary.wiley.com/doi/10.1002/%28SICI%291521-3838%28200002%2919:1%3C50::AID-QSAR50%3E3.0.CO;2-%23%2Fabstract>.
16. Zhang HY. Structure-activity relationships and rational design strategies for radical-scavenging dihydroxyflavone. *Curr Comput-Aided Drug Des.* 2005; 1:257–273.
17. Huang C, Ghavtadze N, Chattopadhyay B, Gevorgyan V. Synthesis of catechols from phenols via Pd-catalyzed silanol-directed C-H oxygenation. *J Am Chem Soc.* 2011; 133(44):17630–3. doi: [10.1021/ja208572v](https://doi.org/10.1021/ja208572v) PMID: [21999512](https://pubmed.ncbi.nlm.nih.gov/21999512/)
18. Notomista E, Scognamiglio R, Troncone L, Donadio G, Pezzella A, Di Donato A et al. Tuning the specificity of the recombinant multicomponent toluene o-xylene monooxygenase from *Pseudomonas* sp. strain OX1 for the biosynthesis of tyrosol from 2-phenylethanol. *Appl. Environ. Microbiol.* 2011; 77(15):5428–37. Available: <http://aem.asm.org/content/77/15/5428.full>. doi: [10.1128/AEM.00461-11](https://doi.org/10.1128/AEM.00461-11) PMID: [21666013](https://pubmed.ncbi.nlm.nih.gov/21666013/)
19. Torres Pazmino DE, Winkler M, Glieder A, Fraaije MW. Monooxygenases as biocatalysts: classification, mechanistic aspects and biotechnological applications. *J Biotechnol* 2010; 146:9–24. Available: <http://www.ncbi.nlm.nih.gov/pubmed/?term=Monooxygenases+as+biocatalysts%3A+classi%EF%AC%81cation%2C+mechanistic+aspects+and+biotechnological+applications.+J.+Biotechnol.+146%3A9-24>. doi: [10.1016/j.jbiotec.2010.01.021](https://doi.org/10.1016/j.jbiotec.2010.01.021) PMID: [20132846](https://pubmed.ncbi.nlm.nih.gov/20132846/)
20. Brouk M, Fishman A. Protein engineering of toluene monooxygenases for synthesis of hydroxytyrosol. *Food Chem* 2009; 116:114–121. Available: <http://www.sciencedirect.com/science/article/pii/S0308814609002064>.
21. Dror A, Fishman A. Engineering non-heme mono- and dioxygenases for biocatalysis. *Comput. Struct. Biotechnol.* 2012;J. doi: [10.5936/csbj.201209011](https://doi.org/10.5936/csbj.201209011) Available: <http://www.ncbi.nlm.nih.gov/pmc/articles/PMC3962191/>.
22. Murray LJ, Lippard SJ. Substrate trafficking and dioxygen activation in bacterial multicomponent monooxygenases. *Acc Chem Res.* 2007; 40:466–474. Available: <http://www.ncbi.nlm.nih.gov/pubmed/?term=Substrate+traf%EF%AC%81cking+and+dioxygen+activation+in+bacterial+multicomponent+monooxygenases.+Acc.+Chem.+Res.+40%3A466%E2%80%93474>. PMID: [17518435](https://pubmed.ncbi.nlm.nih.gov/17518435/)
23. Notomista E, Lahm A, Di Donato A, Tramontano A. Evolution of bacterial and archaeal multicomponent monooxygenases. *J. Mol Evol.* 2003; 56:435–44. Available: <http://www.ncbi.nlm.nih.gov/pubmed/?term=Evolution+of+bacterial+and+archaeal+multicomponent+monooxygenases.+J.+Mol.+Evol.+56%3A435%E2%80%9344>. PMID: [12664163](https://pubmed.ncbi.nlm.nih.gov/12664163/)
24. Cafaro V, Scognamiglio R, Viggiani A, Izzo V, Passaro I, Notomista E et al. Expression and purification of the recombinant subunits of toluene/o-xylene monooxygenase and reconstitution of the active complex. *Eur. J. Biochem* 2002; 269:5689–5699. Available: <http://onlinelibrary.wiley.com/doi/10.1046/j.1432-1033.2002.03281.x/abstract;jsessionid=6559BDA93C647648DB9B27607AE64321.f04t02>. PMID: [12423369](https://pubmed.ncbi.nlm.nih.gov/12423369/)
25. Cafaro V, Izzo V, Scognamiglio R, Notomista E, Capasso P, Casbarra A, et al. Phenol hydroxylase and toluene/o-xylene monooxygenase from *Pseudomonas stutzeri* OX1: interplay between two enzymes. *Appl Environ Microbiol.* 2004; 70:2211–2219. Available: <http://aem.asm.org/content/70/4/2211.long>. PMID: [15066815](https://pubmed.ncbi.nlm.nih.gov/15066815/)
26. Notomista E, Cafaro V, Bozza G, Di Donato A. Molecular determinants of the regioselectivity of toluene/o-xylene monooxygenase from *Pseudomonas* sp. strain OX1. *Appl Environ Microbiol.* 2009; 75:823–836. Available: <http://www.ncbi.nlm.nih.gov/pubmed/?term=Molecular+determinants+of+the+regioselectivity+of+toluene%2Fo-xylene+monooxygenase+from+Pseudomonas+sp.+strain+OX1.+Appl.Environ.Microbiol.75%3A823%E2%80%93836>. doi: [10.1128/AEM.01951-08](https://doi.org/10.1128/AEM.01951-08) PMID: [19074607](https://pubmed.ncbi.nlm.nih.gov/19074607/)

27. Cafaro V, Notomista E, Capasso, Di Donato A. Mutation of glutamic acid 103 of toluene o-xylene monoxygenase as a means to control the catabolic efficiency of a recombinant upper pathway for degradation of methylated aromatic compounds. *Appl Environ Microbiol* 2005; 71:4744–4750. Available: <http://aem.asm.org/content/71/8/4744.long>. PMID: 16085871
28. Feingersch R, Shainsky J, Wood TK, Fishman A. Protein engineering of toluene monoxygenases for synthesis of chiral sulfoxides. *Appl Environ Microbiol*. 2008; 74:1555–1566. (<http://www.ncbi.nlm.nih.gov/pmc/articles/PMC2258606/>). doi: 10.1128/AEM.01849-07 PMID: 18192418
29. Sazinsky MH, Bard J, Di Donato A, Lippard SJ. Crystal structure of the toluene/o-xylene monoxygenase hydroxylase from *Pseudomonas stutzeri* OX1. Insight into the substrate specificity, substrate channeling, and active site tuning of multicomponent monoxygenases. *J. Biol Chem* 2004; 279:30600–30610. Available: <http://www.jbc.org/content/279/29/30600.full>. PMID: 15096510
30. Vardar G, Wood TK. Protein Engineering of Toluene-o-Xylene Monoxygenase from *Pseudomonas stutzeri* OX1 for Synthesizing 4-Methylresorcinol, Methylhydroquinone, and Pyrogallol. *Appl Environ Microbiol*. 2004; 70(6):3253–3262. Available: <http://aem.asm.org/content/70/6/3253>. PMID: 15184119
31. Vardar G, Ryu K, Wood TK. Protein engineering of toluene-o-xylene monoxygenase from *Pseudomonas stutzeri* OX1 for oxidizing nitrobenzene to 3-nitrocatechol, 4-nitrocatechol, and nitrohydroquinone. *J Biotechnol*. 2005; 115(2):145–56. Available: <http://www.ncbi.nlm.nih.gov/pmc/articles/PMC427803/>. PMID: 15607233
32. Bernini R, Merendino N, Romani A, Velotti F. Naturally occurring hydroxytyrosol: synthesis and anticancer potential. *Curr Med Chem* 2013; 20(5):655–70. Available: <http://www.eurekaselect.com/106829/article>. PMID: 23244583
33. Granados-Principal S, Quiles JL, Ramirez-Tortosa CL, Sanchez-Rovira P, Ramirez-Tortosa MC. Hydroxytyrosol: from laboratory investigations to future clinical trials. *Nutr Rev*. 2010; 68(4):191–206. Available: <http://nutritionreviews.oxfordjournals.org/content/68/4/191>. doi: 10.1111/j.1753-4887.2010.00278.x PMID: 20416016
34. Manna C, Migliardi V, Sannino F, De Martino A, Capasso R. Protective effects of synthetic hydroxytyrosol acetyl derivatives against oxidative stress in human cells. *J. Agric Food Chem*. 2005; 53:9602–9607. Available: <http://www.ncbi.nlm.nih.gov/pubmed/?term=Protective+effects+of+synthetic+hydroxytyrosol+acetyl+derivatives+against+oxidative+stress+in+human+cells.+J.+Agric.+Food+Chem.+53%3A9602%E2%80%9939607>. PMID: 16302783
35. Rietjens SJ, Bast A, Haenen GR. New insights into controversies on the antioxidant potential of the olive oil antioxidant hydroxytyrosol. *J. Agric Food Chem*. 2007; 55:7609–7614. Available: <http://www.ncbi.nlm.nih.gov/pubmed/?term=+.New+insights+into+controversies+on+the+antioxidant+potential+of+the+olive+oil+antioxidant+hydroxytyrosol.+J.+Agric.+Food+Chem.+55%3A7609%E2%80%937614>. PMID: 17683140
36. Waterman E, Lockwood B. Active components and clinical applications of olive oil. *Altern Med Rev*. 2007; 12:331–342. Available: <http://www.ncbi.nlm.nih.gov/pubmed/?term=Active+components+and+clinical+applications+of+olive+oil.+Altern.+Med.+Rev.+12%3A331%E2%80%93342>. PMID: 18069902
37. Huang D, Ou B, Prior RL. The Chemistry behind Antioxidant Capacity Assays. *J. Agric Food Chem*. 2005; 53(6):1841–1856. PMID: 15769103
38. Kedare SB, Singh RP. Genesis and development of DPPH method of antioxidant assay. *J. Food Sci Technol*. 2011; 48(4):412–422. Available: <http://www.ncbi.nlm.nih.gov/pmc/articles/PMC3551182/?report=reader>. doi: 10.1007/s13197-011-0251-1 PMID: 23572765
39. Watkins SJ, Borthwick GM, Arthur HM. The H9c2 cell line and primary neonatal cardiomyocyte cells show similar hypertrophic responses in vitro. *In Vitro Cell Dev Biol Anim*. 2011; 47, 125–31. Available: <http://www.ncbi.nlm.nih.gov/pubmed/21082279>. doi: 10.1007/s11626-010-9368-1 PMID: 21082279
40. Zordoky BN, El-Kadi AO. H9c2 cell line is a valuable in vitro model to study the drug metabolizing enzymes in the heart. *J. Pharmacol Toxicol Methods*. 2007; 56:317–22. Available: <http://www.ncbi.nlm.nih.gov/pubmed/17662623>. PMID: 17662623
41. Anderson P, Kedersha N. Stress granules: the Tao of RNA triage. *Trends Biochem Sci*. 2008; 33(3):141–50. Available: [http://www.cell.com/trends/biochemical-sciences/abstract/S0968-0004\(08\)00026-?returnURL=http%3A%2F%2Flinkinghub.elsevier.com%2Fretrieve%2Fpii%2FS0968000408000261%3Fshowall%3Dtrue](http://www.cell.com/trends/biochemical-sciences/abstract/S0968-0004(08)00026-?returnURL=http%3A%2F%2Flinkinghub.elsevier.com%2Fretrieve%2Fpii%2FS0968000408000261%3Fshowall%3Dtrue). doi: 10.1016/j.tibs.2007.12.003 PMID: 18291657
42. Buchan JR, Parker R. Eukaryotic stress granules: the ins and outs of translation. *Mol Cell*. 2009; 36:932–41. Available: <http://www.ncbi.nlm.nih.gov/pmc/articles/PMC2813218/>. doi: 10.1016/j.molcel.2009.11.020 PMID: 20064460
43. Kedersha N, Ivanov P, Anderson P. Stress granules and cell signaling: more than just a passing phase? *Trends Biochem Sci*. 2013; 38(10):494–506. Available: <http://www.ncbi.nlm.nih.gov/pmc/articles/PMC3832949/>. doi: 10.1016/j.tibs.2013.07.004 PMID: 24029419

44. Sambrook J, Fritsch E, Maniatis T. *Molecular Cloning. A Laboratory Manual*. Cold Spring Harbor Laboratory Press, Cold Spring Harbor, New York. 1989; (<http://trove.nla.gov.au/work/13615226>).
45. Ribble D, Goldstein NB, Norris DA, Shellman YG. A simple technique for quantifying apoptosis in 96-well plates. *BMC Biotechnol*. 2005; 5:12. Available: <http://www.biomedcentral.com/1472-6750/5/12>. PMID: [15885144](https://pubmed.ncbi.nlm.nih.gov/15885144/)
46. Jimenez-Escrig A, Jimenez-Jimenez I, Sanchez-Moreno C, Saura-Calixto F. Evaluation of free radical scavenging of dietary carotenoids by the stable radical 2,2-diphenyl-1-picrylhydrazyl. *J. Sci Food Agric*. 2000; 80(11):1686–1690. Available: <http://onlinelibrary.wiley.com/doi/10.1002/1097-0010%2820000901%2980:11%3C1686::AID-JSFA694%3E3.0.CO;2-Y/abstract>.
47. Owen RW, Giacosa A, Hull WE, Haubner R, Würtele G, Spiegelhalder B, et al. Olive-oil consumption and health: the possible role of antioxidants. *Lancet Oncol*. 2000; 1:107–12. Available: <http://www.ncbi.nlm.nih.gov/pubmed/11905662>. PMID: [11905662](https://pubmed.ncbi.nlm.nih.gov/11905662/)
48. Mohajeri A, Somayeh Asemari S. Theoretical investigation on antioxidant activity of vitamins and phenolic acids for designing a novel antioxidant. *J. Mol Struct*. 2009; 930 (1–3): 15–20. Available: <https://www.infona.pl/resource/bwmeta1.element.elsevier-ddbabf11-45d3-374b-9151-f3e89cb0a36a>.



# Antioxidant Supplementation in the Treatment of Aging-Associated Diseases

Valeria Conti<sup>††</sup>, Viviana Izzo<sup>††</sup>, Graziamaria Corbi<sup>2\*</sup>, Giusy Russomanno<sup>1</sup>,  
Valentina Manzo<sup>1</sup>, Federica De Lise<sup>3</sup>, Alberto Di Donato<sup>3</sup> and Amelia Filippelli<sup>1</sup>

<sup>1</sup> Department of Medicine and Surgery, University of Salerno, Baronissi, Italy, <sup>2</sup> Department of Medicine and Health Sciences, University of Molise, Campobasso, Italy, <sup>3</sup> Department of Biology, University of Naples Federico II, Naples, Italy

## OPEN ACCESS

### Edited by:

Filippo Caraci,  
University of Catania, Italy

### Reviewed by:

Fabio Tascedda,  
University of Modena and Reggio  
Emilia, Italy

Giovanni Li Volti,  
University of Catania, Italy

### \*Correspondence:

Graziamaria Corbi  
graziamaria.corbi@unimol.it

<sup>††</sup>These authors have contributed  
equally to this work.

### Specialty section:

This article was submitted to  
Experimental Pharmacology and Drug  
Discovery,  
a section of the journal  
Frontiers in Pharmacology

**Received:** 14 December 2015

**Accepted:** 25 January 2016

**Published:** 12 February 2016

### Citation:

Conti V, Izzo V, Corbi G,  
Russomanno G, Manzo V, De Lise F,  
Di Donato A and Filippelli A (2016)  
Antioxidant Supplementation  
in the Treatment of Aging-Associated  
Diseases. *Front. Pharmacol.* 7:24.  
doi: 10.3389/fphar.2016.00024

Oxidative stress is generally considered as the consequence of an imbalance between pro- and antioxidants species, which often results into indiscriminate and global damage at the organismal level. Elderly people are more susceptible to oxidative stress and this depends, almost in part, from a decreased performance of their endogenous antioxidant system. As many studies reported an inverse correlation between systemic levels of antioxidants and several diseases, primarily cardiovascular diseases, but also diabetes and neurological disorders, antioxidant supplementation has been foreseen as an effective preventive and therapeutic intervention for aging-associated pathologies. However, the expectations of this therapeutic approach have often been partially disappointed by clinical trials. The interplay of both endogenous and exogenous antioxidants with the systemic redox system is very complex and represents an issue that is still under debate. In this review a selection of recent clinical studies concerning antioxidants supplementation and the evaluation of their influence in aging-related diseases is analyzed. The controversial outcomes of antioxidants supplementation therapies, which might partially depend from an underestimation of the patient specific metabolic demand and genetic background, are presented.

**Keywords:** vitamins, resveratrol, sirtuins, hormesis, oxidative stress

## INTRODUCTION

Reactive oxygen species (ROS) comprise both free radicals such as superoxide ( $O_2^{\bullet-}$ ), and non-radical species such as hydrogen peroxide ( $H_2O_2$ ), (Weseler and Bast, 2010; Gülçin, 2012). These molecules, continuously produced in the cell, are involved in physiological events such as cell differentiation, primary immune defense, and signaling (Poli et al., 2004; Shah and Sauer, 2006; Gülçin, 2012). Indeed, some ROS such as  $H_2O_2$  are versatile players of the molecular signaling machinery because they are small, highly diffusible, and can be rapidly generated and degraded (Gough and Cotter, 2011).

Both radical and non-radical ROS are pro-oxidant species capable of oxidizing in the cell different biomolecules (Sies, 1991), which leads to a sequence of chain reactions that may end up in molecular and cellular damage (Gülçin, 2012).

The balance between beneficial and detrimental effects of ROS is preserved in the cell by the activity of a complex array of non-enzymatic and enzymatic detoxification mechanisms collectively

known as antioxidants (Sies, 1993; Bast and Haenen, 2015). Antioxidants are able to counteract, at relatively low concentrations, the damage induced in cells by ROS, thus protecting physiological targets such as lipids, DNA and proteins (Loguercio et al., 2012; Bast and Haenen, 2015). Noteworthy, antioxidants may also act indirectly by regulating redox-sensitive signal transduction pathways including transcription factors, and inhibition of poly (ADP-ribose) polymerase (PARP-1) (Weseler and Bast, 2010).

An imbalance of either the pro-oxidant and/or the antioxidant parties is at the origin of a complex physiological status known as “oxidative stress” (Davies, 1995; Conti et al., 2015a,b), which may be also favored by external sources, and by the presence of dietary compounds of pro-oxidant nature such as quinones (Gülçin, 2012).

Elderly people are more susceptible to oxidative stress due to a reduction in the efficiency of their endogenous antioxidant systems. Organs such as heart and brain, with limited replication rate and high levels of oxygen consumption, are particularly vulnerable to this phenomenon, thus explaining almost in part the high prevalence of neurological and cardiovascular diseases (CVD) in elderly (Ames et al., 1993; Stadtman and Berlett, 1997; Corbi et al., 2008).

A substantial body of literature reported an inverse correlation between serum or plasma total antioxidant capacity and both the onset and progression of several diseases, primarily CVD (Ciancarelli et al., 2012), but also diabetes (Opara et al., 1999), respiratory (Gumral et al., 2009) and neurological disorders (Schrag et al., 2013).

Consequently, antioxidants supplementation was suggested as a promising therapy in line with the general acceptance of the Free Radical Theory of Aging (FRTA) (Harman, 1956, 2006). First presented in Harman (1956), this theory is based on the assumption that lowering the global level of ROS in the body might retard aging, increase life span and be effective in preventing and treating aging-associated diseases (Sadowska-Bartosz and Bartosz, 2014). Further refinements of this theory addressed the roles of other activated oxygen species in aging in the more generalized Oxidative Stress Theory of Aging (OSTA) (Bokov et al., 2004; Muller et al., 2007).

This awareness resulted from one side in boosting in the scientific community the quest for novel natural or synthetic antioxidants (Donadio et al., 2015), and on the other in establishing several treatment strategies whose aim was to counterbalance oxidative stress by supplementing exogenous antioxidants, either singularly or in combination (Bouayed and Bohn, 2010).

However, the clinical expectations of antioxidants-based therapies have been frequently disappointed. The interplay between endogenous and exogenous antioxidants with the overall redox system in humans is very complex and represents a topical issue that is still under debate in the scientific community.

In this review a selection of recent clinical studies concerning antioxidants supplementation and the evaluation of their influence in aging-related diseases is analyzed (Table 1).

## NATURAL ANTIOXIDANTS USED IN RECENT CLINICAL STUDIES

Many natural compounds have been considered, either singularly or in combination, for supplementation therapies. Among them, we devoted particular attention to a specific subset of molecules such as vitamin C, vitamin E, resveratrol, curcumin, hydroxytyrosol and coenzyme Q10.

Ascorbic acid is the main form of vitamin C in the human body and acts as the co-substrate for several enzymes that are important for the organism’s functioning. Its antioxidant activity relies on the ability to be reversibly oxidized to ascorbyl radical and then to dehydroascorbate (DHA) (Wells and Xu, 1994).

The distribution and the concentration of vitamin C in the organs depend on their specific ascorbate requirements and on the tissue distribution of sodium-dependent vitamin C transporter 1 and 2 (SVCT1 and SVCT2) (Figueroa-Mendez and Rivas-Arancibia, 2015).

Vitamin C (ascorbic acid) has different important roles in the cell; as a reducing agent and an antioxidant, ascorbate is able to react and inactivate ROS and, most importantly, reduces in membranes LDL and  $\alpha$ -tocopheroxyl radicals to regenerate  $\alpha$ -tocopherol (Vitamin E) (Chambial et al., 2013).

One of the several biological functions mediated by ascorbate is the enhancement of nitric oxide bioavailability, which is essential to preserve endothelial homeostasis (Carr and Frei, 1999). A recent meta-analysis (Ashor et al., 2014) revealed that vitamin C supplementation counteracts endothelial dysfunction (ED), which is doubtless one of the major contributors for both the development and progression of CVDs (Versari et al., 2009; Conti et al., 2012b, 2013; Corbi et al., 2012; Zhang et al., 2014), suggesting a clinical impact of supplementation only in subjects at higher CVDs risk. Antoniadou et al. (2004) found that a vitamin C supplementation of 2 g/day for 4 weeks increased forearm vasodilator response to reactive hyperemia in patients with combined diabetes (DM) and coronary artery diseases (CAD).

An interesting study by Mullan et al. (2002) showed that an oral administration of ascorbic acid (500 mg/day) for 1 month lowered blood pressure and reduced systemic arterial stiffness; conversely, other two randomized controlled trials failed to prove a blood pressure-lowering effect of vitamin C supplementation (Lovat et al., 1993; Ghosh et al., 1994).

However, the role played by vitamin C in aging-associated diseases has not been adequately investigated in clinical trials mainly because this antioxidant was often used in combination with other molecules (Watanabe et al., 1998; Salonen et al., 2003).

When referring to vitamin E, a family of 8 isoforms classified in two categories is considered: four saturated analogs ( $\alpha$ ,  $\beta$ ,  $\gamma$ , and  $\delta$ ) called tocopherols and four unsaturated analogs indicated as tocotrienols, which differ for the methylation pattern (Cardenas and Ghosh, 2013). These molecules are hydrophobic fat-soluble compounds found in a variety of food sources such as corn oil, peanuts, vegetable oils, fruits and vegetables (Cardenas and Ghosh, 2013). Most of the studies presented in literature have been performed using  $\alpha$ -tocopherol (Wallert et al., 2014; Hanson et al., 2015) that is considered the most active isomer

**TABLE 1 | Clinical studies performed with the main antioxidants.**

Antioxidant	Disease	Primary results	Reference
Vitamin C	Type 2 DM and CAD	↑ Forearm vasodilator response	Antoniades et al., 2004
	DM	↓ Arterial blood pressure and improvement of arterial stiffness	Mullan et al., 2004
	IHD	Prevention of nitrate tolerance	Watanabe et al., 1998
Vitamin E	CAD	↓ Rate of non-fatal MI	Stephens et al., 1996
	CVD and DM	No effect on cardiovascular outcomes	Yusuf et al., 2000
	Vascular disease and DM	↑ Risk for HF	Lonn et al., 2005
	Prior MI	↑ Chronic HF in patients with LVD	Marchioli et al., 2006
Resveratrol	CAD	↓ Plasma biomarkers of oxidative stress and inflammation	Devaraj et al., 2007
	Hypertension and dyslipidemia	↓ Endothelial dysfunction	Carrizzo et al., 2013
Coenzyme Q10	DM	Improvement of glucose control and insulin sensitivity	Liu et al., 2014
	CAD	↑ Antioxidant enzymes activities and ↓inflammation	Lee et al., 2013
Vitamin E and C	Hypercholesterolemia	↓ atherosclerotic progression	Salonen et al., 2003
Vitamins C, E and β-carotene (alone or in combination)	CVD	No overall effects on cardiovascular events	Cook et al., 2007

DM, diabetes mellitus; CAD, coronary artery disease; IHD, ischemic heart disease; CVD, cardiovascular disease; MI, myocardial infarction; HF, heart failure; LVD, left ventricular dysfunction.

within this group and the main hydrophobic antioxidant in cell membranes and circulating lipoproteins. Its antioxidant function is strongly supported by the regeneration promoted by vitamin C  $\alpha$ -Tocopherol exhibits strong antioxidant capacity *in vitro* and has been shown to inhibit LDL oxidation (Wallert et al., 2014).

In addition,  $\alpha$ -tocopherol shows a remarkable anti-inflammatory action by inhibiting, for example, cyclooxygenase-2 (COX2) (O'Leary et al., 2004). Next to its anti-inflammatory and antioxidative properties, vitamin E shows other properties, such as the modulation of the expression of genes encoding proteins involved in signaling (Cardenas and Ghosh, 2013). In addition vitamin E is also involved in the uptake, transport and degradation of tocopherols, as well as the uptake of lipoproteins and the storage and export of lipids such as cholesterol (Cardenas and Ghosh, 2013).

The beneficial effects of vitamin E dietary intake have been described (O'Leary et al., 2004; Hanson et al., 2015), whereas the data concerning vitamin E supplementation are controversial. An old randomized controlled trial by Stephens et al. (1996) showed that in patients with CAD, 1 year of  $\alpha$ -tocopherol supplementation reduced the rate of non-fatal myocardial infarction. However, very few human studies have confirmed the efficacy of vitamin E supplementation in aging-associated diseases, and most of them focused on the role of vitamin E supplementation in influencing aspects of aging phenotypes, such as oxidative stress and inflammation biomarkers. In this specific context some investigations, performed both in animals models and in humans, effectively demonstrated benefits of vitamin E supplementation (Iuliano et al., 2000; Navarro et al., 2005; Abdala-Valencia et al., 2012), while others showed negative impact (Bjelakovic et al., 2012), or no effect at all (Morley and Trainor, 2001; Hemilä and Kaprio, 2011).

Two large randomized trials (Yusuf et al., 2000; Lonn et al., 2005) investigated the impact of vitamin E supplementation on CVDs and cardiovascular events in patients at high risk. The "Heart Outcomes Prevention Evaluation (HOPE)" analyzed

the efficacy of a treatment with vitamin E in preventing cardiovascular outcomes in 9,541 patients with CVD or diabetes in addition to at least one other risk factor (Yusuf et al., 2000). This study, with mean follow-up of 4.5 years, showed that vitamin E did not reduce the incidence of cardiovascular events when compared to placebo, thus suggesting the lack of an evident beneficial effect exerted by this antioxidant (Yusuf et al., 2000).

The "HOPE-TOO" (Lonn et al., 2005) an extension of the HOPE study, was aimed at assessing whether longer duration of the treatment with vitamin E could prevent cancer and/or CVD during a follow-up of 7 years. The HOPE-TOO, involving 7,030 patients, confirmed that administration of 400 IU of vitamin E had no evident impact either on cancer outcomes or on major cardiovascular events and death. Furthermore, during the HOPE-TOO study, the investigators advanced the hypothesis that vitamin E supplementation might even be responsible to increase the risk of heart failure (Lonn et al., 2005).

Another clinical trial explored the effect of vitamin E on the development of chronic heart failure (CHF) in 8,415 post-infarction patients without CHF at baseline (Marchioli et al., 2006). The authors found that vitamin E treatment was associated with a 50% increase of CHF in patients with left ventricular dysfunction, thus confirming the conclusion raised by the HOPE trial investigators.

More recently, Devaraj et al. (2007) evaluated the effect of a high dose of  $\alpha$ -tocopherol (1,200 IU/die for 2 years) in CAD patients with high levels of oxidative stress. The authors demonstrated that vitamin E supplementation lowered plasmatic levels of inflammation markers, such as high-sensitivity C-reactive protein and tumor necrosis factor- $\alpha$ , and the levels of oxidative stress biomarkers, such as plasmatic oxidized LDL, urinary F2-isoprostanes and monocytes superoxide anion concentrations (Devaraj et al., 2007). However,  $\alpha$ -tocopherol supplementation failed to induce any change in intima-media thickness of carotid arteries and no significant differences in

cardiovascular events were observed between patients treated with vitamin E and those with placebo (Devaraj et al., 2007).

As previously underlined, vitamins E and C have been frequently used in combination in clinical trials concerning aging-associated diseases. The “Women’s antioxidant Cardiovascular Study (WACS)” (Cook et al., 2007) investigated the effect of vitamins C, E and  $\beta$ -carotene (alone or in combination) in preventing cardiovascular events in 8,171 patients with either a history of CVD or at least three cardiovascular risk factors, and during an average 9.4 year follow-up (Cook et al., 2007). Results from WACS, as in the case of other antioxidant trials performed with women, failed to find any preventive effects of the antioxidants used on CVD.

The Physicians’ Health Study II (PHS II) (Sesso et al., 2008) randomized trial investigated instead the effects of vitamins E and C in the prevention of CVD in men during a mean follow-up of 8 years. This trial did not evidence any benefit from antioxidant supplementation on major CVD outcomes; moreover, vitamin E was associated with an increased risk of stroke (Sesso et al., 2008).

In a recent prospective study performed with 3,919 aged men, Wannamethee et al. (2013) showed that higher plasma levels of vitamin C, but not those of vitamin E, are inversely associated with cardiovascular risk factors, including blood lipids and blood pressure. Notably, whereas the dietary intake of vitamin C did not exert any influence, the dietary intake of vitamin E was significantly correlated with increased risk of HF (Wannamethee et al., 2013). The authors of this interesting investigation suggested that the reason for the association between vitamin E intake and HF might depend by the fact that vitamin E ( $\alpha$ -tocopherol) may become a pro-oxidant in an environment characterized by high oxidative stress, such as an aged biological system (Wannamethee et al., 2013).

Resveratrol (3, 4', 5-trihydroxystilbene) is a phytoalexin that belongs to the stilbene class of compounds, abundant in many plants, such as peanuts, blueberries, pine nuts and grapes where it mainly accumulates in a glycosylated form, and that is synthesized in response to fungal infection and to some environmental stresses like climate, ozone and ultraviolet irradiation (Harikumar and Aggarwal, 2008).

Resveratrol appears to modulate numerous cell-signaling pathways through the regulation of different molecular targets including the AMP-regulated kinase AMPK and the NAD-dependent deacetylase Sirt-1 (Yun et al., 2014; Conti et al., 2015a). The variety of molecular mechanisms mediated by this compound translates into a plethora of biological actions, primarily, antioxidant and anti-inflammatory effects. Resveratrol is a good antioxidant and blocks *in vitro* LDL oxidation, a biological phenomenon associated with the risk of coronary heart disease and myocardial infarction (Khurana et al., 2013). In rodents, resveratrol supplementation has been shown to decrease cardiovascular risk factor, including blood lipids and VCAM-1, to improve cardiovascular function and physical capacity and to decrease inflammation in the vasculature of aged

animals leading to improved vascular function (Gliemann et al., 2013).

The anti-inflammatory properties of resveratrol have been proved by several *in vitro* experiments. For instance, resveratrol was showed to suppress NF- $\kappa$ B activity induced by beta-amyloid in PC12 neuron cell lines, (Jang and Surh, 2003) and to reduce the production of IL-1 beta and TNF-alpha induced by LPS or beta-amyloid in the microglia (Capiralla et al., 2012; Zhong et al., 2012), suggesting a neuroprotective effect that has also been confirmed in cellular models of neurodegenerative disorders, such as Parkinson’s and Alzheimer’s diseases (Albani et al., 2009). Resveratrol anti-inflammatory effect has been demonstrated also *in vivo*, i.e., in an animal model of asthma in which this molecule mitigated structural airway remodeling (Royce et al., 2011) or in rats with LPS-induced liver failure where resveratrol improved hepatotoxic markers by multiple mechanisms such as downregulation of NOS-2, and modification of oxidative stress parameters (Farghali et al., 2009).

Despite the promising results reported *in vitro* (Zhang et al., 2011; Montesano et al., 2013) and in animal models (Saleh et al., 2014), few studies have been performed directly in humans and the results obtained are not quite convergent.

Recent studies underlined the importance of patient selection in evaluating the potential therapeutic effects of resveratrol. Recently, Carrizzo et al. (2013) conducted an *ex vivo* study to investigate the effects of resveratrol on superior thyroid artery obtained from 59 patients (63 years of mean age) with hypertension and dyslipidemia, and found that resveratrol reduced ED via modulation of NO metabolism and attenuation of vascular oxidative stress. Interestingly, resveratrol failed to exert any effect in vessels from patients without hypertension or dyslipidemia (Carrizzo et al., 2013). A differential effect of resveratrol influenced by the initial health status was also suggested by a recent meta-analysis by Liu et al. (2014) which highlighted that resveratrol improves glucose control and insulin sensitivity in diabetic patients but does not affect glycemic values in non-diabetic subjects.

In a recent work published by Gliemann et al. (2013), the authors tested for the first time the combined effect of exercise training (ET) and resveratrol on vascular function in aged humans. In this trial 27 healthy physically inactive aged men were randomized into 8 weeks of daily intake of either 250 mg of trans-resveratrol or of placebo and were subjected to concomitant high-intensity ET (Gliemann et al., 2013).

The main aim of the study was to confirm if oral resveratrol supplementation improved the positive cardiovascular adaptations to ET in aged subjects by specifically increasing sirtuin 1 (SIRT1) mediated signaling and by promoting the endogenous antioxidant system. Interestingly, results showed that, whereas ET effectively improved several cardiovascular health parameters in aged men, concomitant resveratrol supplementation somehow blunted most of these effects leading, among others, to a significantly lower improvement in the training-induced increase in maximal oxygen uptake (Gliemann et al., 2013).

Curcumin is a lipophilic bioactive phenol derived from the rhizome of *Curcuma longa*, which shows low solubility and stability in aqueous solution. It is contained in culinary curry and used as a coloring agent in food (Bhullar et al., 2013). Orally ingested curcumin is metabolized into the active metabolite tetrahydrocurcumin by a reductase found in the intestinal epithelium (Sadowska-Bartosz and Bartosz, 2014). Extensive research during the last few decades has suggested a strong therapeutic and pharmacological potential of this molecule as antioxidant, antimutagenic, antiprotozoal and antibacterial agent (Bhullar et al., 2013).

Curcumin strong medicinal properties are also associated with reported anti-cancer and neuroprotective effect such as in Alzheimer disease (Brondino et al., 2014). A hormetic mechanism of action of this compound is suggested from studies showing that expression levels of the stress response protein Heme Oxygenase-1 (HO-1) were increased in cultured hippocampal neurons treated with curcumin (Scapagnini et al., 2006). Moreover, this phenolic compound has been shown to reverse chronic stress-induced impairment of hippocampal neurogenesis and increase expression of brain-derived neurotrophic factor (BDNF) in an animal model of depression (Xu et al., 2007). Several studies also showed that curcumin interacts with NF- $\kappa$ B, and through this interaction exerts protective function also in the regulation of T-cell-mediated immunity (Kou et al., 2013). Recently González-Reyes et al. (2013) identified curcumin as a neuroprotector against hemin, the oxidized form of heme, which induced damage in primary cultures of cerebellar granule neurons of rats. In this study, a pretreatment of the neurons with 5–30  $\mu$ M curcumin increased by 2.3–4.9 fold HO-1 expression and by 5.6–14.3-fold Glutathione (GSH) levels. Moreover, 15  $\mu$ M curcumin lowered by 55% the increase in ROS production, by 94% the reduction of GSH/glutathione disulfide ratio, and by 49% cell death induced by hemin. Furthermore, curcumin induced the translocation into the nucleus of nuclear factor related factor-2 (Nrf2), thereby stimulating an inflammatory and antioxidant response against hemin-induced neuronal death (González-Reyes et al., 2013).

Curcumin effects on both the arterial endothelial function and the central arterial compliance was recently evaluated in post-menopausal women that underwent a daily ingestion of 150 mg of curcumin (Akazawa et al., 2012). In 32 post-menopausal women the Flow Mediated Dilation (FMD) measured arterial endothelial function, before and after 8 weeks of curcumin ingestion or ET. After this time, the authors observed that FMD increased significantly both in the exercise and curcumin groups, whereas no significant change in FMD was detected in the control group (Akazawa et al., 2012). The results obtained suggested that a regular ingestion of curcumin could improve endothelial function and might be a potential alternative treatment for patients who are unable to exercise. In a different study performed by the same group (Akazawa et al., 2013) and involving this time 51 post-menopausal women, the effects of curcumin ingestion alone and in combination with aerobic ET on central arterial compliance were evaluated. In this case also, the regular ingestion of curcumin, as the ET alone,

significantly increased carotid arterial compliance in the group analyzed. Interestingly, the combination of ET and curcumin ingestion, differently from what observed with resveratrol (Gliemann et al., 2013), led to a cumulative beneficial effect in the improvement of the arterial compliance (Akazawa et al., 2013).

Hydroxytyrosol is an ortho-diphenol (a catechol) abundant in olive, fruits and extra virgin olive oil (Waterman and Lockwood, 2007). This compound, due to its catecholic structure, shows a marked antioxidant activity and is able to scavenge oxygen and nitrogen free radicals, inhibit LDL oxidation, platelet aggregation and endothelial cell activation, and protects DNA from oxidative damage (Waterman and Lockwood, 2007; Notomista et al., 2011; Bulotta et al., 2014). Hydroxytyrosol is also a metal chelator and is able to scavenge the peroxy radicals and break peroxidative chain reactions producing very stable resonance structures (Bulotta et al., 2014). Interestingly, scavenging activity of hydroxytyrosol has also been demonstrated with respect to hypochlorous acid (HOCl) (Visioli et al., 1998) a potent oxidant produced *in vivo* at the site of inflammation, a phenomenon which may be critical for the protection from atherosclerosis, since HOCl can oxidize the apoprotein component of LDL. Moreover, it has been recently reported (Giordano et al., 2014) that hydroxytyrosol is endowed with the ability to modulate an adaptive signaling pathway activated after endoplasmic reticulum (ER) stress and to improve ER homeostasis itself.

The antioxidant activity of hydroxytyrosol seems to be related *in vivo* to its high bioavailability: various studies have in fact documented a high degree of absorption of this compound, which is fundamental to exert its biological activities (Bulotta et al., 2014). Several studies, mostly performed in cell and animal models, have suggested beneficial effects of hydroxytyrosol in the prevention or treatment of chronic and degenerative diseases, especially CVD and cancer (Facchini et al., 2014). Most of the studies currently presented in literature on hydroxytyrosol are performed *in vitro* on cultured eukaryotic cells and very few are the clinical trials performed in humans and more specifically on elderly people. One of the main reasons is probably the fact that purified hydroxytyrosol is still very expensive, which hampers its use for long-lasting trials. Currently, the attention of the scientific community is focused more on the effect of olive oil supplementation on health, but olive oil is a complex mixture containing variable amounts of triacylglycerols, fatty acids and polyphenols (Waterman and Lockwood, 2007), thus no conclusive hypothesis of the use of purified hydroxytyrosol can yet be drawn from these studies.

Oliveras-López et al. (2013) evaluated the effects of daily consumption of extra virgin olive oil in 62 subjects aged 65–96 years. After a 6-weeks daily intake of polyphenol-rich olive oil with high oleuropein derivative contents, the authors found a significant improvement in lipid profiles, including a reduction of total cholesterol and a significant increase of HDL levels. Moreover, in the same subjects, an increase of serum total antioxidant capacity, and a concomitant significant increase of catalase in erythrocytes and decrease in superoxide dismutase and glutathione peroxidase activities were also observed (Oliveras-López et al., 2013).

Coenzyme Q10 (CoQ10), referred to as ubiquinol in its most active (95%) and reduced form (Q10H<sub>2</sub>), is a lipophilic molecule present in the membranes of almost all human tissues, and essential for the respiratory transport chain (Onur et al., 2014). The side chain serves to keep the molecule anchored in the inner mitochondrial membrane, and the quinone ring, which is easily and reversibly reduced to the quinol form, enables it to fulfill its function of transferring electrons from complexes I and II to complex III in the respiratory chain, ultimately resulting in the reduction of oxygen to water and the generation of ATP (Nowicka and Kruk, 2010; Laredj et al., 2014). CoQ10 is also capable of recycling and regenerating other antioxidants such as  $\alpha$ -tocopherol and ascorbate. CoQ10 has also been identified as a modulator of gene expression, inflammatory processes and apoptosis (Bhagavan and Chopra, 2007). The quinol prevents lipid peroxidation by inhibiting the initial formation and propagation of lipid peroxy radicals, and in the process it is oxidized to the quinone and H<sub>2</sub>O<sub>2</sub> is produced. In addition, it has been shown to protect proteins from oxidation by a similar mechanism (Forsmark-Andrée et al., 1995), and to prevent oxidative DNA damage such as strand breakages. As well as its role in the cellular membranes, CoQ is also believed to function in the blood to protect lipoproteins such as very low density (VLDL), low density (LDL) and high density (HDL) lipoproteins from oxidation (Bentinger et al., 2007). Current evidence suggests that CoQ has a number of independent anti-inflammatory effects (Schmelzer et al., 2007). It has been shown to reduce the secretion of pro-inflammatory cytokines in monocytes and lymphocytes after an inflammatory stimulus by influencing the expression of NF- $\kappa$ B-dependent genes (Schmelzer et al., 2009; Bentinger et al., 2010). Furthermore, dietary supplementation with CoQ10 has been reported to improve ED in patients with diabetes by up-regulating nitric oxide production (patients received 200 mg CoQ10/day for 12 weeks) (Watts et al., 2002), and to decrease hepatic inflammatory stress caused by obesity in mice (Sohet et al., 2009).

Coenzyme Q10 supplementation at 300 mg/day was reported to significantly enhance antioxidant enzymes activities and lower inflammation in patients who have CAD during therapy with statins (Lee et al., 2013). Statins can effectively lower CoQ synthesis as they inhibit 3-hydroxy-3-methylglutaryl Coenzyme A reductase (HMG-CoA reductase), the rate-limiting enzyme in the pathway of cholesterol synthesis which includes the formation of the isoprenoid units required to produce CoQ (Goldstein and Brown, 1990). Moreover, CoQ levels may be pathologically modified in conditions associated with oxidative stress and in aging (Potgieter et al., 2013; Botham et al., 2015).

Data presented in literature on CoQ10 supplementation are heterogeneous and involve a very large number of pathologies. As for HF, no conclusions can be drawn on the benefits or harms of coenzyme Q10 as trials published in literature lack fundamental information concerning clinically relevant endpoints (Madmani et al., 2014). More in detail, reports on the effect of CoQ10 in diseases depending on oxidative stress in elderly people are scarce. In a recent study (Bloomer et al., 2012), 15 exercise-trained individuals (10 men and 5 women; 30–65 years) received

300 mg of reduced CoQ10 per day or a placebo for 4 weeks in a random order, double blind, crossover design. Treatment with CoQ10 resulted in a significant increase in total blood CoQ10 and reduced blood CoQ10, but did not translate into improved exercise performance or decreased oxidative stress (Bloomer et al., 2012).

## HORMESIS AND GENETIC VARIABILITY INFLUENCE ON THE OUTCOMES OF ANTIOXIDANTS SUPPLEMENTATION

As previously reported, clinical trials involving the use of antioxidants supplementation often show conflicting results and lead to dangerous misconceptions, either too positive or too negative, on the use of these molecules in the treatment of several aging-associated diseases. Amid this debate, the first aspect that should be considered is that there are several limitations concerning FRTA, the basic hypothesis on which the antioxidants supplementation therapies are mainly based. This theory, as already underlined, suggests a linear dose-response relationship between increasing amounts of ROS and biological damages, which potentially culminates in diseases and mortality. Therefore, oxidative stress should represent the main driving force of aging and a major determinant of lifespan (Sadowska-Bartosz and Bartosz, 2014). To date, many investigations have urged to reexamine FRTA leading to a modernized view of this theory that takes also in account the so-called “mitohormesis.” According to this concept, a large amount of ROS causes detrimental effects on the cells, whereas low or moderate levels of ROS may exert an opposite effect improving biological outcomes (Ristow and Schmeisser, 2014; Yun and Finkel, 2014). The beneficial effects of caloric restriction (CR) and ET are a good example because they can be considered both as oxidative stressors or inducer of the endogenous antioxidant system activation by favoring a transient cellular increase of ROS (Corbi et al., 2012). Many independent investigations raised the possibility that an initial induction of ROS triggered by CR promotes an adaptive stimulation of antioxidant enzymes at the steady state, consequentially CR is now considered as the first example of mitohormesis (Agarwal et al., 2005; Schulz et al., 2007; Mesquita et al., 2010; Zarse et al., 2012). CR likely induces an adaptive hormetic response through different molecular pathways, one of these involving sirtuins, a family of NAD<sup>+</sup>-dependent deacetylases conserved from yeasts to humans (Banerjee et al., 2012). SIRT1, the first member of sirtuins characterized in humans, plays a crucial role in inducing mitochondrial biogenesis and mediating oxidative stress response through a number of proteins that promote the expression of antioxidant genes, such as peroxisome proliferator-activated receptor (PPAR) gamma coactivator-1 alpha 5 (PGC-1 $\alpha$ ) (St-Pierre et al., 2006) and Forkhead transcription factors member, FOXO3a. SIRT1 interacts with FOXO3a in cells in response to oxidative stress increasing FOXO3 ability to induce cell cycle arrest and resistance to oxidative stress and, at the same time inhibiting FOXO3 ability to induce cell death (Brunet et al., 2004). Ferrara et al. (2008) demonstrated that exercise-induced

increase in SIRT1 activity in the heart of aged rats caused an increase in the expression of FOXO3a and an up-regulation of FOXO3a targets involved in the oxidative stress response, including SOD and catalase.

Exercise training, as CR, is to date considered an intervention triggering a cellular hormetic adaptation (Radak et al., 2005; Ji et al., 2006). Physical inactivity is indeed one of the major risk factors for CVD, neurodegenerative disorders and many other diseases; consequentially, regular physical exercise exerts health promoting effect on such clinical conditions and in general on aging-related diseases (Hu et al., 2001; Conti et al., 2012b; Brown et al., 2013). Exercise is strictly correlated to enhanced mitochondrial biogenesis and increased production of ROS and may promote longevity through pathways common to those of CR (Lanza et al., 2008). However, the benefits linked to ET strictly depend on the type and workload of exercise and, in particular, overtraining can result in maladaptation and possibly cellular damage (Alessio and Goldfarb, 1988; Chevion et al., 2003; Conti et al., 2012a, 2013). ET has been reported to activate PGC-1 $\alpha$ , which controls mitochondrial gene expression by a variety of transcription factors (Nikolaidis and Jamurtas, 2009). This regulation culminates in enhanced oxygen consumption in muscle fibers, which, in turn, promotes ROS generation. Moreover, beyond skeletal muscle, other tissues, such as blood, heart and lung, represent a source of ROS during exercise (Nikolaidis and Jamurtas, 2009). Concomitantly to enhanced ROS production, regular exercise leads to the up-regulation of several antioxidant enzymes, including SODs, catalase and glutathione peroxidase, reinforcing the concept that a certain amount of ROS is necessary for exercise health-promoting effects (Nikolaidis and Jamurtas, 2009).

It is not surprising, then, that both older and recent studies showed that purified antioxidants supplementation might be inadequate or even damaging for athletes, as they seem to abolish ET benefits, including prevention of certain diseases. A very interesting study by Ristow et al. (2009) investigated whether exercise could promote insulin-sensitizing abilities in a ROS-dependent manner in healthy humans. The authors measured insulin sensitivity by glucose infusion rate (GIR) and the amount of ROS within skeletal muscle of trained subjects (previously untrained) in the presence or absence of antioxidant supplementation with vitamin E and vitamin C. As expected, ET induced ROS formation, which was counteracted by the antioxidant treatment. However, concomitantly to the increase of TBARs, ET was able to stimulate the expression of antioxidant molecules, such as SOD and GPx and induced an increase of GIR; these effects were also inhibited by antioxidants supplementation. The conclusion of this study was that a transient increase of oxidative stress may contribute to prevent insulin resistance and type 2 diabetes and, most importantly, antioxidant supplementation may abrogate these results (Ristow et al., 2009).

In addition to hormesis another aspect that should be considered for the conflicting results obtained in the clinical trials is the genetic background of the patients enrolled in the studies. In the last decade an increasing number of studies have suggested that longevity depends not only on life style habits

but also on the genetic background. Oxidative stress response is one of the most evolutionary conserved pathways involved in determination of lifespan from yeast to humans (Vijg and Suh, 2005; vB Hjelmborg et al., 2006) and, indeed, genome wide association studies (GWAS) have identified genetic determinants associated to the levels of circulating antioxidants, which could be linked to human diseases (Ahn et al., 2010). A GWAS authored by Major et al. (2012) revealed that three single nucleotide polymorphisms (SNPs), two located in genes involved in vitamin E transport and metabolism (BUD13 and CYP4F2), and one in NKAIN3, the gene encoding a Na<sup>+</sup>/K<sup>+</sup> transport membrane protein, are associated with response to vitamin E supplementation in humans. The authors concluded that genetic variation contributes to the variability of serologic vitamin E status and may have potential application in determining the regimen of antioxidant supplementation required in complex diseases such as CVD and diabetes (Major et al., 2012). Very interesting data concern Haptoglobin (Hp), a protein encoded by a polymorphic gene with 2 common alleles denoted 1 and 2, which counteracts the increase of ROS induced by hemoglobin activity (Sadrazadeh et al., 1984). As previously reported, the HOPE trial, which investigated the potential protective effect of vitamin E in cardiovascular patients, showed that treatment with vitamin E had no effect on cardiovascular outcomes in patients at high risk for cardiovascular events (Yusuf et al., 2000). Later, Milman et al. (2008) verified such results moving from the hypothesis that HOPE study failed to prove the benefit of vitamin E supplementation because of the inadequate selection of patient genotype. To this end, the authors planned a prospective double-blinded clinical trial in a subgroup of individuals from the HOPE study with type 2 diabetes and found that vitamin E supplementation was effectively able to reduce cardiovascular events in patients with the Hp 2-2 genotype (Milman et al., 2008). Other studies confirmed the impact of Hp genotyping in determining potential benefits from antioxidant therapy, and strongly supported the efficacy of a pharmacogenomic strategy to personalize and fine-tune the treatment with vitamin E in patients with type 2 diabetes (Blum et al., 2010).

## CONCLUSION

Redox state homeostasis in living systems is very complex and life style factors undeniably concur in determining the impact of changes in oxidative stress response in both unhealthy and healthy subjects.

A large part of studies investigating the effectiveness of antioxidant supplementation therapy in humans raised contrasting results. This is due to many aspects among which the often-limited statistic power of the studies, the patient genetic background, the bioavailability of the molecules used, and the non-specific effects that antioxidants might have in the human body, should be taken into account.

Mainly in the elderly, the clinical trials conducted so far often suffer from an incorrect initial selection of the patients. Further investigations should be planned to improve patients selection by performing, for example, quantitative characterizations of the

redox state for each individual and taking into account both the individual patient demand and genetic background.

In addition it is worth to underline that, when dealing with either natural or synthetic antioxidants, clinical trials should consider other two important aspects. First, antioxidants bearing different functional moieties can be profoundly diverse in terms of chemical structure and mode of action; therefore, it should be recommended to identify the right antioxidant to treat a specific pathological condition (Bast and Haenen, 2013). Secondly, the validity of the biomarkers used to determine the effects of antioxidants on human health are still under debate (van Ommen

et al., 2009). Antioxidants, in fact, might be responsible of subtle effects specific for human health optimization and/or disease prevention, which are processes that can be very different in many aspects from disease onset and progression.

## AUTHOR CONTRIBUTIONS

VC, VI, and GC conceived and designed the review and wrote the paper; GR and VM performed the bibliographic research; FD and AD edited the manuscript; AF contributed to write the paper.

## REFERENCES

- Abdala-Valencia, H., Berdnikovs, S., and Cook-Mills, J. M. (2012). Vitamin E isoforms differentially regulate intercellular adhesion molecule-1 activation of PKC in human microvascular endothelial cells. *PLoS ONE* 7:e41054. doi: 10.1371/journal.pone.0041054
- Agarwal, S., Sharma, S., Agrawal, V., and Roy, N. (2005). Caloric restriction augments ROS defense in *S. cerevisiae*, by a Sir2p independent mechanism. *Free Radic. Res.* 39, 55–62. doi: 10.1080/10715760400022343
- Ahn, J., Yu, K., Stolzenberg-Solomon, R., Simon, K. C., McCullough, M. L., Gallicchio, L., et al. (2010). Genome-wide association study of circulating vitamin D levels. *Hum. Mol. Genet.* 19, 2739–2745. doi: 10.1093/hmg/ddq155
- Akazawa, N., Choi, Y., Miyaki, A., Tanabe, Y., Sugawara, J., Ajisaka, R., et al. (2012). Curcumin ingestion and exercise training improve vascular endothelial function in postmenopausal women. *Nutr. Res.* 32, 795–799. doi: 10.1016/j.nutres.2012.09.002
- Akazawa, N., Choi, Y., Miyaki, A., Tanabe, Y., Sugawara, J., Ajisaka, R., et al. (2013). Effects of curcumin intake and aerobic exercise training on arterial compliance in postmenopausal women. *Artery Res.* 7, 67–72. doi: 10.1016/j.artres.2012.09.003
- Albani, D., Polito, L., Batelli, S., De Mauro, S., Fracasso, C., Martelli, G., et al. (2009). The SIRT1 activator resveratrol protects SK-N-BE cells from oxidative stress and against toxicity caused by alpha-synuclein or amyloid-beta (1–42) peptide. *J. Neurochem.* 110, 1445–1456. doi: 10.1111/j.1471-4159.2009.06228.x
- Alessio, H. M., and Goldfarb, A. H. (1988). Lipid peroxidation and scavenger enzymes during exercise: adaptive response to training. *J. Appl. Physiol.* 64, 1333–1336.
- Ames, B. N., Shigenaga, M. K., and Hagen, T. M. (1993). Oxidants, antioxidants, and the degenerative diseases of aging. *Proc. Natl. Acad. Sci. U.S.A.* 90, 7915–7922. doi: 10.1073/pnas.90.17.7915
- Antoniades, C., Tousoulis, D., Tountas, C., Tentolouris, C., Toutouza, M., Vasiliadou, C., et al. (2004). Vascular endothelium and inflammatory process, in patients with combined Type 2 diabetes mellitus and coronary atherosclerosis: the effects of vitamin C. *Diabet. Med.* 21, 552–558. doi: 10.1111/j.1464-5491.2004.01201.x
- Ashor, A. W., Lara, J., Mathers, J. C., and Siervo, M. (2014). Effect of vitamin C on endothelial function in health and disease: a systematic review and meta-analysis of randomised controlled trials. *Atherosclerosis* 235, 9–20. doi: 10.1016/j.atherosclerosis.2014.04.004
- Banerjee, K. K., Ayyub, C., Ali, S. Z., Mandot, V., Prasad, N. G., and Kolthur-Seetharam, U. (2012). dSir2 in the adult fat body, but not in muscles, regulates life span in a diet-dependent manner. *Cell Rep.* 2, 1485–1491. doi: 10.1016/j.celrep.2012.11.013
- Bast, A., and Haenen, G. R. (2013). Ten misconceptions about antioxidants. *Trends Pharmacol. Sci.* 34, 430–436. doi: 10.1016/j.tips.2013.05.010
- Bast, A., and Haenen, G. R. M. M. (2015). “Nutritional antioxidants: it is time to categorise,” in *Antioxidants in Sport Nutrition*, Chap. 2, ed. M. Lamprecht (Boca Raton, FL: CRC Press).
- Bentinger, M., Brismar, K., and Dallner, G. (2007). The antioxidant role of coenzyme Q. *Mitochondrion* 7, S41–S50. doi: 10.1016/j.mito.2007.02.006
- Bentinger, M., Tekle, M., and Dallner, G. (2010). Coenzyme Q–biosynthesis and functions. *Biochem. Biophys. Res. Commun.* 396, 74–79. doi: 10.1016/j.bbrc.2010.02.147
- Bhagavan, H. N., and Chopra, R. K. (2007). Plasma coenzyme Q10 response to oral ingestion of coenzyme Q10 formulations. *Mitochondrion* 7, S78–S88. doi: 10.1016/j.mito.2007.03.003
- Bhullar, K. S., Jha, A., Youssef, D., and Rupasinghe, H. P. (2013). Curcumin and its carbocyclic analogs: structure-activity in relation to antioxidant and selected biological properties. *Molecules* 18, 5389–5404. doi: 10.3390/molecules18055389
- Bjelakovic, G., Nikolova, D., Gluud, L. L., Simonetti, R. G., and Gluud, C. (2012). Antioxidant supplements for prevention of mortality in healthy participants and patients with various diseases. *Cochrane Database Syst. Rev.* 3, CD007176. doi: 10.1002/14651858.CD007176.pub2
- Bloomer, R. J., Canale, R. E., McCarthy, C. G., and Farney, T. M. (2012). Impact of oral ubiquinol on blood oxidative stress and exercise performance. *Oxid. Med. Cell. Longev.* 2012, 465020. doi: 10.1155/2012/465020
- Blum, S., Vardi, M., Brown, J. B., Russell, A., Milman, U., Shapira, C., et al. (2010). Vitamin E reduces cardiovascular disease in individuals with diabetes mellitus and the haptoglobin 2-2 genotype. *Pharmacogenomics* 11, 675–684. doi: 10.2217/pgs.10.17
- Bokov, A., Chaudhuri, A., and Richardson, A. (2004). The role of oxidative damage and stress in aging. *Mech. Ageing Dev.* 125, 811–826. doi: 10.1016/j.mad.2004.07.009
- Botham, K. M., Napolitano, M., and Bravo, E. (2015). The emerging role of disturbed CoQ metabolism in nonalcoholic fatty liver disease development and progression. *Nutrients* 7, 9834–9846. doi: 10.3390/nu7125501
- Bouayed, J., and Bohn, T. (2010). Exogenous antioxidants – Double-edged swords in cellular redox state: health beneficial effects at physiologic doses versus deleterious effects at high doses. *Oxid. Med. Cell. Longev.* 3, 228–237. doi: 10.4161/oxim.3.4.12858
- Brondino, N., Re, S., Boldrini, A., Cuccomarino, A., Lanati, N., Barale, F., et al. (2014). Curcumin as a therapeutic agent in dementia: a mini systematic review of human studies. *Sci. World J.* 2014, 174282. doi: 10.1155/2014/174282
- Brown, B. M., Peiffer, J. J., and Martins, R. N. (2013). Multiple effects of physical activity on molecular and cognitive signs of brain aging: can exercise slow neurodegeneration and delay Alzheimer’s disease? *Mol. Psychiatry* 18, 864–874. doi: 10.1038/mp.2012.162
- Brunet, A., Sweeney, L. B., Sturgill, J. F., Chua, K. F., Greer, P. L., Lin, Y., et al. (2004). Stress-dependent regulation of FOXO transcription factors by the SIRT1 deacetylase. *Science* 303, 2011–2015. doi: 10.1126/science.1094637
- Bulotta, S., Celano, M., Lepore, S. M., Montalcini, T., Pujia, A., and Russo, D. (2014). Beneficial effects of the olive oil phenolic components oleuropein and hydroxytyrosol: focus on protection against cardiovascular and metabolic diseases. *J. Transl. Med.* 12, 219. doi: 10.1186/s12967-014-0219-9
- Capiralla, H., Vingtdoux, V., Zhao, H., Sankowski, R., Al-Abed, Y., Davies, P., et al. (2012). Resveratrol mitigates lipopolysaccharide- and A $\beta$ -mediated microglial inflammation by inhibiting the TLR4/NF- $\kappa$ B/STAT signaling cascade. *J. Neurochem.* 120, 461–472. doi: 10.1111/j.1471-4159.2011.07594.x
- Cardenas, E., and Ghosh, R. (2013). Vitamin E: a dark horse at the crossroad of cancer management. *Biochem. Pharmacol.* 86, 845–852. doi: 10.1016/j.bcp.2013.07.018
- Carr, A. C., and Frei, B. (1999). Toward a new recommended dietary allowance for vitamin C based on antioxidant and health effects in humans. *Am. J. Clin. Nutr.* 69, 1086–1107.

- Carrizzo, A., Puca, A., Damato, A., Marino, M., Franco, E., Pompeo, F., et al. (2013). Resveratrol improves vascular function in patients with hypertension and dyslipidemia by modulating NO metabolism. *Hypertension* 62, 359–366. doi: 10.1161/HYPERTENSIONAHA.111.01009
- Chambial, S., Dwivedi, S., Shukla, K. K., John, P. J., and Sharma, P. (2013). Vitamin C in disease prevention and cure: an overview. *Indian J. Clin. Biochem.* 28, 314–328. doi: 10.1007/s12291-013-0375-3
- Chevion, S., Moran, D. S., Heled, Y., Shani, Y., Regev, G., Abbou, B., et al. (2003). Plasma antioxidant status and cell injury after severe physical exercise. *Proc. Natl. Acad. Sci. U.S.A.* 100, 5119–5123. doi: 10.1073/pnas.0831097100
- Ciancarelli, I., Di Massimo, C., De Amicis, D., Carolei, A., and Tozzi Ciancarelli, M. G. (2012). Evidence of redox unbalance in post-acute ischemic stroke patients. *Curr. Neurovasc. Res.* 9, 85–90. doi: 10.2174/156720212800410885
- Conti, V., Corbi, G., Russomanno, G., Simeon, V., Ferrara, N., Filippelli, W., et al. (2012a). Oxidative stress effects on endothelial cells treated with different athletes' sera. *Med. Sci. Sports Exerc.* 44, 39–49. doi: 10.1249/MSS.0b013e318227f69c
- Conti, V., Russomanno, G., Corbi, G., and Filippelli, A. (2012b). Exercise training in aging and diseases. *Transl. Med. UniSa* 3, 74–80.
- Conti, V., Corbi, G., Simeon, V., Russomanno, G., Manzo, V., Ferrara, N., et al. (2015a). Aging-related changes in oxidative stress response of human endothelial cells. *Aging Clin. Exp. Res.* 27, 547–553. doi: 10.1007/s40520-015-0357-9
- Conti, V., Forte, M., Corbi, G., Russomanno, G., Formisano, L., Landolfi, A., et al. (2015b). Sirtuins: a possible clinical implication in cardio- and cerebro-vascular systems. *Curr. Drug Targets* doi: 10.2174/1389450116666151019095903 [Epub ahead of print].
- Conti, V., Russomanno, G., Corbi, G., Guerra, G., Grasso, C., Filippelli, W., et al. (2013). Aerobic training workload affects human endothelial cells redox homeostasis. *Med. Sci. Sports Exerc.* 45, 644–653. doi: 10.1249/MSS.0b013e318279fb59
- Cook, N. R., Albert, C. M., Gaziano, J. M., Zaharris, E., MacFadyen, J., Danielson, E., et al. (2007). A randomized factorial trial of vitamins C and E and beta carotene in the secondary prevention of cardiovascular events in women: results from the Women's Antioxidant Cardiovascular Study. *Arch. Intern. Med.* 167, 1610–1618. doi: 10.1001/archinte.167.15.1610
- Corbi, G., Acanfora, D., Iannuzzi, G. L., Longobardi, G., Cacciatore, F., Furgi, G., et al. (2008). Hypermagnesemia predicts mortality in elderly with congestive heart disease: relationship with laxative and antacid use. *Rejuvenation Res.* 11, 129–138. doi: 10.1089/rej.2007.0583
- Corbi, G., Conti, V., Russomanno, G., Rengo, G., Vitulli, P., Ciacarelli, A. L., et al. (2012). Is physical activity able to modify oxidative damage in cardiovascular aging? *Oxid. Med. Cell. Longev.* 2012, 728547. doi: 10.1155/2012/728547
- Davies, K. J. (1995). Oxidative stress: the paradox of aerobic life. *Biochem. Soc. Symp.* 61, 1–31. doi: 10.1042/bss0610001
- Devaraj, S., Tang, R., Adams-Huet, B., Harris, A., Seenivasan, T., de Lemos, J. A., et al. (2007). Effect of high-dose alpha-tocopherol supplementation on biomarkers of oxidative stress and inflammation and carotid atherosclerosis in patients with coronary artery disease. *Am. J. Clin. Nutr.* 86, 1392–1398.
- Donadio, G., Sarcinelli, C., Pizzo, E., Notomista, E., Pezzella, A., Di Cristo, C., et al. (2015). The toluene o-xylene monooxygenase enzymatic activity for the biosynthesis of aromatic antioxidants. *PLoS ONE* 10:e0124427. doi: 10.1371/journal.pone.0124427
- Facchini, A., Cetrullo, S., D'Adamo, S., Guidotti, S., Minguzzi, M., Facchini, A., et al. (2014). Hydroxytyrosol prevents increase of osteoarthritis markers in human chondrocytes treated with hydrogen peroxide or growth-related oncogene  $\alpha$ . *PLoS ONE* 9:e109724. doi: 10.1371/journal.pone.0109724
- Farghali, H., Cerný, D., Kameníková, L., Martínek, J., Horínek, A., Kmoníčková, E., et al. (2009). Resveratrol attenuates lipopolysaccharide-induced hepatitis in D-galactosamine sensitized rats: role of nitric oxide synthase 2 and heme oxygenase-1. *Nitric Oxide* 21, 216–225. doi: 10.1016/j.niox.2009.09.004
- Ferrara, N., Rinaldi, B., Corbi, G., Conti, V., Stiuso, P., Boccuti, S., et al. (2008). Exercise training promotes SIRT1 activity in aged rats. *Rejuvenation Res.* 11, 139–150. doi: 10.1089/rej.2007.0576
- Figuroa-Mendez, R., and Rivas-Arancibia, S. (2015). Vitamin C in health and disease: its role in the metabolism of cells and redox state in the brain. *Front. Physiol.* 6:397. doi: 10.3389/fphys.2015.00397
- Forsmark-Andrée, P., Dallner, G., and Ernster, L. (1995). Endogenous ubiquinol prevents protein modification accompanying lipid peroxidation in beef heart submitochondrial particles. *Free Radic. Biol. Med.* 19, 749–757. doi: 10.1016/0891-5849(95)00076-A
- Ghosh, S. K., Ekpo, E. B., Shah, I. U., Girling, A. J., Jenkins, C., and Sinclair, A. J. (1994). A double-blind placebo-controlled parallel trial of vitamin C treatment in elderly patients with hypertension. *Gerontology* 40, 268–272. doi: 10.1159/000213595
- Giordano, E., Davalos, A., Nicod, N., and Visioli, F. (2014). Hydroxytyrosol attenuates tunicamycin-induced endoplasmic reticulum stress in human hepatocarcinoma cells. *Mol. Nutr. Food Res.* 58, 954–962. doi: 10.1002/mnfr.201300465
- Gliemann, L., Schmidt, J. F., Olesen, J., Bienso, R. S., Peronard, S. L., Grandjean, S. U., et al. (2013). Resveratrol blunts the positive effects of exercise training on cardiovascular health in aged men. *J. Physiol.* 591, 5047–5059. doi: 10.1113/jphysiol.2013.258061
- Goldstein, J. L., and Brown, M. S. (1990). Regulation of the mevalonate pathway. *Nature* 343, 425–430. doi: 10.1038/343425a0
- González-Reyes, S., Guzmán-Beltrán, S., Medina-Campos, O. N., and Pedraza-Chaverri, J. (2013). Curcumin pretreatment induces Nrf2 and an antioxidant response and prevents hemin-induced toxicity in primary cultures of cerebellar granule neurons of rats. *Oxid. Med. Cell. Longev.* 2013, 801418. doi: 10.1155/2013/801418
- Gough, D. R., and Cotter, T. G. (2011). Hydrogen peroxide: a Jekyll and Hyde signalling molecule. *Cell Death Dis.* 2, e213. doi: 10.1038/cddis.2011.96
- Gülçin, İ. (2012). Antioxidant activity of food constituents: an overview. *Arch. Toxicol.* 86, 345–391. doi: 10.1007/s00204-011-0774-2
- Gumral, N., Naziroglu, M., Ongel, K., Beydilli, E. D., Oztunçer, F., Sutcu, R., et al. (2009). Antioxidant enzymes and melatonin levels in patients with bronchial asthma and chronic obstructive pulmonary disease during stable and exacerbation periods. *Cell Biochem. Funct.* 27, 276–283. doi: 10.1002/cbf.1569
- Hanson, C., Lyden, E., Furtado, J., Campos, H., Sparrow, D., Vokonas, P., et al. (2015). Serum tocopherol levels and vitamin E intake are associated with lung function in the normative aging study. *Clin. Nutr.* doi: 10.1016/j.clnu.2015.01.020 [Epub ahead of print].
- Harikumar, K. B., and Aggarwal, B. B. (2008). Resveratrol: a multitargeted agent for age-associated chronic diseases. *Cell Cycle* 7, 1020–1035. doi: 10.4161/cc.7.8.5740
- Harman, D. (1956). Aging: a theory based on free radical and radiation chemistry. *J. Gerontol.* 2, 298–300. doi: 10.1093/geronj/11.3.298
- Harman, D. (2006). Free radical theory of aging: an update. Increasing the functional life span. *Ann. N. Y. Acad. Sci.* 1067, 10–21. doi: 10.1196/annals.1354.003
- Hemilä, H., and Kaprio, J. (2011). Vitamin E may affect the life expectancy of men, depending on dietary vitamin C intake and smoking. *Age Ageing* 40, 215–220. doi: 10.1093/ageing/afq178
- Hu, F. B., Manson, J. E., Stampfer, M. J., Colditz, G., Liu, S., Solomon, C. G., et al. (2001). Diet, lifestyle, and the risk of type 2 diabetes mellitus in women. *N. Engl. J. Med.* 345, 790–797. doi: 10.1056/NEJMoa010492
- Iuliano, L., Mauriello, A., Sbarigia, E., Spagnoli, L. G., and Violi, F. (2000). Radiolabeled native low-density lipoprotein injected into patients with carotid stenosis accumulates in macrophages of atherosclerotic plaque: effect of vitamin E supplementation. *Circulation* 101, 1249–1254. doi: 10.1161/01.CIR.101.11.1249
- Jang, J. H., and Surh, Y. J. (2003). Protective effect of resveratrol on beta-amyloid-induced oxidative PC12 cell death. *Free Radic. Biol. Med.* 34, 1100–1110. doi: 10.1016/S0891-5849(03)00062-5
- Ji, L. L., Gomez-Cabrera, M. C., and Vina, J. (2006). Exercise and hormesis: activation of cellular antioxidant signaling pathway. *Ann. N. Y. Acad. Sci.* 1067, 425–435. doi: 10.1196/annals.1354.061
- Khurana, S., Venkataraman, K., Hollingsworth, A., Piche, M., and Tai, T. C. (2013). Polyphenols: benefits to the cardiovascular system in health and in aging. *Nutrients* 5, 3779–3827. doi: 10.3390/nu5103779
- Kou, M. C., Chiou, S. Y., Weng, C. Y., Wang, L., Ho, C. T., and Wu, M. J. (2013). Curcuminoids distinctly exhibit antioxidant activities and regulate expression

- of scavenger receptors and heme oxygenase-1. *Mol. Nutr. Food Res.* 57, 1598–1610. doi: 10.1002/mnfr.201200227
- Lanza, I. R., Short, D. K., Short, K. R., Raghavakaimal, S., Basu, R., Joyner, M. J., et al. (2008). Endurance exercise as a countermeasure for aging. *Diabetes Metab. Res. Rev.* 57, 2933–2942. doi: 10.2337/db08-0349
- Laredj, L. N., Licitra, F., and Puccio, H. M. (2014). The molecular genetics of coenzyme Q biosynthesis in health and disease. *Biochimie* 100, 78–87. doi: 10.1016/j.biochi.2013.12.006
- Lee, B. J., Tseng, Y. F., Yen, C. H., and Lin, P. T. (2013). Effects of coenzyme Q10 supplementation (300 mg/day) on antioxidation and anti-inflammation in coronary artery disease patients during statins therapy: a randomized, placebo-controlled trial. *Nutr. J.* 12, 142. doi: 10.1186/1475-2891-12-142
- Liu, K., Zhou, R., Wang, B., and Mi, M. T. (2014). Effect of resveratrol on glucose control and insulin sensitivity: a meta-analysis of 11 randomized controlled trials. *Am. J. Clin. Nutr.* 99, 1510–1519. doi: 10.3945/ajcn.113.082024
- Loguercio, C., Andreone, P., Brisc, C., Brisc, M. C., Bugianesi, E., Chiamonte, M., et al. (2012). Silybin combined with phosphatidylcholine and vitamin E in patients with nonalcoholic fatty liver disease: a randomized controlled trial. *Free Radic. Biol. Med.* 52, 1658–1665. doi: 10.1016/j.freeradbiomed.2012.02.008
- Lonn, E., Bosch, J., Yusuf, S., Sheridan, P., Pogue, J., Arnold, J. M., et al. (2005). Effects of long-term vitamin E supplementation on cardiovascular events and cancer: a randomized controlled trial. *JAMA* 293, 1338–1347. doi: 10.1001/jama.293.11.1338
- Lovat, L. B., Lu, Y., Palmer, A. J., Edwards, R., Fletcher, A. E., and Bulpitt, C. J. (1993). Double-blind trial of vitamin C in elderly hypertensives. *J. Hum. Hypertens.* 7, 403–405.
- Madmani, M. E., Yusuf Solaiman, A., Tamr Agha, K., Madmani, Y., Shahrour, Y., Essali, A., et al. (2014). Coenzyme Q10 for heart failure. *Cochrane Database Syst. Rev.* 6, CD008684. doi: 10.1002/14651858.CD008684.pub2
- Major, J. M., Yu, K., Chung, C. C., Weinstein, S. J., Yeager, M., Wheeler, W., et al. (2012). Genome-wide association study identifies three common variants associated with serologic response to vitamin E supplementation in men. *J. Nutr.* 142, 866–871. doi: 10.3945/jn.111.156349
- Marchioli, R., Levantesi, G., Macchia, A., Marfisi, R. M., Nicolosi, G. L., Tavazzi, L., et al. (2006). Vitamin E increases the risk of developing heart failure after myocardial infarction: results from the GISSI-Prevenzione trial. *J. Cardiovasc. Med. (Hagerstown)* 7, 347–350. doi: 10.2459/01.JCM.0000223257.09062.17
- Mesquita, A., Weinberger, M., Silva, A., Sampaio-Marques, B., Almeida, B., Leão, C., et al. (2010). Caloric restriction or catalase inactivation extends yeast chronological lifespan by inducing H<sub>2</sub>O<sub>2</sub> and superoxide dismutase activity. *Proc. Natl. Acad. Sci. U.S.A.* 107, 15123–15128. doi: 10.1073/pnas.1004432107
- Milman, U., Blum, S., Shapira, C., Aronson, D., Miller-Lotan, R., Anbinder, Y., et al. (2008). Vitamin E supplementation reduces cardiovascular events in a subgroup of middle-aged individuals with both type 2 diabetes mellitus and the haptoglobin 2-2 genotype: a prospective double-blinded clinical trial. *Arterioscler. Thromb. Vasc. Biol.* 28, 341–347. doi: 10.1161/ATVBAHA.107.153965
- Montesano, A., Luzzi, L., Senesi, P., Mazzocchi, N., and Terruzzi, I. (2013). Resveratrol promotes myogenesis and hypertrophy in murine myoblasts. *J. Transl. Med.* 11, 310. doi: 10.1186/1479-5876-11-310
- Morley, A. A., and Trainor, K. J. (2001). Lack of an effect of vitamin E on lifespan of mice. *Biogerontology* 2, 109–112. doi: 10.1023/A:1011589218219
- Mullan, B. A., Ennis, C. N., Fee, H. J. P., Young, I. S., and McCance, D. R. (2004). Protective effects of ascorbic acid on arterial hemodynamics during acute hyperglycemia. *Am. J. Physiol. Heart Circ. Physiol.* 287, H1262–H1268. doi: 10.1152/ajpheart.00153.2003
- Mullan, B. A., Young, I. S., Fee, H., and McCance, D. R. (2002). Ascorbic acid reduces blood pressure and arterial stiffness in type 2 diabetes. *Hypertension* 40, 804–809. doi: 10.1161/01.HYP.0000039961.13718.00
- Muller, F. L., Lustgarten, M. S., Jang, Y., Richardson, A., and Van Remmen, H. (2007). Trends in oxidative aging theories. *Free Radic. Biol. Med.* 43, 477–503. doi: 10.1016/j.freeradbiomed.2007.03.034
- Navarro, A., Gómez, C., Sánchez-Pino, M. J., González, H., Bández, M. J., Boveris, A. D., et al. (2005). Vitamin E at high doses improves survival, neurological performance, and brain mitochondrial function in aging male mice. *Am. J. Physiol. Regul. Integr. Comp. Physiol.* 289, R1392–R1399. doi: 10.1152/ajpregu.00834.2004
- Nikolaïdis, M. G., and Jamurtas, A. Z. (2009). Blood as a reactive species generator and redox status regulator during exercise. *Arch. Biochem. Biophys.* 490, 77–84. doi: 10.1016/j.abb.2009.08.015
- Notomista, E., Scognamiglio, R., Troncone, L., Donadio, G., Pezzella, A., Di Donato, A., et al. (2011). Tuning the specificity of the recombinant multicomponent toluene o-xylene monooxygenase from *Pseudomonas* sp. strain OX1 for the biosynthesis of tyrosol from 2-phenylethanol. *Appl. Environ. Microbiol.* 77, 5428–5437. doi: 10.1128/AEM.00461-11
- Nowicka, B., and Kruk, J. (2010). Occurrence, biosynthesis and function of isoprenoid quinones. *Biochim. Biophys. Acta* 1797, 1587–1605. doi: 10.1016/j.bbabi.2010.06.007
- O’Leary, K. A., de Pascual-Teresa, S., Needs, P. W., Bao, Y. P., O’Brien, N. M., and Williamson, G. (2004). Effect of flavonoids and vitamin E on cyclooxygenase-2 (COX-2) transcription. *Mutat. Res.* 551, 245–254. doi: 10.1016/j.mrfmmm.2004.01.015
- Oliveras-López, M. J., Molina, J. J., Mir, M. V., Rey, E. F., Martín, F., and de la Serrana, H. L. (2013). Extra virgin olive oil (EVOO) consumption and antioxidant status in healthy institutionalized elderly humans. *Arch. Gerontol. Geriatr.* 57, 234–242. doi: 10.1016/j.archger.2013.04.002
- Onur, S., Niklowitz, P., Jacobs, G., Nöthlings, U., Lieb, W., Menke, T., et al. (2014). Ubiquinol reduces gamma glutamyltransferase as a marker of oxidative stress in humans. *BMC Res. Notes* 7:427. doi: 10.1186/1756-0500-7-427
- Opara, E. C., Abdel-Rahman, E., Soliman, S., Kamel, W. A., Souka, S., Lowe, J. E., et al. (1999). Depletion of total antioxidant capacity in type 2 diabetes. *Metabolism* 48, 1414–1417. doi: 10.1016/S0026-0495(99)90152-X
- Poli, G., Leonarduzzi, G., Biasi, F., and Chiarpotto, E. (2004). Oxidative stress and cell signalling. *Curr. Med. Chem.* 11, 1163–1182. doi: 10.2174/0929867043365323
- Potgieter, M., Pretorius, E., and Pepper, M. S. (2013). Primary and secondary coenzyme Q10 deficiency: the role of therapeutic supplementation. *Nutr. Rev.* 71, 180–188. doi: 10.1111/nure.12011
- Radak, Z., Chung, H. Y., and Goto, S. (2005). Exercise and hormesis: oxidative stress-related adaptation for successful aging. *Biogerontology* 6, 71–75. doi: 10.1007/s10522-004-7386-7
- Ristow, M., and Schmeisser, K. (2014). Mitohormesis: promoting health and lifespan by increased levels of reactive oxygen species (ROS). *Dose Response* 12, 288–341. doi: 10.2203/dose-response.13-035
- Ristow, M., Zarse, K., Oberbach, A., Klötting, N., Birringer, M., Kiehnopf, M., et al. (2009). Antioxidants prevent health-promoting effects of physical exercise in humans. *Proc. Natl. Acad. Sci. U.S.A.* 106, 8665–8670. doi: 10.1073/pnas.0903485106
- Royce, S. G., Dang, W., Yuan, G., Tran, J., El Osta, A., Karagiannis, T. C., et al. (2011). Resveratrol has protective effects against airway remodeling and airway hyperreactivity in a murine model of allergic airways disease. *Pathobiol. Aging Age Relat. Dis.* 1, 7134. doi: 10.3402/PBA.v1i0.7134
- Sadowska-Bartosz, I., and Bartosz, G. (2014). Effect of antioxidants supplementation on aging and longevity. *Biomed Res. Int.* 2014, 404680. doi: 10.1155/2014/404680
- Sadrzadeh, S. M., Graf, E., Panter, S. S., Hallaway, P. E., and Eaton, J. W. (1984). Hemoglobin: a biologic fenton reagent. *J. Biol. Chem.* 259, 14354–14356.
- Saleh, M. C., Connell, B. J., Rajagopal, D., Khan, B. V., Abd-El-Aziz, A. S., Kucukkaya, I., et al. (2014). Co-administration of resveratrol and lipoic acid, or their synthetic combination, enhances neuroprotection in a rat model of ischemia/reperfusion. *PLoS ONE* 9:e87865. doi: 10.1371/journal.pone.0087865
- Salonen, R. M., Nyssönen, K., Kaikkonen, J., Porkkala-Sarataho, E., Voutilainen, S., Rissanen, T. H., et al. (2003). Six-year effect of combined vitamin C and E supplementation on atherosclerotic progression: the Antioxidant Supplementation in Atherosclerosis Prevention (ASAP) Study. *Circulation* 107, 947–953. doi: 10.1161/01.CIR.0000050626.25057.51
- Scapagnini, G., Colombrita, C., Amadio, M., D’Agata, V., Arcelli, E., Sapienza, M., et al. (2006). Curcumin activates defensive genes and protects neurons against oxidative stress. *Antioxid. Redox Signal.* 8, 395–403. doi: 10.1089/ars.2006.8.395
- Schmelzer, C., Lorenz, G., Rimbach, G., and Döring, F. (2007). Influence of Coenzyme Q<sub>10</sub> on release of pro-inflammatory chemokines in the human monocytic cell line THP-1. *Biofactors* 31, 211–217. doi: 10.1002/biof.5520310308

- Schmelzer, C., Lorenz, G., Rimbach, G., and Döring, F. (2009). In vitro effects of the reduced form of coenzyme Q(10) on secretion levels of TNF-alpha and chemokines in response to LPS in the human monocytic cell line THP-1. *J. Clin. Biochem. Nutr.* 44, 62–66. doi: 10.3164/jcbsn.08-182
- Schrag, M., Mueller, C., Zabel, M., Crofton, A., Kirsch, W. M., Ghribi, O., et al. (2013). Oxidative stress in blood in Alzheimer's disease and mild cognitive impairment: a meta-analysis. *Neurobiol. Dis.* 59, 100–110. doi: 10.1016/j.nbd.2013.07.005
- Schulz, T. J., Zarse, K., Voigt, A., Urban, N., Birringer, M., and Ristow, M. (2007). Glucose restriction extends *Caenorhabditis elegans* life span by inducing mitochondrial respiration and increasing oxidative stress. *Cell Metab.* 6, 280–293. doi: 10.1016/j.cmet.2007.08.011
- Sesso, H. D., Buring, J. E., Christen, W. G., Kurth, T., Belanger, C., MacFadyen, J., et al. (2008). Vitamins E and C in the prevention of cardiovascular disease in men: the Physicians' Health Study II randomized controlled trial. *JAMA* 300, 2123–2133. doi: 10.1001/jama.2008.600
- Shah, A. M., and Sauer, H. (2006). Transmitting biological information using oxygen: reactive oxygen species as signalling molecules in cardiovascular pathophysiology. *Cardiovasc. Res.* 71, 191–194. doi: 10.1016/j.cardiores.2006.05.018
- Sies, H. (1991). Role of reactive oxygen species in biological processes. *Klin. Wochenschr.* 69, 965–968. doi: 10.1007/BF01645140
- Sies, H. (1993). Strategies of antioxidant defense. *Eur. J. Biochem.* 215, 213–219. doi: 10.1111/j.1432-1033.1993.tb18025.x
- Sohet, F. M., Neyrinck, A. M., Pachikian, B. D., de Backer, F. C., Bindels, L. B., Niklowitz, P., et al. (2009). Coenzyme Q10 supplementation lowers hepatic oxidative stress and inflammation associated with diet-induced obesity in mice. *Biochem. Pharmacol.* 78, 1391–1400. doi: 10.1016/j.bcp.2009.07.008
- Stadtman, E. R., and Berlett, B. S. (1997). Reactive oxygen-mediated protein oxidation in aging and disease. *Chem. Res. Toxicol.* 10, 485–494. doi: 10.1021/tx960133r
- Stephens, N. G., Parsons, A., Schofield, P. M., Kelly, F., Cheeseman, K., and Mitchinson, M. J. (1996). Randomised controlled trial of vitamin E in patients with coronary disease: cambridge heart antioxidant study (CHAOS). *Lancet* 347, 781–786. doi: 10.1016/S0140-6736(96)90866-1
- St-Pierre, J., Drori, S., Uldry, M., Silvaggi, J. M., Rhee, J., Jäger, S., et al. (2006). Suppression of reactive oxygen species and neurodegeneration by the PGC-1 transcriptional coactivators. *Cell* 127, 397–408. doi: 10.1016/j.cell.2006.09.024
- van Ommen, B., Keijer, J., Heil, S. G., and Kaput, J. (2009). Challenging homeostasis to define biomarkers for nutrition related health. *Mol. Nutr. Food Res.* 53, 795–804. doi: 10.1002/mnfr.200800390
- vB Hjelmberg, J., Iachine, I., Skytthe, A., Vaupel, J. W., McGue, M., Koskenvuo, M., et al. (2006). Genetic influence on human lifespan and longevity. *Hum. Genet.* 119, 312–321. doi: 10.1007/s00439-006-0144-y
- Versari, D., Daghini, E., Virdis, A., Ghiadoni, L., and Taddei, S. (2009). Endothelium-dependent contractions and endothelial dysfunction in human hypertension. *Br. J. Pharmacol.* 157, 527–536. doi: 10.1111/j.1476-5381.2009.00240.x
- Vijg, J., and Suh, Y. (2005). Genetics of longevity and aging. *Annu. Rev. Med.* 56, 193–212. doi: 10.1146/annurev.med.56.082103.104617
- Visioli, F., Bellomo, G., and Galli, C. (1998). Free radical-scavenging properties of olive oil polyphenols. *Biochem. Biophys. Res. Commun.* 247, 60–64. doi: 10.1006/bbrc.1998.8735
- Wallert, M., Schmözl, L., Galli, F., Birringer, M., and Lorkowski, S. (2014). Regulatory metabolites of vitamin E and their putative relevance for atherogenesis. *Redox Biol.* 2, 495–503. doi: 10.1016/j.redox.2014.02.002
- Wannamethee, S. G., Bruckdorfer, K. R., Shaper, A. G., Papacosta, O., Lennon, L., and Whincup, P. H. (2013). Plasma vitamin C, but not vitamin E, is associated with reduced risk of heart failure in older men. *Circ. Heart Fail.* 6, 647–654. doi: 10.1161/CIRCHEARTFAILURE.112.000281
- Watanabe, H., Kakiyama, M., Ohtsuka, S., and Sugishita, Y. (1998). Randomized, double-blind, placebo-controlled study of the preventive effect of supplemental oral vitamin C on attenuation of development of nitrate tolerance. *J. Am. Coll. Cardiol.* 31, 1323–1329. doi: 10.1016/S0735-1097(98)00085-0
- Waterman, E., and Lockwood, B. (2007). Active components and clinical applications of olive oil. *Altern. Med. Rev.* 12, 331–342.
- Watts, G. F., Playford, D. A., Croft, K. D., Ward, N. C., Mori, T. A., and Burke, V. (2002). Coenzyme Q(10) improves endothelial dysfunction of the brachial artery in Type II diabetes mellitus. *Diabetologia* 45, 420–426. doi: 10.1007/s00125-001-0760-y
- Wells, W. W., and Xu, D. P. (1994). Dehydroascorbate reduction. *J. Bioenerg. Biomembr.* 26, 369–377. doi: 10.1007/BF00762777
- Weseler, A. R., and Bast, A. (2010). Oxidative stress and vascular function: implications for pharmacologic treatments. *Curr. Hypertens. Rep.* 12, 154–161. doi: 10.1007/s11906-010-0103-9
- Xu, Y., Ku, B., Cui, L., Li, X., Barish, P. A., Foster, T. C., et al. (2007). Curcumin reverses impaired hippocampal neurogenesis and increases serotonin receptor 1A mRNA and brain-derived neurotrophic factor expression in chronically stressed rats. *Brain Res.* 1162, 9–18. doi: 10.1016/j.brainres.2007.05.071
- Yun, H., Park, S., Kim, M. J., Yang, W. K., Im, D. U., Yang, K. R., et al. (2014). AMP-activated protein kinase mediates the antioxidant effects of resveratrol through regulation of the transcription factor FoxO1. *FEBS J.* 281, 4421–4438. doi: 10.1111/febs.12949
- Yun, J., and Finkel, T. (2014). Mitohormesis. *Cell Metab.* 19, 757–766. doi: 10.1016/j.cmet.2014.01.011
- Yusuf, S., Dagenais, G., Pogue, J., Bosch, J., and Sleight, P. (2000). Vitamin E supplementation and cardiovascular events in high-risk patients. The Heart Outcomes Prevention Evaluation Study Investigators. *N. Engl. J. Med.* 342, 154–160.
- Zarse, K., Schmeisser, S., Groth, M., Priebe, S., Beuster, G., Kuhlow, D., et al. (2012). Impaired insulin/IGF1 signaling extends life span by promoting mitochondrial L-proline catabolism to induce a transient ROS signal. *Cell Metab.* 15, 451–465. doi: 10.1016/j.cmet.2012.02.013
- Zhang, C., Feng, Y., Qu, S., Wei, X., Zhu, H., Luo, Q., et al. (2011). Resveratrol attenuates doxorubicin-induced cardiomyocyte apoptosis in mice through SIRT1-mediated deacetylation of p53. *Cardiovasc. Res.* 90, 538–545. doi: 10.1093/cvr/cvr022
- Zhang, X. G., Zhang, Y. Q., Zhao, D. K., Wu, J. X., Zhao, J., Jiao, X. M., et al. (2014). Relationship between blood glucose fluctuation and macrovascular endothelial dysfunction in type 2 diabetic patients with coronary heart disease. *Eur. Rev. Med. Pharmacol. Sci.* 18, 3593–3600.
- Zhong, L. M., Zong, Y., Sun, L., Guo, J. Z., Zhang, W., He, Y., et al. (2012). Resveratrol inhibits inflammatory responses via the mammalian target of rapamycin signaling pathway in cultured LPS-stimulated microglial cells. *PLoS ONE* 7:e32195. doi: 10.1371/journal.pone.0032195

**Conflict of Interest Statement:** The authors declare that the research was conducted in the absence of any commercial or financial relationships that could be construed as a potential conflict of interest.

Copyright © 2016 Conti, Izzo, Corbi, Russomanno, Manzo, De Lise, Di Donato and Filippelli. This is an open-access article distributed under the terms of the Creative Commons Attribution License (CC BY). The use, distribution or reproduction in other forums is permitted, provided the original author(s) or licensor are credited and that the original publication in this journal is cited, in accordance with accepted academic practice. No use, distribution or reproduction is permitted which does not comply with these terms.



Contents lists available at ScienceDirect

## Journal of Molecular Catalysis B: Enzymatic

journal homepage: [www.elsevier.com/locate/molcatb](http://www.elsevier.com/locate/molcatb)

## RHA-P: Isolation, expression and characterization of a bacterial $\alpha$ -L-rhamnosidase from *Novosphingobium* sp. PP1Y



Federica De Lise<sup>a,1</sup>, Francesca Mensitieri<sup>a,1</sup>, Vincenzo Tarallo<sup>b</sup>, Nicola Ventimiglia<sup>a</sup>, Roberto Vinciguerra<sup>b</sup>, Annabella Tramice<sup>c</sup>, Roberta Marchetti<sup>b</sup>, Elio Pizzo<sup>a</sup>, Eugenio Notomista<sup>a</sup>, Valeria Cafaro<sup>a</sup>, Antonio Molinaro<sup>b</sup>, Leila Birolo<sup>b</sup>, Alberto Di Donato<sup>a</sup>, Viviana Izzo<sup>d,\*</sup>

<sup>a</sup> Dipartimento di Biologia, Università Federico II di Napoli, Via Cinthia I, 80126 Napoli, Italy

<sup>b</sup> Dipartimento di Scienze Chimiche, Università Federico II di Napoli, via Cinthia I, 80126 Napoli, Italy

<sup>c</sup> Istituto di Chimica Biomolecolare, Consiglio Nazionale delle Ricerche, Via Campi Flegrei 34, 80072 Pozzuoli (NA), Italy

<sup>d</sup> Dipartimento di Medicina, Chirurgia e Odontoiatria "Scuola Medica Salernitana", Università degli Studi di Salerno, via S. Allende, 84081 Baronissi (SA), Italy

## ARTICLE INFO

## Article history:

Received 29 July 2016

Received in revised form

23 September 2016

Accepted 3 October 2016

Available online 3 October 2016

## Keywords:

 $\alpha$ -L-Rhamnosidases

Flavonoids

*Novosphingobium* sp. PP1Y

Glycosyl hydrolases

Biotransformation

## ABSTRACT

$\alpha$ -L-Rhamnosidases ( $\alpha$ -RHAs) are a group of glycosyl hydrolases of biotechnological potential in industrial processes, which catalyze the hydrolysis of  $\alpha$ -L-rhamnose terminal residues from several natural compounds. A novel  $\alpha$ -RHA activity was identified in the crude extract of *Novosphingobium* sp. PP1Y, a marine bacterium able to grow on a wide range of aromatic polycyclic compounds. In this work, this  $\alpha$ -RHA activity was isolated from the native microorganism and the corresponding *orf* was identified in the completely sequenced and annotated genome of strain PP1Y. The coding gene was expressed in *Escherichia coli*, strain BL21(DE3), and the recombinant protein, rRHA-P, was purified and characterized as an inverting monomeric glycosidase of ca. 120 kDa belonging to the GH106 family. A biochemical characterization of this enzyme using pNPR as substrate was performed, which showed that rRHA-P had a moderate tolerance to organic solvents, a significant thermal stability up to 45 °C and a catalytic efficiency, at pH 6.9, significantly higher than other bacterial  $\alpha$ -RHAs described in literature. Moreover, rRHA-P was able to hydrolyze natural glycosylated flavonoids (naringin, rutin, neohesperidin dihydrochalcone) containing  $\alpha$ -L-rhamnose bound to  $\beta$ -D-glucose with either  $\alpha$ -1,2 or  $\alpha$ -1,6 glycosidic linkages. Data presented in this manuscript strongly support the potential use of RHA-P as a biocatalyst for diverse biotechnological applications.

© 2016 Elsevier B.V. All rights reserved.

## 1. Introduction

$\alpha$ -L-Rhamnosidases ( $\alpha$ -RHAs) are a group of glycosyl hydrolases (GHs) that catalyze the hydrolysis of terminal residues of

**Abbreviations:**  $\alpha$ -RHAs,  $\alpha$ -L-rhamnosidases; GHs, glycosyl hydrolases; GTs, glycosyl transferases; PPMM, potassium phosphate minimal medium; pNPR, *p*-nitrophenyl- $\alpha$ -L-rhamnopyranoside; MOPS, 3-(*N*-morpholino) propanesulfonic acid; pNP, *p*-nitrophenolate; BSA, bovine serum albumin; LB, Luria Bertani medium; LB-N, Luria Bertani medium containing a final concentration of 0.5 M NaCl; LB-BS, Luria Bertani medium supplemented with 1 mM of both betaine and sorbitol; LB-NBS, Luria Bertani medium containing a final concentration of 0.5 M NaCl and 1 mM of both betaine and sorbitol; IPTG, Isopropyl  $\beta$ -D-1-thiogalactopyranoside.

\* Corresponding author.

E-mail address: [vizzo@unisa.it](mailto:vizzo@unisa.it) (V. Izzo).<sup>1</sup> These authors equally contributed to the work.<http://dx.doi.org/10.1016/j.molcatb.2016.10.002>

1381-1177/© 2016 Elsevier B.V. All rights reserved.

$\alpha$ -L-rhamnose from a large number of natural compounds [1]. L-Rhamnose is widely distributed in plants as component of flavonoid glycosides, terpenyl glycosides, pigments, signaling molecules, and in cell walls as a component of complex heteropolysaccharides, such as rhamnogalacturonan and arabinogalactan-proteins [2–7]. In bacteria, L-rhamnose appears to be included in membrane rhamnolipids [8,9] and polysaccharides [10]. According to the similarities among their amino acidic sequences,  $\alpha$ -RHAs are grouped in the CAZy (carbohydrate-active enzymes) database ([www.cazy.org](http://www.cazy.org)) into four different families: GH28, GH78, GH106, and NC (non-classified).

In the last decade,  $\alpha$ -RHAs have attracted a great deal of attention due to their potential application as biocatalysts in a variety of industrial processes and in particular in the food industry [1]. Several dietary products are rich in glycosylated flavonoids that show the presence of either a rutinoid (6- $\alpha$ -L-rhamnosyl- $\beta$ -D-glucose)

or a neohesperidoside (2- $\alpha$ -L-rhamnosyl- $\beta$ -D-glucose) disaccharidic unit. In particular, naringin, hesperidin and rutin, flavanone glycosides found in grapefruit juices, lemons, sweet oranges and vegetables, have gained increasing recognition for their potential antioxidant, antitumor and anti-inflammatory properties [11–14].

The ability to hydrolyze glycosylated flavonoids has been used to mitigate the bitterness of citrus juices, which is primarily caused by naringin. Rhamnose removal from naringin allows softening the bitter taste of citrus juice [15,16]. Moreover, the corresponding de-rhamnosylated compound, prunin, is endowed with antimicrobial properties [14], and shows an improved intestinal assimilation when compared to naringin. Other applications of  $\alpha$ -RHAs are gaining popularity in the oenological industry, where these enzymes are used to hydrolyze terpenyl glycosides and enhance aroma in wine, grape juices and derived beverages [17–19].

Application of  $\alpha$ -RHAs to improve flavonoids bioavailability has also been recently described [20]. In humans, flavonoids absorption occurs primarily in the small intestine where the attached glucose (or possibly arabinose or xylose) is removed by endogenous  $\beta$ -glucosidases [21–23]. Terminal rhamnose is not a suitable substrate for human  $\beta$ -glucosidases. Therefore, unabsorbed rhamnosylated flavonoids arrive unmodified in the colon, where they are hydrolyzed by  $\alpha$ -rhamnosidase activities expressed by the local microflora [24]. To improve intestinal absorption of rhamnosylated flavonoids, and thus their bioavailability in humans, a removal of the terminal rhamnose group catalyzed by  $\alpha$ -RHAs would be indeed beneficial [25–27].

The absence of human  $\alpha$ -RHAs has been the key to the development of a novel targeted drug delivery strategy, indicated as LEAPT (Lectin-directed enzyme activated prodrug therapy) [28,29], a bipartite system based on the internalization of an engineered  $\alpha$ -RHA bearing a glycosidic moiety that is recognized by specific lectins present on the surface of different eukaryotic cell lines. In the LEAPT system, the intake of a rhamnosylated prodrug, which cannot be processed by mammalian enzymes, allows a site-selective action of the drug in cells where the engineered  $\alpha$ -RHA has been prelocalized.

To date, microbial  $\alpha$ -RHAs have been mainly purified from fungal strains such as *Penicillium* and *Aspergillus* [30–32]; only one example of  $\alpha$ -RHA isolated from a viral source has been described [33], and it is noteworthy that only a limited number of bacterial rhamnosidases has been fully characterized [34–39]. One of the main differences between fungal and bacterial  $\alpha$ -RHAs is their different optimal pH values, with the fungal enzymes showing more acidic pH optima when compared to the bacterial counterparts, for which neutral and alkaline values have generally been described. This characteristic suggests diverse applications for fungal and bacterial enzymes, making bacterial  $\alpha$ -RHAs suitable in biotechnological processes requiring good activity in more basic solutions such as, for example, the production of L-rhamnose from the hydrolysis of naringin or hesperidin, flavonoids whose solubility strongly increases at higher pH values [40]. In addition, bacterial rhamnosidases could be ideal candidates for dietary supplements having activity across the entire gastrointestinal (GI) tract, and more specifically in the small intestine where flavonoids absorption should mostly occur to enhance the beneficial effect of these molecules on human health.

In order to elucidate the real biotechnological potential of bacterial  $\alpha$ -RHAs, further investigation is undoubtedly needed. Few details on the catalytic mechanism of bacterial  $\alpha$ -RHAs are available, and most importantly, to the best of our knowledge, no attempt to improve the catalytic efficiency or modify substrate specificity of these enzymes by mutagenesis has been performed yet. This is in part consequential to the fact that only a very limited number of crystal structures of  $\alpha$ -RHAs are currently available, such as the  $\alpha$ -L-rhamnosidase B (BsRhaB) from *Bacillus* sp. GL1 [41], and

the  $\alpha$ -L-rhamnosidase from *Streptomyces avermitilis* [42]. Therefore, it is evident that bacterial  $\alpha$ -RHAs represent a yet unexplored reservoir of potential biocatalysts for which more functional and structural data are required.

A member of the order of the Sphingomonadales, recently isolated and microbiologically characterized, *Novosphingobium* sp. PP1Y [43,44], appears to be a valuable source for the isolation of  $\alpha$ -RHA activities. Sphingomonadales are a group of Gram-negative  $\alpha$ -proteobacteria whose genomes show the presence of a great abundance of both glycosyl hydrolases (GHs) and glycosyltransferases (GTs). These activities are probably involved in the biosynthesis of complex extracellular polysaccharides and microbial biofilms [45]. The interest for *Novosphingobium* sp. PP1Y carbohydrate-active enzymes has grown as the sequencing and annotation of the whole genome, recently completed, allowed the identification of a great number of genes encoding for both GHs (53 orfs) and GTs (57 orfs) [46].

Recently, a  $\alpha$ -RHA activity in *Novosphingobium* sp. PP1Y crude extract was described, which showed an alkaline pH optimum and a moderate tolerance to organic solvents [47]. *Novosphingobium* sp. PP1Y crude extract expressing this enzymatic activity was used for the bioconversion of naringin, rutin and hesperidin. Based on these preliminary results, a more detailed biochemical characterization of the  $\alpha$ -RHA activity was essential.

In this work, the isolation, recombinant expression and partial characterization of a  $\alpha$ -RHA from *Novosphingobium* sp. PP1Y is reported. This enzyme, named RHA-P, belongs to the GH106 family [48], a subgroup for which, according to our knowledge, no crystal structure is available yet. As evident from our analyses, RHA-P is a promising candidate for several biotechnological applications.

## 2. Materials and methods

### 2.1. Generals

General molecular biology techniques were performed according to Sambrook et al. [49]. Bacterial growth was followed by measuring the optical density at 600 nm ( $OD_{600}$ ). pET22b(+) expression vector and *E. coli* strain BL21(DE3) were from Amersham Biosciences; *E. coli* strain Top10 was purchased from Life Technologies. *N. sp.* PP1Y was isolated from polluted seawater in the harbor of Pozzuoli (Naples, Italy) as previously described [43].

The thermostable recombinant DNA polymerase used for PCR amplification was TAQ Polymerase from Microtech Research Products. dNTPs, T4 DNA ligase, and the Wizard PCR Preps DNA purification system for elution of DNA fragments from agarose gels were purchased from Promega. The QIAprep Spin Miniprep Kit for plasmid DNA purification was from QIAGEN. Enzymes and other reagents for DNA manipulation were from New England Biolabs. Oligonucleotides synthesis and DNA sequencing were performed by MWG-Biotech. N-terminus of rRHA-P was sequenced by Proteome Factory AG. The presence and location of a potential signal peptide cleavage site on the amino acidic sequence of RHA-P was analyzed using SignalP 4.1 server (<http://www.cbs.dtu.dk/services/SignalP>).

Q-Sepharose Fast Flow and *p*-nitrophenyl- $\alpha$ -L-rhamnopyranoside (pNPR) were from Sigma Aldrich; Sephacryl S200 High Resolution was purchased from Amersham Biosciences. IPTG (isopropyl  $\beta$ -D-1-thiogalactopyranoside) was obtained from Applichem.

Solvents used in enzymatic assays were either from Applichem (DMSO) or from Romil (acetone). TLC silica gel plates were from E. Merck (Darmstadt, Germany).

## 2.2. Growth of *Novosphingobium* sp. PP1Y cells

*N. sp.* PP1Y cells were grown in Potassium Phosphate Minimal Medium (PPMM) at 30 °C for 28 h under orbital shaking at 220 rpm. A pre-inoculum in LB was prepared by transferring 50 µL from a glycerol stock stored at –80 °C to a 50 mL Falcon tube containing 12.5 mL of sterile LB. The pre-inoculum was allowed to grow at 30 °C O/N under orbital shaking and then used to inoculate 1 L of PPMM at an initial cell concentration of 0.01–0.02 OD<sub>600</sub>. 0.3 mM naringine was added to the medium and used as an inducer of the α-RHA activity, as previously described [47].

## 2.3. Cloning of *orfPP1Y\_RS05470* and construction of the *pET22b(+)/rha-p* expression vector

Genomic DNA was extracted from a 50 mL saturated culture of *N. sp.* PP1Y as described elsewhere [44]. *orfPP1Y\_RS05470* coding for the α-RHA activity was amplified in two contiguous fragments, owing to the considerable length of the *orf* (3441 bp). The first fragment, named *rha-up* (1816 bp), was amplified using an internal downstream primer, RHA-Intdw (5'-AGGCGCCATGCGAATGT-3'), which included an internal *NcoI* site already present in *orfPP1Y\_RS05470*, and an upstream primer, RHA-up (5'-GGGAATCCATATGCCGCGCTTCGCT-3'), designed to add a *NdeI* restriction site at 5' of *orfPP1Y\_RS05470*. The second half of the gene, named *rha-dw* (1625 bp), was amplified using the upstream primer RHA-Intup (5'-ACATCCCATGGCCGCT-3'), complementary to RHA-Intdw, and the downstream primer RHA-dw (5'-AAAACCGAGCTCTCAATGCCGCGCTG-3') that was intended to incorporate a *SacI* restriction site downstream of the amplified *orf*.

The amplified fragments, *rha-up* and *rha-dw*, were purified from agarose gel, digested, respectively, with *NdeI/NcoI* and *NcoI/SacI*, and individually cloned in *pET22b(+)* vector previously cut with the same enzymes.

Ligated vectors were used to transform *E. coli*, strain Top10, competent cells. The resulting recombinant plasmids, named *pET22b(+)/rha-up* and *pET22b(+)/rha-dw*, were verified by DNA sequencing. Next, the construction of complete *rha-p* gene in *pET22b(+)* was performed. First, both *pET22b(+)/rha-dw* and *pET22b(+)/rha-up* were digested with *NcoI/SacI* restriction endonucleases to obtain, respectively, fragment *rha-dw* and linearized *pET22b(+)/rha-up*.

Digestion products were purified from agarose gel electrophoresis, eluted and ligated. Ligation products were used to transform *E. coli* Top10 competent cells and the resulting recombinant plasmid, named *pET22b(+)/rha-p* was verified by DNA sequencing.

## 2.4. α-L-Rhamnosidase recombinant expression

Protein expression was carried out in *E. coli* BL21(DE3) strain transformed with *pET22b(+)/rha-p* plasmid.

All the media described in this paragraph contained 100 µg/mL of ampicillin.

### 2.4.1. Analytical expression

*E. coli* BL21(DE3) competent cells transformed with plasmid *pET22b(+)/rha-p* were inoculated in a sterile 50 mL Falcon tube containing 12.5 mL of either LB [50] or LB containing a final concentration of 0.5 M NaCl (LB-N). Cells were grown under constant shaking at 37 °C up to 0.6–0.7 OD<sub>600</sub>. This preinoculum was diluted 1:100 in 12.5 mL of either one of the four following media: LB, LB-N, LB supplemented with 1 mM of both betaine and sorbitol (LB-BS), or LB containing a final concentration of 0.5 M NaCl and 1 mM of both betaine and sorbitol (LB-NBS). Cells were grown under constant shaking at 37 °C up to 0.7–0.8 OD<sub>600</sub>. RHA-P recombinant expression was induced with 0.1 mM IPTG at either 23 °C or 37 °C; growth

was continued in constant shaking for 3 h. Cells were collected by centrifugation (5,524 × *g* for 15 min at 4 °C) and suspended in 25 mM MOPS pH 6.9 at a final concentration of 14 OD<sub>600</sub>. Cells were disrupted by sonication (12 times for a 1-min cycle, on ice) and an aliquot of each lysate was centrifuged at 22,100 × *g* for 10 min at 4 °C. Both soluble and insoluble fractions were analyzed by SDS-PAGE. The soluble fraction was assayed for the presence of α-RHA enzymatic activity.

### 2.4.2. Large scale expression

Fresh transformed cells were inoculated into 10 mL of LB-N and incubated in constant shaking at 37 °C O/N. The preinoculum was diluted 1:100 in four 2 L Erlenmeyer flasks containing each 500 mL of LB-NBS and incubated in constant shaking at 37 °C up to 0.7–0.8 OD<sub>600</sub>.

Expression of the recombinant protein, named rRHA-P, was induced with 0.1 mM IPTG and growth was continued for 3 h at 23 °C. Cells were collected by centrifugation (5,524 × *g* for 15 min at 4 °C) and stored at –80 °C until needed.

## 2.5. Native and recombinant α-L-rhamnosidase purification

Both native and recombinant RHA-P were purified following three chromatographic steps. Cell paste was suspended in 25 mM MOPS pH 6.9, 5% glycerol (buffer A), at a final concentration of 100 OD<sub>600</sub> and cells were disrupted by sonication (10 times for a 1-min cycle, on ice). Cell debris were removed by centrifugation at 22,100 × *g* for 60 min at 4 °C and the supernatant was collected and filtered through a 0.45 µm PVDF Millipore membrane.

Afterwards, cell extract was loaded onto a Q Sepharose FF column (30 mL) equilibrated in buffer A. The column was washed with 50 mL of buffer A, after which bound proteins were eluted by using a 300 mL linear gradient of buffer A from 0 to 0.4 M NaCl at a flow rate of 15 mL/h. The chromatogram was obtained by analyzing fractions absorbance at λ = 280 nm and the presence of the recombinant α-RHA activity was detected using the pNPR assay. Relevant fractions were analyzed by SDS-PAGE, pooled and concentrated at a final volume of ~ 0.5 mL using a 30 kDa Amicon ultra membrane, Millipore. The sample was then loaded onto a Sephacryl HR S200 equilibrated with buffer A containing 0.2 M NaCl (buffer B).

Proteins were eluted from the gel filtration column with 250 mL of buffer B at a flow rate of 12 mL/h. Fractions were collected, analyzed and screened for the presence of α-RHA activity as previously described. At this stage, NaCl was removed from pooled fractions by repeated cycles of ultrafiltration and dilution with buffer A. The sample was then loaded on a Q Sepharose FF column (30 mL) equilibrated in buffer A. The column was washed with 50 mL of buffer A, after which bound proteins were eluted with 300 mL of a linear gradient of buffer A from 0 to 0.25 M NaCl at a flow rate of 13 mL/h. Fractions were collected, analyzed by SDS-PAGE and screened for the presence of α-RHA activity. Relevant fractions were pooled, concentrated, purged with nitrogen, and stored at –80 °C until use.

## 2.6. Analytical gel filtration

Analytical gel-filtration experiments were carried out as follows: 100 µL of a 40 pM protein sample was loaded on a Superdex 200 HR 10/300 column previously equilibrated in buffer B, installed on an AKTA™FPLC™ (GE Healthcare Life Science). Samples were eluted isocratically at RT at a flow rate of 0.5 mL/min. Protein elution was monitored at λ = 280 nm. A molecular weight calibration was performed in the same buffer with the following proteins of known molecular weight: β-amylase (200 kDa), glyceraldehyde-3-phosphate dehydrogenase (143 kDa), carbonic anhydrase (29 kDa).

## 2.7. Enzyme activity assays

$\alpha$ -RHA activity was determined using *p*NPR as substrate (*p*NPR assay). Otherwise stated, all activity assays were performed at RT. The reaction mixture contained, in a final volume of 0.5 mL of 50 mM MOPS pH 6.9, *p*NPR at a final concentration of 600  $\mu$ M and variable amounts of the sample tested. The reaction was blocked after 10 and 20 min by adding 0.5 M  $\text{Na}_2\text{CO}_3$ ; the product, *p*-nitrophenolate (*p*NP), was detected spectrophotometrically at  $\lambda=405$  nm. The extinction coefficient used was  $\epsilon_{405} = 18.2 \text{ mM}^{-1} \text{ cm}^{-1}$ . One unit of enzyme activity was defined as the amount of the enzyme that releases one micromole of *p*NP per min.

### 2.7.1. Kinetic parameters determination

Kinetic parameters were obtained at pH 6.9 using a *p*NPR concentration in the range 0.025–1 mM. All kinetic parameters were determined by a non-linear regression curve using GraphPad Prism (GraphPad Software; [www.graphpad.com](http://www.graphpad.com)).

### 2.7.2. pH optimum

pH optimum for  $\alpha$ -RHA activity was determined in the range 4.7–8.8. Enzyme assays were performed as described above, using the following buffers: 50 mM potassium acetate (pH 4.7–5.7), 50 mM MOPS/NaOH (pH 5.7–7.7) and 50 mM Tris/HCl (pH 7.7–8.8).

### 2.7.3. Temperature optimum and stability

Optimum temperature was evaluated by performing the standard *p*NPR assay and incubating the reaction mixture at different temperatures, in the range 25–55 °C.

The thermal stability of the enzyme was determined by incubating the enzyme for one and 3 h at 30, 40, 50, 60 °C and measuring, after each incubation, the residual specific activity.

### 2.7.4. Organic solvents tolerance

The tolerance of the enzymatic activity to the presence of organic solvents in the reaction mixture, such as DMSO, acetone or ethanol, was evaluated by performing the standard *p*NPR assay in 50 mM MOPS pH 6.9 to which either 10% or 50% of solvent was added.

## 2.8. Substrate specificity

Reactions were carried out in 0.6 mL of 50 mM Na-phosphate buffer pH 7.0 under magnetic stirring at 40 °C in the presence of 20 mM of either aryl glycoside and 0.25 U of rRHA-P. Reactions were monitored over time (0–24 h) by TLC analysis (system solvent: EtOAc:MeOH:H<sub>2</sub>O 70:20:10). Compounds on TLC plates were visualized under UV light or charring with  $\alpha$ -naphthol reagent.

Hydrolysis reactions of maltose, pullulan, starch, amylopectin, sucrose, raffinose, lactose, xylan from birchwood, xylan from oat spelt, hyaluronic acid,  $\alpha$ -cellulose, cellobiose, chitosan,  $\beta$ -Glucan from barley, laminarin, curdlan, fucoidan from *Fucus vesiculosus*, rhamnogalacturonan, rutinose were performed using 2.5 mg of each substrate, which was suspended in 0.5 mL of 50 mM Na-phosphate buffer pH 7.0. The reaction was carried out at 40 °C under magnetic stirring, in the presence of 0.25 U of rRHA-P. Hydrolysis products were monitored by TLC analysis (system solvent HCOOH:HAc:H<sub>2</sub>O:2-propanol: EtOAc:1:10:15:5:25).

Flavonoidic compounds such as naringin, rutin, neohesperidin dihydrochalcone, were screened as possible substrates. In this case, a 6 mM solution of each compound in a final volume of 1 mL of 50 mM Na-phosphate buffer pH 7 was incubated at 40 °C in the presence of 0.25 U of rRHA-P. Reactions were checked over time by TLC analysis ( $t=0, 15', 30', 60', 90', 120', 150', 180', 24$  h) with

the following solvent system: EtOAc:MeOH:H<sub>2</sub>O 70:20:10. An additional hydrolysis reaction of naringin was performed in conditions similar to those reported above in the presence of 10% DMSO, and the reaction was monitored over time.

In all experiments, TLC standard solutions of pure reagents and products were used for comparison.

## 2.9. Mass spectrometry analysis

Identification of native and recombinant RHA-P by mass spectrometry was performed by enzymatic digestion, either in solution or *in situ* after separation by SDS-PAGE.

When digesting in solution, the protein sample was lyophilized and then dissolved in denaturing buffer (300 mM Tris/HCl pH 8.8, 6 M urea, 10 mM EDTA). Cysteines were reduced with 10 mM dithiothreitol in denaturing buffer at 37 °C for 2 h, and then carbamidomethylated with 55 mM iodoacetamide dissolved in the same buffer at RT for 30 min, in the dark. Protein sample was desalted by size exclusion chromatography on a Sephadex G-25 M column (GE Healthcare, Uppsala, Sweden). Fractions containing RHA-P were lyophilized and then dissolved in 10 mM  $\text{NH}_4\text{HCO}_3$  buffer (pH 8.0). Enzyme digestion was performed using proteases with different specificity such as trypsin, chymotrypsin and endoproteinase GluC (V8-DE) (Sigma), using a protease/RHA-P ratio of 1:50 (w/w) at 37 °C for 16 h.

For the enzymatic digestion *in situ*, Coomassie blue stained bands excised from polyacrylamide gels were destained by several washes with 0.1 M  $\text{NH}_4\text{HCO}_3$  pH 7.5 and acetonitrile. Cysteines were reduced for 45 min in 100  $\mu$ L of 0.1 M  $\text{NH}_4\text{HCO}_3$ , 10 mM dithiothreitol, pH 7.5. Carbamidomethylation of thiols was achieved after 30 min in the dark by adding 100  $\mu$ L of 55 mM iodoacetamide dissolved in the same buffer. Enzymatic digestion was carried out on different bands of RHA-P by using 100 ng of proteases with different specificity (same as above) in 10 mM  $\text{NH}_4\text{HCO}_3$  buffer, pH 7.5. Samples were incubated for 2 h at 4 °C. Afterwards, the enzyme solution was removed and a fresh protease solution was added; samples were incubated for 18 h at 37 °C. Peptides were extracted by washing the gel spots/bands with acetonitrile and 0.1% formic acid at RT, and were filtered using 0.22  $\mu$ m PVDF filters (Millipore) following the recommended procedures.

Peptide mixtures were analyzed either by matrix-assisted laser-desorption/ionization mass spectrometry (MALDI-MS) or capillary liquid chromatography with tandem mass spectrometry detection (LC-MS/MS).

MALDI-MS experiments were performed on a 4800 Plus MALDI TOF/TOF mass spectrometer (Applied Biosystems, Framingham, MA) equipped with a nitrogen laser (337 nm). The peptide mixture (1  $\mu$ L) was diluted (1:1, v/v) in acetonitrile/50 mM citrate buffer (70:30 v/v) containing 10 mg/mL of  $\alpha$ -cyano-4-hydroxycinnamic acid. Mass calibration was performed using external peptide standards purchased from Applied Biosystems.

Spectra were acquired using a mass ( $m/z$ ) range of 300–4000 amu and raw data were analyzed using Data Explorer Software provided by the manufacturer. Experimental mass values were compared with calculated masses derived from an *in silico* digestion of RHA-P obtained with different proteases, using MS-Digest, a proteomics tool from Protein Prospector software ([prospector.ucsf.edu/](http://prospector.ucsf.edu/)).

Peptide mixtures were analyzed by nanoLC-MS/MS on a CHIP MS 6520 QTOF equipped with a capillary 1200 HPLC system and a chip cube (Agilent Technologies, Palo Alto, Ca). After sample loading, the peptide mixture was first concentrated and then washed at 4 nL/min in a 4 nL enrichment column (Agilent Technologies chip) with 2% acetonitrile + 0.1% formic acid.

The sample was then fractionated on a C18 reverse-phase capillary column at a flow rate of 400 nL/min by using a two-solvents

system consisting of 2% acetonitrile + 0.1% formic acid (solvent A) and 95% acetonitrile + 0.1% formic acid (solvent B). Separation was carried out with a 50 min linear gradient from 5 to 60% of solvent B.

Peptide analysis was performed using data-dependent acquisition of one MS scan (mass range from 300 to 2,000  $m/z$ ) followed by MS/MS scans of the five most abundant ions in each MS scan.

MS/MS spectra were acquired automatically when the MS signal detected upraised the threshold of 50,000 counts. Double and triple charged ions were isolated and fragmented. The acquired MS/MS spectra were transformed in Mascot Generic format (.mgf) and used to query either a NCBI nr 02–2015 (21,322,359,704 amino acid sequences; 10,835,265,410 residues) or a *N. sp. PP1Y* (4635 amino acid sequences; 1,493,994 residues) sequence database.

A licensed version (2.4.0.) of MASCOT software ([www.matrixscience.com](http://www.matrixscience.com)) was used with the following search parameters: trypsin, chymotrypsin or GluC endoproteinase as enzyme; 3 or 2 as allowed number of missed cleavages; carbamidomethylation of cysteines as fixed modification; 10 ppm MS tolerance and 0.6 Da MS/MS tolerance; peptide charge from +2 to +3. Oxidation of methionine and formation of pyroglutamic acid from glutamine residues at the N-terminal position of peptides were considered as variable modifications. Ions score is  $-10 \cdot \log(P)$ , where P is the probability that the observed match is a random event. Individual ions score >14 indicate identity or extensive homology ( $p < 0.05$ ). Protein scores derive from ion scores as a non-probabilistic basis for ranking protein hits. Individual ion score threshold provided by MASCOT software, necessary to evaluate the quality of matches in MS/MS data and to calculate protein score, was 52 in NCBI nr database and 14 in PP1Y Database. In Table 1 only peptides with ion score  $\geq 10$  are reported.

### 2.10. NMR Analysis

All the experiments were performed at 298 K on a Bruker 600 MHz DRX spectrometer equipped with a cryo probe. pNPR was dissolved in  $D_2O$  to a final concentration of 3 mM in a 5-mm NMR tube. The ligand proton resonances were assigned by a combination of 1D and 2D NMR experiments including COSY, TOCSY and HSQC.  $^1H$  NMR spectra were acquired with 32 k data points. Double quantum-filtered phase sensitive COSY and TOCSY experiments were performed by using data sets of  $2096 \times 256$  ( $t_1 \times t_2$ ) points. Total Correlation Spectroscopy (TOCSY) spectrum was recorded with a spin lock time of 100 ms. Heteronuclear single quantum coherence (HSQC) experiment was measured in the  $^1H$ -detected mode via single quantum coherence with proton decoupling in the  $^{13}C$  domain, by using data sets of  $2048 \times 256$  points. Experiments were carried out in the phase-sensitive mode according to the method of States and coworkers [51]. In all homonuclear spectra the data matrix was zero-filled in the F1 dimension to give a matrix of  $4096 \times 2048$  points and resolution was enhanced in both dimensions by a cosine-bell function before Fourier transformation.

After the acquisition of the initial spectra of the ligand alone, rRHA-P was added to a final concentration of  $\sim 1 \mu M$  ( $\sim 60 \mu g$ ) in the NMR tube from a  $\sim 5.9 \mu M$  solution in 25 mM MOPS containing 5% glycerol. The NMR sample was immediately placed in the spectrometer probe to record experiments on the mixture.

Data acquisition and processing were performed with TOPSPIN 2.1 software.

### 2.10. Analytical methods

Protein concentration was measured using the Bio-Rad Protein System [52] using bovine serum albumin (BSA) as standard. Polyacrylamide gel electrophoresis was carried out using standard techniques [53]. SDS-PAGE 15% Tris-glycine gels were run under

denaturing conditions and proteins were stained with Coomassie brilliant blue G-250. "Wide range" (200–6.5 kDa) molecular weight standard was from Sigma (ColorBurst™ Electrophoresis Marker).

## 3. Results

### 3.1. Isolation and identification of a $\alpha$ -RHA from *Novosphingobium sp. PP1Y*

In a previous work [47], a  $\alpha$ -RHA activity was detected in the crude extract of *N. sp. PP1Y* grown in minimal medium and in the presence of 0.3 mM naringin. In order to identify and characterize this enzymatic activity, *N. sp. PP1Y* cells were grown under the same experimental conditions described by the authors [47]. Cells were collected by centrifugation after 24 h of growth in PPMM (optical density of  $\sim 1 OD_{600}$ ) at  $5,524 \times g$  for 15 min at 4 °C.  $\alpha$ -RHA purification was carried out following the procedures described in this work in Materials and Methods. In all three chromatographic steps used for the purification of *N. sp. PP1Y* crude extract, a unique peak of  $\alpha$ -RHA activity was always detected, but no major protein band was ever evident from the SDS-PAGE analysis of the corresponding active fractions (data not shown).

Peak fractions obtained from the first two chromatographic steps were digested with trypsin and analyzed by LC-MS/MS analysis. Raw data were used to search NCBI database (Bacteria as taxonomy restriction) with the MS/MS ion search program of Mascot software. Among the identified proteins, a member of the glycoside hydrolase family (*Novosphingobium sp. PP1Y:WP.013837086.1*) was identified with 10 (20% of sequence coverage) and 32 peptides (46% of sequence coverage) in the first and in the second chromatographic step, respectively (data not shown). The putative MW, deduced from the amino acid sequence, was of 124,225 Da.

Peak fractions obtained from the last chromatographic step (Q-sepharose) showed the presence of a relatively limited number of protein bands (Fig.S1, Supplementary material). Five bands migrating as expected for proteins of MW higher than 100 kDa were selected and excised from the polyacrylamide gel stained with Colloidal Coomassie Blue. Bands were digested *in situ* with trypsin, and the resulting peptides mixture was analyzed by LC-MS/MS. Raw data were used to search NCBI database (Bacteria as taxonomy restriction) with MASCOT software.

One of the protein bands analyzed, indicated in Fig. S1 by a red arrow, was identified (52 peptides, 71% sequence coverage, Table 1) as the protein encoded by the *orfPP1Y\_RS05470*; this latter is located in one of the extrachromosomal elements of *N. sp. PP1Y*, the Megaplasmid referred to as *Mpl* [44]. This protein, from now on indicated as RHA-P, had been previously annotated as a member of the GHs family and is composed by 1,146 aa for a calculated molecular weight of about 124,225 Da.

### 3.2. Cloning, recombinant expression and purification of recombinant RHA-P

The recombinant plasmid pET22b(+)/*rha-p* (Materials and Methods), in which *orf PP1Y\_RS05470* was cloned, was used to transform *E. coli* BL21(DE3) strain. First attempts of expression of the recombinant protein at 37 °C showed the presence of a protein band with the expected molecular weight of recombinant RHA-P (rRHA-P) almost exclusively in the insoluble fraction of the induced culture (Fig. S2). As evident from Fig. S2 of the Supplementary material, when *E. coli* was instead induced at 23 °C [54], the presence of a protein band with the expected MW for rRHA-P in the soluble fraction (lane 5) appeared to be markedly increased when compared to the soluble fraction obtained after an induction performed

**Table 1**  
Identification of native RHA-P by *in situ* digestion followed by LC–MS/MS analysis.

Protein [Species] NCBI nr Accession number	Mass	Protein score	Sequence coverage (%)	n° of peptides	Ion score <sup>a</sup> and peptide sequence
Glycoside hydrolase family protein [ <i>Novosphingobium</i> sp. PP1Y] gi 334145605 ref  WP.013837086.1]	124,225	2318	71	52	34 R.TGDAIK.A 31 R.VGGFYGK.G 38 R.GVVQNEK.R 28 R.LDNELVR.G 21 R.GPEIEPVK.A 11 R.VLPITGRK.A 19KVGSKNEPR.G 37 R.AVAEAAFDK.V 42 R.GVVQNEKR.Q 48KLSSPNAMALR.A 13KLSSPNAMALR.A+Oxidation (M) 37 R.DITDQVPVLR.L 13 R.ITVVGDIITMDR.L 41 R.ITVVGDIITMDR.L+Oxidation (M) 32 R.LGRPEDYVVK.L 17KAPIVSVTLYYK.V 24KVEKWFGQIPR.G 55KVGLHILGGLASSR.L 52 R.VKQAQAEELAQK.L 61 R.LDATAIAEAQER.L 35 R.TFVVSAPVQADR.T 28 R.MGWLLPAVTQDK.L 15 R.MGWLLPAVTQDK.L+Oxidation (M) 27 R.KAPIVSVTLYYK.V 52 R.DLAAMAALTPAQVK.A 70 R.DLAAMAALTPAQVK.A+Oxidation (M) 74 R.AVVSTLSGEIGGLER.V 32 R.LKPMLEQAFGAWK.A 31 R.LKPMLEQAFGAWK.A+Oxidation (M) 74KGATLAEGQVYSDDPAK.Y 28 R.RAVVSTLSGEIGGLER.V 50KFVLANGLTTIVHTDR.K 18KSAAPVKPLGAAVPAQGR.I 23 R.NWTAPGINDPDPALK.V 37 R.MGWLLPAVTQDKLTK.Q 33 R.MGWLLPAVTQDKLTK.Q+Oxidation (M) 47 R.AVAEAAFDKVLADYLR.D 65 R.ALPNQFETNAAVQAIR.K 25KGWSYGVYSSVTQPTGPR.T 29KWMSRPVYALNVVPGPR.T 26KWMSRPVYALNVVPGPR.T+Oxidation (M) 20 R.TFVVSAPVQADRTGDAIK.A 18KGATLAEGQVYSDDPAKYK.R 36 R.IVLIDRPNPQSVIMAGR.V 43 R.IVLIDRPNPQSVIMAGR.V+Oxidation (M) 58KADTEALGLANDVLGGFLSR.L 47 R.GPEIEPVKAGPVTLPAPLSR.D 55 R.HATIGSMADLDAATLTDVVRK.W 56 R.HATIGSMADLDAATLTDVVRK.W+Oxidation (M) 21 R.EEKGWSYGVYSSVTQPTGPR.T 46KAIADVGFAPGQKIPITQEEQQR.V 70 R.TNYVETVPTGALDLALFMESDR.M 50 R.AIEASANEFLRPGGMTYVVVGDR.K 59 R.AIEASANEFLRPGGMTYVVVGDR.K+Oxidation (M) 65 R.AIEASANEFLRPGGMTYVVVGDRK.I 54 R.QGDNQPYGLFDYAQADGLLPVGHYPYR.H+ Gln->pyro-Glu (N-term Q) 71 R.QGDNQPYGLFDYAQADGLLPVGHYPYR.H 23 R.LNKDLREEKGWSYGVYSSVTQPTGPR.T 38KWFTEHYGPNNVVLVLSGDIDAATARPK.V 35KIVEPQLEGLPLIDVQQAPQAAADDQSVE.- 55 R.KIVEPQLEGLPLIDVQQAPQAAADDQSVE.- 40 R.ALGSTLFGQHPYAQPTDGLGNAASLAALTPAALR.A

<sup>a</sup> In the table only peptides with ion score  $\geq 10$  are reported.

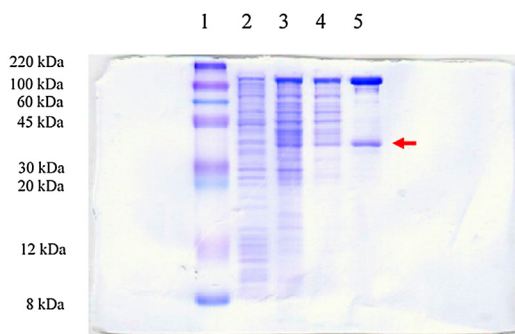
at 37 °C (lane 3). Neither the use of different IPTG concentrations nor the variation of the induction time seemed to improve rRHA-P solubility.

To increase the yield of active rRHA-P in the soluble fraction of cell cultures induced at 23 °C, a novel set of analytical expression experiments using either LB or LB-N (Materials and Methods) supplemented with 1 mM of both betaine and sorbitol (two osmolytes),

were performed. Data in literature suggest that the addition of these molecules to the growth medium of induced recombinant cells of *E. coli* might increase protein solubility. This effect should be improved by the co-presence in the medium of a high salt concentration (LB-N medium), which might *it* increase the uptake rate in the cytoplasm of betaine and sorbitol from the extracellular

**Table 2**  
Purification Table of rRHA-P.

	Total Units <sup>b</sup>	Specific Activity (Units/mg) <sup>b</sup>	P.F. <sup>a</sup>	Yield (%)
Cell lysate	13,728.8	49.8		
I Q-Sepharose	5,939.6	54.7	1.1	43.3
Gel filtration	1,370.6	66.1	1.3	9.9
II Q-Sepharose	920.9	346.9	6.9	6.7

<sup>a</sup> Purification Factor.<sup>b</sup> Standard deviations, expressed as percentage errors, were always within 20%.**Fig. 1.** SDS-PAGE analysis of rRHA-P purification steps. Lane 1: MW standard. Lane 2: cell lysate of *E. coli* strain BL21(DE3). Lane 3: peak fraction after the first Q-sepharose. Lane 4: peak fraction after S200-gel filtration chromatography. Lane 5: purified rRHA-P; the red arrow in this line indicates the contaminant protein found at the end of purification. For each sample an amount of ca. 4 µg of total proteins was loaded. (For interpretation of the references to colour in this figure legend, the reader is referred to the web version of this article.)

environment [55], and/or **ii**) induce the expression of additional heat-shock proteins assisting in protein folding [56].

For these experiments, IPTG concentration and induction time were respectively 0.1 mM and 3 h. Activity assays showed that the best expression of active rRHA-P was obtained inducing the cultures at 23 °C and using LB-NBS (LB-N to which 1 mM of both betaine and sorbitol were added) as growth medium. In this case, specific activity of cell extract was 46 times higher than what obtained with the soluble fraction of recombinant cells grown in LB and induced at 37 °C.

Large-scale recombinant expression was performed by using the optimized conditions suggested by the analytical experiments.

rRHA-P purification was carried out following three different chromatographic steps. The purification table (Table 2) showed a final purification factor (PF) of 6.9. SDS-PAGE analysis of peak fractions representative of each purification step (Fig. 1) showed in the final purified sample of rRHA-P the additional presence of a major contaminant protein with an approximate MW of ~35 kDa.

The 35 kDa protein band was excised, digested *in situ* with trypsin and analyzed by LC-MS/MS. The protein, identified by searching the *E. coli* sequence database (Materials and Methods), resulted to be glyceraldehyde 3-phosphate dehydrogenase, as identified by 17 peptides matches for a sequence coverage of 71%.

Purified rRHA-P amino acid sequence was verified up to a 94% coverage, by MS Mapping analysis carried out by MALDI-TOF and LC-MS/MS. However, it is worth noting that the protein N-terminus, detected by MS analysis, lacks the first 23 amino acids from the expected cloned sequence (Fig. 2 and Fig. S3).

To confirm the lack of the putative N-terminal peptide, purified rRHA-P was subjected to both a MALDI-TOF and LC-MS/MS analysis after an *in situ* digestion with either trypsin or chymotrypsin, and to the N-terminus sequencing. Mass spectrometry analysis allowed the identification of peptides <sup>23</sup>ESRDDAAEVAPSTRPEPSLEQAF<sup>45</sup> (MH<sup>+</sup> 2502.17 ppm) and <sup>23</sup>ESRDDAAEVAPSTR<sup>36</sup> (MH<sup>+</sup> 1503.70) when rRHA-P was digested with chymotrypsin or trypsin, respec-

**Table 3**  
TLC results of RHA-P-catalyzed reaction using different pNP-α- and pNP-β- derivatives as substrates.

	Substrates <sup>a</sup>	Hydrolysis		Transglycosylation	
		3 h	20 h	3 h	20 h
1	pNP-α-D-Glcp	-	-	-	-
2	pNP-β-D-Glcp	-	-	-	-
3	pNP-α-D-Galp	-	-	-	-
4	pNP-β-D-Galp	-	-	-	-
5	pNP-α-D-Manp	-	-	-	-
6	pNP-β-D-Manp	-	-	-	-
7	pNP-β-D-Xylp	-	-	-	-
8	pNP-α-L-Fucp	-	-	-	-
9	pNP-β-D-Fucp	-	-	-	-
10	pNP-α-L-Araf	-	-	-	-
11	pNP-β-L-Araf	-	-	-	-
12	pNP-α-L-Rhap	+	+	-	-
13	pNP-β-GlcAp	-	-	-	-
14	pNP-β-D-NAGlcp	-	-	-	-
15	pNP-β-D-NAGalp	-	-	-	-

<sup>a</sup> Ara, arabinose; Fuc, fucose; Gal, galactose; Glc, glucose; Man, mannose; NAGlc, N-acetylglucosamine; NAGal, N-acetylgalactosamine; GlcA: glucuronic acid, Rha, Rhamnose; Xyl, xylose.

tively. This evidence was also confirmed by N-terminus sequencing results, which showed that the first 5 amino acids of the recombinant protein are **ESRDD**. Interestingly, also in native RHA-P the same N-terminal peptide, obtained by fragmentation spectrum of the triple charged ion at 834.73 *m/z* from the *in situ* digestion of the protein with chymotrypsin (Fig. S4), had been detected in the first place. The scarce amount of native protein, however, did not allow us to confirm the effective lack of the N-terminus peptide by direct amino acid sequencing.

### 3.3. Biochemical characterization of rRHA-P

#### 3.3.1. Analytical gel filtration

The oligomeric state of rRHA-P was verified by analytical gel filtration using a Superdex 200 analytical column; the protein eluted as a single peak with an apparent molecular weight of 101,500 ± 5,000 Da, which indicates that rRHA-P is a monomer.

#### 3.3.2. Substrate specificity

To investigate rRHA-P substrate specificity in hydrolysis and self-condensation processes, several pNP-α- and pNP-β- derivatives were used as substrates in enzymatic assays performed as described in Materials and Methods. Reactions were followed over time by TLC analysis and data are reported in Table 3. As evident from Table 3, the purified enzyme showed activity only on pNPR, confirming that rRHA-P is indeed an α-L-rhamnosidase. Moreover, no activity on pNP-β-D-Glc was detected, excluding that rRHA-P might act as a naringinase, a class of glycosyl hydrolase having both α-L-rhamnosidase and β-D-glucosidase activities [40]. Furthermore, oligo- and polysaccharides such as rutinose, maltose, sucrose, lactose, pullulan, starch, amylopectin, raffinose, xylan from birchwood, xylan from oat spelt, hyaluronic acid, α-cellulose, cellobiose, chitosan, β-Glucan from barley, laminarin, curdlan, fucoidan from *Fucus vesiculosus*, were also tested as substrates for rRHA-P. TLC analysis of all these reactions, performed as described in Materials and Methods, showed the lack of activity of this enzyme on any of these compounds.

#### 3.3.3. Mechanism of action

To understand whether rRHA-P behaves as an inverting or a retaining glycosidase [1], <sup>1</sup>H NMR spectroscopy was used to monitor the stereochemical course of pNPR cleavage. As shown in Fig. 3, after the addition of the enzyme, a mixture of α and β

```

1  PRLSLRIVLCLATALSTLPVHAESRDDAAEVAPSTRPEPSLEQAFKDPSSARPRVWVHWMNGNITKDGIRKDLWEMKRV  80
81  GIGGLQNFNDANLQTPQIVDHRLLVYMTPEWKDAFRFAAHEADRLDLELAIAASPGWSETGGPWVKPQDGLKLVWSETTLA  160
161 GGQRFVGRLASPPGTGTFPOTLHPPVTIEEIIISGVPAAETGGVSYAGEVGVLAFFVPDIASLPVPRALDGAENVLAGKALV  240
241 DADIAGGVTLARVDGKAPLLRLDYQRVTVRSATVFPVNVRI PFAGAAFAGTLESSQDGKTWTPIKALELSNVPTTISFA  320
321 PVEAAHFRLVLNPGQPDAALGSPAPGVAGNDLFGAIAASKRAGQPI MVGQFELHSDALVDRYETKAGFVMSRDYYALVGP  400
401 DNVTVGVDPSVIDLDTDKLKADGTLDAAPKLPAGQHWRVRLRIGYSLGTTNHPAPPEATGLEVDKFDGEAVREYLEHYIG  480
481 MYKDAAGPDMVGKRGVRRALLTDSIEVGEANWTPRMLEQFQRLRGYDARPWLPAITGTLVGTREQSDRFLYDVRRLADLL  560
561 ASEHYGTVADVAHENDLKVYGEGLDHRPMLGDDMAMRSHADI PMAALWTFNRDEGPRQTLIADMKGAA SVAHLYGQNLV  640
641 AAESMTASMAPWAFAPKDLKRFIDLEFVTGVNRPVIHTSVHVPVDDKPKGLSLAIFGQYFNROESWAEMARPVVDYIARS  720
721 SLLIQTGRNVADVAYFYGEEAPLTGLYGDEPVADAPVRYAYDYINFNALTELLANDGEDLVAPSGARYKTIYLGSSSHM  800
801 TLAALRKLAALVVGATVVGKAPIATPSNTSAQEGDLTEWSSSLVARLWPGSGDARV GKGRVIASQDIESALQAMDVAPDF  880
881 TFTGADAGVKIPFVHRRDGKGEIYYLVNQEEAAQSIEAHFRVTGKQPELWHPETGKSEPI SYRISGGETVVPLHLDGDEA  960
961 VFVVFRRKAAARDRVTLARQGERAVATLDGAWQVAFQADRGA PASIELARLEPLDKSADPGVKYFSGIATYSRNRFRVTGKY  1040
1041 GEGRSLWLDLGRVGDLAQVSVNGVDVGTAWHAPYRLDIGKAVRKGQNTLEIRVANTWVNRLIGDQOQEGAQKITWTAMPTY  1120
1121 RADAPLRPSGLIGPVRLIEETTGGH  1145

```

**Fig. 2.** rRHA-P sequence coverage by MS analysis. Highlighted in grey are the peptides, identified by MS analysis (MALDI-TOF and/or LC-MSMS), of the enzymatic digestions of rRHA-P carried out either *in situ* or in solution with proteases of different specificity: trypsin, chymotrypsin and endoproteinase GluC (V8-DE). A global sequence coverage of 94% was obtained. Crossed is the N-terminus sequence expected for rRHA-P (reference sequence WP\_013837086.1) and not retrieved, either by N-terminus or by MS analysis.

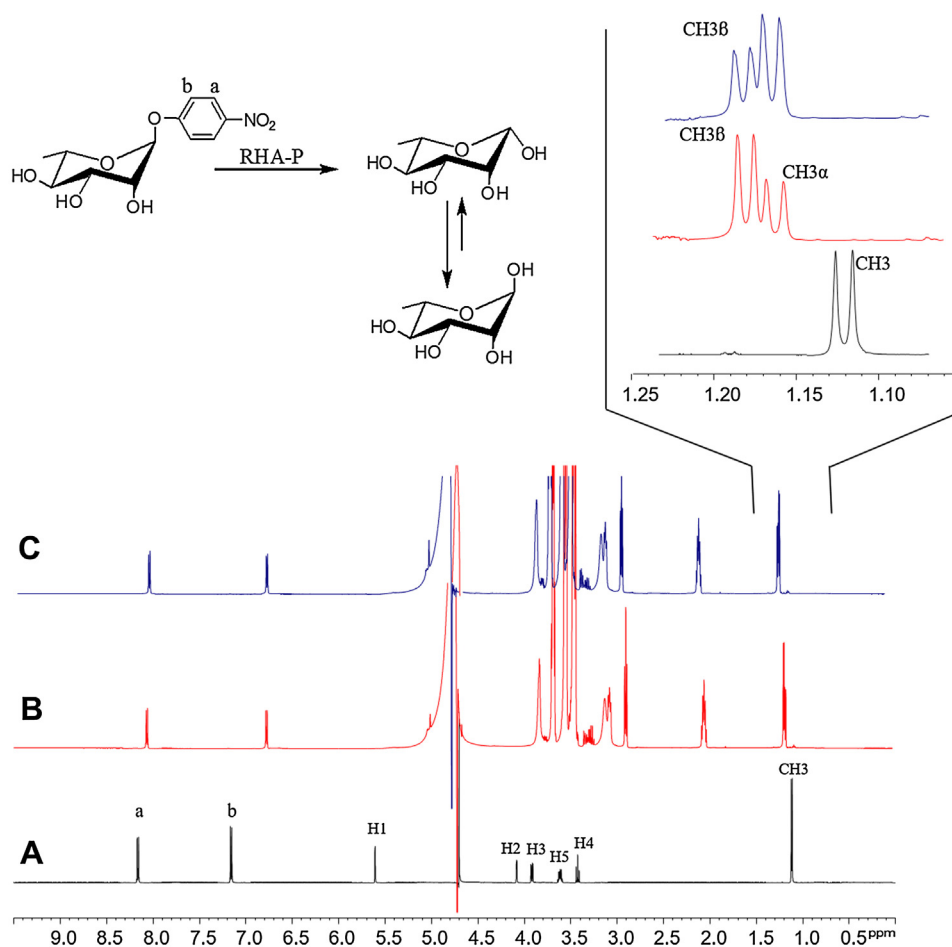


**Fig. 3.**  $^1\text{H}$  NMR analysis of pNPR after rRHA-P catalyzed hydrolysis. A. Spectrum of the ligand alone in solution (3 mM). B. Spectrum following the addition of the enzyme to the NMR tube ( $\sim 60\ \mu\text{g}$ ), which showed the appearance of  $\text{CH}_3$  signals relative to  $\alpha$ - and  $\beta$ -anomers. C. Spectrum obtained after a 30 min reaction; a mixture of  $\alpha$ - and  $\beta$ -anomers with a different relative ratio was observed due to emiacetal equilibrium.

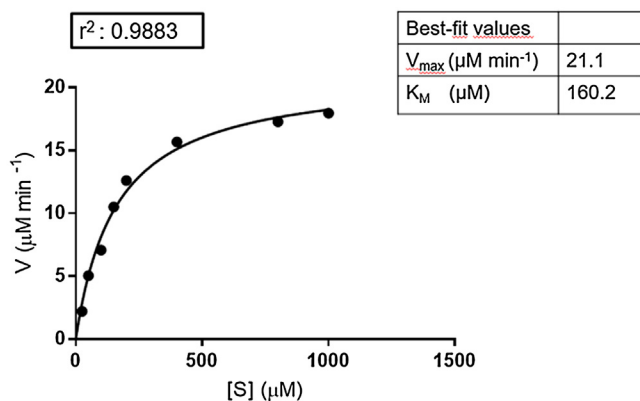


Fig. 4. rRHA-P kinetic behavior. Reaction rate expressed in  $\mu\text{M}/\text{min}$  is plotted as a function of  $p\text{NPR}$  concentration.

rhamnose anomers was observed in solution, as evident from the presence of two different methyl group resonances. TOCSY spectrum allowed the assignment of both  $\alpha$  and  $\beta$  spin systems up to the methyl group resonances located at position 6 of each rhamnose residue. Therefore, the less shielded methyl signal was assigned to  $\beta$ -rhamnose. The analysis of the intensity of the different methyl proton signals showed that the thermodynamically unfavorable  $\beta$ -rhamnose prevailed soon after the addition of rRHA-P (Fig. 3B). Afterwards, as a consequence of the equilibrium established by a reducing monosaccharide in water, the relative ratio of the two peaks changed up to the point in which the  $\alpha$  anomeric product was predominant (Fig. 3C). Hence, the data suggested that rRHA-P acts as an inverting enzyme as it cleaves the  $\alpha$ -glycoside ligand yielding a  $\beta$ -anomer, which in water solution equilibrates according to the anomeric effect.

### 3.3.4. Enzymatic characterization

All enzymatic assays described in this subsection are detailed in Materials and Methods section and were performed using  $p\text{NPR}$  as substrate. Kinetic constants on  $p\text{NPR}$  were determined using a substrate concentration ranging from 0.025 to 1 mM. The reaction rate ( $\mu\text{M}/\text{min}$ ), plotted as a function of the substrate concentration ( $\mu\text{M}$ ), showed a typical Michaelis-Menten trend and is reported in Fig. 4.  $K_M$  constant was of  $160.2 (\pm 17.3) \mu\text{M}$ , a value significantly lower than most other  $\alpha$ -RHAs described in literature [32,57], indicating a higher affinity of rRHA-P for  $p\text{NPR}$ . A  $V_{max}$  of  $21.1 (\pm 8.0) \mu\text{M}/\text{min}$ , a  $k_{cat}$  of  $734.4 (\pm 212.9) \text{sec}^{-1}$  and a  $K_S$  of  $4.6 (\pm 1.7) \text{sec}^{-1} \mu\text{M}^{-1}$  were obtained.

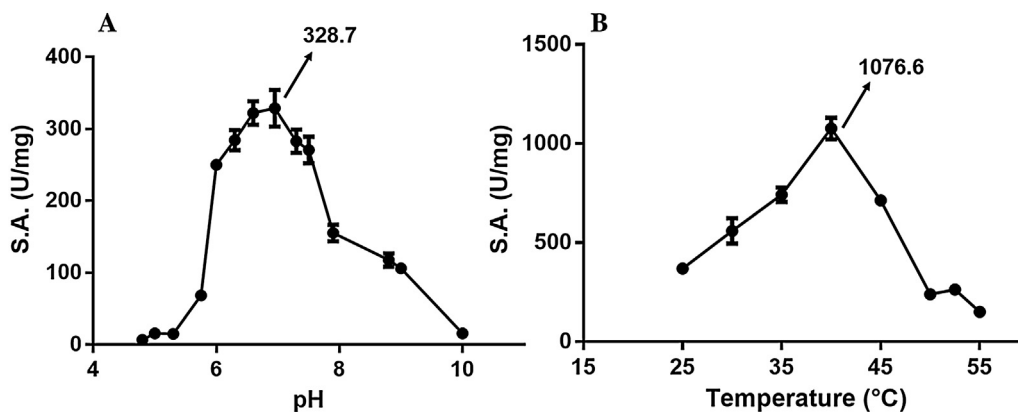


Fig. 5. rRHA-P activity assays. pH (A) and temperature (B) optimum curves. In both graphs specific activity (S.A.) is plotted as a function of pH and temperature, respectively. The maximum value of S.A. obtained is reported in both graphs and indicated by a black arrow.

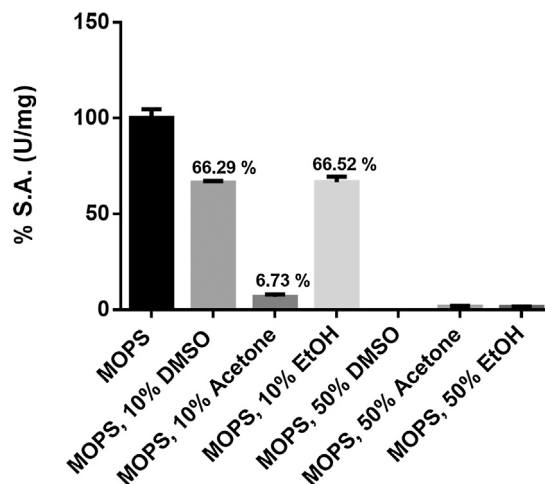


Fig. 6. rRHA-P tolerance to organic solvents. Data are reported as percentage of residual specific activity (S.A.) compared to the control (25 mM MOPS, pH 6.9). MOPS buffer is used at a final concentration of 25 mM and at pH 6.9.

rRHA-P revealed an optimal activity in the range 6.0–7.5 with an optimum at pH 6.9 (Fig. 5A), retaining 47% and 36% of activity at pH 7.9 and 8.8, respectively. In addition, rRHA-P activity was assayed in the temperature range  $25\text{--}55\text{ }^\circ\text{C}$ . Data are presented in Fig. 5B and show an optimal activity temperature at ca.  $40.9\text{ }^\circ\text{C}$ , with a 44% retaining of its initial value up to  $50\text{ }^\circ\text{C}$ . To evaluate the thermal stability of rRHA-P in the same range used to determine the optimal temperature, an incubation of the purified protein for either one or 3 h was performed at different temperatures; afterwards, the residual rhamnosidase activity of the enzyme was calculated (Fig. S5). The enzymatic activity appeared to be stable between 25 and  $40\text{ }^\circ\text{C}$ , independently from the duration of the incubation. At  $40\text{ }^\circ\text{C}$ , corresponding to the temperature optimum, the activity is stable up to 24 h (data not shown).

In order to establish the tolerance of the enzymatic activity of rRHA-P to the presence of organic solvents,  $p\text{NPR}$  assay in 50 mM MOPS pH 6.9 containing 10% or 50% of either DMSO, acetone or ethanol was performed (Fig. 6). While activity dramatically decreased in all concentration of acetone and in 50% of ethanol and DMSO, a 66% of activity was still recovered in the presence of 10% of either DMSO or ethanol.

### 3.3.5. Activity on flavonoids

The ability of rRHA-P to hydrolyze natural flavonoids was evaluated. Enzymatic assays using naringin, rutin and neohesperidin

dihydrochalcone were performed and followed by TLC analysis, as described in Materials and Methods. To this purpose, a 6 mM solution of each compound was incubated with purified rRHA-P in 50 mM Na-phosphate buffer pH 7.0 at 40 °C, and the reaction was monitored by TLC analyses over time. After 3 h of incubation, TLC analysis of the reaction mixtures showed a 40–60% hydrolysis of neohesperidin dihydrochalcone and rutin in the corresponding derhamnosylated neohesperidin dihydrochalcone and quercetin-3- $\beta$ -glucopyranoside (isoquercitrin). Besides, a total conversion of naringin was observed as the corresponding products, rhamnose and prunin, were the only compounds observed on the TLC plate. Reaction on naringin was also carried out in the presence of 10% DMSO. In this case, in our experimental conditions, the complete conversion of naringin in prunin and rhamnose occurred after just 1 h.

#### 4. Discussion

$\alpha$ -RHAs are a group of glycosyl hydrolases (GHs) that have attracted a great deal of attention due to their potential application as biocatalysts in a variety of industrial processes. These enzymes are of particular interest for the biotransformation of several natural compounds used in pharmaceutical and food industry. Enzymatic derhamnosylation catalyzed by  $\alpha$ -RHAs can be used, for example, in functional foods and beverages containing molecules with enhanced health-related properties. Some examples encompass the biotransformation of natural steroids, antibiotics, flavonoids, and terpenyl glycosides responsible for wine aromas [2,40].

Bacterial  $\alpha$ -RHAs are still poorly characterized, but their biochemical properties might be of key importance for biotransformation processes involving reactions conditions that are unfavorable for fungal rhamnosidases. In this work, we have successfully expressed and partially characterized a novel recombinant  $\alpha$ -RHA from *Novosphingobium* sp. PP1Y, named RHA-P. The  $\alpha$ -RHA activity has been isolated from the native source and the corresponding protein sequence was verified by MS analysis. The sequence was used for a BLAST search against all protein databases, and resulted to be homologous to GHs present in the genomes of several Sphingomonads; among these, a 48% sequence identity of RHA-P with the  $\alpha$ -RHA (rhaM) from *Sphingomonas paucimobilis* FP2001, was retrieved [58]. Noteworthy, an analysis of the amino acidic sequence of RHA-P highlighted the presence of a 23 amino acids long signal peptide [59] located at the N-terminus of the protein.

The new  $\alpha$ -RHA identified is encoded by *orf*PP1Y\_RS05470, a 3,441 bp gene located in Megaplasmid Mpl of *N. sp.* PP1Y [44], which was amplified and cloned into pET22b (+) plasmid to allow for the recombinant expression in *E. coli* BL21(DE3) strain. First attempts of expression of the recombinant protein, rRHA-P, resulted in the foremost presence of the protein in the insoluble portion of the induced cultures. A lower induction temperature, shifted from 37 °C to 23 °C, along with the use of a high-salt LB formulation containing both betaine and sorbitol, which presumably act as “chemical chaperones”, efficiently concurred in improving the yield of soluble, active rRHA-P [54–56].

rRHA-P was purified following a three-step purification protocol. The relatively poor yield obtained at the end of the purification was not unexpected at this stage, as we chose after each step to avoid collecting rRHA-P active fractions that showed the presence of too many protein contaminants.

Purified rRHA-P sequence was verified by MS mapping. It is interesting to underline that the protein N-terminus expected from the cloned sequence was never detected, either by MS analysis (both native and recombinant RHA-P) or by N-terminus sequenc-

ing (only recombinant RHA-P). The lack of this peptide, which had been expected by a preliminary analysis of the amino acidic sequence, confirmed the presence of a signal peptide presumably cleaved through a post-translational proteolytic processing. A similar evidence has been described for the  $\alpha$ -RHA isolated from *S. paucimobilis* FP2001 and recombinantly expressed in *E. coli* [58]. Takeshi M. and coworkers reported in this case the presence of a putative signal peptide cleaved between positions A24 and N25 [58]. Similarly, in rRHA-P the cleavage site is located between A23 and E24. The amino acidic sequence of the N-terminus of both  $\alpha$ -RHA from strain FP2001 and strain PP1Y revealed several peculiarities owned by bacterial signal peptides, such as the presence of a charged region (2–5 residues) followed by a hydrophobic stretch of ~12 aa, along with the presence of small and apolar residues located 1 and 3 aa upstream of the cleavage site [60]. The functional role of this cleavage, as well as the possible sorting of these processed proteins in the periplasmic space of the native bacteria, needs to be further investigated.

A preliminary structural characterization showed that rRHA-P is a monomeric protein with an approximate molecular weight of 101,500  $\pm$  5,000 Da. Mechanism of action, kinetic parameters and optimum reaction conditions were determined using a synthetic substrate, pNPR.

As for the reaction mechanism, GHs are generally grouped in two main classes, inverting and retaining. A typical inverting glycosidase requires the presence of a catalytic acid residue and a catalytic basic residue, whereas a typical retaining glycosidase contains a general acid/base residue and a nucleophile. These different hydrolysis mechanisms lead, respectively, to an inversion or to a retention of the anomeric oxygen configuration in the product compared to the substrate [61]. NMR experiments showed that rRHA-P acts as an inverting GH; further investigation will give additional insights in identifying residues in the active site of this enzyme, which are directly involved in catalysis.

rRHA-P catalytic efficiency, defined by a  $K_S$  value of 4.6 s<sup>-1</sup>  $\mu$ M<sup>-1</sup>, underlined that the activity of this enzyme resulted to be comparable or even higher than that of other bacterial  $\alpha$ -RHAs described in literature. When clearly reported, such as in lactic acid bacteria *Lactobacillus plantarum*, and *Pediococcus acidilactici*,  $K_S$  values on pNPR range in fact from 0.01 s<sup>-1</sup>  $\mu$ M<sup>-1</sup> to 0.019 s<sup>-1</sup>  $\mu$ M<sup>-1</sup> [38,39]. In addition,  $K_S$  of rRHA-P resulted to be approximately 3 times higher than the  $K_S$  of 1.74 s<sup>-1</sup>  $\mu$ M<sup>-1</sup> reported for the  $\alpha$ -RHA isolated from *S. paucimobilis* FP2001 [57]. The comparison among the  $K_M$  values present in literature, ranging from 1.18 mM for *S. paucimobilis* FP 2001 to 16.2 mM for the  $\alpha$ -RHA isolated from *P. acidilactici*, showed a higher apparent affinity of rRHA-P for pNPR ( $K_M$  of 160  $\mu$ M), which might be in part responsible for the great differences found in  $K_S$  values.

To investigate the effective potential of using rRHA-P in biotechnological processes involving the biotransformation of flavonoids, optimal reaction conditions in terms of pH, temperature and presence of organic solvents were evaluated. In particular, rRHA-P, in line with other bacterial  $\alpha$ -RHAs [34–38,55], has an optimal activity at pH 6.9, a value that highlights a marked difference with fungal  $\alpha$ -RHAs acting at pH values ranging from 4 to 5 [17,31,32]. rRHA-P shows an optimal activity at 40.9 °C and a significant overall thermal stability, retaining ~66% of the activity up to 45 °C, a temperature range mainly used in most industrial processes. In this respect, also a great majority of other fungal and bacterial enzymes exhibit similar values of temperature stability and optimal activity [17,32,34,37,38,55], whereas only a limited number of  $\alpha$ -RHAs is more thermophilic and has an optimum of temperature at ca. 60 °C [31,36,37,39]. rRHA-P has a moderate tolerance to organic solvents, usually employed for the biotransformation of flavonoids that are poorly soluble in water, retaining the 66% of activity on pNPR in solutions containing 10% of either DMSO or ethanol. Naringin con-

version is even faster in 10% DMSO than in the absence of this solvent, probably owing to the fact that this flavonoid is more soluble in the presence of DMSO. Noteworthy, flavonoids conversion catalyzed by other  $\alpha$ -RHA has been described in the presence of 2–5% DMSO [37–39]; higher concentration of DMSO, as the one used for our bioconversion, might further increase the solubility of many flavonoids of commercial interest. These data altogether suggest a higher tolerance of rRHA-P to the presence of solvents compared to  $\alpha$ -RHAs described in literature for which a residual 20–30% activity in 12% ethanol and a 24% activity in 25% DMSO has been reported [17,39]. It is worth mentioning that rRHA-P residual activity in ethanol-containing buffers might be of additional importance as many biologically relevant rhamnosylated flavonoids are found in wine and possibly citrus derived alcoholic beverages.

As previously underlined, the kinetic data obtained so far for this enzyme undoubtedly encourage its use for the bioconversion of glycosylated natural flavonoids that are more soluble at high temperature (ca. 50 °C) [62], basic pH values, and in the presence of organic solvents. In this context, experiments to verify the hydrolytic properties of rRHA-P on few natural flavonoids containing either  $\alpha$ -1,2 or  $\alpha$ -1,6 glycosidic linkages between  $\alpha$ -L-rhamnose and  $\beta$ -D-glucose were performed. TLC analysis on naringin ( $\alpha$ -1,2), rutin ( $\alpha$ -1,6) and neohesperidin ( $\alpha$ -1,6) showed a total conversion of naringin in the corresponding prunin and rhamnose, while a partial hydrolysis of rutin and neohesperidin was observed, thus confirming the ability of this enzyme to hydrolyze both  $\alpha$ -1,2 and  $\alpha$ -1,6 linkages. Likewise, the majority of other bacterial and fungal  $\alpha$ -RHAs exhibit similar substrate specificity, even though these enzymes often show a slight preference for the hydrolysis of  $\alpha$ -1,6 linkages [31,32,37–39].

In conclusion, the results described in this work boost the interest toward a further biochemical characterization of RHA-P activity using for example a wide array of glycosylated flavonoids, to investigate the effective potential of this novel enzyme for various biomass and food-processing applications aimed at recovering high-value added compounds from complex vegetable matrixes.

## Acknowledgment

This research was supported by FARB 2014 ORSA 132082. The funder had no role in study design, data collection and analysis, decision to publish, or preparation of the manuscript.

## Appendix A. Supplementary data

Supplementary data associated with this article can be found, in the online version, at <http://dx.doi.org/10.1016/j.molcatb.2016.10.002>.

## References

- [1] B. Henrissat, A classification of glycosyl hydrolases based on amino-acid sequence similarities, *Biochem. J.* 280 (1991) 309–316.
- [2] P. Manzanares, S. Vallés, D. Ramón, M. Orejas,  $\alpha$ -L-Rhamnosidases: old and new insights, industrial enzymes, structure, function and application, in: J. Polaina, A.P. MacCabe (Eds.), *Industrial Enzymes*, Springer, 2007, pp. 117–140.
- [3] M. Mutter, G. Beldman, H.A. Schols, A.G.J. Voragen, Rhamnogalacturonan  $\alpha$ -L-rhamnopyranohydrolase. A novel enzyme specific for the terminal nonreducing rhamnosyl unit in rhamnogalacturonan regions of pectin, *Plant Physiol.* 106 (1) (1994) 241–250.
- [4] D.C. Crick, S. Mahapatra, P.J. Brennan, Biosynthesis of the arabinogalactan-peptidoglycan complex of *Mycobacterium Tuberculosis*, *Glycobiology* 11 (9) (2001) 107R–118R.
- [5] E.G. Maxwell, I.J. Colquhoun, H.K. Chau, A.T. Hotchkiss, K.W. Waldron, V.J. Morris, N.J. Belshaw, Rhamnogalacturonan I containing homogalacturonan inhibits colon cancer cell proliferation by decreasing ICAM1 expression, *Carbohydr. Polym* 132 (2015) 546–553.
- [6] E. Nguema-Ona, M. Vicié-Gibouin, M. Gotté, B. Plancot, P. Lerouge, M. Bardor, A. Driouch, Cell wall O-glycoproteins and N-glycoproteins: aspects of biosynthesis and function, *Front. Plant Sci.* 5 (2014) 499.
- [7] W. Hashimoto, O. Miyake, H. Nankai, K. Murata, Molecular identification of an  $\alpha$ -L-rhamnosidase from *Bacillus* sp. strain GL1 as an enzyme involved in complete metabolism of gellan, *Arch. Biochem. Biophys.* 415 (2) (2003) 235–244.
- [8] R. Rahim, U.A. Ochsner, C. Olvera, M. Graninger, P. Messner, J.S. Lam, G. Soberón-Chávez, Cloning and functional characterization of the *Pseudomonas aeruginosa* rhlC gene that encodes rhamnosyltransferase 2, an enzyme responsible for di-rhamnolipid biosynthesis, *Mol. Microbiol.* 40 (3) (2001) 708–718.
- [9] -W. Nereus, I.V. Gunther, A. Nun'ez, W. Fett, D.K.Y. Solaiman, Production of rhamnolipids by *Pseudomonas chlororaphis*, a nonpathogenic bacterium, *Appl. Environ. Microb.* 71 (5) (2005) 2288–2293.
- [10] E. Champion, I. Andre, L.A. Mulard, P. Monsan, M. Remaud-Simeon, S. Morel, Synthesis of L-rhamnose and N-acetyl-D-glucosamine derivatives entering in the composition of bacterial polysaccharides by use of glucanases, *J. Carbohydr. Chem.* 28 (2009) 142–160.
- [11] E.Jr. Middleton, T.C. Theoharides, The effects of plant flavonoids on mammalian cells: implications for inflammation, heart disease, and cancer, *Pharmacol. Rev.* 4 (52) (2000) 673–751.
- [12] F.L. Perez-Vizcaino, J. Duarte, Flavonols and cardiovascular disease, *Mol. Aspects Med.* 31 (6) (2010) 478–494.
- [13] P. Fresco, F. Borges, M.P.M. Marques, C. Diniz, The anticancer properties of dietary polyphenols and its relation with apoptosis, *Curr. Pharm. Des.* 16 (2010) 114–134.
- [14] G. Ceñiz, M.C. Audisio, M. Daz, Antimicrobial properties of prunin, a citric flavanone glucoside, and its prunin 6-O-lauroyl ester, *J. Appl. Microbiol.* 109 (4) (2010) 1450–1457.
- [15] M. Puri, S.S. Marwaha, R.M. Kothari, J.F. Kennedy, Biochemical basis of bitterness in citrus fruit juices and biotech approaches for debittering, *Crit. Rev. Biotechnol.* 16 (1996) 145–155.
- [16] R. González-Barrio, L.M. Trindade, P. Manzanares, L.H. de Graaff, F.A. Tomás-Barberán, J.C. Espín, Production of bioavailable flavonoid glucosides in fruit juices and green tea by use of fungal  $\alpha$ -L-rhamnosidases, *J. Agric. Food Chem.* 52 (20) (2004) 6136–6142.
- [17] M.V. Gallego, F. Piñaga, D. Ramón, S. Vallés, Purification and characterization of an  $\alpha$ -L-rhamnosidase from *Aspergillus terreus* of interest in winemaking, *J. Food Sci.* 66 (2) (2001) 204–209.
- [18] Z. Gunata, S. Bitteur, J.M. Brillouet, C. Bayonove, R. Cordonnier, Sequential enzymatic hydrolysis of potentially aromatic glycosides from grape, *Carbohydr. Res.* 184 (1988) 139–149.
- [19] P. Manzanares, M. Orejas, J.V. Gil, L.H. de Graaff, J. Visser, D. Ramón, Construction of a genetically modified wine yeast strain expressing the *Aspergillus aculeatus* rhaA gene, encoding an  $\alpha$ -L-rhamnosidase of enological interest, *Appl. Environ. Microbiol.* 69 (12) (2003) 7558–7562.
- [20] M.E. Melo Branco de Araújo, Y.E. Moreira Franco, T. Grandio Alberto, M. Alves Sobreiro, M.A. Conrado, D. Gonçalves Priolli, A.C.H. Frankland Sawaya, A.L.T.G. Ruiz, J.E. de Carvalho, P. de Oliveira Carvalho, Enzymatic de-glycosylation of rutin improves its antioxidant and antiproliferative activities, *Food Chem.* 141 (2013) 266–273.
- [21] V.D. Bokkenheuser, C.H. Shackleton, J. Winter, Hydrolysis of dietary flavonoid glycosides by strains of intestinal Bacteroides from humans, *Biochem. J.* 248 (3) (1987) 953–956.
- [22] A.J. Day, J.M. Gee, M.S. DuPont, I.T. Johnson, G. Williamson, Absorption of quercetin-3-glucoside and quercetin-4'-glucoside in the rat small intestine: the role of lactase phlorizin hydrolase and the sodium-dependent glucose transporter, *Biochem. Pharmacol.* 65 (7) (2003) 1199–1206.
- [23] S. Wolfram, M. Block, P. Ader, Quercetin-3-glucoside is transported by the glucose carrier SGLT1 across the brush border membrane of rat small intestine, *J. Nutr.* 132 (4) (2002) 630–635.
- [24] A. Scalbert, G. Williamson, Dietary intake and bioavailability of polyphenols, *J. Nutr.* 130 (2000) 2073S–2085S.
- [25] P.C. Hollman, J.M. van Trijp, M.N. Buysman, M.S. van der Gaag, M.J. Mengelers, J.H. de Vries, M.B. Katan, Relative bioavailability of the antioxidant flavonoid quercetin from various foods in man, *FEBS Lett.* 418 (1997) 152–156.
- [26] K. Németh, G.W. Plumb, J.G. Berrin, N. Juge, R.J. Hassan, H.Y. Naim, G. Williamson, D.M. Swallow, P.A. Kroon, Deglycosylation by small intestinal epithelial cell  $\beta$ -glucosidases is a critical step in the absorption and metabolism of dietary flavonoid glycosides in humans, *Eur. J. Nutr.* 42 (2003) 29–42.
- [27] P.C. Hollman, M.N. Bijsman, Y. van Gameren, E.P. Cossen, J.H. de Vries, M.B. Katan, The sugar moiety is a major determinant of the absorption of dietary flavonoid glycosides in man, *Free Radic. Res.* 31 (6) (1999) 569–573.
- [28] P. Garnier, X.T. Wang, M.A. Robinson, S. van Kasteren, A.C. Perkins, M. Frier, A.J. Fairbanks, B.G. Davis, Lectin-directed enzyme activated prodrug therapy (LEAPT): synthesis and evaluation of rhamnose-capped prodrugs, *J. Drug Target.* 18 (10) (2010) 794–802.
- [29] M.A. Robinson, S.T. Charlton, P. Garnier, X.T. Wang, S.S. Davis, A.C. Perkins, M. Frier, R. Duncan, T.J. Savage, D.A. Wyatt, S.A. Watson, B.G. Davis, LEAPT: lectin-directed enzyme-activated prodrug therapy, *Proc. Natl. Acad. Sci.* 101 (40) (2004) 14527–14532.
- [30] N.M. Young, R.A.Z. Johnston, J.C. Richards, Purification of the  $\alpha$ -L-rhamnosidase of *Penicillium decumbens* and characteristics of two glycopeptide components, *Carbohydr. Res.* 191 (1989) 53–62.

- [31] T. Koseki, Y. Mese, N. Nishibori, K. Masaki, T. Fujii, T. Handa, Y. Yamane, Y. Shiono, T. Murayama, H. Iefuji, Characterization of an alpha-L-rhamnosidase from *Aspergillus kawachii* and its gene, *Appl. Microbiol. Biotechnol.* 80 (6) (2008) 1007–1013.
- [32] P. Manzanares, H.C. van den Broeck, L.H. de Graaff, J. Visser, Purification and characterization of two different alpha-L-rhamnosidases, RhaA and RhaB, from *Aspergillus aculeatus*, *Appl. Environ. Microbiol.* 67 (5) (2001) 2230–2234.
- [33] J.E. Chua, P.A. Manning, R. Morona, The Shigella flexneri bacteriophage Sf6 tailspike protein (TSP)/endo rhamnosidase is related to the bacteriophage P22 TSP and has a motif common to exo- and endoglucanases and C-5 epimerases, *Microbiology* 145 (7) (1999) 1649–1659.
- [34] W. Hashimoto, H. Nankai, N. Sato, S. Kawai, K. Murata, Characterization of alpha-L-rhamnosidase of *Bacillus* sp. GL1 responsible for the complete depolymerization of gellan, *Arch. Biochem. Biophys.* 415 (2) (1999) 56–60.
- [35] A.G. Orrillo, P. Ledesma, O.D. Delgado, G. Spagna, J.D. Breccia, Cold-active alpha-L-rhamnosidase from psychrotolerant bacteria isolated from a sub-Antarctic ecosystem, *Enz. Microbiol. Technol.* 40 (2) (2007) 236–241.
- [36] V.V. Zverev, C. Hertel, K. Bronnenmeier, A. Hroch, J. Kellermann, W.H. Schwarz, The thermostable alpha-L-rhamnosidase RamA of *Clostridium stercorarium*: biochemical characterization and primary structure of a bacterial alpha-L-rhamnosidase hydrolase a new type of inverting glycoside hydrolase, *Mol. Microbiol.* 35 (2000) 173–179.
- [37] M. Avila, M. Jaquet, D. Moine, T. Requena, C. Peláez, F. Arigoni, I. Jankovic, Physiological and biochemical characterization of the two alpha-L-rhamnosidases of *Lactobacillus plantarum* NCC245, *Microbiology* 155 (2009) 2739–2749.
- [38] J. Beekwilder, D. Marcozzi, S. Vecchi, R. de Vos, P. Janssen, C. Francke, J. van Hylckama Vlieg, R.D. Hall, Characterization of rhamnosidases from *Lactobacillus plantarum* and *Lactobacillus acidophilus*, *Appl. Environ. Microbiol.* 75 (2009) 3447–3454.
- [39] H. Michlmayr, W. Brandes, R. Eder, C. Schumann, A.M. del Hierro, K.D. Kulbe, Characterization of two distinct glycosyl hydrolase family 78 alpha-L-rhamnosidases from *Pediococcus acidilactici*, *Appl. Environ. Microbiol.* 77 (18) (2011) 6524–6530.
- [40] M. Puri, Updates on naringinase: structural and biotechnological aspects, *Appl. Microbiol. Biotechnol.* 93 (1) (2012) 49–60.
- [41] Z. Cui, Y. Maruyama, B. Mikami, W. Hashimoto, K. Murata, Crystal structure of glycoside hydrolase family 78 alpha-L-rhamnosidase from *Bacillus* sp. GL1, *J. Mol. Biol.* 374 (2) (2007) 384–398.
- [42] Z. Fujimoto, A. Jackson, M. Michikawa, T. Maehara, M. Momma, B. Henrissat, H.J. Gilbert, S. Kaneko, The structure of a *Streptomyces avermitilis* alpha-L-rhamnosidase reveals a novel carbohydrate-binding module CBM67 within the six-domain arrangement, *J. Biol. Chem.* 288 (17) (2013) 12376–12385.
- [43] E. Notomista, F. Pennacchio, V. Cafaro, G. Smaldone, V. Izzo, L. Troncone, M. Varcamonti, A. Di Donato, The marine isolate *Novosphingobium* sp. PP1Y shows specific adaptation to use the aromatic fraction of fuels as the sole carbon and energy source, *Microb. Ecol.* 61 (3) (2011) 582–594.
- [44] V. D'Argenio, M. Petrillo, P. Cantiello, B. Naso, L. Cozzuto, E. Notomista, G. Paoletta, A. Di Donato, F. Salvatore, De novo sequencing and assembly of the whole genome of *Novosphingobium* sp. strain PP1Y, *J. Bacteriol.* 193 (16) (2011) 4296.
- [45] W. Hashimoto, K. Murata, Alpha-L-rhamnosidase of *Sphingomonas* sp. R1 producing an unusual exopolysaccharide of sphingan, *Biosci. Biotechnol. Biochem.* 62 (6) (1998) 1068–1074.
- [46] V. D'Argenio, E. Notomista, M. Petrillo, P. Cantiello, V. Cafaro, V. Izzo, B. Naso, L. Cozzuto, L. Durante, L. Troncone, G. Paoletta, F. Salvatore, A. Di Donato, Complete sequencing of *Novosphingobium* sp. PP1Y reveals a biotechnologically meaningful metabolic pattern, *BMC Genomics* 15 (2014) 384.
- [47] V. Izzo, P. Tedesco, E. Notomista, E. Pagnotta, A. Di Donato, A. Trinconcone, A. Tramice, Rhamnosidase activity in the marine isolate *Novosphingobium* sp. PP1Y and its use in the bioconversion of flavonoids, *J. Mol. Catal. B: Enzym.* 105 (2014) 95–103.
- [48] B.L. Cantarel, P.M. Coutinho, C. Rancurel, T. Bernard, V. Lombard, B. Henrissat, The carbohydrate-Active EnZymes database (CAZy): an expert resource for glycogenomics, *Nucl. Acids Res.* 37 (2009) D233–D238.
- [49] J. Sambrook, E.F. Fritsch, T. Maniatis, *Molecular Cloning. A Laboratory Manual*, 2nd ed., Cold Spring Harbor Lab. Press, 1982, pp. 545.
- [50] P. Gerhardt, R.G.E. Murray, W.A. Wood, N.R. Krieg, *Methods for General and Molecular Bacteriology*, ASM Press, Washington D.C., 1994.
- [51] D.J. States, R.A. Haberkorn, D.J. Ruben, A two-dimensional nuclear overhauser experiment with pure absorption phase in four quadrants, *J. Magn. Reson.* 48 (1982) 286–292.
- [52] M.M. Bradford, A rapid and sensitive method for the quantitation of microgram quantities of protein utilizing the principle of protein-dye binding, *Anal. Biochem.* 72 (1976) 248–254.
- [53] F. He, Laemmli-SDS-PAGE, Bio-protocol. 2011. Bio101:e80. <http://www.bio-protocol.org/e80>.
- [54] J.R. Blackwell, R. Horgan, A novel strategy for production of a highly expressed recombinant protein in an active form, *FEBS Lett.* 295 (1–3) (1991) 10–12.
- [55] N. Oganessian, I. Ankudinova, S.H. Kim, R. Kimb, Effect of osmotic stress and heat shock in recombinant protein overexpression and crystallization, *Prot. Expr. Purif.* 52 (2) (2007) 280–285.
- [56] M. Kilstrup, S. Jacobsen, K. Hammer, F.K. Vogensen, Induction of heat shock proteins DnaK, GroEL, and GroES by salt stress in *Lactococcus lactis*, *Appl. Environ. Microbiol.* 63 (5) (1997) 1826–1837.
- [57] F. Miake, T. Satho, H. Takesue, F. Yanagida, N. Kashige, K. Watanabe, Purification and characterization of intracellular alpha-L-rhamnosidase from *Pseudomonas paucimobilis* FP2001, *Arch. Microbiol.* 173 (1) (2000) 65–70.
- [58] M. Takeshi, K. Nobuhiro, S. Tomomitsu, Y. Tadatashi, A. Yoichi, M. Fumio, Cloning, Sequence analysis, and expression of the gene encoding *Sphingomonas paucimobilis* FP2001 alpha-L-rhamnosidase, *Curr. Microbiol.* 51 (2005) 105–109.
- [59] T.N. Petersen, S. Brunak, G. von Heijne, H. Nielsen, SignalP 4.0: discriminating signal peptides from transmembrane regions, *Nat. Methods* 8 (2011) 785–786.
- [60] L.M. Gierasch, Signal sequences, *Biochemistry* 28 (1989) 923–930.
- [61] B. Cobucci-Ponzano, M. Moracci, Glycosidases and glycosynthases, in: *Biocatalysis in Organic Synthesis of Faber K, Fessner W-D Turner NJ*, 2016, pp. 483–506.
- [62] T. Sathishkumar, R. Baskar R, S. Shanmugam, P. Rajasekaran, S. Sadasivam, V. Manikandan, Optimization of flavonoids extraction from the leaves of *Tabernaemontana heyneana* Wall using L<sub>16</sub> Orthogonal design, *Naturesci* 6 (3) (2008), 1545–0740.

## REVIEW ARTICLE

# Novel Drug Targets for the Treatment of Cardiac Diseases

Marine Pingeon<sup>1</sup>, Bruno Charlier<sup>1</sup>, Federica De Lise<sup>2</sup>, Francesca Mensitieri<sup>2</sup>,  
Fabrizio Dal Piaz<sup>1</sup> and Viviana Izzo<sup>1,\*</sup>

<sup>1</sup>Department of Medicine, Surgery and Dentistry “Scuola Medica Salernitana”, University of Salerno, Baronissi (Salerno), Italy; <sup>2</sup>Department of Biology, University of Naples Federico II, Naples, Italy

**Abstract: Background:** Cardiovascular disease is the leading cause of morbidity and mortality worldwide in developed countries, and its social and economic burden is expected to increase dramatically over the next decades. Despite significant improvement in the pharmacological treatment, and the huge advances in prevention, the quest for new molecular targets and for novel, more efficient and personalized therapies is still a priority for this group of pathologies.

**Objective:** The paramount complexity of the metabolic networks responsible for the onset and progression of cardiovascular disease is highlighted by the wide and diverse array of new molecular targets recently described in literature. In this brief review, we focused our interest on a subset of promising molecular targets for the development of new pharmacological treatments specific for cardiac diseases such as coronary artery disease, heart failure and myocardial infarction.

**Conclusions:** The global quest for new molecular targets for the treatment of cardiac diseases is leading to an impressive amount of records in the more recent literature. Although several promising molecular pathways have been identified so far, great caution should be used in considering all these targets effective in promoting the production of new drugs. The identification of suitable therapeutic targets is in fact an ongoing challenge that often lacks enough pre-clinical and clinical studies, which hinders the effective utilization of several new drugs due to a lack of efficacy or induction of safety liabilities.

---

**ARTICLE HISTORY**

Received: January 24, 2017  
Revised: March 10, 2017  
Accepted: April 15, 2017

DOI:  
10.2174/1875692115666170503105402

**Keywords:** Cardiovascular disease, coronary artery disease, heart failure, myocardial infarction, drug discovery, drug targets.

## INTRODUCTION

The cardiovascular system (CVS) is responsible to transport oxygen and nutrients, remove metabolic waste, and carry endocrine factors and immune cells throughout the body.

Cardiovascular pressure/volume complex homeostasis mainly depends upon the tight regulation of a neurohormonal system, which involves the interplay between the renin-angiotensin-aldosterone system (RAAS) and the sympathetic nervous system (SNS), together with the cardiac natriuretic peptides and the arginine vasopressin-mediated action [1].

Cardiovascular disease (CVD) is currently the leading cause of mortality and morbidity worldwide and is caused by a wide array of dysfunctions affecting the heart and/or blood vessels, which include aging, hypertension, diabetes, atherosclerosis and coronary artery disease (CAD) [2]. In September 2016, the World Health Organization (WHO) has estimated that more than 17 million people die annually from CVD and has launched the “Global Hearts” initiative, aimed at facing the global threat of these diseases [3].

Early onset of CVD involves complex cellular and molecular signaling cascades that regulate, among others, cardiac myocytes growth, electrical conduction, contractility, redox balance, metabolic homeostasis, extracellular matrix remodeling (EMR), necrosis and apoptosis [4-6].

CAD is the result of a progressive narrowing and damage of blood vessels that supply blood to the heart

---

\*Address correspondence to this author at the Department of Medicine, Surgery and Dentistry “Scuola Medica Salernitana”, University of Salerno, Baronissi (Salerno), Italy;  
Tel/Fax: +39(0)89965225/5116; E-mail: [vizzo@unisa.it](mailto:vizzo@unisa.it)

muscle and it is usually caused by atherosclerosis, a process of hardening of arteries due to the buildup of an atheromatous plaque inside the artery walls. CAD include less severe manifestations, such as stable angina (SA) or unstable angina (UA) and more severe forms like acute coronary syndrome (ACS) and myocardial infarction (MI).

Heart Failure (HF) is the final endpoint of many heart diseases [7], and is characterized by several hemodynamic abnormalities, ultimately leading to an inadequate systemic perfusion that does not respond to the body metabolic demand in conditions of stress or increased activity [8]. In the early onset of HF, compensatory neurohormonal mechanisms are activated to maintain cardiovascular homeostasis; however, an increase in cardiac mass along with alterations in the extracellular matrix (ECM) later drive the alteration in heart function and structure, usually referred to as "cardiac remodeling". The late stage of HF is clinically characterized by cardiac enlargement and by a progressive worsening of the contractile function [7, 8].

Age, male sex, left ventricular hypertrophy (LVH), MI, CAD, valvular heart disease, obesity, and diabetes are among the main risk factors described so far for HF development [7, 9]. Among others, hypertension, a multifactorial disease characterized by high blood pressure and involving both genetic and environmental factors, is a major contributor to the population burden of HF because of its great prevalence [7, 10]. Hypertension is characterized by high arterial pressure resulting from increased peripheral vascular resistance, which can be consequent to both enhanced contractility of vascular smooth muscle cells (VSMCs) and arterial wall remodeling. Systemic hypertension induces LVH, fibrosis and diastolic dysfunction, increases the risk of CAD, which leads to congestive HF.

Elevated cholesterol levels are recognized as an important independent risk factor for the onset of CAD; therefore, dyslipidemia is also directly linked to the development of HF. It is worth noting that elevated levels of total cholesterol are not a strong predictor of new-onset HF, whereas an increased ratio of total cholesterol to HDL cholesterol seems to be effectively associated with high HF risk [7].

Despite a substantial progress in the treatment of HF with the all-time classics angiotensin-converting-enzyme (ACE) inhibitors, angiotensin receptor blockers (ARB), diuretics, beta blockers and aldosterone antagonists, no further improvement has been observed in the late 10 years for patients prognosis [7]. HF remains a deadly clinical syndrome and a major public health concern for western countries, being the most frequent reason for hospitalization in elderly patients; both the prevalence of this disorder and the cost of healthcare are expected to dramatically increase over next decades [11-15].

HF patients are frequently re-hospitalized and generally experience a very poor quality of life. Thus, there is undoubtedly an urgent need of identifying new targets for the development of innovative pharmacological treatments for HF. Insights into the molecular and cellular determinants responsible for the development of HF are shedding light on several anomalies in cell function and signaling that could be used as potential therapeutic targets in the near future [8, 13].

MI is an irreversible damage of myocardial tissue, which occurs as a consequence of myocardial cell death due to protracted ischemia and hypoxia. This most commonly happens when blood flow is blocked by the occlusion of a coronary artery, possibly occurring as the consequence of the rupture of an atherosclerotic plaque that leads to the formation of a blood clot. Major modifiable risk factors of MI are hypertension, high blood cholesterol level, diabetes (mellitus), smoking/tobacco use, obesity, poor nutrition/diet, physical inactivity, stress, and the exposure to dangerous conditions at work [16]. The major non-modifiable risk factors for MI include age, family history, and race. Likely, combinations of these risk factors, which appear to be different in men and women, are important in the aetiology of the disease [16].

After MI, necrotic cardiac myocytes trigger the onset of an inflammatory response, which might be beneficial in terms of wound healing, but is responsible to further damage the left ventricle. A complex tissue remodeling follows MI event, which involves both cellular and ECM components [17]. The initial loss of cardiomyocytes in MI, due to the primary ischemic event, directly affects the survival and long-term prognosis of the patient, which may experience arrhythmogenesis, adverse remodeling and contractile dysfunction. The fast recovery of coronary blood flow using percutaneous coronary intervention (PCI) as primary state care remains of utmost importance to preserve myocardial viability in patients with MI. However, PCI can also trigger molecular events that contribute to the process known as "ischemic/ reperfusion" (I/R) injury [17, 18]. In this process, the restoration of blood flow boosts the over-production of reactive oxygen species (ROS) [19], an intracellular  $\text{Ca}^{2+}$  overload, and the up-regulation of pro-inflammatory molecules triggering cell death in vital spared myocytes, thus leading to additional cardiac damage and complications [20].

In conclusion, clinical evidence suggests for several CVDs the growing need of identifying novel targets to improve the pharmacotherapy efficiency. It should be underlined that, for the complexity of the metabolic pathways involved, multiple molecular targets, and not single molecules, should be considered for future

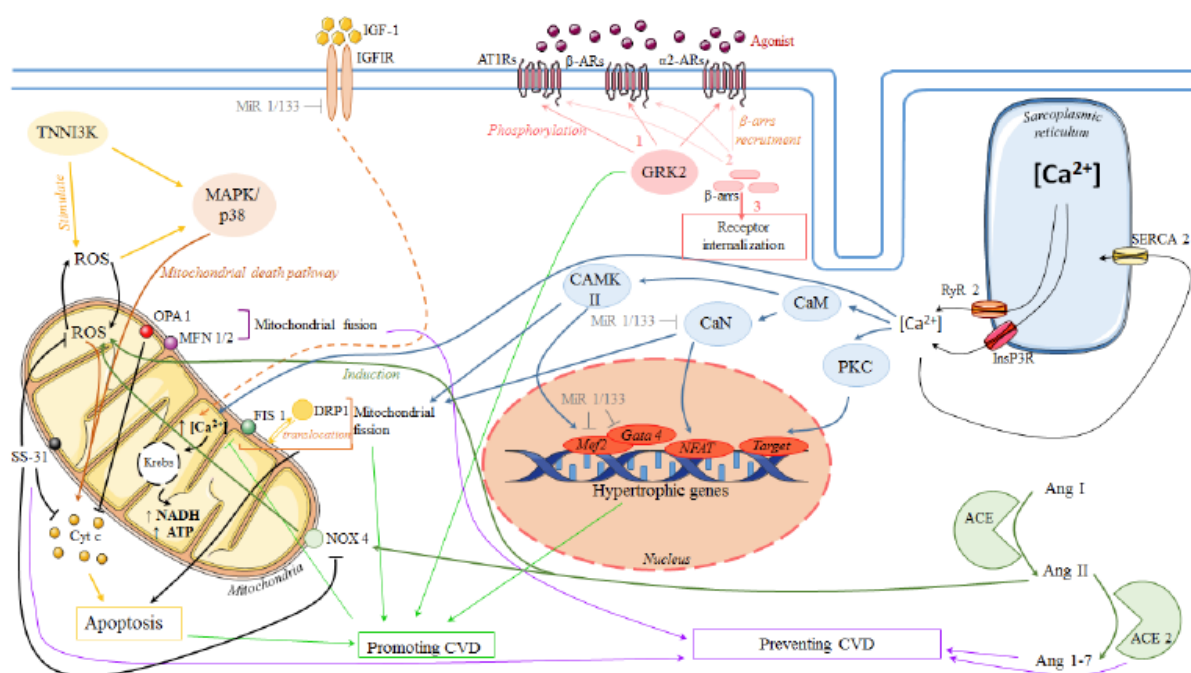


**Fig. (1).** A schematic and simplified view of the molecular targets described in this paper highlighting their interconnections in cardiac myocyte and their role in either promoting or preventing cardiac diseases.

therapeutic management. This approach, along with the characterization of the genetic background of the patient, will concur in developing in the near future a far more personalized approach in the treatment of these diseases. In this brief review, we focused our interest on a subset of promising molecular targets (Fig. 1), recently described in the literature, for the development of new pharmacological treatments specific for cardiac diseases such as atherosclerosis, CAD, HF and MI.

### NOVEL MOLECULAR TARGETS FOR THE TREATMENT OF CARDIAC DISEASES.

#### ROS Metabolism, Oxidative Stress and I/R Injury

ROS include several oxygen and nitrogen-derived species such as superoxide ( $O_2^{\cdot-}$ ), hydroxyl radical ( $\cdot OH$ ), hydrogen peroxide ( $H_2O_2$ ), and peroxynitrite ( $ONOO^-$ ) [19]. An imbalance between ROS production and the cell/systemic antioxidant defense capacity is responsible for the onset of the metabolic condition generally called “oxidative stress” [19, 21]. ROS are a double-edged sword as they are undoubtedly essential in cell signaling, proliferation, and differentiation pathways, but if their levels increase in an unregulated manner they are responsible for cell damage, necrosis, and apoptosis *via* oxidation of lipids, proteins, and DNA [22, 23]. Physiology and pathophysiology of CVD are clearly related to both oxidative stress and ROS, even though not all molecular details have been fully elucidated yet. The multiple effects of ROS are particularly evident, for example, in the different stages

underlying I/R injury [24, 25]. In this case, during ischemia, ROS-producing enzymes are activated and up-regulated, and hypoxia is responsible to decrease ATP production and uncouple the electron transport chain. During the reperfusion phase, the re-establishment of the blood supply abruptly restores molecular oxygen, thus resulting in a sharp increase of ROS generation. ROS trigger a cascade of molecular events involving the expression of proinflammatory stimuli, the expression of adhesion molecules by endothelial cells and leukocytes, which contribute to the infiltration and activation of neutrophils, T cells and monocytes. In the third stage, after early reperfusion, tissue repair takes place. At this stage, low levels of ROS are generated, which act as signaling molecules to activate the transcription of growth factors and promote cell proliferation, differentiation and migration. The result of this repair stage is tissue and vascular remodeling, which helps restoring organ function, but at the same time causes tissue fibrosis, which eventually contributes to HF onset.

Reactive Nitrogen Species (RNS) derived from nitric oxide (NO), also play a central role in the cellular and systemic response to I/R. Indeed, interactions between ROS and RNS are responsible to influence the extent of injury *via* the production of reactive nitrogen oxide species (RNOS), such as  $ONOO^-$ . RNOS are responsible for several detrimental effects at this stage including damage/modification of macromolecules, induction of death of endothelial and/or parenchymal cells, stimulation of production/release of pro-inflam-

matory mediators and of adhesion molecules supporting leukocyte/lymphocyte-endothelial cell adhesive interactions, along with a diminished global availability of protective NO [25].

It is evident that the interplay between ROS (and RNS) homeostasis and CVD is quite complex, and this is probably one of the main reasons explaining the conflicting results often described in literature when general antioxidant treatments are used to mitigate CVD [19, 24]. Nonetheless, ROS redox therapy still shows promising signs of being a possible treatment option, as long as new molecular details of this complex relationship continue to be unraveled.

Peroxisome proliferator activated receptors (PPARs) are involved in several biological processes such as energy homeostasis, cell proliferation and differentiation, fatty acid catabolism, and adipogenesis [26]. Among the three PPAR isotypes identified, PPAR $\delta$  is the predominant subtype in cardiac cells and is involved in the regulation of cardiac lipid metabolism. There is a great interest for this nuclear receptor due to its important role in apoptosis and cell proliferation, and for its function as a key regulator of fatty acid metabolism [26]. In the framework of the inflammatory response following cardiac I/R it is worth to note that PPAR $\delta$  activation by one of its synthetic ligand, GW610742, reduces inflammatory cytokine expression, ending up in a reduction of plasma levels of interleukin-6 (IL-6) and interleukin-8 (IL-8) [26]. Recently, the therapeutic effects of GW610742 treatment on cardiac healing in post-MI rats was investigated [27]. Interestingly, GW610742 treatment promoted the onset of cardiac fibrosis and angiogenesis in the early infarct site after MI. The prolonged pharmacological PPAR $\delta$  activation did not lead to beneficial effects on cardiac function in that specific study, despite the histological advance of the healing process in the early phase after MI [27].

Recently, cardiac troponin I-interacting protein kinase (TNNI3K), a cardiomyocyte-specific kinase over-expressed in patients with HF, was shown to promote I/R injuries through the onset of a marked oxidative stress, thereby promoting the death of cardiomyocytes [28, 29]. To shed light on the significance of this increased expression, a pre-clinical study based on rodent models was conducted [29]. In TNNI3K overexpressing mice, ischemic injury was worsened and cardiomyocyte death was promoted; this was driven by an increase in O<sub>2</sub><sup>-</sup> production and a stimulation of the mitogen-activated protein kinase (MAPK) p38, an enzyme that responds to stress signals in cells (Fig. 1). The combination of both activities stimulated mitochondrial death pathway in cardiac cells, which worsened I/R injury. Conversely, in loss-of-function mice, O<sub>2</sub><sup>-</sup> production and p38 activation were markedly reduced and heart lesion, dysfunction and fibrosis were

limited [29]. Active site-binding small molecules that selectively inhibited TNNI3K, when delivered at reperfusion, decreased infarct size and significantly reduced ROS [29]. Results on TNNI3K are encouraging especially because this kinase appears to be cardiospecific, thus the use of inhibitors should produce limited negative effects on systemic kinase inhibition. TNNI3K inhibition might represent a novel pharmacological option after coronary angioplasty in acute state of MI, and in chronic coronary syndromes, characterized by the frequent occurrence of multiple episodes of I/R injury. However, further studies in pre-clinical animal models are still required to better detail the signaling pathways effectively involved [30].

### **Mitochondrial Metabolism**

Mitochondria play a very important role in the regulation of cardiovascular cell function and, consequently, in the onset of CVD [24, 25]. The high energetic demand of the cardiac tissue mainly relies on the metabolism of mitochondria, which show a critical role in regulating cardiomyocyte apoptosis as well. Consequently, the high consumption of oxygen in cardiomyocytes can potentially prompt the cells to oxidative stress. Mitochondria are an important source of ROS, which has profound implications for the cardiovascular system. Mitochondrial metabolic impairment can be associated with abnormal mitochondrial dynamics, increased oxidative stress and abnormal Ca<sup>2+</sup> handling, and seems to play a critical role in the myocardial remodeling process responsible for HF onset [31]. Some of the recently published strategies for the treatment of CVD encompass the exploitation of different mitochondrial targets.

During the last decades, several evidences have shown that mitochondria are quite “dynamic” organelles as their morphology, subcellular distribution and activity can be modified according to the cell metabolic status [32]. Mitochondria continually divide (fission) and fuse, even in resting cells, and several reports have demonstrated a direct correlation between the extent of mitochondrial fusion and the capacity for oxidative phosphorylation [33]. Tissues with high energy requirements (*e.g.* heart and skeletal muscle) show a predominantly fused mitochondrial morphology with tightly packed cristae [33]. A fine-tuned interplay between mitochondrial fission and fusion guarantees a proper mitochondrial function, and a close relationship between a remodeling of mitochondrial architecture and the changes in metabolism does exist [32].

Dynamamin-related GTPases mitofusins (MFN1, MFN2) and optic atrophy protein 1 (OPA1), respectively expressed in the outer and inner mitochondrial membrane, are the main regulators of mitochondrial fusion [33, 34], whereas mitochondrial fission 1 protein

(Fis1) and Dynamin-related protein 1 (DRP1) are mostly responsible for mitochondrial fission [33].

Data in literature support the idea that changes in mitochondrial morphology may be relevant to various aspects of CVD, including I/R injury, HF, and dilated cardiomyopathy, where disorganized small mitochondria have been retrieved [35].

Mitochondria observed in failing hearts of rats are small and fragmented, which is consistent with a decreased fusion rate. HF in both human and rat cardiomyocytes is characterized by a marked decrease in OPA1 levels, which leads to cell apoptosis [35, 36]. In some HF models, levels of OPA1 are reduced but there is no change in the amount of MFN1, MFN2, DRP1, or Fis1. Expression of OPA1 mRNA does not seem to be directly influenced, thus indicating that the decrease of OPA-1 proteins might be likely due to post-transcriptional modification or degradation [35, 36]. Deficiency of this protein, which normally prevents release of cytochrome c from the mitochondria, is related to mitochondrial respiratory dysfunction [36]. Ong and coworkers [37] observed that transfection of HL-1 cells with MFN1 or MFN2 supported mitochondrial elongation and reduced cell death following simulated ischaemia; transfection with the mitochondrial fission protein Fis1 promoted instead mitochondrial fragmentation and increased cell death. These data suggest that prevention of ischaemia-induced mitochondrial fragmentation might be cardioprotective [37]. In conclusion, therapeutic approaches aimed at either inhibiting mitochondrial fission or stimulating mitochondrial fusion might protect the heart from failure and ischemia.

As previously underlined, mitochondria are a site of massive production of free radicals, and are consequently one of the first molecular targets for oxidative damage [38]. During cardiac remodeling and HF, both cytosolic and mitochondrial ROS are unbalanced, thus leading to oxidative damage, mitochondrial dysfunction and ultimately cell death [38]. Since mitochondrial ROS are involved in cardiac hypertrophy and remodeling, several groups have developed specific strategies for the targeted delivery of antioxidants to mitochondria, as an innovative therapeutic approach to prevent cardiac failure. As an example, Dai and coworkers demonstrated that mitochondrial-targeted catalase partially protects the heart from failure [39]. They used the mitochondrial-targeted antioxidant peptide Szeto-Schiller (SS-31) to reduce mitochondrial oxidative stress in hypertensive cardiomyopathy [40]. SS-31 peptide belongs to a family of aromatic cationic peptides that selectively target the mitochondrial inner membrane and are endowed with the ability to scavenge  $H_2O_2$ , ONOO<sup>-</sup> and <sup>•</sup>OH, and to inhibit lipid peroxidation. These peptides reduce mitochondrial ROS, thus

inhibiting cytochrome c release and preventing oxidant-induced cell death. Preclinical studies strongly support the use of these peptides in case of I/R injury and neurodegenerative disorders [41]. Among others, peptide SS-31 reduced Ang II-induced NOX4 up-regulation and prevented apoptosis. Experimental results highlighted that SS-31 is a multifunctional mitochondrioprotective compound that promotes bioenergetics, reducing ROS production, scavenging excess ROS, inhibiting cardiolipin peroxidation, and preserving mitochondrial structure, all properties that are particularly effective in minimizing I/R injury. However, further pre-clinical and clinical studies are still required in order to evaluate the efficacy and toxicity of mitochondrial-targeted antioxidants.

In the last two decades a new role of  $Ca^{2+}$  in programming reactive hypertrophic signaling has emerged [42].  $Ca^{2+}$  is stored mainly in the sarcoplasmic reticulum (SR), which regulates its release into the cytoplasm. The main regulative  $Ca^{2+}$  channels involved in this function are the inositol 1,4,5-triphosphate receptor (InsP3R) and the ryanodine receptor (RyR). Following a release, low cytoplasmic concentration of  $Ca^{2+}$  is preserved because  $Ca^{2+}$  ions are rapidly pumped back through the action of the sarcoendoplasmic reticulum  $Ca^{2+}$  ATPase (SERCA) [42]. Mitochondrial  $Ca^{2+}$  is also important for cell bioenergetics; an increase in mitochondrial  $Ca^{2+}$  concentration is responsible for stimulating Krebs Cycle activity and increasing NADH levels, thus leading to a global increase in ATP synthesis [43].

Cytoplasmic  $Ca^{2+}$  increase activates the  $Ca^{2+}$ -calmoduline dependent protein II (CAMKII), calcineurin (CaN) and protein kinase C (PKC), which in turn induce a characteristic genetic program involved in the development of cardiac hypertrophy. Moreover, the activation of CAMKII and CaN promotes mitochondrial fission and, consequently, cardiomyocyte apoptosis.

Several reports focused their attention on the variation of mitochondrial  $Ca^{2+}$  metabolism in HF [44]. Interestingly, cardiomyocytes from failing hearts show a reduced mitochondrial  $Ca^{2+}$  sensitivity that might be directly responsible for the reduction in mitochondrial metabolism. Therefore, the stimulation of mitochondrial  $Ca^{2+}$  has been investigated as a potential therapeutic strategy to prevent HF [44]. In this context, insulin-like growth factor-1 (IGF-1) was reported to prompt mitochondrial  $Ca^{2+}$  uptake and mitochondrial respiration and to prevent a fall in ATP synthesis, thus reducing cell death [45].

Future studies aimed at elucidating the interplay between mitochondrial morphology, metabolism, and cardiac function will undoubtedly provide new interesting insight for the prevention and treatment of CVD.

## Cholesterol Metabolism

CVD, like atherosclerosis, is closely related to alterations in cholesterol metabolism. Innovative pharmacological approaches aiming at counteracting cholesterol imbalance show a promising therapeutic potential. Some therapeutic agents are already used to attenuate atherogenesis such as niacin, fibrates and statins; these latter often fail to achieve treatment goals, and residual CVD risk remains high.

HDL cholesterol has numerous anti-atherosclerotic properties [46]; a key function of HDL is in fact to promote reverse cholesterol transport from the periphery to the liver, thus removing excess cholesterol from membranes of peripheral cells, macrophages and foam [47, 48]. Cholesterol efflux by HDL is also important for lipoprotein signaling in endothelial cells, which leads to the activation of endothelial nitric oxide synthase (eNOS), thus supporting endothelial repair and inducing angiogenesis [49, 50]. Structural and functional changes of HDL, which may affect their anti-atherogenic properties, have been reported in the chronic inflammatory process of atherosclerosis and in pathological states such as oxidative stress, inflammation and diabetes [51, 52].

Therapeutic interventions aimed at preventing atherosclerosis and CVD should not only focus on raising HDL levels, but should also address the improvement of their structural and functional properties [52]. Apolipoproteins Apo A-I and A-II are major protein components of human HDL. The cycling of Apo A-I between lipid-poor and lipid-rich forms of HDL plays a key role in the transport of cholesterol by these particles. Beneficial effects of raising Apo A-I levels on the anti-atherosclerotic properties of HDL are validated by experiments of transgenic overexpression or intravenous infusion of Apo A-I in mice models, which resulted in a marked reduction of atherosclerosis [53]. Promising research has also been performed on the therapeutic effect of mimetic peptides structurally related to Apo A-I, but further studies need to be performed in this direction [54].

Reducing circulating levels of low-density lipoproteins (LDL) is clearly another important aspect in the development of new therapies to counteract atherosclerosis. In this framework an interesting target is the serine protease proprotein convertase subtilisin/kexin type 9 (PCSK9), which binds and vehiculate to the lysosome for degradation the LDL receptor (LDLR) [55]. The decreased number of LDLR available on the cell surface leads to an increase in circulating LDL particles. Among the specific inhibitors recently discussed in literature, antibodies directed against PCSK9 are probably the most promising ones, with multiple phase III and cardiovascular endpoint trials already underway [55]. These fully human monoclonal antibodies have

shown to be effective in subjects with statin intolerance, as adjuvant to statin therapy, as monotherapy and in patients with familial hypercholesterolemia [55].

## Epicardial Adipose Tissue

The perivascular adipose tissue (PVAT) is the adipose tissue that virtually surrounds all large arteries in the body and is an active endocrine and paracrine organ influencing vascular homeostasis through the production of local cytokines and chemokines, collectively known as adipokines [56, 57]. An impairment in the secretion of these molecules leads to multiple pathological conditions such as atherosclerosis and CAD [58, 59].

Recently, the attention has been specifically focused on the adipose tissue present on the surface of the heart surrounding large coronary arteries and on the surface of the ventricles, known as epicardial perivascular adipose tissue (EAT), whose dysfunction has been involved in the onset of the inflammatory burden affecting coronary plaque development and phenotype [58, 59]. EAT, in physiologic conditions, has several protective functions for the heart [56, 57]; however, it is known that EAT might produce several pro-inflammatory and pro-atherogenic cytokines, such as Tumor Necrosis Factor  $\alpha$  (TNF- $\alpha$ ), Monocyte chemoattractant protein-1 (MCP-1), IL-6, Interleukin 1 $\beta$  (IL-1 $\beta$ ), plasminogen activator inhibitor-1 (PAI-1), resistin, leptin, visfatin and chemerin [57]. Noteworthy, in CAD patients local levels of these inflammatory mediators do not correlate with plasma concentrations of circulating cytokines and are independent of several clinical variables, such as obesity, and diabetes [58]. Not all adipokines are pro-inflammatory and pro-atherogenic; adiponectin, as an example, has been associated with endothelial improvement and vascular protection [56]. More specifically, adiponectin stimulates NO production in vascular endothelial cells and seems to ameliorate endothelial function through eNOS-dependent pathways [56]. Thus, there is a substantial body of evidence showing that several adipokines might effectively represent novel therapeutic targets for the treatment of CAD. It is still quite unclear, however, whether future therapies should aim at either increasing anti-atherogenic adipokine or inhibiting pro-atherogenic adipokine levels or combining both strategies [56].

## Endoplasmic Reticulum Metabolism

The endoplasmic reticulum (ER) plays a crucial role in the folding of secretory and membrane proteins, calcium homeostasis, and lipid biosynthesis [60]. ER function can be hindered in response to a wide variety of stressors, which leads to the accumulation of unfolded and misfolded proteins, thus activating transcriptional and translational pathways known as the unfolded protein response (UPR) [61].

Adaptive and pro-apoptotic pathways of UPR have been related to the pathophysiology of human diseases, including CVD, neurodegenerative diseases, diabetes mellitus, obesity, and liver diseases. Advanced atherosclerotic plaques can cause ER stress and activate UPR pathways [62, 63], thus inducing oxidized lipids production, inflammation cascade and metabolic stress [64]. A growing number of evidences indicates that the ER stress-induced macrophage apoptosis is a key cellular event in the conversion of benign to vulnerable atherosclerotic plaques. Moreover, a strong association between ER stress markers such as CHOP (CCAAT/enhancer binding protein (C/EBP) homologous Protein) and Glucose-regulated protein 78 (GRP78) and ruptured atherosclerotic plaques in human coronary artery lesions was retrieved [65], suggesting that ER stress is likely involved in the development of plaque rupture in humans. Pharmacological agents that directly activate or deactivate UPR components will be potentially useful in treating CVD. Potential components of the UPR, such as Activation Transcription Factor 6 (ATF6), inositol-requiring enzyme 1 (IRE1), spliced X-Box binding Protein 1 (XBP1), PERK, eukaryotic initiation factor 2 (eIF2), and the proteasome, could be initial targets for therapeutic design. In several studies, activation of ATF6 had cardioprotective effects against I/R injury [66, 67].

CHOP is a pro-apoptotic transcription factor; deletion of the gene encoding for this protein protects against cell death induced by a pharmacological ER stressor [68]. CHOP inhibitors might attenuate cardiac hypertrophy and failure and prevent atherosclerosis. GRP78 is a Heat shock protein 70 (HSP70)-like chaperone, which recognizes and binds exposed hydrophobic residues in misfolded or denatured proteins; overexpression of GRP78 attenuates ER stress and cardiac damage by I/R or proteasome inhibition [69]. In this framework, it would be interesting to determine whether chemical chaperones, which have been successfully used in other animal models of UPR-associated diseases, might have a beneficial effect on advanced atherosclerotic lesion progression [70].

### Other Targets

**GRK2.** G-protein-coupled receptors (GPCRs) are the largest superfamily of cell surface receptors; they are crucial molecular sensors for many physiological processes and represent the clinical target of a significant percentage of all drugs currently used [71]. Agonist binding promotes interaction of the GPCR with heterotrimeric G proteins, which initiates the classical intracellular signaling cascade. Drugs targeting GPCRs either directly block the ligand-receptor access or modulate the production of the target GPCR ligand. The majority of GPCRs are regulated by agonist-promoted desensitization and downregulation [72]. At

the molecular level, this process is triggered by the phosphorylation of the receptor catalyzed by GPCR kinases (GRKs), followed by the binding of  $\beta$ -arrestins ( $\beta$ arrs);  $\beta$ arrs uncouple the receptor from its cognate G proteins, sterically hinder its further binding to them, thus targeting the receptor for internalization into endosomes [73]. GRKs are serine-threonine protein kinases comprising seven isoforms (GRK1-7), among which GRK2 is mainly expressed in the heart. GRK2 is a cytoplasmic protein in its inactive state, which recognizes, binds and phosphorylates agonist-bound GPCR, including  $\beta$ - and  $\alpha$ 2-adrenergic receptors ( $\beta$ -ARs and  $\alpha$ 2-ARs) and angiotensin II type 1 receptor (AT1Rs) [73]. During HF different neurohormonal systems are hyperactive, which leads to a marked increase in circulating levels of catecholamines such as adrenaline and noradrenaline. This overstimulation of the  $\beta$ -adrenergic system, which is of course part of a compensatory mechanism, is responsible at the same time to produce toxic effects on the heart on the long run and plays a key pathogenic role in HF progression. GRK2 is upregulated in several different pathologic conditions, such as cardiac ischemia, hypertrophy, and hypertension, in line with a protective mechanism whose aim is to counteract the effects of an excessive catecholaminergic stimulation by reducing signaling through  $\beta$ ARs [74]. Moreover, in HF, cardiac GRK2 protein levels are increased in the early stages of the disease and an increasing body of evidence suggests that this protein can be considered as a potential novel biomarker of cardiac dysfunction in human [74-76]. In line with this, the prognostic value of GRK2 to predict cardiovascular death and all-cause mortality was recently assessed [75, 76].

GRK2 upregulation is detrimental for the heart and provokes the functional uncoupling of  $\beta$ AR *in vivo*. An ever-growing body of pre-clinical evidence presented in literature supports cardiac GRK2 inhibition as a valid pharmacological approach to improve cardiac function and reduce the cardiac damage in patients with HF [77-82]. Studies in knock-out mice using a GRK2 inhibitor peptide, known as bARKct, revealed a beneficial effect on cardiac function in several other animal models [77, 78]. The use of a wide array of small molecules and peptides to inhibit GRK2 is currently under investigation [80, 81] and will certainly offer in the near future many advantages for the patient suffering from HF.

Interestingly, adrenal glands were recently pinpointed as a possible target organ for GRK2 therapy; adrenal GRK2, indeed, seems to play an important role in regulation of heart sympathetic stimulation and in HF damages [73]. The inhibition, *via* adenoviral-mediated  $\beta$ ARKct adrenal-specific gene delivery, led to a marked reduction in catecholamines circulating levels, restoring both adrenal and cardiac functions [73].

Among others, the serotonin reuptake inhibitor (SSRI) paroxetine showed strong affinity for GRK2 and revealed significant inhibitory properties on GRK2 both *in vitro* and *in vivo* [79]. Paroxetine binds in the active site of GRK2 and stabilizes the kinase domain in a novel conformation, in which a unique regulatory loop forms part of the ligand-binding site [79]. A major limitation for the use of this drug, however, is the requirement of a very high dosage to inhibit the kinase. The effective doses exceed those approved for the use of paroxetine in humans, provoking unavoidable effects on the central nervous system [8].

All these data strongly support the use of inhibition mechanisms on GRK2 activity in HF treatment [82]. However, the incoming evidence about the multiple role of GRK2 in cellular physiology is prompting further studies to identify its subcellular localization and function in the different organelles, thus better detailing the molecular determinants of its inhibition.

**ACE2.** Angiotensin-converting enzyme (ACE), a dipeptidyl carboxypeptidase, is a key enzyme in the renin-angiotensin system (RAS) and is involved in the conversion of the inactive decapeptide, angiotensin I (Ang I; or Ang 1-10), to the active octapeptide Ang II (or Ang 1-8), and in the inactivation of the vasodilator bradykinin [83]. The canonical view of RAS has been confronted by the recent discovery of the enzyme ACE2, a monocarboxypeptidase that converts Ang II into angiotensin 1-7 (Ang 1-7), which counteracts the molecular and cellular effects of Ang II [84]. It has been proposed that ACE2, widely expressed in cardiomyocytes, cardiofibroblasts, and coronary endothelial cells, might protect against blood pressure increase caused by Ang II action [83]. Indeed, recent preclinical translational studies confirmed that an increase of ACE2 level prevents and reverses the HF phenotype. Recombinant human ACE2 has been shown to effectively lower plasma levels of Ang II and to increase Ang 1-7 levels, and, most importantly, was considered safe in both phase I and II of clinical trials [84].

**RhoA/ROCK pathway.** Rho-kinases (ROCKs) are the first and the best-characterized effectors of the small G-protein RhoA, and play important roles in many intracellular signaling pathways [85-89]. ROCK are serine/threonine kinases for which two isoforms, ROCK1 and ROCK2 have been identified in humans [86]. The RhoA/ROCK pathway has been so far well described in endothelial cells and in VSMCs, where a large number of ROCK targets are related to actin-filament dynamics, organization of the cytoskeleton and regulation of contractility [87]. The Rho/ROCK cascade seems to be interacting with other signaling cascades, like NO-signaling, that are also important regulators of vascular smooth muscle contractility [85]. ROCKs activity regulates major morphogenetic events

during embryonic development including cardiomyocyte differentiation [85].

Several studies have clearly shown an important pathophysiological involvement of this pathway in the cardiovascular system and in diseases such as atherosclerosis, I/R injury, hypertension, HF and stroke [85-89]. Among others, the interplay between ROCKs activation and ROS production plays a crucial role in myocardial damage after I/R. Pretreatment with the ROCK inhibitor Fasudil before reperfusion prevented endothelial dysfunction and reduced the extent of MI in several animal models [87].

Among others, increased activity of the Rho/Rho-kinase pathway has also been shown to have an important role in the development and maintenance of hypertension [85-87]. Modifications in the RhoA/ROCK pathway are likely related to an upstream event in the hypertensive state. One upstream signaling molecule possibly involved is Ang II and its receptor type 1 (AT1R). Interestingly, another upstream event that is linked to activation of RhoA and ROCKs in hypertension is the formation of ROS [86].

ROCKs specific inhibitors, such as Fasudil and Y-27632, inhibit kinase activity by competing with ATP at the Rho-binding site [87]. Since the two ROCK isoforms seem to have different functions in smooth muscle cells under different conditions, clinical applications require more specific ROCK inhibitors, which might have multiple beneficial effects on vascular function.

Even though the use of ROCKs inhibitors have drawn much attention in cardiovascular medicine, their use should be avoided during pregnancy due to the crucial role of ROCKs in cardiac development [87]. Moreover, it should be also taken in account that several medications, including statins, calcium channel blockers and eicosapentaenoic acid share an indirect inhibitory effect on Rho-kinase.

Recently, it was shown that Arhgef1 is the RhoA guanine exchange factor responsible for angiotensin II-induced activation of RhoA signaling in arterial smooth muscle cells [88, 89]. The authors showed that control of RhoA signaling through Arhgef1 is central to the development of angiotensin II-dependent hypertension and identify Arhgef1 as a potential target for the treatment of hypertension [88, 89].

**PTX3.** Pentraxine (PTXs) superfamily includes evolutionary conserved proteins involved in the acute inflammatory phase [90]. Among them, particular attention has been focused on pentraxine 3 (PTX3); this protein regulates the inflammatory response and is also involved in several important mechanisms, including the onset of vascular diseases. Indeed, during inflammation, blood vessels produce a large amount of PTX3;

these high levels are also detected in several pathological conditions affecting the cardiovascular system [91]. Furthermore, the protein is abundantly expressed in the endothelial cells in advanced atherosclerotic lesions and in patients with vasculitis [91]. This suggests that PTX3 is involved in a variety of molecular mechanisms leading to vascular damage; in addition, it has been shown that its elevated plasma levels might effectively represent a predictor of fragility in hypertensive patients [92, 93]. Interestingly, recent work by Bonacina and coworkers showed that PTX3 produced by vascular cells plays a protective role in arterial thrombosis, reducing collagen and fibrinogen induced platelet aggregation. Injection of recombinant PTX3 restored, at least partially, phenotype observed in PTX3-deficient knockout mice and had beneficial effects on cardiovascular dysfunctions in wild-type mice [94].

**miRNA.** miRNAs, small non-coding RNAs of 20-25 nucleotides, are a group of key regulators that modulate the development of various diseases, including CVD. Considering the role of miRNA in gene regulation, miRNAs may thus be deeply involved in cardiac hypertrophy and HF and show a great potential for diagnostic and therapeutic utilization [95-98]. miRNAs modulate gene expression at the posttranscriptional level through several mechanisms [99], and are extremely abundant in humans; it has been estimated that these molecules, whose expression seems to be tissue specific, participate in modulating the expression of more than 60% of protein-coding genes [100, 101]. miRNAs downregulate gene expression by either cleaving and degrading mRNA or blocking translation through different mechanisms such as inhibition of mRNA translation, de-adenylation and sequestration [102].

Generally, a mature miRNA regulates gene expression by binding motifs in the 3' UTR sequences, but recent studies suggest that miRNA may also target 5' UTR or exons and may potentially undergo base pairing with regulatory-DNA sequences to modulate transcription [102].

As already underlined in this review, CVD is the result of cardiac remodeling involving several processes such as cardiomyocyte hypertrophy, cardiomyocyte apoptosis, interstitial fibrosis and aberrant cardiac conduction. All these processes, ultimately, impair the myocardium electromechanical performance. Pathological cardiac hypertrophy is characterized by an increase in cell size, enhanced protein synthesis, and heightened organization of the sarcomere. *In vivo* and *in vitro* studies in cardiac hypertrophy models have revealed both up- and down- regulation of miRNAs responsible for either positive or negative regulatory effects on cardiac hypertrophic pathways. In literature, several studies show the involvement of miR-

1/miR133 cluster in hypertrophy remodeling [103, 104]. It has been shown that they are downregulated in cardiac disease and cardiac hypertrophy models [104]. Furthermore, miR-1/miR133 cluster participates in hypertrophic program because they repress CaN/NFAT (Nuclear Factor of activated T-cells) and IGF signaling pathways, a key regulator of cardiomyocytes growth and differentiation [103]. Even though the precise role of miR-1 remains to be defined, the observed effects *in vitro* and *in vivo* of these molecules suggest that their pharmacological potential might be of preventing cardiac hypertrophy during cardiac diseases [105].

To date, more than 11 miRNAs have been experimentally established to be involved in the pathogenesis of CVD; among these, the best characterized are miR-1, 133, 129, 18b, 195, 21, 23a, 23b, 24, 208, and 212 [106]. Down-regulation of miR-1 has been for example identified in three different hypertrophic models, including transverse aortic arch-constricted mice, transgenic mice with selective cardiac overexpression of a constitutively active mutant of the Akt kinase, and exercised rats [107, 108]. miR-1 was also reported to negatively regulate the expression of hypertrophy-associated genes, myocyte enhancer factor-2 (Mef2a) and transcription factor Gata4, and to attenuate cardiomyocyte hypertrophy in cultured neonatal rat cardiomyocytes and in the intact adult heart [109]. Increasing evidence indicates that miRNAs such as miR-1/106, miR-133, miR-21, miR-320, miR-199a and miR-92a, are also implicated in CAD. It was recently shown that miR-1 level is markedly elevated in ischemic myocardium where apoptotic cell death plays an important role in the detrimental changes of the diseased heart [110]. Aberrant proliferation of VSMCs and the formation of neointimal lesion is a key pathological process of a variety of proliferative vascular diseases, such as atherosclerosis, CAD, postangioplasty restenosis and transplantation arteriopathy [111]. It was suggested that miR-21, miR-221, and miR-222 were significantly upregulated in carotid arteries after angioplasty and the depletion of the aberrantly overexpressed miR-21, miR-221, or miR-222, *via* antisense-mediated knock-down, has a significantly negative effect on neointimal lesion formation in rat artery after angioplasty, forced overexpression of these miRNAs promotes instead VSMCs proliferation [112].

For those miRNAs that are aberrantly upregulated and play a causal role in disease states, the anti-miRNA techniques suppressing their expression are an appealing therapeutic approach. The inhibition of miRNAs expression can be achieved by using antisense inhibitor oligonucleotides (AMO) technique, thus designing oligonucleotides fully complementary to their target miRNAs (antagomiR), which block the targeted miRNAs with unknown mechanisms [113, 114]. Several

studies have validated so far the therapeutic effects of antagomiR in cardiac hypertrophy and infarction [115].

## CONCLUSION

CVD is globally recognized as the leading cause of human morbidity and mortality in developed countries, although a profound gap still exists between high-income countries and low and middle-income countries in terms of major and fatal clinical events [116].

Despite the existence of well-established therapies for these dysfunctions, their social and economic burden, due to high mortality and morbidity rates, continues to increase and, as a very limited number of new drugs survive phase III trials, there is a critical need for safer and more effective therapies.

Aim of this brief review has been to describe some among the most interesting molecular targets currently investigated for the development of new therapeutics for cardiac diseases.

The global quest for new molecular targets is leading to an impressive amount of records in the more recent literature. However, great caution should be used in considering all these targets effective in promoting the production of new drugs, as past lessons have shown the fail in clinical development of several new molecules due to a lack of efficacy or induction of safety liabilities [117]. The drawbacks responsible for discontinuing the pipeline to the development of commercially available drugs are different and include, among others, a very high bar of the existing medicines and the increasing cost of mega-trials. In addition, several studies lack independent and large-scale population studies from which novel targets with strong correlation to clinical phenotypes should be inferred, and do not show the fundamental pre-clinical and clinical validations. Furthermore, many molecular targets for CVD treatment are correctly selected, based on their involvement in critical metabolic pathways in cellular models but, since they play functional roles in other biological processes outside the cardiovascular system, they lack specificity.

Lastly, but most importantly, the complexity of CVD -caused by interconnected multiple genetic, environmental and physiological factors- cannot be addressed by a single “magic bullet”. To maximize the chance for successful clinical drug development, CVD onset should be analyzed based on the entire body of genetic and biochemical knowledge associated with the clinical traits, even though today it is still very important to add further details to the cellular and molecular basis of cardiovascular dysfunctions.

In this light, an increasing interest has been aroused in “omics” sciences, which allow performing the untargeted investigation of complex biological systems.

In particular, proteomic approaches are very attractive to CVD research, since these multifactorial pathologies depend on alterations involving large protein networks. Proteomics emerged as one of the most powerful tools to identify biomarkers for early diagnosis of CVD and risk prediction [118], responsible to identify tens of new promising candidates both in plasma and urine. Moreover, it could provide information concerning the proteins playing key roles in the onset and progression of CVD, also unveiling the relationships occurring among proteins affecting different pathways [119]. Therefore, proteomics-based studies could lead to the identification of new therapeutic targets, possibly consisting of groups of proteins [120, 121].

## CONFLICT OF INTEREST

The authors confirm that this article content has no conflict of interest.

## ACKNOWLEDGEMENTS

Declared none.

## REFERENCES

- [1] Wong LL, Wang J, Liew OW, Richards AM, *et al.* MicroRNA and Heart Failure. *Int J Mol Sci.* 2016; 17(4): 502.
- [2] Cabrera-Fuentes HA, Aragonés J, Bernhagen J, *et al.* From basic mechanisms to clinical applications in heart protection, new players in cardiovascular diseases and cardiac theranostics: meeting report from the third international symposium on "New frontiers in cardiovascular research". *Basic Res Cardiol.* 2016; 111(6): 69.
- [3] [http://www.who.int/cardiovascular\\_diseases/global-hearts](http://www.who.int/cardiovascular_diseases/global-hearts).
- [4] Kehat I, Molkentin JD. Molecular pathways underlying cardiac remodeling during pathophysiologic stimulation. *Circulation.* 2010; 122(25): 2727-2735.
- [5] Johnson FL. Pathophysiology and etiology of heart failure. *Cardiol Clin.* 2014; 32(1): 9-19.
- [6] Walters AM, Porter GA Jr, Brookes PS. Mitochondria as a drug target in ischemic heart disease and cardiomyopathy. *Circ Res.* 2012; 111(9): 1222-36.
- [7] Bui AL, Horwich TB, Fonarow GC. Epidemiology and risk profile of heart failure. *Nat Rev Cardiol.* 2011; 8(1): 30-41.
- [8] Sorriento D, Ciccarelli M, Cipolletta E, *et al.* "Freeze, Don't Move": How to Arrest a Suspect in Heart Failure - A Review on Available GRK2 Inhibitors. *Front Cardiovasc Med.* 2016; 3: 48.
- [9] Joubert M, Jagu B, Montaigne D, *et al.* The SGLT2 Inhibitor Dapagliflozin Prevents Cardiomyopathy in a Diabetic Lipodystrophic Mouse Model. *Diabetes.* 2017; pii: db160733.
- [10] Randriamboavonjy JI, Loirand G, Vaillant N, *et al.* Cardiac Protective Effects of Moringa oleifera Seeds in Spontaneous Hypertensive Rats. *Am J Hypertens.* 2016; 29(7): 873-81.
- [11] George M, Rajaram M, Shanmugam E, VijayaKumar TM. Novel drug targets in clinical development for heart failure. *Eur J Clin Pharmacol.* 2014; 70(7): 765-74.
- [12] Chatterjee K. Neurohormonal activation in congestive heart failure and the role of vasopressin. *Am J Cardiol.* 2005; 95(9A): 8B-13B.
- [13] Bonsu KO, Owusu IK, Buabeng KO, *et al.* Review of novel therapeutic targets for improving heart failure treatment

- based on experimental and clinical studies. *Ther Clin Risk Manag*. 2016; 12: 887-906.
- [14] Greenberg B. Gene therapy for Heart Failure. *J Cardiol*. 2015; 66: 195-200.
- [15] Gong B, Zicheng Li Z, and Philip Ching Yat Wong P. Levosimendan treatment for heart failure: a systematic review and meta-analysis. *J Cardiothorac Vasc Anesth*. 2015; 29(6): 1415-1425.
- [16] Gonzales TK, Yonker JA, Chang V, *et al*. Myocardial infarction in the Wisconsin Longitudinal Study: the interaction among environmental, health, social, behavioural and genetic factors. *BMJ Open*. 2017; 7(1): e011529.
- [17] Yabluchanskiy A, Li Y, Chilton RJ, *et al*. Matrix metalloproteinases: drug targets for myocardial infarction. *Curr Drug Targets*. 2013; 14(3): 276-86.
- [18] Hausenloy DJ, Yellon DM. Myocardial ischemia-reperfusion injury: a neglected therapeutic target. *J Clin Invest*. 2013; 123(1): 92-100.
- [19] Conti V, Izzo V, Corbi G, *et al*. Antioxidant Supplementation in the Treatment of Aging-Associated Diseases. *Front Pharmacol*. 2016; 7: 24.
- [20] Conti V, Forte M, Corbi G, *et al*. Sirtuins: possible clinical implications in cardio and cerebrovascular diseases. *Curr Drug Targets*. 2017; 18(4): 473-484.
- [21] He F, Zuo L. Redox Roles of Reactive Oxygen Species in Cardiovascular Diseases. *Int J Mol Sci*. 2015; 16(11): 27770-27780.
- [22] De Marchi E, Baldassari F, Bononi A, *et al*. Oxidative Stress in Cardiovascular Diseases and Obesity: Role of p66Shc and Protein Kinase C. *Oxid Med Cell Longev*. 2013; Article ID 564961.
- [23] Sugamura K, Keaney JF Jr. Reactive Oxygen Species in Cardiovascular Disease. *Free Radic Biol Med*. 2011; 51(5): 978-992.
- [24] Kalogeris T, Bao Y, Korthuis RJ. Mitochondrial reactive oxygen species: a double edged sword in ischemia/reperfusion vs preconditioning. *Redox Biol*. 2014; 2: 702-714.
- [25] Kalogeris T, Baines CP, Krenz M, *et al*. Cell Biology of Ischemia/Reperfusion Injury. *Int Rev Cell Mol Biol*. 2012; 298: 229-317.
- [26] Tesse A, Andriantsitohaina R, Ragot T. PPAR $\delta$  activity in Cardiovascular Diseases: a Potential Pharmacological Target. *PPAR Res*. 2009; 2009: 745821.
- [27] Park JR, Ahn JH, Jung MH. Effects of Peroxisome Proliferator-Activated Receptor- $\delta$  Agonist on Cardiac Healing after Myocardial Infarction. *PLoS One*. 2016; 11(2): e0148510.
- [28] Zhao Y, Meng XM, Wei YJ, *et al*. Cloning and characterization of a novel cardiac-specific kinase that interacts specifically with cardiac troponin I. *J Mol Med (Berl)* 2003; 81(5): 297-304.
- [29] Vagnozzi RJ, Gatto GJ Jr, Kallander LS *et al*. Inhibition of the cardiomyocyte-specific kinase TNNI3K limits oxidative stress, injury, and adverse remodeling in the ischemic heart. *Sci Transl Med* 2013; 5 (207): 207-141.
- [30] Lal H, Ahmad F, Parikh S, *et al*. TNNI3K, a novel cardiac-specific kinase, emerging as a molecular target for the treatment of cardiac disease. *Circ J* 2014; 78(7): 1514-1519.
- [31] Ballinger SW. Mitochondrial dysfunction in cardiovascular disease. *Free Radic Biol Med*. 2005; 38(10): 1278-95.
- [32] Parra V, Verdejo H, del Campo A, *et al*. The complex interplay between mitochondrial dynamics and cardiac metabolism. *J Bioenerg Biomembr*. 2011; 43(1): 47-51
- [33] Berman SB, Pineda FJ, Hardwick JM. Mitochondrial fission and fusion dynamics: the long and short of it. *Cell Death Differ*. 2008; 15(7): 1147-52
- [34] Song Z, Ghochani M, McCaffery JM, *et al*. Mitofusins and OPA1 Mediate Sequential Steps in Mitochondrial Membrane Fusion. *Mol Biol Cell*. 2009; 20(15): 3525-3532.
- [35] Chen L, Gong Q, Stice JP, *et al*. Mitochondrial OPA1, apoptosis, and heart failure. *Cardiovasc Res*. 2009; 84(1): 91-99.
- [36] Frezza C, Cipolat S, Martins de Brito O, *et al*. OPA1 controls apoptotic cristae remodeling independently from mitochondrial fusion. *Cell*. 2006; 126(1): 177-89.
- [37] Ong SB, Subrayan S, Lim SY, *et al*. Inhibiting mitochondrial fission protects the heart against ischemia/reperfusion injury. *Circulation*. 2010; 121(18): 2012-22.
- [38] Hare JM. Oxidative stress and apoptosis in heart failure progression. *Circ Res*. 2001; 89(3): 198-200.
- [39] Dai DF, Santana LF, Vermulst M, *et al*. Overexpression of catalase targeted to mitochondria attenuates murine cardiac aging. *Circulation*. 2009; 119(21): 2789-2797.
- [40] Dai DF, Chen T, Szeto H, *et al*. Mitochondrial targeted antioxidant Peptide ameliorates hypertensive cardiomyopathy. *J Am Coll Cardiol*. 2011; 58(1): 73-82.
- [41] Rocha M, Hernandez-Mijares A, Garcia-Malpartida K, *et al*. Mitochondria-targeted antioxidant peptides. *Curr Pharm Des*. 2010; 16(28): 3124-31.
- [42] Bers DM. Calcium cycling and signaling in cardiac myocytes. *Annu Rev Physiol*. 2008; 70: 23-49.
- [43] Cardenas C, Miller RA, Smith I, *et al*. Essential regulation of cell bioenergetics by constitutive InsP3 receptor Ca<sup>2+</sup> transfer to mitochondria. *Cell*. 2010; 142: 270-83.
- [44] Liu T, O'Rourke B. Enhancing mitochondrial Ca<sup>2+</sup> uptake in myocytes from failing hearts restores energy supply and demand matching. *Circ Res*. 2008; 103: 279-88.
- [45] Troncoso R, Vicencio JM, Parra V, *et al*. Energy-preserving effects of IGF-1 antagonist starvation-induced cardiac autophagy. *Cardiovasc Res*. 2011; 93: 320-9
- [46] deGoma EM, deGoma RL, Rader DJ. Beyond high-density lipoprotein cholesterol levels evaluating high-density lipoprotein function as influenced by novel therapeutic approaches. *J Am Coll Cardiol* 2008; 51: 2199-211.
- [47] Rader DJ, Alexander ET, Weibel GL *et al*. The role of reverse cholesterol transport in animals and humans and relationship to atherosclerosis. *J Lipid Res* 2009; 50: Suppl: S189-S194.
- [48] Otocka-Kmiecik A, Mikhailidis DP, Nicholls SJ, *et al*. Dysfunctional HDL: A novel important diagnostic and therapeutic target in cardiovascular disease? *Progress In Lipid Research* 2012; 51:314-324.
- [49] Assanasen C, Mineo C, Seetharam D, *et al*. Cholesterol binding, efflux, and a PDZ-interacting domain of scavenger receptor-BI mediate HDL-initiated signaling. *J Clin Invest* 2005; 115: 969-77.
- [50] Saddar S, Carriere V, Lee WR, *et al*. Scavenger receptor class B type I is a plasma membrane cholesterol sensor. *Circ Res* 2013; 112: 140-51.
- [51] Wadham C, Albanese N, Roberts J, *et al*. Highdensity lipoproteins neutralize C-reactive protein proinflammatory activity. *Circulation* 2004; 109: 2116-22.
- [52] Eren E, Yilmaz N, Aydin O. High Density Lipoprotein and its Dysfunction. *Open Biochem J* 2012; 6: 78-93.
- [53] Wacker BK, Dronadula N, Zhang J, *et al*. Local vascular gene therapy with apolipoprotein A-I to promote regression of atherosclerosis. *Arterioscler Thromb Vasc Biol* 2017; 37(2): 316-327.
- [54] Navab M, Anantharamaiah GM, Reddy ST, *et al*. Peptide mimetics of apolipoproteins improve HDL function. *J Clin Lipidol* 2007; 1: 142-7.
- [55] Eisen A, Giugliano RP. Advances in the field of proprotein convertase subtilisin kexin type 9 inhibitors. *Curr Opin Cardiol*. 2016 Nov; 31(6): 644-653.

- [56] Payne GA, Kohr MC, Tune JD. Epicardial perivascular adipose tissue as a therapeutic target in obesity-related coronary artery disease. *Br J Pharmacol.* 2012; 165(3): 659–669.
- [57] Talman AH, Psaltis PJ, Cameron JD, *et al.* Epicardial adipose tissue: far more than a fat depot. *Cardiovasc Diagn Ther.* 2014; 4(6): 416–429.
- [58] Parisi V, Rengo G, Perrone-Filardi P, *et al.* Increased Epicardial Adipose Tissue Volume Correlates With Cardiac Sympathetic Denervation in Patients With Heart Failure. *Circ Res.* 2016; 118(8): 1244–53.
- [59] Parisi V, Rengo G, Pagano G, *et al.* Epicardial adipose tissue has an increased thickness and is a source of inflammatory mediators in patients with calcific aortic stenosis. *Int J Cardiol.* 2015; 186: 167–9.
- [60] Minamino T, Komuro I, Kitakaze M. Endoplasmic Reticulum Stress As a Therapeutic Target in Cardiovascular Disease. *Circulation Research* 2010; 107: 1071–1082.
- [61] Ron D, Walter P. Signal integration in the endoplasmic reticulum unfolded protein response. *Nat Rev Mol Cell Biol* 2007; 8: 519–529.
- [62] Kim I, Xu W, Reed JC. Cell death and endoplasmic reticulum stress disease relevance and therapeutic opportunities. *Nat Rev Drug Discov* 2008; 7: 1013–1030.
- [63] Minamino T, Kitakaze M. ER stress in cardiovascular disease. *J Mol Cell Cardiol.* 2010; 48: 1105–1110.
- [64] Hansson GK. Inflammation, atherosclerosis, and coronary artery disease. *N Engl J Med* 2005; 352: 1685–1695.
- [65] Myoishi M, Hao H, Minamino T, *et al.* Increased endoplasmic reticulum stress in atherosclerotic plaques associated with acute coronary syndrome. *Circulation* 2007; 116: 1226–1233.
- [66] Belmont PJ, Chen WJ, San Pedro MN, *et al.* Roles for endoplasmic reticulum-associated degradation and the novel endoplasmic reticulum stress response gene Derlin-3 in the ischemic heart. *Circ Res* 2010; 106: 307–316.
- [67] Avery J, Etzion S, DeBosch BJ, *et al.* TRB3 function in cardiac endoplasmic reticulum stress. *Circ Res* 2010; 106: 1516–1523.
- [68] Tajiri S, Oyadomari S, Yano S, *et al.* Ischemia-induced neuronal cell death is mediated by the endoplasmic reticulum stress pathway involving CHOP. *Cell Death Differ* 2004; 11: 403–415.
- [69] Fu HY, Minamino T, Tsukamoto O, *et al.* Overexpression of endoplasmic reticulum-resident chaperone attenuates cardiomyocyte death induced by proteasome inhibition. *Cardiovasc Res* 2008; 79: 600–610.
- [70] Ozcan U, Yilmaz E, Ozcan L, *et al.* Chemical chaperones reduce ER stress and restore glucose homeostasis in a mouse model of type 2 diabetes. *Science* 2006; 313: 1137–1140.
- [71] Salon JA, David T, Lodowski DT, *et al.* The Significance of G Protein-Coupled Receptor Crystallography for Drug Discovery. *Pharmacol Rev.* 2011; 63(4): 901–937.
- [72] Siryk-Bathgate A, Dabul S, Lympopoulos A. Current and future G protein-coupled receptor signaling targets for heart failure therapy. *Drug Des Devel Ther.* 2013; 7: 1209–1222.
- [73] Lympopoulos A, Rengo G, Koch WJ. GRK2 inhibition in heart failure: something old, something new. *Curr Pharm Des* 2012; 18(2): 186–191.
- [74] Woodall MC, Ciccarelli M, Koch WJ, *et al.* G protein-coupled receptor kinase 2: a link between myocardial contractile function and cardiac metabolism. *Circ Res* 2014; 114(10): 1661–70.
- [75] Rengo G, Pagano G, Filardi PP, *et al.* Prognostic Value of Lymphocyte G Protein-Coupled Receptor Kinase-2 Protein Levels in Patients With Heart Failure. *Circ Res.* 2016; 118(7): 1116–24.
- [76] Rengo G, Galasso G, Femminella GD, *et al.* Reduction of lymphocyte G protein-coupled receptor kinase-2 (GRK2) after exercise training predicts survival in patients with heart failure. *Eur J Prev Cardiol.* 2014; 21(1): 4–11.
- [77] Raake P. W, Schlegel P, Ksienzyk J, *et al.* AAV6.βARKct cardiac gene therapy ameliorates cardiac function and normalizes the catecholaminergic axis in a clinically relevant large animal heart failure model. *Eur Heart J* 2013; 34(19): 1437–1447.
- [78] Rengo G, Lympopoulos A, Zincarelli C, *et al.* Myocardial adeno-associated virus serotype 6-βARKct gene therapy improves cardiac function and normalizes the neurohormonal axis in chronic heart failure. *Circulation* 2009; 119(1): 89–98.
- [79] Thal DM, KT Homan, Chen J, *et al.* Paroxetine is a direct inhibitor of g protein-coupled receptor kinase 2 and increases myocardial contractility. *ACS Chem. Biol* 2012; 7(11): 1830–1839.
- [80] Carotenuto A, Cipolletta E, Gomez-Monterrey I, *et al.* Design, synthesis and efficacy of novel G protein-coupled receptor kinase 2 inhibitors. *Eur J Med Chem.* 2013; 69: 384–92.
- [81] Sorriento D, Santulli G, Franco A, *et al.* Integrating GRK2 and NFκB in the Pathophysiology of Cardiac Hypertrophy. *J Cardiovasc Transl Res.* 2015; 8(8): 493–502.
- [82] Cannavo A, Liccardo D, Koch WJ. Targeting cardiac beta-adrenergic signaling via GRK2 inhibition for heart failure therapy. *Front Physiol* 2013; 4: 264.
- [83] Der Sarkissiana S, Huentelmana MJ, Stewart J, *et al.* ACE2: A novel therapeutic target for cardiovascular diseases. *Prog Biophys Mol Biol* 2006; 91(1–2): 163–98.
- [84] Patel VB, Zhong JC, Grant MB, *et al.* Role of the ACE2/Angiotensin 1–7 Axis of the Renin-Angiotensin System in Heart Failure. *Circ Res.* 2016; 118(8): 1313–26.
- [85] Loirand G, Gue'rin P, Pacaud P. Rho Kinases in Cardiovascular Physiology and Pathophysiology. *Circ Res* 2006; 98: 322–334.
- [86] Wirth A. Rho Kinase and Hypertension. *Biochim Biophys Acta.* 2010; 1802 (12): 1276–1284.
- [87] Shimokawa H, Sunamura S, Satoh K. RhoA/Rho-Kinase in the Cardiovascular System. *Circ Res.* 2016; 118(2): 352–66.
- [88] Guilluy C, Brégeon J, Toumaniantz G, *et al.* The Rho exchange factor Arhgef1 mediates the effects of angiotensin II on vascular tone and blood pressure. *Nat Med.* 2010; 16(2): 183–90.
- [89] Carbone ML, Brégeon J, Devos N, *et al.* Angiotensin II activates the RhoA exchange factor Arhgef1 in humans. *Hypertension.* 2015; 65(6): 1273–8.
- [90] Bottazzi B, Vouret-Craviari V, Bastone A, *et al.* Multimer formation and ligand recognition by the long pentraxin PTX3. Similarities and differences with the short pentraxins C-reactive protein and serum amyloid P component. *J Biol Chem.* 1997; 272: 32817–32823.
- [91] Presta M, Camozzi M, Salvatori G, *et al.* Role of the soluble pattern recognition receptor PTX3 in vascular biology. *J Cell Mol Med.* 2007; 11: 723–738.
- [92] Fornai F, Carrizzo A, Forte M, *et al.* The inflammatory protein Pentraxin 3 in cardiovascular disease. *Immunity & Ageing.* 2016; 13: 25.
- [93] Carrizzo A, Lenzi P, Procaccini C, *et al.* Pentraxin 3 Induces Vascular Endothelial Dysfunction Through a P-selectin/Matrix Metalloproteinase-1 Pathway. *Circulation.* 2015; 131: 1495–1505.
- [94] Bonacina F, Barbieri SS, Cutuli L, *et al.* Vascular pentraxin 3 controls arterial thrombosis by targeting collagen and fibrinogen induced platelets aggregation. *Biochim Biophys Acta* 2016; 1862(6): 1182–1190.

- [95] Li M, Marin-Muller C, Bharadwaj U, *et al.* MicroRNAs: control and loss of control in human physiology and disease. *World J Surg* 2009; 33: 667–84.
- [96] Latronico MV, Catalucci D, Condorelli G. Emerging role of microRNAs in cardiovascular biology. *Circ Res* 2007; 101: 1225–36.
- [97] Wang GK, Zhu JQ, Zhang JT *et al.* Circulating microRNA: a novel potential biomarker for early diagnosis of acute myocardial infarction in humans. *Eur Heart J*. 2010; 31(6): 659–66.
- [98] Montgomery RL, Hullinger TG, Semus HM. Therapeutic inhibition of miR-208a improves cardiac function and survival during heart failure. *Circulation*. 2011; 124(14): 1537–47.
- [99] Filipowicz W, Bhattacharyya SN, Sonenberg N. Mechanisms of post-transcriptional regulation by microRNAs: are the answers insight? *Nat Rev Genet*. 2008, 9(2): 102–14.
- [100] Kozomara A, Griffiths-Jones S. miRBase: annotating high confidence microRNAs using deep sequencing data. *Nucleic Acids Res*. 2014 Jan 1; 42 (Database issue): D68–D73.
- [101] Kloosterman WP, Wienholds E, de Bruijn E, *et al.* *In situ* detection of miRNAs in animal embryos using LNA-modified oligonucleotide probes. *Nat Methods*. 2006; 3(1): 27–9.
- [102] Ørom UA, Nielsen FC, Lund AH. MicroRNA-10a binds the 5'UTR of ribosomal protein mRNAs and enhances their translation. *Mol Cell*. 2008 May 23; 30(4): 460–71.
- [103] Care A, Catalucci D, Felicetti F *et al.* MicroRNA-133 controls cardiac hypertrophy. *Nat Med*. 2007; 13: 613–618.
- [104] Liu N, Williams AH, Kim Y, *et al.* An intragenic MEF2-dependent enhancer directs muscle-specific expression of microRNAs 1 and 133. *Proc Natl Acad Sci U S A*. 2007; 104(52): 20844–9.
- [105] Elia L, Contu R, Quintavalle M, *et al.* Reciprocal regulation of microRNA-1 and insulin-like growth factor-1 signal transduction cascade in cardiac and skeletal muscle in physiological and pathological conditions. *Circulation*. 2009; 120(23): 2377–85.
- [106] Sayed D, Hong C, Chen IY, *et al.* MicroRNAs play an essential role in the development of cardiac hypertrophy. *Circ Res* 2007; 100: 416–24.
- [107] Yang B, Lin H, Xiao J, *et al.* The muscle-specific microRNA miR-1 regulates cardiac arrhythmogenic potential by targeting GJA1 and KCNJ2. *Nat Med* 2007; 13: 486–91.
- [108] Care A, Catalucci D, Felicetti F, *et al.* MicroRNA-133 controls cardiac hypertrophy. *Nat Med* 2007; 13: 613–8.
- [109] Hedley PL, Carlsen AL, Christiansen KM, *et al.* MicroRNAs in cardiac arrhythmia: DNA sequence variation of MiR-1 and MiR-133A in long QT syndrome. *Scandinavian Journal of Clinical and Laboratory Investigation*. 2014; 74(6): 485–491.
- [110] Pan Z, Lu Y, Yang B. MicroRNAs: a novel class of potential therapeutic targets for cardiovascular diseases. *Acta Pharmacologica Sinica* 2010; 31(1): 1–9.
- [111] Yang B, Lin H, Xiao J, *et al.* The muscle-specific microRNA miR-1 regulates cardiac arrhythmogenic potential by targeting GJA1 and KCNJ2. *Nat Med* 2007; 13: 486–91.
- [112] Sayed D, Hong C, Chen IY, *et al.* MicroRNAs play an essential role in the development of cardiac hypertrophy. *Circ Res* 2007; 100: 416–24.
- [113] Lu Y, Xiao J, Lin H, *et al.* A single anti-microRNA antisense oligodeoxyribonucleotide (AMO) targeting multiple microRNAs offers an improved approach for microRNA interference. *Nucleic Acids Res* 2009; 37.
- [114] Cheng AM, Byrom MW, Shelton J, *et al.* Antisense inhibition of human miRNAs and indications for an involvement of miRNA in cell growth and apoptosis. *Nucleic Acids Res* 2005; 33: 1290–7.
- [115] van Rooij E, Sutherland LB, Thatcher JE, *et al.* Dysregulation of microRNAs after myocardial infarction reveals a role of miR-29 in cardiac fibrosis. *Proc Natl Acad Sci USA* 2008; 105: 13027–32.
- [116] Schwalm JD, McKee M, Huffman MD, *et al.* Resource Effective Strategies to Prevent and Treat Cardiovascular Disease. *Circulation*. 2016; 133(8): 742–55.
- [117] Tall AR, The Failure of Torcetrapib: Was it the Molecule or the Mechanism? Alan R. Tall, Laurent Yvan-Charvet and Nan Wang *Arterioscler Thromb Vasc Biol*. 2007; 27: 257–260.
- [118] Lam MP, Ping P, Murphy E. Proteomics Research in Cardiovascular Medicine and Biomarker Discovery. *J Am Coll Cardiol*. 2016; 68(25): 2819–2830.
- [119] MacNamara J, Eapen DJ, Quyyumi A, *et al.* Novel biomarkers for cardiovascular risk assessment: current status and future directions. *Future Cardiol*. 2015; 11(5): 597–613.
- [120] Izzo V, Leo G, Scognamiglio R, *et al.* PHK from phenol hydroxylase of *Pseudomonas* sp. OX1. Insight into the role of an accessory protein in bacterial multicomponent monooxygenases. *Arch Biochem Biophys*. 2011; 505 (1): 48–59.
- [121] Mesaros C, Blair IA. Mass spectrometry-based approaches to targeted quantitative proteomics in cardiovascular disease *Clin Proteomics*. 2016; 13: 20. eCollection 2016.